final report

Project code: B.FLT.3010

Prepared by: Tony Batterham, Brad White, Luciano Gonzalez
Apiam Animal Health; Precision Animal Solutions, LLC; University of Sydney

Date published: 25-Aug-2022

PUBLISHED BY
Meat and Livestock Australia Limited
Locked Bag 1961
NORTH SYDNEY NSW 2059

Determination of bovine respiratory disease diagnostic accuracy for multiple modalities

Meat & Livestock Australia acknowledges the matching funds provided by the Australian Government to support the research and development detailed in this publication.

Abstract

Accurate and rapid diagnosis of bovine respiratory disease (BRD) remains a major limitation in mitigating negative disease impact, including death, and associated costs due to reduced animal performance. The project was conducted using two replicates (March 2020, March 2021, n = 200, 190 respectively) of commercially sourced feeder cattle monitored at a collaborating feedlot. In each replicate, cattle were monitored for visual signs of BRD and enrolled in the study at the time of illness as a CASE or CONTROL (CONT) animal, based on specific criteria including clinical signs of illness, rectal temperature, and pulmonary lesions demonstrated at necropsy. The remaining cattle in each cohort had carcass and pulmonary lesion data collected at slaughter to facilitate assessment of ability to detect subclinical illness. Based on case definition at the time of illness and necropsy confirmation, 10 x CASE and 10 x CONT animals were identified during the feeding phase. A total of 361 animals received pulmonary scoring at slaughter harvest with 45 (12.5%) having either a pleurisy score of > 1 and/or pulmonary consolidation of 5% or greater.

Multiple diagnostic methods were applied to each animal throughout the study period and at the time of diagnosis. For CASE and CONT, the best models for each modality examined resulted in ultrasound reporting as the most accurate (Se: 100%, Sp: 90%), followed by plasma haptoglobin (Se: 100%, Sp: 78%) and metabolomics (model random forest for visual / clinical signs from B.FLT.0164; Se: 100%, Sp: 78%), reticulo-rumen bolus (model classification tree T-180; Se: 100%, Sp: 70%), the REDI system (model REDI_ds3; Se: 90%, Sp: 80%), and computer aided auscultation (Se: 60%, Sp: 60%).

Executive summary

The health, performance, and economic impact of bovine respiratory disease (BRD) is significant in the cattle feeding industry. Common diagnostic modalities currently available for BRD in the field include visual (subjective) assessment and rectal temperature. Less common, but more sophisticated modalities include continuous behavioural monitoring, continuous reticulo-rumen temperature, thoracic ultrasound, plasma metabolomics and acute phase proteins (haptoglobin), nasopharyngeal microbiota profile, and computer aided auscultation. Although many methods exist, little work has been done to robustly validate each of these potential diagnostic modalities due to the lack of a gold standard in live animals at the time of clinical illness. The objective of the present study was to evaluate different diagnostic modalities and the viability of each in isolation, or their potential in combination, to improve diagnostic functionality and performance in commercial feedlot clinical settings.

A trial was performed with two replicates to identify BRD CASEs at the time of clinical presentation using clinical illness scores and rectal temperature confirmed by pulmonary lesions at necropsy. The same process was undertaken to identify and confirm CONT animals to pair with the confirmed CASEs. Diagnostic modalities were applied at specific time points such as at arrival, at disease diagnosis (ultrasound, haptoglobin, computer aided auscultation, nasopharyngeal microbiota, metabolomics) or for continuous monitoring (behaviour collar tags for the Remote Early Disease Identification (REDI) system, reticulo-rumen thermobolus temperature monitoring). Cattle not selected as CASE or CONT were allowed to finish the feeding phase, then pulmonary and pleural lesions were measured at harvest slaughter. A number of diagnostic modalities were used to compare CASE/CONT with respect to pulmonary lesions present at slaughter to evaluate diagnostic accuracy in this (subclinical) population.

A total of 390 cattle were enrolled in the trial in two replicates (2020 and 2021) and 10 x CASE and 10 x CONT animals were identified from the population. A total of 361 animals received pulmonary scoring at harvest with 45 trial animals (12.5%) having either a pleurisy score > 1 and/or pulmonary (total lung) consolidation of 5% or greater.

Multiple diagnostics were applied to each animal throughout the study period and at the time of diagnosis. Ultrasound scanning of the lungs was the most accurate (Se: 100%, Sp: 90%), followed by plasma haptoglobin (Se: 100%, Sp: 78%) and metabolomics (model random forest for visual / clinical signs from B.FLT.0164Se: 100%, Sp: 78%), reticulo-rumen bolus (model classification tree T-180Se: 100%, Sp: 70%), the REDI system (model REDI_ds3Se: 90%, Sp: 80%), metabolomics (model neural networks for lung lesions from B.FLT.0164; Se: 90%, Sp: 78%), reticulo-rumen bolus (model classification tree T-250; Se: 90%, Sp: 70%), the REDI system (model REDI_rn4call; Se: 80%, Sp: 80%) and the REDI system (model REDI_rn2call; Se: 80%, Sp:80%), metabolomics (model classification tree for visual signs from B.FLT.0164; Se 80%, Sp: 78%), the REDI system (model REDI_dccal; Se: 100%, Sp: 60%), reticulo-rumen bolus (model classification tree T-100; Se: 100%, Sp: 60%), reticulo-rumen bolus (model classification tree T-350; Se: 70%, Sp: 80%) and lastly computer aided auscultation (Se: 60%, Sp: 60%).

Changes from baseline (induction) nasopharyngeal microbiota diversity of CASE and CONT animals were also examined. This process does not fall into the standard description of a diagnostic test, therefore has not been reported in terms of sensitivity and specificity. Nonetheless, it's possible that interpreting the microbiota profile at feedlot arrival, and subsequent change from this baseline, might be predictive of BRD susceptibility if a sufficient dataset is available.

Subclinical CASEs were evaluated by considering pulmonary and pleural lesions at slaughter. Analysis of this population was possible through the two remote monitoring modalities: the REDI system and reticulo-rumen thermobolus. These two modalities were applied at induction into the study as wearable / in-situ devices on the cattle and were removed at the time of necropsy or harvest slaughter. The REDI system showed a sensitivity of 10-62% and specificity of 45-82% among the algorithms. The reticulo-rumen thermobolus showed sensitivity between 60-95% and specificity between 15-48% among different algorithms.

During normal feedlot (visual) surveillance operations, (29) study animals were detected and attributed a clinical illness score that would typically warrant removal from the pen for treatment, and record one of the required three scores for candidature as a preliminary CASE per the study criteria. None of these animals ultimately presented for enrollment as CASEs and only (3) demonstrated respiratory pathology at slaughter, representing 7% of the cohort.

Ultrasound of the chest was attempted as a modality screening for subclinical pulmonary lesions in the last 14 days before exit to harvest slaughter. An incomplete database was generated because the duration of time required to conduct bilateral (both sides) chest ultrasound surveys was too long for the handling facility designated and/or the facility couldn't provide bilateral access.

Subsequently, ultrasound detected the presence of subclinical pulmonary lesions with 8.7% sensitivity and 100% specificity but there were significant limitations present applying this diagnostic test.

The dataset forming the basis of this report does not provide sufficient power to interpret the findings with full confidence. A minimum of 20 CASE/CONT pairs *per* replicate was estimated to be required to power the study to the generally agreed level of 80%. 30 to 150 CASE / CONT pairs are required to achieve sufficient power, with the upper estimate giving robust confidence.

In adding these extra replicates, a modified design could be utilised whereby a smaller suite of modalities are employed. The modalities prioritised would be those reporting highest accuracies to date, and/or are most likely to be adapted to typical feedlot operating environments to further examine adoptability and commercial viability.

The working conclusions arising from the outcomes of this study, despite the insufficient statistical power estimate, can be summarised as follows:

- An accurate standard for BRD diagnosis in living animals facilitates future research and negates the requirement to euthanase specifically for confirmatory diagnosis.
- Sensitivity and specificity are widely used metrics, however other measurements should be considered when designing an overall diagnostic strategy for research or commercial purposes such as accuracy, prevalence, repeatability, amongst others. A highly specific test may not be very useful when the disease condition has high (true) prevalence, but in clinical settings where there is low prevalence, a highly specific test will protect against the inefficiency of many false positive detections and the work practices and operations this generates.
- This study confirms that the standard feedlot visual observation method, with rectal temperature not utilised, has low operating accuracy compared to CASEs with lung pathology.
- Adding rectal temperature (40.0°C threshold) to visual observation and clinical illness scoring did improve diagnosis in terms of rejecting preliminary CASEs for enrolment in that ultimately were never enrolled as CASEs at later dates in the study, and did not demonstrate respiratory pathology at slaughter. However, there were instances of false positive and false negative CASE and CONT animals on the basis of rectal temperature, with 40.0°C as the threshold for final determination.
- In the course of this study, no animal in the study pen was a non-detection misdiagnosis by visual observation as the method, to the extent of discovering animals very advanced with BRD and/or spontaneous deaths due to BRD without any preceding detection. It is important to note however, that these cattle were observed twice daily and for longer periods per session than the industry norm (up to 30 minutes in total daily). Even with this augmented version of the typical feedlot process, many of the cattle with pulmonary lesions at harvest were not identified as clinically ill.
- Ultrasound performs well as a BRD diagnostic method but requires training to conduct the surveys and interpret images, minimum machine capability, an appropriate restraint facility that allows access to both sides of the chest and the forward chest area, and a minimum of 5 minutes available to conduct the more basic level survey. It should also be noted that presumptive CASEs presented for examination had demonstrated a minimum of three clinical illness scores of 2 or greater over a 24-hour period. These CASEs therefore represent moderate to severe morbidity where the disease (and lung lesions) are allowed to progress unlike in typical feedlot clinical settings. Nonetheless, this diagnostic modality showed the best accuracy. For commercial application, where a truncated survey would be required to save time, prioritising anteroventral (forward and low) positions on the right hemithorax (right chest side) would yield the best probability of detecting pulmonary lesions if they are present.
- Remote, continuous monitoring through wearable technologies demonstrated promising accuracy with the added advantage of early detection in the case of REDI, especially in

comparison to the industry standard of visual observation. Reticulorumen thermobolus modalities have the potential for early detection however more advanced algorithms would need to be developed, targeting above threshold temperature counts in a more condensed time period near the presentation of clinical illness.

- Remote continuous monitoring offers the most promise commercially because of the ability to capture clinical and subclinical cases across the whole cohort under surveillance, as opposed to select animals presented to a restraint facility. As such, remote continuous monitors can facilitate early, targeted, treatment intervention across both clinical presentations and maximise treatment, productivity and welfare outcomes.
- Diagnostic tests can also be made more sensible or switched on in periods with prior high probability estimates of the disease in a typical clinical setting. In the case of BRD in Australian beef feedlots, the usual epidemiology involves incidence concentrating between approximately 10 and 60 days after arrival. The continuous monitoring modality REDI made all its detection of BRD CASEs in this period. This is a significant advantage for the REDI modality.
- Remote continuous monitoring can be utilised as a screening diagnostic test, with confirmation determination carried out by ultrasound, haptoglobin, or metabolomics. At this stage, combining these modalities would define the best working practical gold standard of BRD diagnosis in living animals for research purposes and for further validation of the continuous monitors. For commercial purposes, considering real-time requirements, combining the continuous monitoring screening test with ultrasound as confirmation, defines the best working practical gold standard of BRD diagnosis in living animals with the disease allowed to progress enough to cause lung tissue damage.
- Remote continuous monitoring modalities carry the capacity to operate with varying mixes of diagnostic sensitivity and specificity, which can be applied to varying levels of BRD risk as presented in the feedlot clinical setting. A working example could be utilising more sensitive algorithms for high BRD risk cohorts that are candidates for targeted metaphylaxis and/or more intensive daily pen riding.
- Haptoglobin is an acute phase protein that performed well as a diagnostic for BRD in this study, however specific cut-offs for levels of haptoglobin present in plasma have not been established for BRD, and this modality remains very non-specific to a spectrum of disease conditions. BRD is necessarily a very inflammatory process, so elevated levels in enrolled CASEs can be expected, however there remains low differentiation from other inflammatory disease processes.
- Plasma metabolomics in this study utilised a set of algorithms generated from an independent dataset and project (B.FLT.0164). There was good overall performance classifying CASE and CONT status in this group of study animals, with the random forest for visual / clinical signs model likely being a good candidate for confirmatory diagnostic test as part of a wider diagnostic strategy.
- Nasopharyngeal microbiota offers potential in the living animal to describe changes in the structure of microbiota that might align with increased resilience or susceptibility to BRD. In this study, the most prominent identified phyla across all CASE and CONT samples were Proteobacteria (40.50%), Tenericutes (33.27%), Firmicutes (8.78%), Bacteroidetes (6.22%), and Actinobacteria (6.21%). However, the order of both phyla and genera by abundance differed between experimental CASEs and CONTs, and between induction and CASE/CONT enrolment sample types. The most prominent identified genera across all CASE and CONT samples were *Mycoplasma* (32.15 %), *Psychrobacter* (12.68%), *Actinobacillus* (4.54%), *Histophilus* (4.14%), and *Nicotella* (3.04%). However, the order of genera by abundance differed between experimental groups and sample types (Genus abundance) Genera also varied between individual animals across experimental groups and sample types (individual

animal abundance). It was notable that CASE animals possessed comparatively higher abundance of *Mycoplasma* at induction and CASE enrolment.

- Computer aided electronic auscultation performed with low accuracy, as well as low repeatability (precision) in this study, across all animals in both replicates. A significant limitation of this modality is the requirement to limit all ambient noise to conduct the recording, which involves at minimum, removing all animals from the restraint apparatus adjacent to the presented patient. This results in considerable interruption to animal flow through the facility. To ensure mitigation of ambient noise further and obtain a diagnostic recording, vehicles travelling on the feedlot must be diverted from proximity to the restraint facility. Even under these conditions, computer aided electronic auscultation performed with the lowest accuracy and repeatability of all the studied modalities and offers very limited commercial application.
- Staging of disease and assessment of level of severity was not well elucidated in this study. Either the diagnostics employed were performing as a classifier only (i.e. determining disease present or not only), or, severity functions were not fully utilised (ultrasound) or didn't perform well (computer aided auscultation).
- Presence of pulmonary lesions as defined in this study (> 1 pleurisy score and/or => 5% pulmonary consolidation) at slaughter was significantly associated with reduced average daily gain. This highlights a potential value proposition for remote monitoring diagnostic modalities to identify feeder cattle that are subclinical cases so that they can be treated during the feeding phase to realise more optimal health, welfare, and productivity.

Table of contents

1 Background

Bovine respiratory disease (BRD) is the most common and costly disease of feedlot cattle and a major shortfall in mitigating negative disease impact is our inability to rapidly and accurately diagnose BRD. In addition to costs associated with performance loss and animal death, the cattle industry expends significantly each year attempting to prevent and treat BRD. A major opportunity exists to improve BRD diagnostics thereby promoting more efficacious therapy, animal well-being, and appropriate antimicrobial utilization.

Accurate and early disease diagnosis at feedlots is important to improve feedlot performance, health, welfare, and carcase characteristics. Bovine Respiratory Disease (BRD) results from the complex interaction of pathogens with animal, environmental and management risk factors. Human observation combined with current “chute-side” diagnostic technologies such as rectal thermometer, has modest sensitivity and specificity for diagnosis.

Over the past 5 years, numerous technologies for feedlot animal health have been researched with advances in information technology, engineering and diagnostic pathology. Technologies that differentiate between infection and disease (stage and severity of pathology) are required to assist appropriate antimicrobial use. Research to calibrate such technologies against gold standards for infection and disease in live animals is required. Currently the only reliable gold standard involves euthanasia of animals at the time of diagnosis, with subsequent necropsy assessment and pathology analysis.

Our multi-institutional research team with expertise in varied disciplines assessed diverse modalities to improve BRD identification and confirmation. Our objective was to determine diagnostic accuracy (sensitivity, specificity) and ability to determine stage of disease for multiple modalities relative to the gold standard of pulmonary lesions demonstrated at the time of diagnosis. The results contained will be directly applicable to Australian feedlots due to the importance of BRD diagnosis and the high external validity of the trial design. Study conclusions below provide insight for optimal deployment of the technologies examined to improve BRD diagnosis.

2 Project objectives

The principal aim of this research is to establish a gold standard for BRD diagnosis on feedlots in the living feeder animal that supersedes the current post-mortem model. As such, an expected output from this research relates to improving BRD diagnostic ability through an improved understanding of the attributes of multiple modalities that are currently available. The diagnostic accuracy of each tool has been evaluated relative to the gold standard of lung lesions demonstrated at the time of diagnosis to improve understanding of each modality.

The specific objectives set out to achieve this aim were as follows:

(1) Determine diagnostic accuracy and ability to delineate disease severity with BRD screening tests (e.g., acute phase proteins, respiratory microbiota, metabolomics).
(2) Determine diagnostic accuracy and ability to delineate disease severity using confirmatory tests (e.g., thoracic ultrasonography, computer aided thoracic auscultation, acute phase proteins, respiratory microbiota, metabolomics).
(3) Estimate ability of continuous monitoring systems for early identification and delineating BRD severity (e.g., reticulo-rumen temperature bolus and Remote Early Disease Identification, REDI, system).
(4) Comparison and contrasting of potential combinations of diagnostic modalities into a scheme to optimize detection and confirmation of BRD CASEs.

Overall, the objective is to determine diagnostic accuracy (sensitivity, specificity) and ability to determine stage of disease, for multiple modalities relative to the gold standard of pulmonary lesions at the time of diagnosis.

3 Methodology

3.1 Animal Care and Use Committee Approval

All study procedures were conducted in accordance with a protocol approved by the New South Wales Department of Primary Industries Animal Ethics committee.

3.2 Study design

The study was a prospective CASE-CONT trial performed in two replicates to monitor multiple diagnostic modalities and confirm the true BRD status of selected CASE and CONT via necropsy soon after diagnosis. External validity of the study is important; therefore, typical production practices and a natural disease challenge model were utilized. Multiple groups of *Bos taurus* breed steers meeting specification for a domestic short-fed program were sourced through normal procurement practices at high-risk times of year (Autumn: March to May). The first replicate completed during March-June 2020, then the study was subsequently delayed due to significant issues related to COVID-19. The second replicate was initiated in March 2021 and completed in May 2021.

Cattle within each pen were commingled from multiple sources and expected to have high morbidity risk. The same physical pen was used for each replicate and represented a typical open-air facility with in-line bunks, access to shade, and shared water troughs.

Upon arrival each feeder animal was individually weighed, given an identification tag, vaccinated for infectious bovine rhinotracheitis (Rhinogard™, Zoetis, Brisbane) and Mannheimia haemolytica (Bovilis MH+IBR™, Merck, Bendigo). Standard treatments were administered for internal and

external parasites and hormone growth promotant (200mg progesterone / 20mg oestradiol benzoate). Wearable technology utilised for the trial – neck collars (custom made for this study) for REDI (Precision Animal Solutions, Kansas MO, USA), and reticulo-rumen thermoboluses (Thermobolus, New Medria, Chateaubourg, France) – were placed in-situ at the time of induction. The reticulo-rumen boluses were activated as instructed having been calibrated pre-trial by the manufacturer. All biological sampling re deep nasopharyngeal swabs and blood samples were also taken at the point of induction. Study feeder animals were fed a standard feedlot ration twice daily. The study animals were not treated for BRD at any point prior to selection as a CASE or CONT. Any animal deemed ill with any clinical syndrome other than BRD at any point during the trial was treated per the normal feedlot health management protocol.

3.3 Clinical BRD observations

Trial feeder cattle were observed twice daily for signs of BRD and assigned a clinical illness score (CIS) by the same experienced veterinary researcher. Observations occurred in the morning at a time synchronising with standard feedlot operations (approximately 7am pen riding), and again soon after lunch (12pm). Observations made by the feedlot livestock staff conducting the pen riding surveillance were also recorded and cross-referenced with the veterinary researcher observations. The CIS system ranged from 0 (healthy) to 4 (extremely ill) with specific criteria used for each level. The following criteria were used to determine each CIS level: CIS 1 = normal behaviour and appetite, CIS 2 = slight illness, mild depression, and/or a cough, CIS 3 = moderate illness, severe depression, laboured breathing, and/or cough, and CIS 4 = severe illness, where animals may be moribund or have little response to human approach.

3.4 BRD CASE and CONT selection

Cattle were enrolled as potential CASEs or CONTs based on the twice daily visual observations. Trial feeder cattle with 3 consecutive CIS => 2 observations (clinically ill over a 24-hour period) were eligible for initial (presumptive) CASE status and were removed from the pen for further analysis. At this time, a full physical examination was undertaken, and rectal temperature taken. If the recorded rectal temperature was > 40.0°C, these study cattle were considered a preliminary CASE.

Standard feedlot operation would dictate that a feeder animal registering one isolated score of CIS =>2 qualifies as requirement to pull from the pen and treat for BRD. As noted above, these feedlot staff observations were recorded. For the purposes of the study, 3 x consecutive scores => 2 were necessary to qualify as a presumptive CASE.

At arrival, all animals were assigned a random number and after a CASE was identified, the animal with the lowest random number that had not received a CIS > 1 at any time point, was selected as a preliminary CONT. The preliminary CONT was brought to the hospital restraint chute for a thorough clinical examination including (standard) lung auscultation to confirm the trial feeder animal met the criteria as a healthy animal. A rectal temperature was taken on the preliminary CONT and if below 40.0°C, this study animal was considered a preliminary CONT. After meeting initial CASE or CONT criteria, the animals were humanely euthanized, and a full necropsy performed.

Given the reduced ability to transport euthanized cattle after the (12) PM observation period, if trial cattle were observed and met preliminary criteria, all diagnostics were performed in the afternoon (CASE and CONT) and the necropsy and final sample collections were deferred to the following morning. If the animal was identified as a CASE after the AM observation period, the necropsy was

performed on the same day. At necropsy, the lungs were evaluated grossly and the extent of pulmonary lesions in each lobe recorded using the same techniques described by Hanzlicek et al (2010 AJVR 71(3):359-369). Digital pictures were recorded on each animal documenting the level and location of pulmonary lesions. A pulmonary culture was taken from the area of affected lung and submitted to determine bacterial presence. The study animal was formally enrolled and classified as CASE or CONT based on combination of clinical signs (present or absent), rectal temperature (≥ 40°C or < 40°C) and level of lung lesions (≥ 5% or < 5%). Histopathology was performed on affected sections of the pulmonary tissue to further confirm the CASE definition of CASE animals.

3.5 Diagnostic modalities for evaluation

Multiple diagnostic systems were evaluated and compared to determine diagnostic accuracy relative to CASEs (CASE) and CONTs (CONT). These evaluations **(Figure 1)** included systems that could be used to identify clinically ill feeder animals through continuous monitoring (REDI, reticulo-ruminal temperature boluses) and systems that could confirm BRD in clinical CASEs (e.g. haptoglobin, respiratory microbiota, metabolomics, thoracic ultrasonography, computer aided lung auscultation). The sampling strategy timeline utilised at induction and diagnosis as CASE or CONT is outlined in **Figure 1**.

Figure 1. Sampling strategy timeline.

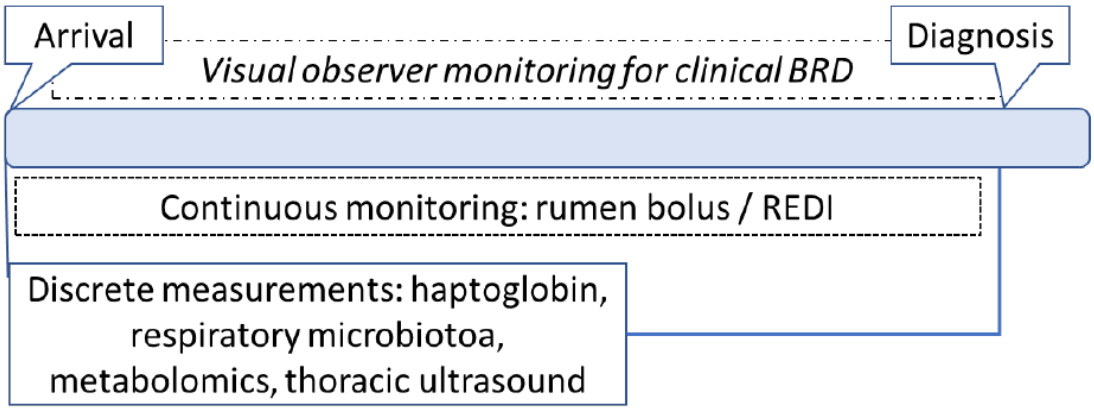

3.5.1 Point of care, "chute-side", diagnostics

3.5.1.1 Thoracic ultrasound

A mock trial was used to modify the procedures to fit the time and facilities constraints for the trial. The mock trial was not performed on analysed study cattle, it was completed prior to initiation of the first replicate group. Based on the results of the mock trial several modifications to existing process were made including:

- The ultrasound survey was truncated to include the following locations which typically limited the survey to less than 10 minutes (including preparation time and switching sides re left and right hemithorax): **Figure 2** (from Rademacher et al 2014):
    - 23, 22, 21 – examine location 20 if lesion detected at 21
    - 19, 18, 17 – examine location 16 if lesion detected at 17

- 15, 14, 13 – examine location 12 if lesion detected at 13
- examine locations 1 – 11 if lesions detected at 12 – 14
- "Apical" locations – as best accessed via the axilla (armpit).

- Describing ultrasound finding based on lesion detection by location, without estimates of cross-sectional area and/or depth of lesions.

Figure 2. Anatomical locations (left thorax, equivalent for right thorax) for ultrasound survey.

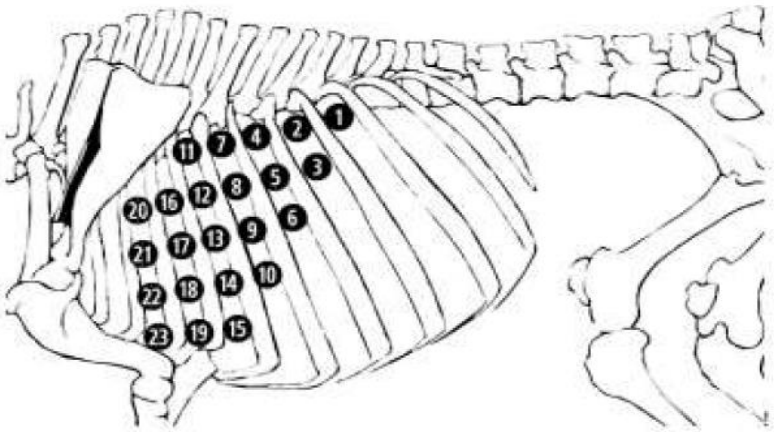

Thoracic ultrasounds were performed by the same experienced clinician using a Sonosite M-Turbo device (Fugifilm, Bothell, WA, USA) with a 5-10 MHz linear (rectal) probe, maximal depth = 15 cm. The thorax of cattle was not shaved or clipped and isopropyl alcohol (70%) was used as a transducing agent. Thoracic ultrasounds were performed on all cattle at induction, in selected CASEs and CONTs immediately prior to euthanasia, and prior to slaughter in remaining animals. Ultrasound results were scored based on presence/absence of lesions in the left and/or right hemithorax, using Ollivett Buczinski Scale (OBS) from 1 to 5 with 1 representing no lesions and 5 representing severe lesions in multiple lung lobes.

3.5.1.2 Haptoglobin

Blood samples were collected on all animals at arrival and at the time of CASE/CONT selection for analysis by Haptoglobin assay (Elizabeth Macarthur Agricultural Institute, Menangle, NSW). Haptoglobin assays were evaluated using excess plasma from lithium heparin tubes used to collect metabolomics samples.

3.5.1.3 Metabolomics

Blood samples were obtained from both BRD CASE and CONT steers euthanised as part of the main project. Samples were centrifuged for 20 min at 20,000 g, plasma harvested and frozen at – 20°C for up to 30 days until samples could be transported to The University of Sydney for long-term storage at – 80°C until chemical analysis. Chemical analysis for metabolomics was performed using H NMR spectroscopy in a Bruker 600 MHz with the process described by Blakebrough-Hall et al. (2020). The NMR dataset of the present study resulted in 264 chemical features instead of 323 in Blakebrough-Hall et al. (2020). Therefore, the 264 peaks were aligned with the 323 peaks using the mid ppm and those peaks that were not present were inputted a value of zero being noises in all CASEs. In addition, a new NMR protocol was explored using a preparation method with the zgesgppe data

acquisition program to determine if the metabolomics data is cleaner and more accurate compared to that used in B.FLT.0164. Final results for this new method will not be presented herein.

CASE steers of the present analysis were defined as those pulled with visual signs of BRD per the study protocol of 3 x consecutive clinical illness scores => 2, confirmed with rectal temperature > 40 ºC and with BRD lesions in the respiratory tract after euthanasia. False positives (n = 3) and false negatives (n = 1) were not included in the analysis. In addition, one blood sample (replicate 1, animal 110) was lost and thus not included in the analysis with the final dataset consisting of 9 CASEs and 10 CONTs.

Various machine learning models were developed to detect sick steers from metabolomics with data collected in project B.FLT.0164 (Blakebrough-Hall et al.; 2020) and these prediction models were then applied to the present study. However, none of the BRD CASE definitions of B.FLT.0164 were the same as used in the present study because animals were not euthanised after detecting the disease and the pulling protocols were different. Therefore, BRD CASE definitions of the tests developed in project B.FLT.0164 included animals with only Visual Signs (Pen Rider), Visual and Clinical Signs (visual signs plus rectal temperature ≥ 40 ºC and Whisper lung auscultation score ≥ 2), and animals that scored for lung lesions at slaughter with blood samples obtained at pulling as described by Blakebrough-Hall et al. (2020).

The machine learning prediction models from B.FLT.0164 were developed with a split of 70% training data and evaluated with the 30% remaining as testing data but these results are not presented herein. In addition, the models trained in B.FLT.0164 were also evaluated using cross-validation with 10 folds and 3 repeats. Blakebrough-Hall et al. (2020) presented the results of the diagnostic accuracy using classification trees on the testing data only. All prediction models were 'tuned' to maximise the area under the receiver operating curve (ROC). The prediction models were then applied to the data collected in B.FLT.3010. All datasets were centred and scaled and used all 323 chemical features detected by the standard recoupling of variables as described elsewhere (Blakebrough-Hall et al., 2020). Confusion matrices were drawn, and metrics of diagnostic accuracy were calculated including accuracy, Kappa coefficient of agreement, specificity, sensitivity, precision, F1 score, positive and negative predictive value. Results are only presented for the prediction models developed in B.FLT.0164 applied on B.FLT.3010.

3.5.1.4 Nasopharyngeal Microbiota

Deep nasopharyngeal swabs were collected on all cattle at induction and on CASE/CONT pairs at the time of enrolment. Each sample was stored in liquid nitrogen tanks prior to transfer to University of Technology, Sydney, for DNA extraction of the enrolled CASE/CONT pairs baseline and diagnostic samples.

Sequence processing

Microbiome bioinformatics were performed with QIIME 2 v2020.11 (Bolyen et al., 2019). Raw sequence data were demultiplexed and quality filtered using the q2-demux plugin. Sequencing data were then denoised with DADA2 (Callahan et al., 2016) (via q2-dada2). All sequencing reads were trimmed from the 3' end down to 270 bases per read. The 270 base length was selected based on the sequencing data quality profiles and to ensure adequate overlap of paired-end reads after

removal of sequencing primers. The forward and reverse 5' 16S primers were trimmed from the sequencing data by trimming the first 21 bases from each read. Reverse compliment primers were not trimmed since the trimmed read length was 270 base pairs; as the approximate length of the V3-V4 region is 443 base pairs, reverse compliments of the forward and reverse 5' primers were trimmed off and therefore were not present in the data. Sequencing data quality was assessed using the qiime2view visualizer on the qime2 website (view.qiime2.org). Once the data quality was deemed acceptable, DADA2 was utilized to filter and trim reads, infer exact sequence variants, and assign taxonomy to variants. Default parameters were used for all DADA2 functions unless expressly mentioned. A parametric error model was then estimated through a form of unsupervised machine-learning using 100 million sequences each for the forward and reverse reads separately. Sequencing reads were then dereplicated. Exact amplicon sequence variants (SVs) were inferred for each sample using the DADA2 sample inference algorithm and the estimated error model. Full, denoised sequences were obtained by merging the inferred forward and reverse reads. An SV table, which is functionally similar to an operational taxonomic unit table, was assembled from the denoised sequences. A Naïve Bayes feature classifier trained on the SILVA 132 (Quast et al., 2013) taxonomic database was used to assemble a taxonomy table by assigning taxonomy to each SV in the SV table. Any SV assigned to chloroplast or mitochondria were then filtered out of the SV and taxonomy tables.

Statistical analyses

Downstream analyses were performed in R v4.1.2 (R Development Core Team, 2010) using multiple functions from phyloseq v1.38.0 (McMurdie and Holmes, 2013), ggpubr v0.4.0 (Kassambara, 2017), and vegan v2.5-7 (Dixon, 2003). An object was constructed from the SV and taxonomy tables in R using phyloseq for subsequent analysis.

Species richness (Chao1) and diversity (Shannon) were calculated as implemented in phyloseq. Pairwise comparisons of alpha-diversity measures were made using Wilcoxon rank-sum and Wilcoxon signed-rank tests, as appropriate, to compare alpha-diversity group means between experimental groups (CASE and Ctrl) and sample types (A = arrival sample and B = enrolment sample) as implemented in ggpubr.

A permutational multivariate analysis of variance (PERMANOVA) using a Bray-Curtis dissimilarity index was used as implemented in vegan to evaluate the effects of experimental group, sample type, Whisper score, and ultrasound score, as well as any potential interactions between these terms, on microbiota composition. Group dispersion homogeneity (beta dispersion) was evaluated using a permutational analysis as implemented in vegan. Non-metric multidimensional scaling was used to visualize community composition by experimental group, sample type, Whisper score, ultrasound score, and haptoglobin concentration.

3.5.1.5 Computer aided auscultation

A computer aided auscultation device (Whisper™, Merck Animal Health) was utilized to evaluate each CASE/CONT pair at the time of enrolment, immediately prior to necropsy. The electronic stethoscope was utilized per manufacturer's instructions and three recordings were captured for each CASE or CONT candidate. For analysis, readings were aggregated with the final value

representing the most common reading (2 of 3 readings) or the median reading (if all three observations displayed unique results).

3.5.2 Remote, continuous monitoring diagnostics

3.5.2.1 Remote Early Disease Identification system

The REDI system consists of a real time location system with an Eliko™ asset tracking tag placed on each feeder animal via a neck band collar, and a series of readers located around the coverage area to record and accumulate feeder location data. The pen was survey mapped, identifying relevant structures of interest including the feeding area, watering area, shade structures, and pen perimeter. Feeder animal location within the pen was measured and recorded every 4 to 12 seconds. The study animal locations were used to calculate specific behavioural characteristics including multiple variables in broad categories of activity (e.g., distance travelled), proximity to areas of interest (e.g., percent time in feed bunk apron), and social behaviour (e.g., time spent in isolation). These variables were calculated on an hourly basis for each study animal throughout the trial for subsequent analyses. Data were used to inform the REDI algorithms that have been previously used and modified for the Australian cattle feeding operations. None of the REDI disease determinations were available to the pen rider at any point during the trial, i.e., the feedlot staff were blinded to the real-time REDI data.

3.5.2.2 Reticulo-ruminal temperature (thermo) boluses

Reticulo-ruminal temperature boluses (Thermobolus, New Medria) were placed in all cattle at induction into the study. This same type of bolus has been used in previous trials (Damiran et al., 2019; Timsit et al., 2011a an 2011b), and recorded reticulo-rumen temperature reading every 5 minutes. The pen rider was blinded to the real-time reticulo-rumen bolus data during the study.

3.5.3 Pulmonary lesions at harvest slaughter

Lung scores, in the form of lung consolidation, pleurisy, and abscesses, were scored by the veterinary researchers at the slaughter plant for every available animal in the group (not previously deemed CASE or CONT). Pulmonary consolidation was calculated based on scoring each segment of the lungs and applying a calculation as previously reported (Rezac et al., 2014). Consolidations scores were categorized into less or greater than 5% to distinguish normal/minor lesions from abnormal lesions. Pleurisy scores ranged from 0 (normal), 1(small fibrin tags on pleural surfaces), 2(significant pleural tags and parts of lung lobe(s) adhered to thoracic wall) to 3 (severe pleural lesions including whole lung lobe adhered to thoracic wall). Pleural adhesion scores were then categorized as normal/minor (0 and 1) or abnormal (2 and 3). A combined pulmonary consolidation/pleural score was created to dichotomize the lesions as described in **Table 1**.

Table 1. Lung categorization table. The rows indicate the categories used for percent lung consolidation and the columns represent the category for pleurisy.

		Pleurisy Score			
		0	**1**	**2**	**3**
Pulmonary Consolidation	**0-5%**	N	N	A	A
	>5%	A	A	A	A

*Normal/Minor N

*Abnormal A

3.6 Data collection

CASE and CONT were selected using aforementioned methods for each replicate until either 20 CASEs and 20 CONTs were identified, or no further animals were eligible. The remainder of the pen was managed in accordance with standard feedlot health protocols. All data from CASE, CONT, and remaining animals in the pen were downloaded and combined for subsequent analysis. Study feeder cattle not identified as CASE or CONT were followed to harvest slaughter and their lung scores recorded.

3.7 Statistical analysis

Data were imported into an open-source statistical program (R, Vienna, Austria) for full evaluation and comparison of parameters. Statistical evaluation was performed on each of the diagnostic modalities comparing the sensitivity and specificity to evaluate each modality. The final CASE definition (based on pulmonary lesions present at necropsy, at the time of clinical diagnosis) was used as the gold standard outcome to determine diagnostic characteristics of each test.

Evaluation of potential associations between final status (CASE and CONT) and performance outcomes were evaluated using mixed models incorporating replicate as a random effect to account for hierarchical structure of these data.

Working definitions of diagnostic sensitivity and specificity are as follows.

- Sensitivity – the ability of the diagnostic test to correctly identify populations of individuals that truly ***have*** disease
- Specificity – the ability of the diagnostic test to correctly identify populations of individuals that truly ***do not have*** disease

Confusion matrices, for each modality examined, report sensitivity and specificity determined in this study. Other diagnostic measures such as positive predictive value, negative predictive value and accuracy, along with apparent prevalence and true prevalence where relevant, are also reported.

Pulmonary lesions at harvest slaughter were used, as is the current standard, for evaluation of the subclinical population of study animals. A secondary project objective was the evaluation of subclinical illness as categorized by pulmonary lesions and subsequent evaluation by continual measures (REDI, reticulo-ruminal thermoboluses) and visual observation/clinical illness scoring. Thoracic ultrasound was designated to be utilised as a screening diagnostic, pre harvest slaughter, to examine lesions consistent with subclinical disease, however operational limitations such as availability of suitable restraint facilities and the rate of throughput required for market specifying activities significantly constrained this diagnostic activity such that a smaller dataset was generated. Statistical analysis for evaluation of the continual measures REDI, and the reticulo-rumen thermobolus, as well as the truncated dataset for thoracic ultrasound, against the industry method of visual observation only, for this subclinical population are also presented in this report.

For nasopharyngeal microbiota, downstream analyses were performed in R v4.1.2 (R Development Core Team, 2010) using multiple functions from phyloseq v1.38.0 (McMurdie and Holmes, 2013),

ggpubr v0.4.0 (Kassambara, 2017), and vegan v2.5-7 (Dixon, 2003). An object was constructed from the SV and taxonomy tables in R using phyloseq for subsequent analysis.

Species richness (Chao1) and diversity (Shannon) were calculated as implemented in phyloseq. Pairwise comparisons of alpha-diversity measures were made using Wilcoxon rank-sum and Wilcoxon signed-rank tests, as appropriate, to compare alpha-diversity group means between experimental groups (Case and Ctrl) and sample types (A = arrival sample and B = enrolment sample) as implemented in ggpubr.

A permutational multivariate analysis of variance (PERMANOVA) using a Bray-Curtis dissimilarity index was used as implemented in vegan to evaluate the effects of experimental group, sample type, Whisper score, and ultrasound score, as well as any potential interactions between these terms, on microbiota composition. Group dispersion homogeneity (beta dispersion) was evaluated using a permutational analysis as implemented in vegan. Non-metric multidimensional scaling was used to visualize community composition by experimental group, sample type, Whisper score, ultrasound score, and haptoglobin concentration.

A total of four negative control samples were sent for metagenomic sequencing. The sequencing results for each negative control were assessed individually, and it was determined that, based on the composition of the reads and the low number of sequences shared between the negative control samples and the study samples, there was insignificant contamination of the study samples due to the DNA extraction and metagenomic sequencing processes. Therefore, there was no need to adjust the study calf DNA sequencing results for possible contaminants.

4 Results and Discussion

Original study planning called for sequential replicates; however, due to COVID-19 delays replicate 1 was initiated in March 2020 and replicate 2 initiated in March 2021. The first replicate (R1) consisted of 200 head while the second replicate (R2) consisted of 190 head (**Table 2**). The average in-weight (Avg In Wt) and average rectal temperature (Avg In Temp) for inducted study cattle are also shown.

Table 2. Induction information of study cattle by date.

Replicate	Induction Date	Head number	Average in-weight (kg)	Average in-temperature
R1	5/3/2020	52	337.1	39.5°C
	6/3/2020	127	294.6	39.5°C
	9/3/2020	21	351.3	39.2°C
R1		***200***	***311.6***	***39.5°C***
R2	3/3/21	29	367.6	39.8°C
	4/3/21	81	364.3	39.5°C
	5/3/21	80	376.3	39.4°C
R2		***190***	***369.8***	***39.5°C***
Total		***390***	***339.9***	***39.5°C***

4.1 Ancillary health conditions

All cattle were observed twice daily throughout the study period and conditions other than BRD were treated in accordance with the standard feedlot health protocol. Within each replicate when cattle were treated for additional syndromes **(Table 3**), this made them ineligible for enrolment as either a CASE or CONT for the entire study.

Table 3. Number of cattle by diagnosis at first ailment.

	Feedlot BRD	Buller	CIS =>2	Lame	Other	Pinkeye	None	CASE	CONT
R1	2	4	15	13	2	6	152	3	3
R2	1	6	14	9	3	0	143	7	7

Cattle with a CIS2 => 2 at least once, would have been pulled and treated in normal feedlot operations per the on-site health management protocol. These animals are "CIS =>2" in Table 3; some individuals in this category scored CIS => 2 more than once. Any animals recording a clinical illness score became ineligible for enrolment as CONT for the entire study. The distinction between CIS =>2 and "Feedlot BRD" was that the Feedlot BRD CASEs did not meet CASE enrolment criteria but were determined to require treatment per the feedlot health management protocol.

The apparent prevalence of BRD, based on CIS =>2, the feedlot protocol CASE(s), and the enrolled study CASEs was 10.0% in replicate 1 (20/200) and 11.6% in replicate 2 (22/190) for an overall prevalence based on visual signs of 10.8% (42/390). Note that, as above, only the "Feedlot BRD" CASEs were removed from the pen and treated per the feedlot health management protocol as the visual signs in these animals were determined to be sufficiently significant to require treatment.

Lameness (= 5.6%) was the next most common issue followed by buller syndrome (= 2.6%) in this overall population. Some of these animals were treated multiple times and the stated diagnosis in Table 3 was based on diagnosis at first ailment.

Several animals did not present at the slaughter facility for pulmonary scoring and subsequently haven't supplied data for this analysis. The first replicate had 2 spontaneous deaths: 1) aspiration of rumen bolus into the larynx during placement at enrolment and the animal expired before a surgical approach could be attempted to dislodge the bolus, and 2) one animal was retained at the feedlot after rest of replicate had exited for slaughter due to inadequate finished live weight and WHP on recent foot infection treatment. This steer died spontaneously of BRD while resident in a hospital pen. Ultrasonographic survey of the chest before death and subsequent necropsy confirmed BRD pathology and BRD as the cause of death.

The second replicate had three animals that could not exit the feedlot for slaughter and were not enrolled as CASE or CONT:

1) Acute onset of blindness midway through the feeding period, rendering this animal unfit to load for transport and further residence at the feedlot, thereby having to be euthanised on animal welfare grounds.
2) Acute presentation of BRD day before intended exit for slaughter. Retained and treated under normal feedlot protocol. Failed to respond sufficiently for delayed slaughter and also euthanised on animal welfare grounds, and

3) Too heavy at drafting for slaughter and out of specification for exit. Diverted to alternate market and distant slaughter facility that didn't allow access for pulmonary scoring.

4.2 CASE and CONTROL (CONT) selection

Study criteria were based on visual observations and CASE required a visual CIS of => 2 for three consecutive readings. Several study animals received at least one visual observation CIS => 2 but did not reach the threshold of 3 consecutive readings. Each trial animal that received at least one diagnosis of CIS >= 2 was no longer eligible to enrol as a CONT animal. The final study criteria resulted in 3 CASE and CONT in R1, and 7 CASE and CONT in R2 **(Table 4)**. Enrolment as a CASE animal relied on gross pathology consistent with BRD being present at necropsy. The percentage (%) of total lung consolidation was calculated using a summation of per lobe consolidation, utilising estimates of individual lung lobe volumes. CONT animals accordingly presented with no pathology at necropsy so reported 0% lung consolidation.

Table 4. Days on feed (DOF), rectal temperature and body weight of BRD CASE and CONTROL animals by replicate at enrolment.

CASES					
Replicate_ID	**DOF 3rd call**	**Date 3rd call**	**Temperature**	**Diagnosis Weight**	**% Lung consolidation**
R1_130	19	25/3/2020	40.8°C	286	12.50%
R1_89	21	27/3/2020	40.9°C	313	12.30%
R1_110*	58	3/5/2020	40.8°C	291	3.40%
R2_25	16	19/3/2021	40.6°C	358	27.68%
R2_101	16	20/3/2021	40.3°C	457	39.97%
R2_59	18	22/3/2021	40.5°C	310	5.76%
R2_181	19	24/3/2021	40.6°C	452	5.79%
R2_58	21	25/3/2021	40.1°C	349	19.59%
R2_2	23	26/3/2021	40.5°C	318	64.11%
R2_8	39	11/4/2021	40.2°C	386	64.32%

**R1_110 enrolment details are discussed below in ultrasound section 4.6.1*

CONTROLS					
Replicate_ID	**DOF 3rd call**	**Date 3rd call**	**Temperature**	**Diagnosis Weight**	**% Lung consolidation**
R1_25	20	25/3/20	39.5	344	0%
R1_92	21	27/3/20	39.1	356	0%
R1_60	59	4/5/20	39.6	337	0%
R2_60	15	19/3/21	39.3	349	0%
R2_113	17	22/3/21	38.7	375	0%
R2_134	17	22/3/21	39.8	432	0%
R2_86	21	25/3/21	39.0	454	0%

R2_76	21	25/3/21	39.0	365	0%
R2_67	22	26/3/21	38.8	303	0%
R2_144	38	12/4/21	39.2	511	0%

In each replicate, preliminary CASE and CONT were rejected at the initial physical examination or necropsy for not meeting the full criteria as a CASE or a CONT **(Table 5)**. Most animals were rejected as CASE due to rectal temperature not above threshold at the time of evaluation, and these animals were excluded from further eligibility for CASE or CONT enrolment. One animal was also rejected as CONT because of presenting with rectal temperature above 40°C.

Table 5. Animals meeting preliminary criteria but not classified as CASE or CONT.

Preliminary CASE rejected

Replicate_ID	DOF at 3rd call	Date reached 3rd call	Temperature	Rejection reason
R1_152	5	9/3/2020	39.5°C	Temperature < 40°C
R1_137	6	10/3/2020	39.8°C	Temperature < 40°C
R2_27	18	23/3/2021	39.5°C	Temperature < 40°C
R2_117	15	20/3/2021	39.1°C	Temperature < 40°C
R2_107	19	24/3/2021	39.2°C	Temperature < 40°C
R2_158	38	13/4/2021	39.8°C	Temperature < 40°C

Preliminary CONTROL rejected

Replicate_ID	DOF at 3rd call	Date reached 3rd call	Temperature	Rejection reason
R1_90	6	10/3/2020	39.4°C	Partner CASE not enrolled
R1_87	6	10/3/2020	39.9°C	Partner CASE not enrolled
R1_82	58	4/5/2020	40.4°C	Temperature > 40°C

False Positives (CASE)

Replicate_ID	DOF at 3rd call	Date reached 3rd call	Temperature	Rejection reason
R1_159	5	9/3/2020	40.2°C	Necropsy = no lesions
R1_113	24	1/4/2020	40.0°C	Necropsy = no lesions
R1_109	23	31/3/2021	40.2°C	Necropsy = no lesions

False Negative (CONTROL)

Replicate_ID	DOF at 3rd call	Date reached 3rd call	Temperature	Rejection reason
R1_168	57	3/5/20	39.4°C	necropsy> 5% lung lesions

Three false positives CASES were identified which met the preliminary enrolment criteria of 3 consecutive CIS =>2, and rectal temperature > 40°C, but on necropsy no lung lesions were identified. Additionally, a study animal from R1 was never identified as sick (no clinical illness scores recorded) and on random selection as CONT candidate, did not have a rectal temperature > 40°C, therefore met preliminary criteria for CONT. However, at necropsy, demonstrated > 5% lung lesion pathology therefore disqualified as a CONT and was not enrolled. These four CASEs highlight the challenges with clinical diagnosis of BRD through visual observation, even with strict enrolment criteria, as when the lungs were examined, BRD was found to be misdiagnosed. An additional example of misdiagnosis applies to animal R2_158 which presented as a preliminary CASE candidate but recorded insufficient rectal temperature. Subsequently, this animal demonstrated ultrasonographically detected respiratory lesions at hospital presentation (same time as CASE rejection) and pathology at slaughter.

Using gross pathology assessment at necropsy as the current gold standard, visual observation per the study protocol, combined with utilising threshold rectal temperature of 40.0°C, detected 10/13 (= 77%) as true BRD CASEs and 10/11 (= 91%) as true healthy animals (CONT).

Most CASE were diagnosed in each replicate during a days on feed (since arrival) period typical of Australian industry BRD incidence, i.e. 15 – 23 days on feed **(Figure 3)**. Outlier CASEs occurred at 39 and 58 days on feed.

Figure 3. Number of cattle diagnosed and confirmed as a CASE by days on feed (DOF) after induction.

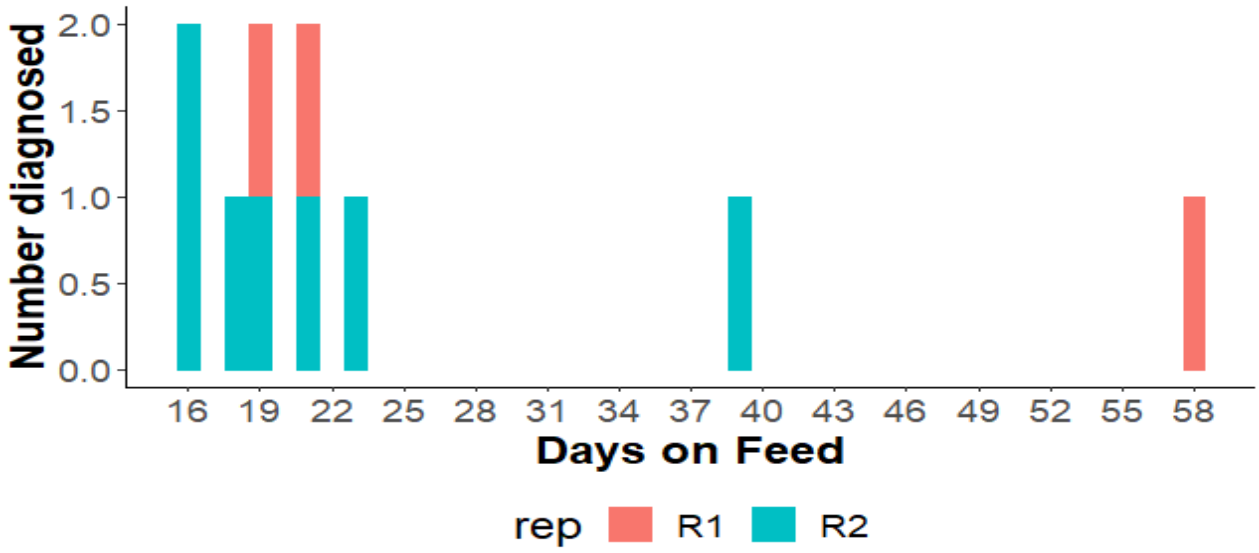

The only statistical difference in CASE/CONT cattle was the temperature at diagnosis was higher in CASES compared to CONTS ($P < 0.01$), but this is expected as it is a critical part of the CASE definition utilised for the study **(Table 6)**. No differences were identified in induction weight, induction temperature or diagnosis weight. As CASE and CONT cattle were enrolled as a pair on the same day no differences in days on feed were present.

Table 6. Body weight and rectal temperature at induction and diagnosis of study animals with or without BRD defined by lung pathology at necropsy (CASE vs CONT).

	CASE	SE	CONT	SE	P-value
Induction Weight	335.5	36.73	339.5	37.20	0.87
Induction Temperature	39.7	0.25	39.4	0.26	0.32
Diagnosis Temperature*	40.6	0.17	39.3	0.17	<0.01
Diagnosis Weight	341.1	35.45	371.7	35.45	0.21

**Temperature was part of the CASE/CONT protocol*

4.3 CASE confirmation: laboratory microbiology and histopathology

Tissue samples submitted were evaluated descriptively for each CASE to confirm presence or absence of pathogens and lesions as identified by histopathology **(Table 7)**. All CASES were confirmed to have either broncho and/or pleuropneumonia based on histopathological examination. CONT animals were confirmed on the basis of gross pathological examination alone. Each CASE was also confirmed by microbiological culture for the presence of at least a single pathogen.

Table 7. Microbiology and histopathology for each CASE.

Replicate and Animal ID	CASE status	Isolate(s)	Histopathology
R1_89	CASE	*Histophilus somni* *Mycoplasma sp*	Pleuropneumonia – bacterial fibroplasia, degenerate white blood cells
R1_110	CASE	*Pasteurella multocida* *Histophilus somni* *Mycoplasma sp*	Bronchopneumonia – fibrinosuppurative and necrotising. Multifocal, severe
R1_130	CASE	*Histophilus somni*	Bronchopneumonia and pleuritis, fibrinosuppurative, severe, diffuse, chronic-active, fibrin thrombi
R1_168	FALSE NEGATIVE	*Histophilus somni* *Mannheimia haemolytica* *Mycoplasma sp*	Bronchopneumonia – caseonecrotising, chronic-active. Multifocal, severe, and significant hyperplasia
R2_002	CASE	*Mycoplasma sp*	Bronchopneumonia and pleuritis, fibrinosuppurative, chronic, multiple foci of caseous necrosis
R2_008	CASE	*Histophilus somni* *Mycoplasma sp*	Pleuropneumonia, fibrinosuppurative, multifocal, chronic-active
R2_025	CASE	*Pasteurella multocida*	Bronchopneumonia and pleuritis, fibrinosuppurative, severe, diffuse, chronic-active

R2_058	CASE	*Pasteurella multocida* *Histophilus somni* *Mycoplasma sp*	Bronchopneumonia, fibrinosuppurative, chronic, severe with multifocal abscessation
R2_059	CASE	*Pasteurella multocida* *Histophilus somni* *Mycoplasma sp*	Bronchopneumonia and pleuritis, fibrinosuppurative, severe, diffuse, subacute
R2_101	CASE	*Histophilus somni* *Mycoplasma sp*	Bronchopneumonia and pleuritis, fibrinosuppurative and histiocytic, severe, diffuse, chronic-active with lytic caseous necrosis
R2_181	CASE	*Histophilus somni* *Mycoplasma sp*	Bronchopneumonia, fibrinosuppurative, chronic, severe, with bronchiolitis obliterans

4.4 Pulmonary Lesions at harvest slaughter

Pulmonary lesions were evaluated at harvest slaughter on all available cattle from each replicate (total n= 361) at the end of the feeding phase as an indicator of subclinical BRD. Lesions in the respiratory tract, i.e. lungs and pleural surfaces, of study animals were measured at slaughter by way of a continuous numerical scale for lung consolidation (lung volume %) and a categorical scale for pleural surface. There were 14 head (11 from R1, and 3 from R2) that scored greater than 5% pulmonary consolidation at harvest slaughter, representing 3% prevalence overall of this higher severity grade. The distribution of scores for these cattle are presented in **Figure 4**.

Figure 4. Distribution of pulmonary consolidation scores of feedlot steers at harvest (n=29 in R1 and n=13 in R2).

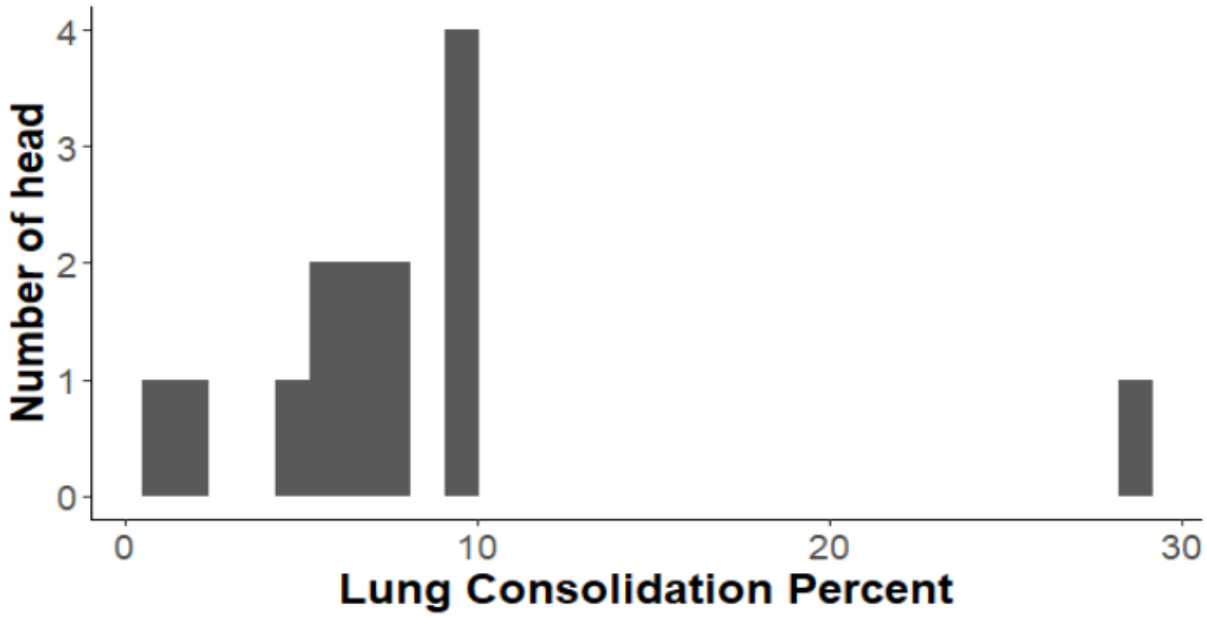

Most cattle received normal pleurisy scores with 8.3% (157 out of 188 in R1 and 70.5% (122 out of 173) in R2 receiving a pleurisy score of 0. Relatively few cattle received the most severe pleurisy score of 3 (**Figure 5**).

Figure 5. Pleurisy scores by replicate.

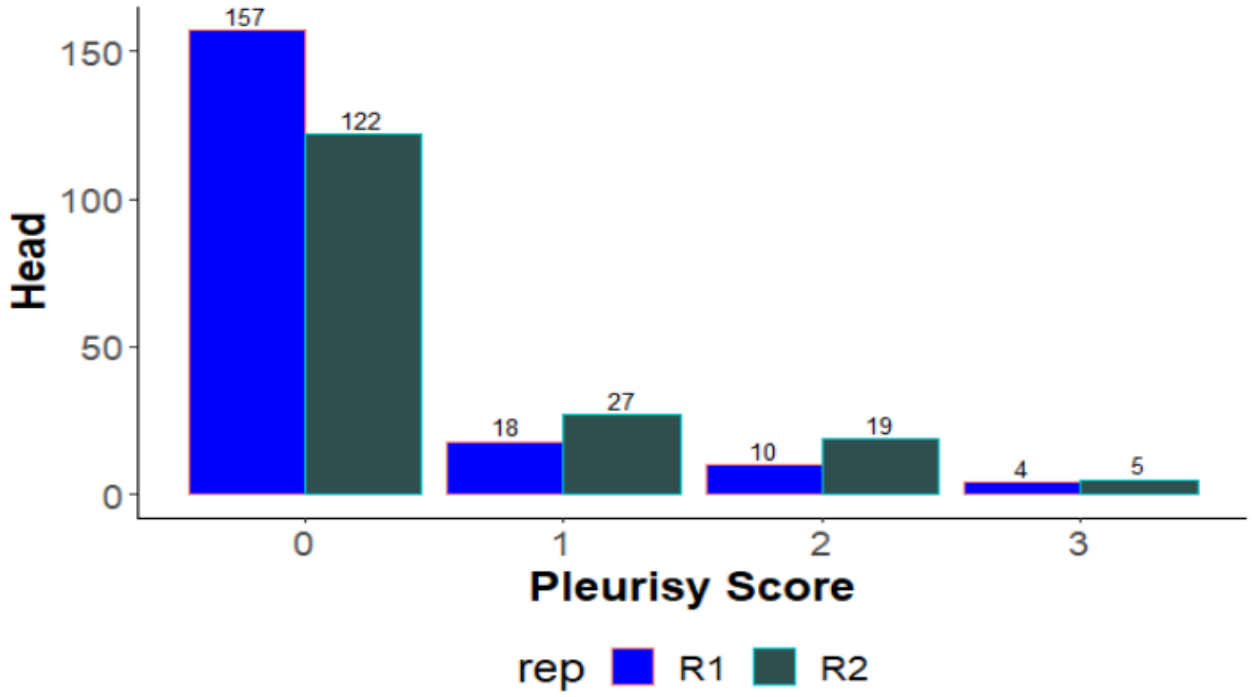

Overall classification of pulmonary status was based on the previously described formula with cattle > 5% lung lesions or pleural score > 1, or both considered abnormal. The summary of cattle scored in each pleural and lung category is summarized in **Table 8**. The replicates resulted in 10.6% (20/188 and 14.4% (25/173) abnormal pulmonary scores respectively.

Table 8. Pleurisy and pulmonary consolidation scores for feedlot cattle in each replicate and aggregate.

Replicate1 n=188

		Pleurisy Score			
		0	**1**	**2**	**3**
Pulmonary Consolidation	**0-5%**	153	15	7	2
	>5%	3	3	3	2

Replicate 2 n=173

		Pleurisy Score			
		0	**1**	**2**	**3**
Pulmonary Consolidation	**0-5%**	122	26	18	4
	>5%	0	1	1	1

Total n=361

		Pleurisy Score			
		0	**1**	**2**	**3**
Pulmonary Consolidation	**0-5%**	275	41	25	6
	>5%	3	4	4	3

**Shaded cells display cattle classified as abnormal.*

Statistical models were created to compare outcomes of interest based on differences in final pulmonary status while accounting for lack of independence due to replicate. Both HSCW and ADG were lower in cattle with abnormal final pulmonary status compared to cattle with normal pulmonary status ($P < 0.05$; **Table 9**). These differences provide support for the classification system of pulmonary lesions as meaningful from a production viewpoint.

Table 9. Performance and carcass traits of steers with normal and abnormal final pulmonary classification.

	Final pulmonary status				
	Normal	**SE**	**Abnormal**	**SE**	**P-value**
Head (n)	316	-	45	-	-
Initial Weight (kg)	339.6	28.04	349.1	28.72	0.14
Initial Temperature (°C)	39.5	0.02	39.5	0.07	0.79
HSCW (kg)	**262.8**	**5.21**	**255.0**	**6.03**	**0.02**
P8 (mm)	10.32	0.787	9.23	0.934	0.06
EMA (cm^2)	64.5	1.36	64.9	1.94	0.99
MSA Index	56.4	0.07	56.09	0.2	0.14
ADG (kg/d)	**2.00**	**0.055**	**1.69**	**0.078**	**<0.01**

4.5 Visual observation and rectal temperature as diagnostic

For the confirmed clinical CASE and CONT study cattle, and additional false negative and false positive animals also confirmed by necropsy during the study, a simple 2x2 table with manual calculations is presented in Table 10. The table reports diagnostic sensitivity and specificity using the method of visual observation, combined with threshold rectal temperature of 40.0°C, compared against the necropsy gold standard.

Table 10: Confusion matrix (2x2 table) of diagnostic sensitivity and specificity for visual observation and rectal temperature combined.

Pulmonary (disease) Status (TRUTH)	***Diagnostic Test: Visual Clinical Illness Score + rectal temperature***		
	ABNORMAL (test positive)	**NORMAL (test negative)**	
ABNORMAL (lesions)	True positives (TP) 10	False negatives (FN) 1	***Sensitivity*** = TP / TP+FN 10 / (10 + 1) = ***91%***
NORMAL (no lesions)	3 False positive (FP)	10 True negatives (TN)	***Specificity*** = TN / TN+FP 10 / (10 + 3) = ***77%***

For the clinical CASEs, under the criteria specified in the study design, visual observation combined with rectal temperature threshold (40.0°C) as a diagnostic performed at 91% sensitivity and 77% specificity. This specificity is based only on cattle receiving 3 consecutive CIS => 2. It is likely that specificity based on only a single score of CIS=>2, per standard feedlot practice for identifying animals for BRD treatment, would be lower.

There were multiple study feeder animals scored with CIS => 2 at least once, but not 3 consecutive times per the study protocol; therefore, these cattle did not qualify as a CASE. Of the 29 called abnormal (respiratory, CIS => 2) at least once by visual observation, not enrolled as CASE animals, not treated for BRD per the feedlot treatment protocol, and ultimately managed to harvest slaughter, only 3 presented with abnormal pulmonary status **(Table 11)**. These study animals were not treated at the feedlot, they might have potentially resolved any pulmonary lesions existing at the time of clinical (visual) scoring, or, were false positive designations at the time of clinical illness scoring.

This illustrates that of the cattle clinically scored by visual means only, and not presented for rectal temperature recording, and then presented for harvest slaughter, the overall sensitivity to detect abnormal pulmonary lesions was 7%. Conversely, for 332 study animals determined to be healthy, and never receiving a CIS > 1, there were 42 that presented with pathology at harvest slaughter. Therefore, overall specificity to detect abnormal pulmonary lesions was 92%.

The 10 x CASE and 10 x CONT identified and confirmed were not included in the analysis of animals assessed at slaughter and as such, their clinical illness scores are not included. Animals with clinical illness scoring that are included however are the study subjects in table 5 that are preliminary CASE

and CONT rejections for the reasons stated. It is interesting to note that of these 9 animals, all but two have been correctly classified into CASE and CONT groups by rectal thermometer at the time of hospital chute presentation – IF – lesions at slaughter are utilised as the diagnostic CASE definition. For all these animals, presentation at the hospital chute was directed by the study protocol clinical observations criteria, so preliminary CASEs received 3 x consecutive scores => 2, rather than just 1 x score per the feedlot practice. The two study animals that were incorrectly classified by rectal thermometer, utilising this CASE definition, are summarised below;

- Preliminary CASE rejection: R2_158
    - 38 days on feed, T = 39.8°C at presentation however lesions detected by ultrasound. Slaughter lung consolidation = 28.3% and pleural score = 3
- Preliminary CONT rejection: R1_82
    - 58 days on feed, T = 40.4°C at presentation, ultrasound survey not conducted. Slaughter lung consolidation = 0% and pleural score = 0

Table 11. Visual observation, by clinical illness scoring, with no rectal temperature recording, diagnostic 2x2 table for the non-clinical (non-study enrolled) dataset.

Pulmonary Status (TRUTH)	***Diagnostic Test: Visual Clinical Illness Score only***		
	ABNORMAL (test positive)	**NORMAL (test negative)**	
ABNORMAL (lesions)	True positives (TP) 3	False negatives (FN) 42	***Sensitivity*** = TP / TP+FN 3 / (42 + 3) = ***7%***
NORMAL (no lesions*)	26 False positive (FP)	290 True negatives (TN)	***Specificity*** = TN / TN+FP 290 / (290 + 26) = ***92%***
**nil or mild lesions per definition in Table 8*	***PPV*** = TP / TP+FP 3 / 29 = ***10%***	***NPV*** = TN / TN+FN 290 / 332 = ***87%***	

Positive predictive value (PPV) is the probability that subjects with a positive result on screening test truly *do* have disease. Negative predictive value (NPV) is the probability that subjects with a negative screening test truly *don't* have disease. These two metrics have also been calculated in **Table 11** for visual observation assessment only against the standard of pulmonary lesions present at slaughter. The "gold standard" remains pulmonary pathology at the time of clinical diagnosis, demonstrated by necropsy. Positive predictive value in this study was reported at 10% and negative predictive value at 87% for the non-clinical study animals' dataset.

Carcass characteristics were also compared between animals without and with visual signs (CIS =>2) in the non-clinical animals' dataset. Interestingly, the initial placement temperature was lower, and initial weight tended to be lower, but not statistically significant (P = 0.07), in cattle that eventually received an abnormal visual illness score (**Table 12**). Carcass traits were not different between

groups except for P8 fat with cattle receiving an abnormal score having thicker P8 fat thickness compared to animals with no visual signs.

Table 12. Performance, rectal temperature, and carcass traits of steers receiving an abnormal (CIS=>2) or normal (CIS < 2) visual assessment score at any point during the feeding phase.

	Visual Assessment				
	Normal	**SE**	**Abnormal**	**SE**	**P-value**
Head (n)	332		29		
Initial Weight (kg)	342.0	28.23	327.6	29.10	0.07
Initial Temperature (C)	**39.5**	**0.02**	**39.3**	**0.09**	**0.02**
HSCW (kg)	262.2	5.11	256.9	6.44	0.21
P8 (mm)	**10.1**	**0.81**	**11.6**	**1.04**	**0.02**
EMA (cm2)	64.7	1.35	63.2	2.24	0.45
MSA Index	56.4	0.07	56.3	0.25	0.90
ADG (kg/d)	1.97	0.059	1.91	0.098	0.51

4.6 Thoracic Ultrasound

Thoracic ultrasound was performed for CASE and CONT study animals at the time of diagnosis. A subset of cattle not selected as CASE or CONT were also scanned near harvest slaughter.

Aligned with the modified survey protocol established after the mock trial, whereby detectable lesions were classified on the basis of size and number in anatomical lung lobes per the scoring system described by Ollivett and Buscinski (Vet Clin Nth Amer 2016). This (OBS) scoring system can be summarised as follows;

0. no lesions detectable
1. pinpoint densities and/or comet tails in single lobes
2. lobular, patchy consolidations – can be present in more than 1 lobe
3. lobar consolidation that has invaded most of 1 (anterior) lobe
4. lobar consolidation that has invaded at least 2 lobes
5. lobar consolidation that has invaded more than 3 lobes.

An OBS >= 3 is considered positive for BRD diagnosis.

4.6.1 CASE and CONT Evaluation

Ten CASE and CON cattle were evaluated at arrival and the time of diagnosis. At the time of clinical diagnosis 8 out of 10 CASES had lesions on the left side (hemithorax) and 8 out of 10 CASES had lesions on the right side (hemithorax) compared with none of the CONT cattle. No CONT cattle scored above a 0 on the (OBS) scoring system, but CASE cattle scored as follows: 0 (n=1), 3 (n=2), 4 (n=1), or 5 (n=6) **(Table 13)**.

Table 13. Thoracic ultrasound status by each CASE and CONT steer at the time of BRD diagnosis (1 indicates presence of lesions, 0 indicates absence of lesions).

Animal ID	Status	Ultrasound Left	Ultrasound Right	Ultrasound OBS Scale	Ultrasound Lesions
R1_110*	CASE	0	0	0	0
R1_130	CASE	1	1	5	1
R1_89	CASE	0	1	3	1
R2_101	CASE	1	1	5	1
R2_181	CASE	1	0	3	1
R2_2	CASE	1	1	5	1
R2_25	CASE	1	1	5	1
R2_58	CASE	1	1	5	1
R2_59	CASE	1	1	4	1
R2_8	CASE	1	1	5	1
R1_25	CONT	0	0	0	0
R1_60	CONT	0	0	0	0
R1_92	CONT	0	0	0	0
R2_113	CONT	0	0	0	0
R2_134	CONT	0	0	0	0
R2_144	CONT	0	0	0	0
R2_60	CONT	0	0	0	0
R2_67	CONT	0	0	0	0
R2_76	CONT	0	0	0	0
R2_86	CONT	0	0	0	0

**CASE animal R1_110*: this animal was ultimately included as a CASE enrolment on the balance of factors that all preliminary criteria were met and pulmonary pathology was present grossly at

necropsy and confirmed by laboratory microbiology. However, initial lung consolidation (%) calculation was in error reporting > 5%; the corrected result was 3.4%. With respect to thoracic ultrasound survey, the veterinary researcher supervising the study on this animal's enrolment date wasn't able to demonstrate lesions at chute presentation and wasn't able to capture still or video images of the survey(s). This researcher scored acceptable (Kappa = 0.6) agreement with the primary veterinary researcher during the mock trial. The primary veterinary researcher conducted the remainder of all CASE/CONT surveys at time of enrolment.
Ultrasound lesions were dichotomized based on overall presence or absence (left or right) and positive score on OBS scale to create a single variable for calculation of sensitivity and specificity **(Table 14)**. Thoracic ultrasound yielded 90% sensitivity and 100% specificity against the gold standard of lung pathology present at necropsy at the time of clinical diagnosis.

Table 14. Confusion matrix (2x2 table) relationship between thoracic ultrasound survey and the 'gold standard' of lung pathology present in euthanised study animals diagnosed with BRD.

		Ultrasound Survey	
		ABNORM	**NORM**
TRUE	**CASE**	9	1
Status	**CONT**	0	10

Sensitivity:	*90%*
Specificity:	*100%*

Ultrasound surveys were conducted on study animals pre-harvest, near the time of exit from the feedlot. These animals had not been enrolled as CASE or CONT and had not died spontaneously at the feedlot, they were slaughtered as per the feedlot program. As the ultrasound survey procedure took time, animals were done as multiple drafts. Due to a technical issue with the handling facility many of the cattle did not receive a survey in Replicate 1. In total, 181 study cattle received both a thoracic ultrasound near exit and lung scores at harvest. The lungs were deemed as having lesions or no lesions utilising the scoring method as described in other parts of this report (no lesions/normal presented with < 5% pulmonary consolidation and < 2 pleurisy score). The US scores were applied using the same scaled scoring system as previously and this system was dichotomized to normal (US score = 0) or abnormal (US score > 3) for the final statistical analysis (noting that a score ***=> 3*** on the Ollivett and Buscinski (2016) scale is considered diagnostic for BRD).

There were 12 head that received an ultrasound score above zero, which included scores of 1 (n=9), 2 (n=1), 3 (n=1) and 4 (n=1). As above, 45 study animals in total received abnormal lung lesion scores at slaughter, with 23 of those occurring in the pre-harvest ultrasound dataset.

The data were dichotomized to determine sensitivity and specificity of ultrasound lesions compared to true lung status at harvest. The sensitivity of US as a diagnosis method was very low at only 8.7% although the specificity was 100%.

Table 15. Sensitivity and specificity of exit thoracic ultrasound score against the presence or absence of lung and pleural lesions at harvest.

		Ultrasound Survey	
		ABNORMAL	**NORMAL**
TRUE	**Lung and pleural lesions**	2	21
Status	**No lung and pleural lesions**	0	158

Sensitivity:	*8.7%*
Specificity:	*100%*

Anatomical features of the bovine respiratory tract and implications for ultrasound surveys exist. Per the description by Fait and Apley (2003), total lung field volume supplied by the right hemithorax lung lobes is 53.6%, compared to the left hemithorax lung lobes of 42.1%, with the accessory lobe constituting 4.3% of the total lung field. Apical lung lobes in the right hemithorax are anatomically more cranial (forward) and ventral (lower) in the thoracic (chest) cavity compared to left hemithorax apical lung lobes. As such, given that the BRD syndrome essentially involves translocation of opportunistic commensal bacteria from the upper respiratory tract, the right hemithorax lung field, particularly the right cranial lung lobes, harbours higher probability of subsequent pathology. This hypothesis is supported by the results of harvest slaughter lung scoring from this study as presented in **(Table 16)** below. For any study animals presenting with any pathology in the form of lung consolidation, particularly significant consolidation qualifying as > 5% total lung field, the predilection of lesions is almost principally in the right hemithorax, and further, the right apical lung lobes. Lesions in the left hemithorax contributed to only 5/41 = 12.2% of all these lesions recorded.

For **(Table 16)** below, the following abbreviations are used. All values are reported in terms of (%) of the associated lung lobe/field.

Lapcr = left cranial apical lobe
Lapcau = left caudal apical lobe
Ldiaph = left diaphragmatic lobe
Rdiaph = right diaphragmatic lobe
Rmid = (right) middle lobe
Rapcr = right cranial apical lobe
Rapcau = right caudal apical lobe
Acc = accessory lobe
Lung cons % = total lung consolidation per Fait and Apley (2003)

US Busc = ultrasound score per Ollivett and Buscinski (2016). The hemithorax examined is indicated in closed brackets as L = left or R = right. If no survey was conducted, a (-) is input

Table 16. Lung and pleural lesion scoring at harvest slaughter and associated ultrasound exit score (Buczinski scale).

ID	Lapcr	Lapcau	Ldiaph	Rdiaph	Rmid	Rapcr	Rapcau	Acc	Pleural	Lung cons %	US Busc
R1_121					75			10	1	5.005	-
R1_188						75	10		2	5.325	-
R1_173					70	5	10	20	0	6.045	-
R1_59						100			1	6.300	-
R1_148					100			10	0	6.530	-
R1_106						50	100		3	9.150	-
R1_191						75	75		3	9.225	-
R1_154						100	50		2	9.300	-
R1_177						100	50		2	9.300	-
R2_174					5	100	10		1	7.205	0 (L)
R2_66					5	75	50		1	8.030	0 (L)
R2_158	75	75	20	10	10	75	50		3	28.325	4 (L&R)
R1_72						5			3	0.315	-
R1_56					10				2	0.610	-
R1_107						25			2	1.575	0 (L)
R1_76		25					10		2	1.825	-
R1_175		50			20				3	3.670	-
R1_55						75			2	4.725	-
R2_154						5			2	0.315	0 (L)
R2_28		20							2	0.980	3 (L)
R2_46					20	20	40		3	4.880	0 (L)
R1_69	2									0.106	-
R1_1		5								0.245	-
R1_20		5								0.245	-
R1_5						5				0.315	-
R1_149						5				0.315	0 (R)
R1_157						5				0.315	-
R1_189							10		1	0.600	-
R1_49				2					1	0.704	0 (R)
R1_195						20				1.260	-
R1_115						25				1.575	-
R1_142			5				5			1.895	-
R1_30						40				2.52	-
R1_93						50			1	3.15	-
R1_4			10							3.19	-
R2_164						5				0.315	0 (L)
R2_168						5				0.315	1 (L)
R2_31						5			1	0.315	0 (L)
R2_129						10				0.630	0 (L)
R2_109						25				1.575	0 (L)
R2_171					75				1	4.575	0 (L)

A direct explanation for the low sensitivity of the ultrasound scores is that animals were scanned only unilaterally during these sessions and depending on the working day at the feedlot, different handling facilities and different sides of the chest employed, albeit most exit surveys were conducted on the left hand side. Therefore, potential lesions may have been contralateral to the hemithorax being surveyed and could have been missed.

Cattle scanned on the left side with significant lesions ipsilateral were identified – note animals R2_158 and R2_28 above in **Table 16** with green shaded cells in the US Busc column. Also note that the final lung score was based on both pleurisy data and pulmonary consolidation which may not have been unilateral at the time of survey scanning. The pre-harvest scans were also time limited, which reduced the overall detection time to find the lesions. For the 21 x false negatives (non detections) reported in this study; 18 were pleural (pleuritis) lesions only, 2 were consolidation lesions present on the right hand side in the second replicate and 1 was a consolidation lesions present on the right hand side in the first replicate. Data is not available on the chest side demonstrating the pleural lesions – this would give better detail as to the diagnostic accuracy.

Statistics were not performed comparing arrival and carcass data based on ultrasound survey due to small numbers of animals with ultrasound-detectable lesions and classification inaccuracy due to unilateral scans.

If lesions are present on the ipsilateral hemithorax to the ultrasonographic survey conducted, there is similar probability of detecting and demonstrating pathology present, as is the case for the clinical CASEs. For the example below in **Figure 6**, this animal (R2_28) was imaged pre exit per the study process before the first harvest slaughter session for the second replicate. This study animal had received a clinical illness score of (2) on 24th March 2021 (= 21 days on feed), but no other clinical illness scores during the rest of the study period. The exit survey was conducted on 27th April 2021 (= 55 days on feed) and demonstrated pathology in the left apical region under the shoulder blade which scored (=3) on the OBS Scale (single lobar lesion). This study animal was not sufficiently grown for the first harvest slaughter session, so was presented for the second harvest slaughter on 24th May 2021 (= 82 days on feed). During pulmonary scoring at slaughter, a 20% consolidation of the left caudal apical lung lobe was recorded, equating to total lung field consolidation of 0.98%, and a pleural score = 2.

Figure 6. Ultrasound survey at pre-exit scanning for R2_28 demonstrating consolidation in the left apical chest field (yellow arrow).

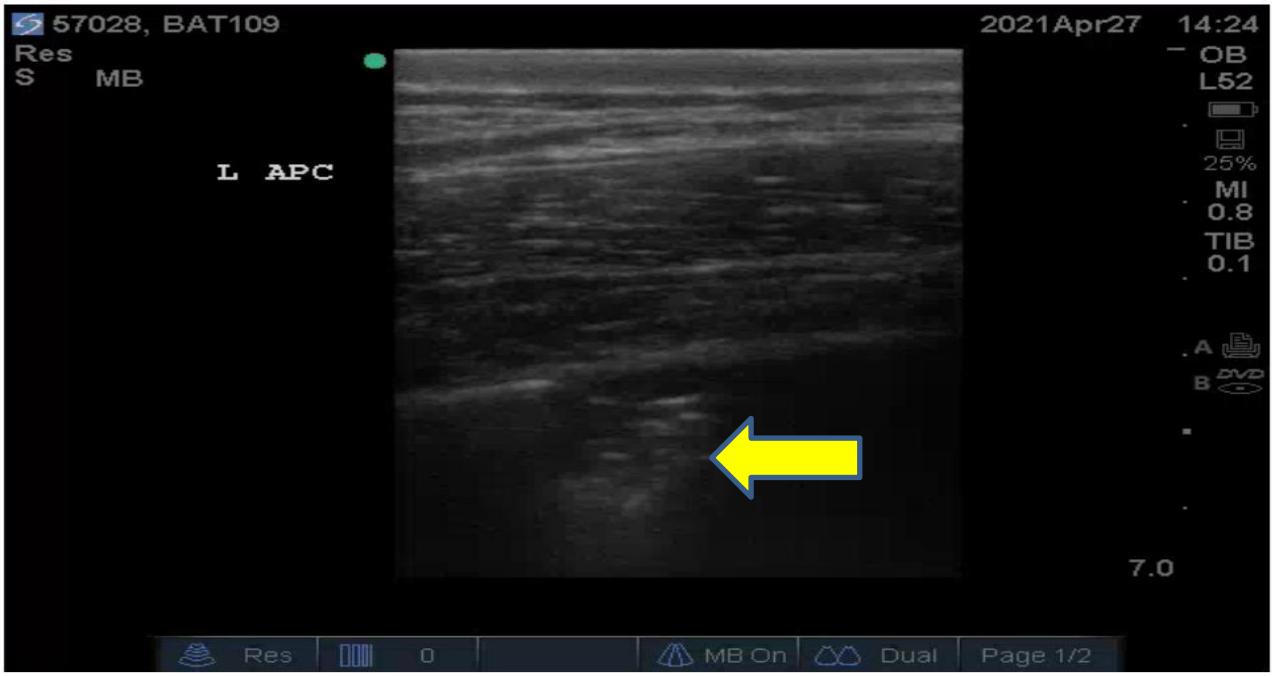

Additional monitoring for study animal R2_28, in the form of continuous reticulo-rumen temperature, is presented in **Figure 7**. Thermobolus data capture is reported in greater detail in section 4.12 below. Note in **Table 34** re thermobolus classification models – all four classified this animal as a CASE. Regarding the presence of pulmonary pathology at slaughter, it is speculative to consider the pathology developed during the feeding period or was present at induction into the feedlot (and the study).

Figure 7. Temporal profile of reticulo-rumen temperature: R2_28.

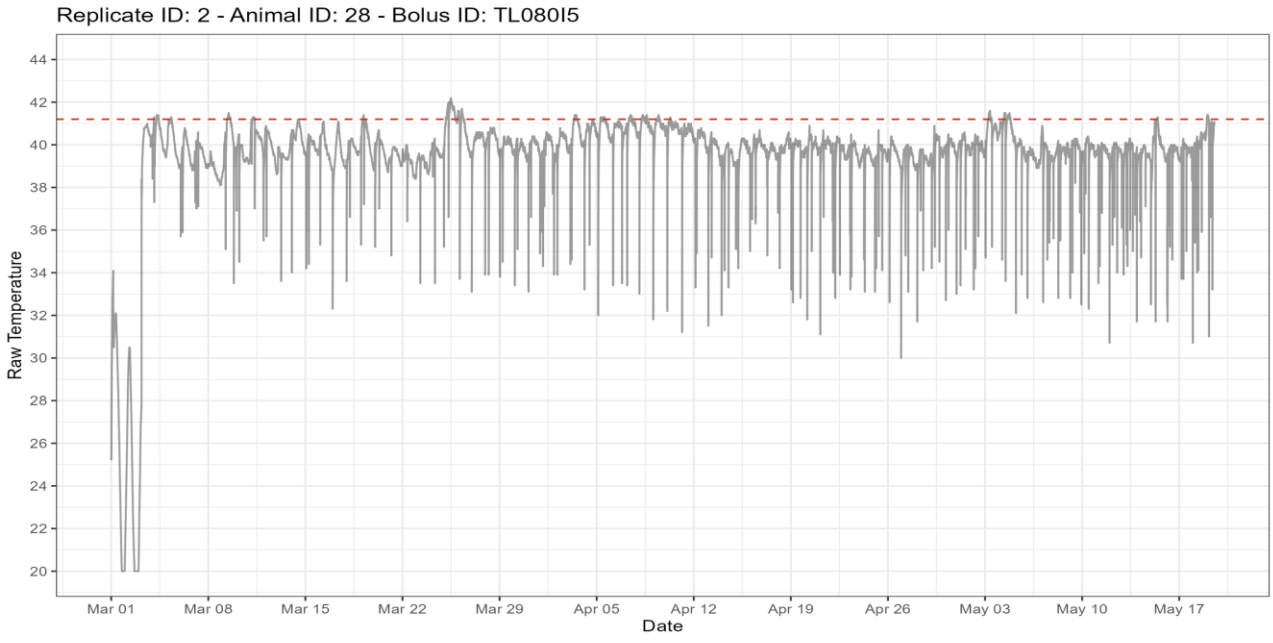

4.7 Haptoglobin

Blood for plasma haptoglobin was collected and submitted for analysis on CASEs and CONTs. Each animal had two samples submitted at arrival and at induction. Haptoglobin is an acute phase protein present in blood that is elevated in many inflammatory diseases, not specifically to BRD alone.

Using the laboratory (Elizabeth MacCarthur Agriculture Institute, Menangle, NSW) cutoff, specific for ruminants, (0.3 g/L) the samples were classified as elevated or normal concentration.

In the first replicate, 2 out of 3 CASES had elevated haptoglobin at arrival, while the second replicate induction group unfortunately had several (4) serum samples misplaced during the extended storage time and were not available for analysis at project completion. Of the 3 CASE samples recovered for testing in replicate 2, one animal (R1_101) returned an elevated haptoglobin at arrival.

No CONT had elevated levels in the first replicate at arrival. All CONT samples from replicate 2 were available for testing at project completion and only one was elevated at arrival in this group (R2_86). The mean haptoglobin for CONT at arrival was 0.5 g/L compared to mean haptoglobin of 1.26 g/L in CASE animals for replicate 1. Only the CONT group for replicate 2 at arrival can be reported usefully given the loss of samples in the CASE animals, and the mean haptoglobin for CONT at arrival was 0.24 g/L.

At the time of diagnosis CASE cattle had mean haptoglobin of 1.42 g/L compared to CONT at 0.19 g/L for the first replicate. The proportion of CONT with elevated haptoglobin at the time of diagnosis was 1/3 in the first replicate. For replicate 2, one CASE and one CONT animal suffered loss of sample during storage for analysis. Of the remaining 6 samples for both CONT and CASE, mean haptoglobin at time of diagnosis for CASE animals was 2.23 g/L compared to 0.26 g/L for CONT animals. For CONT animals in replicate 2, at the time of diagnosis the proportion with elevated haptoglobin was 1/6. For the two replicates combined, mean haptoglobin at the time of diagnosis for CASE animals was 1.96 g/L and for CONT animals was 0.23 g/L CASE

Table 17. Diagnostic accuracy of haptoglobin to detect BRD animals with visual and clinical signs, and lung lesions at euthanasia.

		Haptoglobin	
		ABNORM	**NORM**
TRUE	**CASE**	9	0
Status	**CONT**	2	7

Sensitivity:	*100%*
Specificity:	*78%*

4.8 Metabolomics

The new NMR sample preparation protocol with manual quantification offered the most optimal spectral and reliable quantification with the highest intensity, flattest baseline, and greatest water suppression **(Figure 8)**. However, the protocol filtered out large molecules such as lipids, which potentially removed biomarkers of interest. This protocol also resulted in stronger correlations with disease status (data not shown). However, these data with the new protocol cannot be used with the prediction models developed in B.FLT.0164 because the intensity differ and would not be accurate.

Figure 8. Annotated complete NMR Spectra showing comparison of cattle samples prepared by TMIC (red) and NMR-MP (blue; zgesgppe, 37 °C) methods. Black rectangle highlights water molecules at ~4.5 ppm. (x axis = ppm; y axis = intensity (AU). Ellen Barker honours thesis.

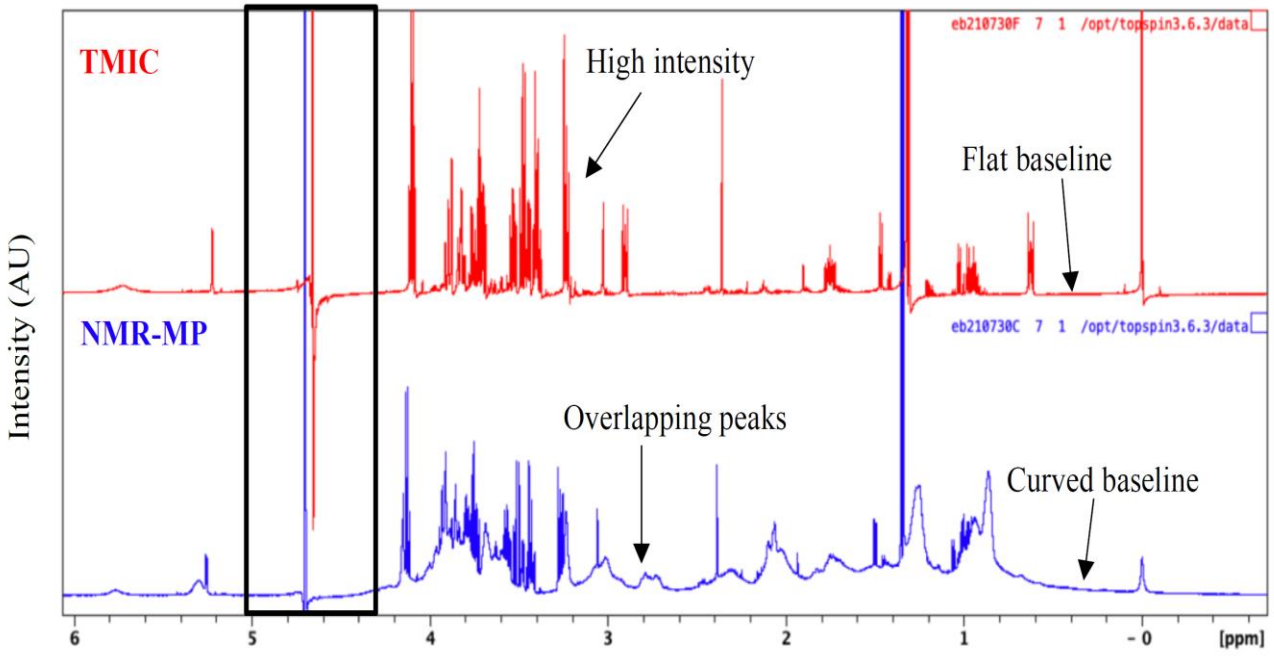

Classification accuracy of animals for the in-sample, cross-validation (resampling), and evaluation datasets from B.FLT.0164 will not be presented for brevity except for a few examples below to demonstrate the process (these could be added upon request). **Figure 9** shows the results from the application of the prediction models on the cross-validation dataset for prediction models of severe lung lesions at slaughter in B.FLT.0164. The three Decision trees models resulted in the smallest Area Under the Receiver Operating Curve (AUROC) of approximately 0.70 to detect animals that later had severe lung lesions upon slaughter. These values are those presented by Blakebrough-Hall et al. (2020). However, random forest, boosted trees and neural networks showed the largest AUROC of approximately 80% with high sensitivity (> 90%) and low specificity (~40%; **Figure 9**).

Figure 9. Resampling results to detect steers with **Severe lung lesions** (reference method) from metabolomics data in B.FLT.0164 using various machine learning models.

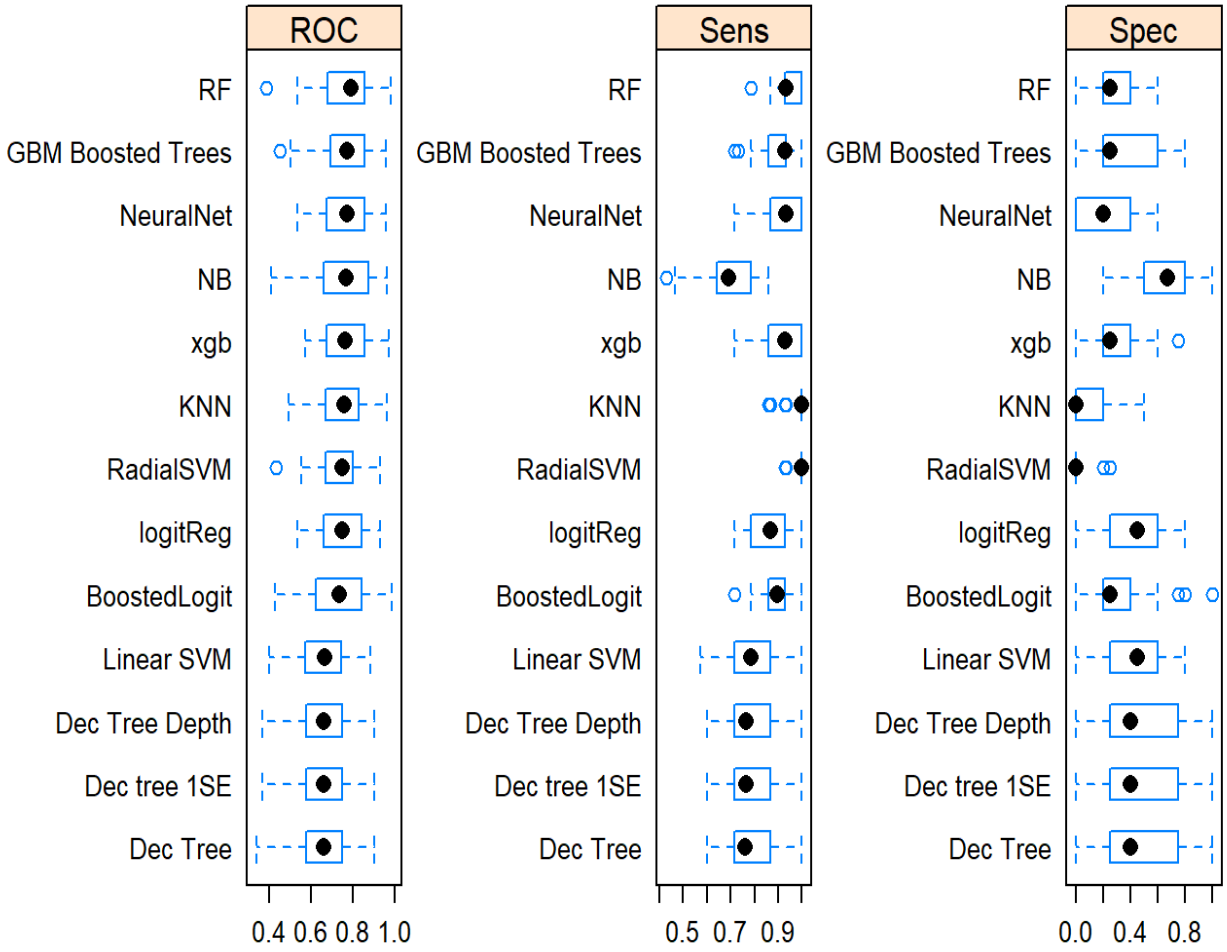

Naïve Bayes classifier resulted in a good trade-off between sensitivity and specificity and the results from the cross-validation dataset in B.FLT.0164 were similar to those obtained on B.FLT.3010 **(Figure 10)**.

Figure 10. Receiver operating curve using Naïve Bayes classifier to detect animals with **Severe lung lesions** at slaughter using the cross-validation dataset in B.FLT.0164 (red line) and the same model applied to B.FLT.3010 dataset (blue line).

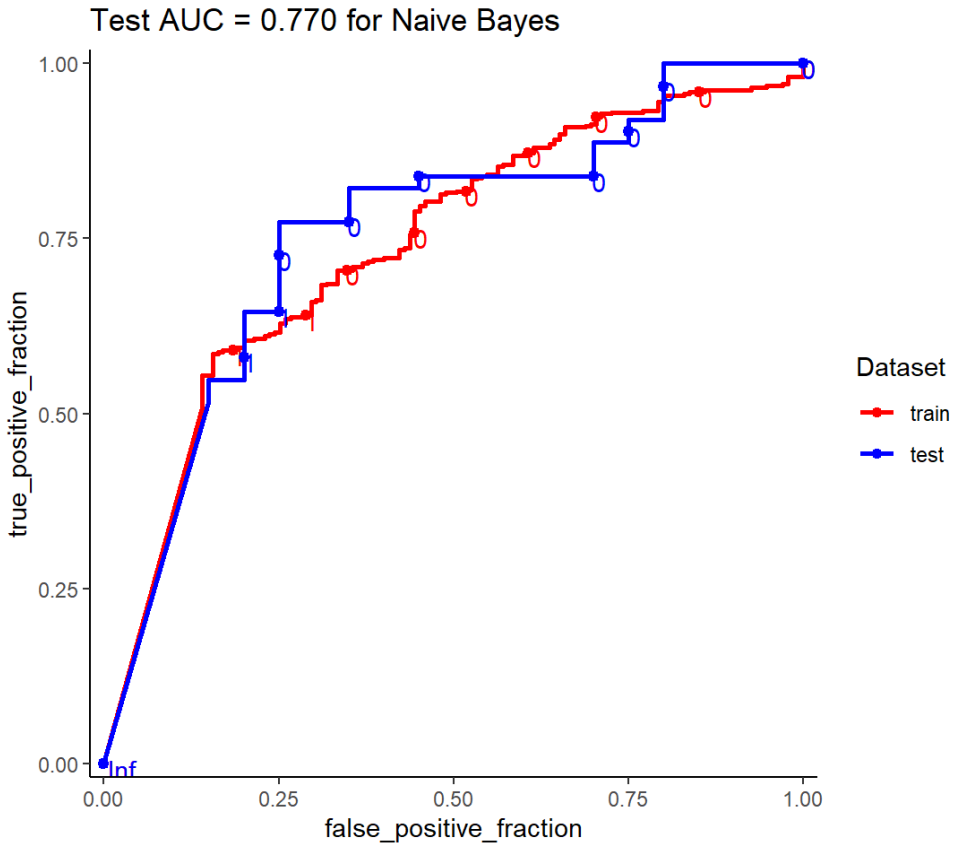

Blood metabolomics detected animals with **Visual signs of BRD** (pen rider observation only, no rectal temperature recording) using classification trees with similar accuracy in B.FLT.3010 (**Table 18** and 19) as in B.FLT.0164 (Blakebrough-Hall et al., 2020) using the unknown biomarker at 5.39 ppm of the NMR spectra (79% accuracy; **Table 19**). Therefore, this biomarker seems to be consistent in both trials and further efforts to identify and possibly develop a crush-side test is encouraged. However, there were other machine learning models applied to B.FLT.3010 that further improved accuracy including random forest (89%), neural networks (84%), and regularised logistic regression (84%; **Table 19**).

Table 18. Diagnostic accuracy of blood metabolomics to detect animals with **Visual Signs of BRD** using various machine learning models developed in B.FLT.0164 applied to data collected in B.FLT.3010 with 52% prevalence (visual and clinical signs with lung lesions at euthanasia).

Technique	True Negative	False Positive	False negative	True positive
Classification Trees	8	2	2	7
K nearest neighbour	8	2	2	7
Naïve Bayes	0	10	1	8
Regularised logistic regression	9	1	2	7
Radial Support vector machines	6	4	2	7
Linear Support Vector Machines	8	2	2	7
Boosted Logistic Regression	8	2	3	6
Random Forest	10	0	2	7
eXtreme Gradient Boosting	10	0	4	5
Neural Networks	9	1	2	7
Gradient boosting machine	10	0	3	6

Detection of animals with both Visual and Clinical signs of BRD showed highest accuracy when random forest (89%) and K nearest neighbour (84%), although other models also yielded >70% accuracy including Regularised Boosted regression, Neural Networks and Radial Support Vector Machines **(Table 20 and 21)**. These results demonstrate consistently high accuracy between independent trials because the models developed in the previous trial were applied to a new dataset from a different feedlot, diets, animals, management, and even different CASE definitions.

Table 19. Diagnostic accuracy of blood metabolomics to detect animals with **visual signs of BRD** using various machine learning models developed in B.FLT.0164 applied to data collected in B.FLT.3010 with 52% prevalence (visual and clinical signs with lung lesions at euthanasia) – heat map of diagnostic metrics.

Technique	Accuracy	Kappa	Sensitivity	Specificity	Pos Pred Value	Neg Pred Value	Precision	Recall	F1	Detection Rate	Detection Prevalence
Classification Trees	0.79	0.58	0.80	0.78	0.80	0.78	0.80	0.80	0.80	0.42	0.53
K nearest neighbour	0.79	0.58	0.80	0.78	0.80	0.78	0.80	0.80	0.80	0.42	0.53
Naïve Bayes	0.42	-0.11	0.00	0.89	0.00	0.44	0.00	0.00	NA	0.00	0.05
Regularised logistic regression	0.84	0.68	0.90	0.78	0.82	0.88	0.82	0.90	0.86	0.47	0.58
Radial Support vector machines	0.68	0.37	0.60	0.78	0.75	0.64	0.75	0.60	0.67	0.32	0.42
Linear Support Vector Machines	0.79	0.58	0.80	0.78	0.80	0.78	0.80	0.80	0.80	0.42	0.53
Boosted Logistic Regression	0.74	0.47	0.80	0.67	0.73	0.75	0.73	0.80	0.76	0.42	0.58
Random Forest	0.89	0.79	1.00	0.78	0.83	1.00	0.83	1.00	0.91	0.53	0.63
eXtreme Gradient Boosting	0.79	0.57	1.00	0.56	0.71	1.00	0.71	1.00	0.83	0.53	0.74
Neural Networks	0.84	0.68	0.90	0.78	0.82	0.88	0.82	0.90	0.86	0.47	0.58
Gradient boosting machine	0.84	0.68	1.00	0.67	0.77	1.00	0.77	1.00	0.87	0.53	0.68

Diagnostic metric definitions:

- **Precision** = repeatability, or reproducibility of the measurement (quality measure)
  - Formula = true positives/(true positives + false positives), i.e. true positives/all positives
- **Recall** = a measure of how many relevant elements were detected in the test (quantity measure)
  - Formula = true positives/(true positives + false negatives), i.e. true positives/number of all samples that should have been identified as positive
- **F1** = harmonic mean of the precision and recall of a test, F-score of 1.0 indicates perfect precision and recall, whereas F-score of 0.0 indicates nil precision and recall
  - Formula = (1 + beta^2)*precision*recall/(beta^2 * precision)+recall)
- **Detection Rate** = the fraction of all patients who have the disease and are called positive by the diagnostic test

  - Formula = true positives/(true positives + false positives + true negatives + false negatives)

- **Apparent (detection) prevalence** = the proportion of the population that tests positive for the disease
  - Formula = (true positives + false positives)/total number of tests

- **True prevalence** = the proportion of the population that is actually infected
  (true positives + false negatives)/total

As above in **Table 19**, Positive predictive value (PPV) is the probability that subjects with a positive result on screening test truly *do* have disease. Negative predictive value (NPV) is the probability that subjects with a negative screening test truly *don't* have disease.

Table 20. Diagnostic accuracy of blood metabolomics to detect animals with **visual and clinical signs of BRD** (visual observation supported by rectal temperature and electronic stethoscope) with various machine learning models developed in B.FLT.0164 applied to data collected in B.FLT.3010 with prevalence of 52.6% (visual and clinical signs and lung lesions at euthanasia).

Technique	True Negative	False Positive	False negative	True positive
K nearest neighbour	9	1	2	7
Naïve Bayes	1	9	1	8
Regularised logistic regression	7	3	2	7
Radial Support Vector Machines	8	2	2	7
Linear Support Vector Machines	6	4	2	7
Regularised Boosted regression	8	2	2	7
Random Forest	10	0	2	7
eXtreme gradient Boosting	9	1	4	5
Neural Networks	8	2	2	7
Gradient boosting machine	7	3	3	6

Table 21. Diagnostic accuracy of blood metabolomics to detect animals with **visual and clinical signs of BRD** (visual observation supported by rectal temperature and electronic stethoscope) with various machine learning models developed in B.FLT.0164 applied to data collected in B.FLT.3010 with prevalence of 52.6% (visual and clinical signs and lung lesions at euthanasia) – heat map of diagnostic metrics.

Technique	Accuracy	Kappa	Sensitivity	Specificity	Pos Pred Value	Neg Pred Value	Precision	Recall	F1	Detection Rate	Detection Prevalence
K nearest neighbour	0.84	0.68	0.90	0.78	0.82	0.88	0.82	0.90	0.86	0.47	0.58
Naïve Bayes	0.47	-0.01	0.10	0.89	0.50	0.47	0.50	0.10	0.17	0.05	0.11
Regularised logistic regression	0.74	0.48	0.70	0.78	0.78	0.70	0.78	0.70	0.74	0.37	0.47
Radial Support Vector Machines	0.79	0.58	0.80	0.78	0.80	0.78	0.80	0.80	0.80	0.42	0.53
Linear Support Vector Machines	0.68	0.37	0.60	0.78	0.75	0.64	0.75	0.60	0.67	0.32	0.42
Regularised Boosted regression	0.79	0.58	0.80	0.78	0.80	0.78	0.80	0.80	0.80	0.42	0.53
Random Forest	0.89	0.79	1.00	0.78	0.83	1.00	0.83	1.00	0.91	0.53	0.63
eXtreme gradient Boosting	0.74	0.46	0.90	0.56	0.69	0.83	0.69	0.90	0.78	0.47	0.68
Neural Networks	0.79	0.58	0.80	0.78	0.80	0.78	0.80	0.80	0.80	0.42	0.53
Gradient boosting machine	0.68	0.37	0.70	0.67	0.70	0.67	0.70	0.70	0.70	0.37	0.53

Detection of CASEs using metabolomics from the prediction models of animals with lung lesions at slaughter developed in B.FLT.0164 are shown in **Table 22 and 23**. Most of the machine learning models yielded very high Sensitivity but low Specificity, or vice versa. The exceptions were Regularised logistic regression with 68% accuracy and neural networks with 84% accuracy, 90% Sensitivity and 78% Sensitivity **(Table 23).** The reason for the disparity of the results between machine learning models is unknown but it is encouraging that the latter two models were also accurate for field applications with an independent dataset.

Table 22. Diagnostic accuracy of blood metabolomics to detect animals with **lung lesions upon euthanasia** with various machine learning models developed in B.FLT.0164 applied to data collected in B.FLT.3010 with 52.6% prevalence (visual and clinical signs, lung lesions evident upon euthanasia).

Model	True Negative	False Positive	False negative	True positive
K Nearest Neighbour	9	1	6	3
Naïve Bayes	10	0	6	3
Regular logistic regression	7	3	3	6
Radial Support Vector Machine	0	10	1	8
Linear Support Vector Machine	8	2	7	2
Regular Boosted regression	10	0	9	0
Decision Trees	10	0	6	3
Random Forest	10	0	8	1
eXtreme gradient Boosting	10	0	8	1
Neural Networks	9	1	2	7
Gradient boosting machine	10	0	8	1

Table 23. Diagnostic accuracy of blood metabolomics to detect animals with **lung lesions upon euthanasia** with various machine learning models developed in B.FLT.0164 applied to data collected in B.FLT.3010 with 52.6% prevalence (visual and clinical signs, lung lesions evident upon euthanasia) – heat map of diagnostic metrics.

Model	Accuracy	Kappa	Sensitivity	Specificity	Pos. Pred. Value	Neg. Pred. Value	Precision	Recall	F1	Detection Rate	Detection Prevalence
K Nearest Neighbour	0.63	0.24	0.90	0.33	0.60	0.75	0.60	0.90	0.72	0.53	0.47
Naïve Bayes	0.68	0.34	1.00	0.33	0.63	1.00	0.63	1.00	0.77	0.53	0.53
Regular logistic regression	0.68	0.37	0.70	0.67	0.70	0.67	0.70	0.70	0.70	0.53	0.37
Radial SVM	0.42	-0.11	0.00	0.89	0.00	0.44	0.00	0.00	NA	0.53	0.00
Linear SVM	0.53	0.02	0.80	0.22	0.53	0.50	0.53	0.80	0.64	0.53	0.42
Regular Boosted regression	0.53	0.00	1.00	0.00	0.53	NA	0.53	1.00	0.69	0.53	0.53
Decision Trees	0.68	0.34	1.00	0.33	0.63	1.00	0.63	1.00	0.77	0.53	0.53
Random Forest	0.58	0.12	1.00	0.11	0.56	1.00	0.56	1.00	0.71	0.53	0.53
eXtreme gradient Boosting	0.58	0.12	1.00	0.11	0.56	1.00	0.56	1.00	0.71	0.53	0.53
Neural Networks	0.84	0.68	0.90	0.78	0.82	0.88	0.82	0.90	0.86	0.53	0.47
Gradient boosting machine	0.58	0.12	1.00	0.11	0.56	1.00	0.56	1.00	0.71	0.53	0.53

4.9 Nasopharyngeal Microbiota

Baseline sequencing data

A total of 2,009,587 reads were obtained across all samples from one sequencing run (CASE = 726,175; Ctrl = 702,373) prior to upstream processing. After processing with DADA2, removing negative CONT samples, and animals which did not have samples at both arrival and enrolment, a total of 908,890 reads remained across all samples (CASE = 444,891; Ctrl = 340,570; False negative = 46,916; False positive = 76,513), with an average coverage of 21,640 reads (range = 15,029-27,616) per sample (CASE = 22,245; Ctrl = 21,286). From these sequences, 5,477 unique SVs were identified across all samples. After removal of all SVs that did not belong to the kingdom Bacteria, a total of 5,349 SVs remained. False positive and false negative samples were excluded from all downstream analyses.

A total of 4 negative CONT samples were sent for metagenomic sequencing. The sequencing results for each negative CONT were assessed individually, and it was determined that, based on the composition of the reads and the low number of sequences shared between the negative CONT samples and the study samples, there was insignificant contamination of the study samples due to the DNA extraction and metagenomic sequencing processes. Therefore, there was no need to adjust the study feeder steer DNA sequencing results for possible contaminants.

Characterization of the nasopharyngeal bacterial microbiota

The most prominent identified phyla across all CASE and CONT samples were Proteobacteria (40.50%), Tenericutes (33.27%), Firmicutes (8.78%), Bacteroidetes (6.22%), and Actinobacteria (6.21%). However, the order of phyla by abundance differed between experimental groups and sample types (Phylum abundance).

Figure 11. Phylum abundance extracted from swabs of the respiratory tract of BRD CASEs and CONTs steers at induction (sample type A) and upon confirmation of BRD (sample type B).

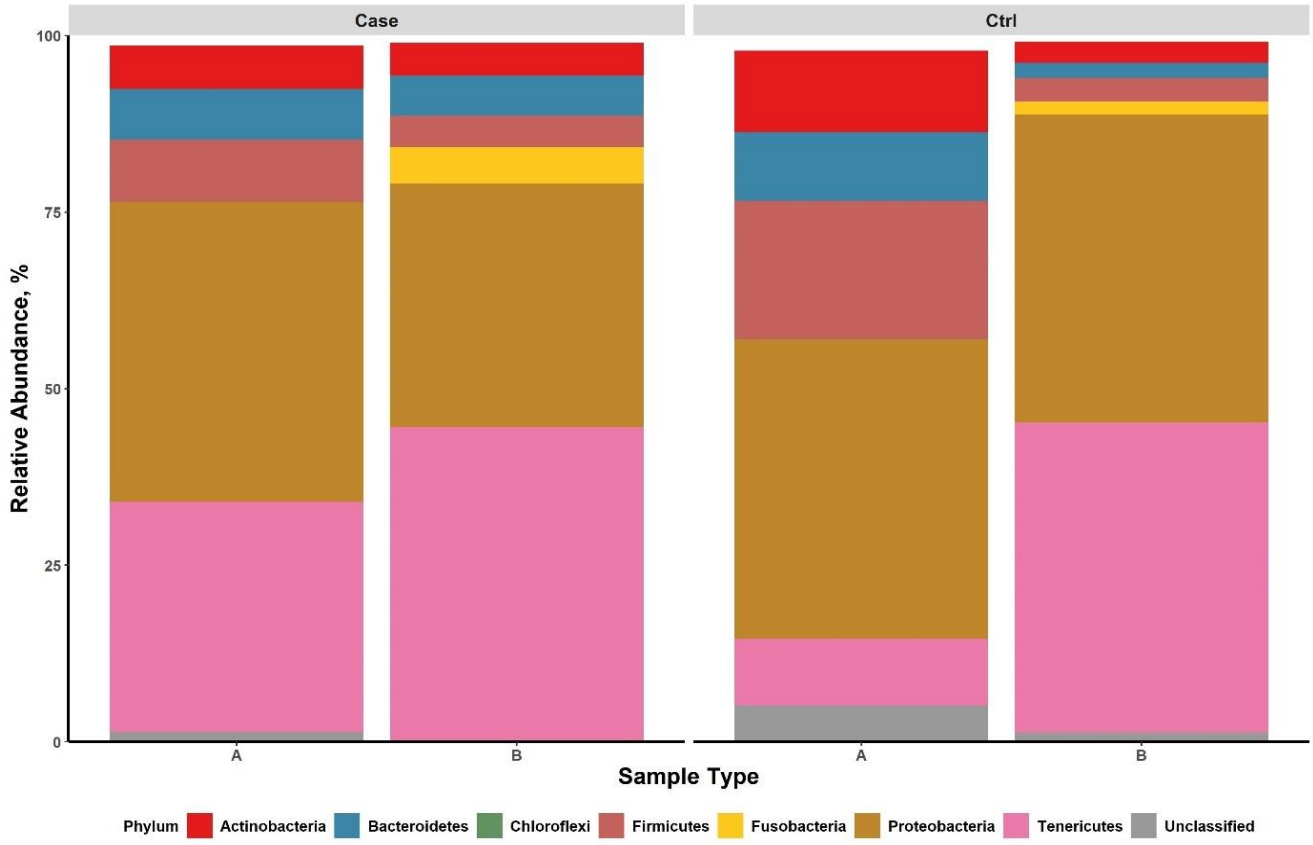

The most prominent identified genera across all CASE and CONT samples were *Mycoplasma* (32.15 %), *Psychrobacter* (12.68%), *Actinobacillus* (4.54%), *Histophilus* (4.14%), and *Nicotella* (3.04%). However, the order of genera by abundance differed between experimental groups and sample types (Genus abundance). Genera also varied between individual animals across experimental groups and sample types (individual animal abundance)

Figure 12. Genus abundance extracted from swabs of the respiratory tract with BRD (CASE) and CONT steers at induction (sample type A) and upon confirmation of BRD (sample type B).

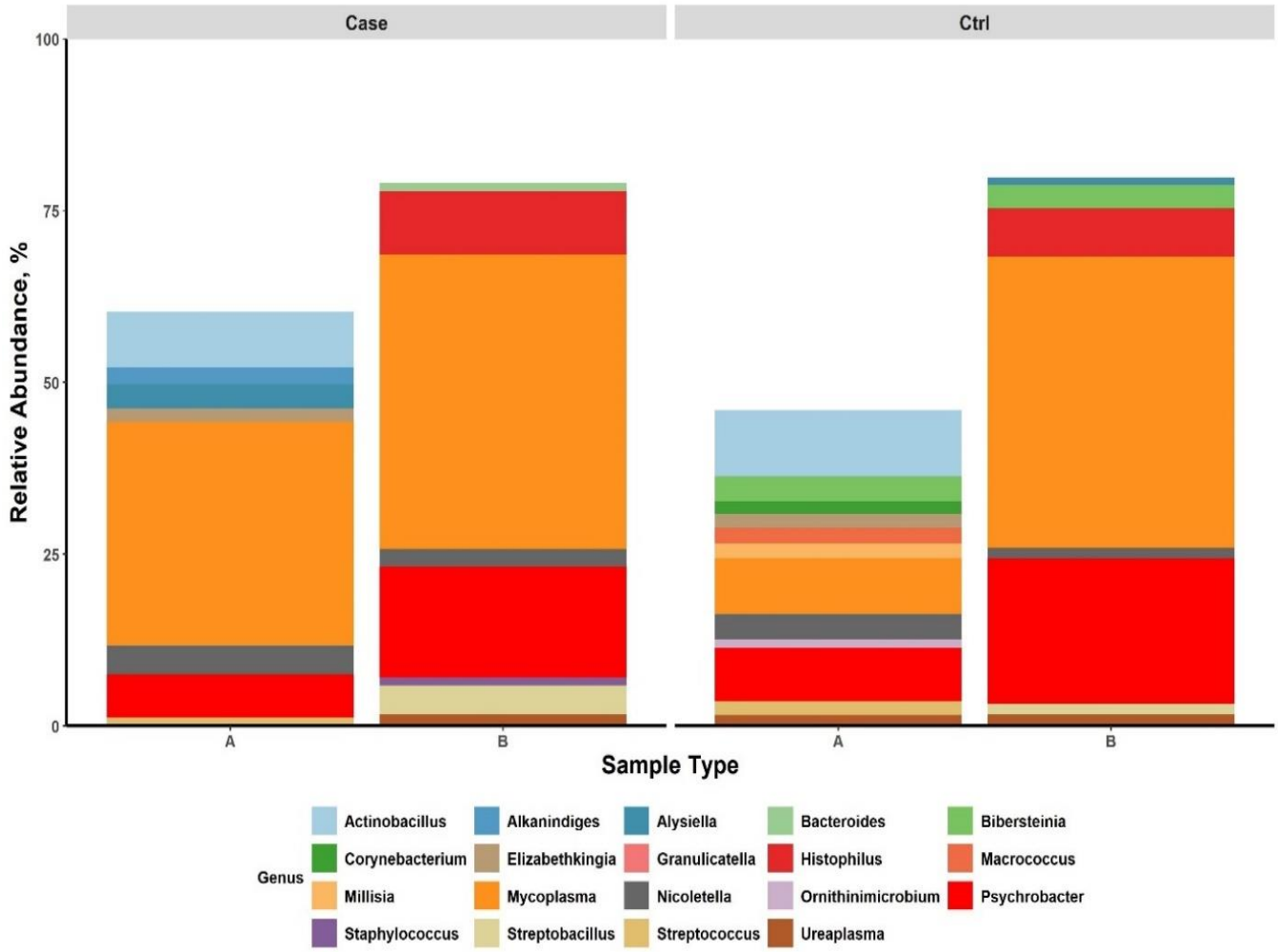

Figure 13. Genus abundance of individual animals (tag number) extracted from swabs of the respiratory tract of steers with BRD (top panel), control (bottom panel) and false positive and negatives (bottom panel) at induction (sample type A) and upon confirmation of BRD (sample type B).

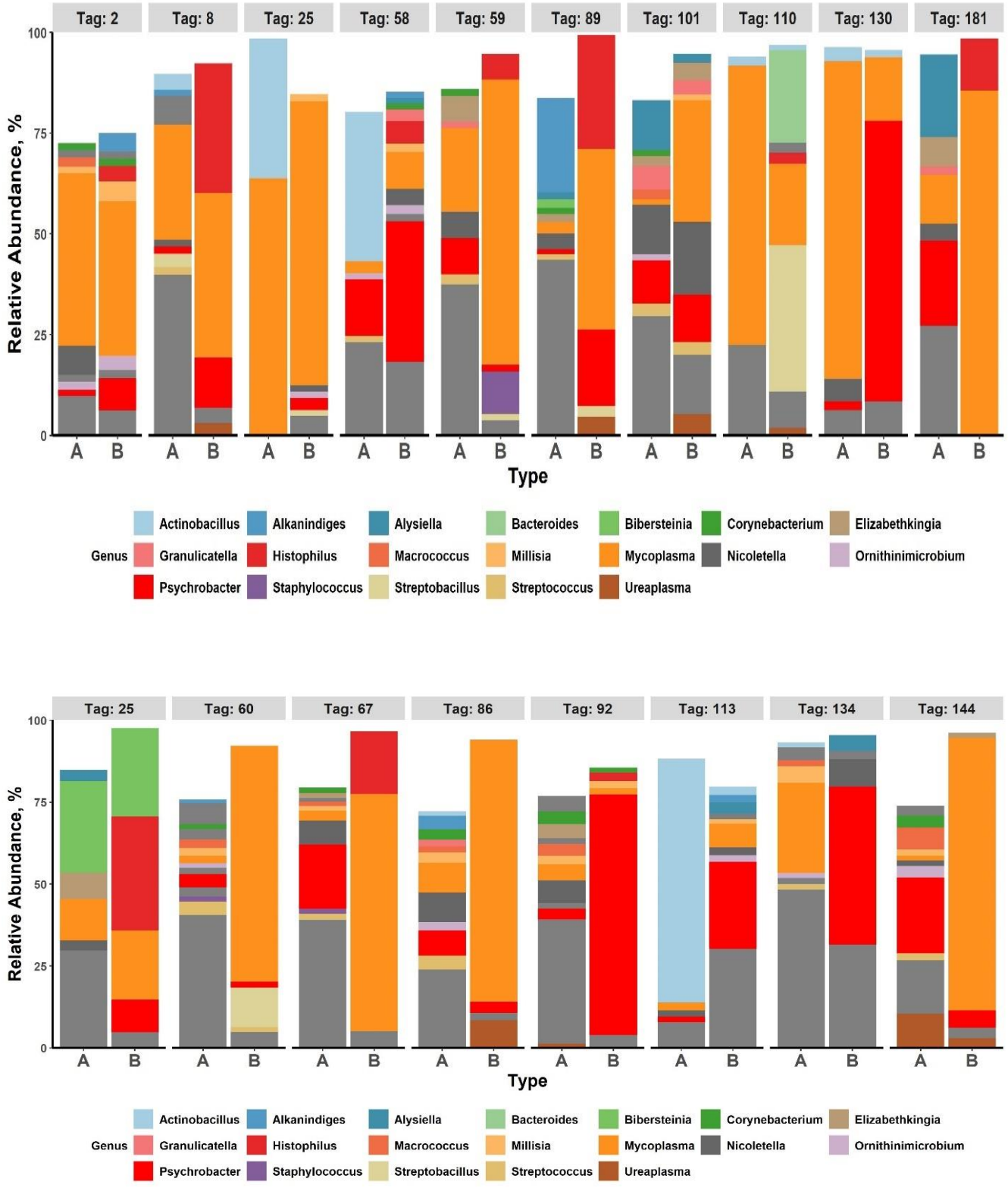

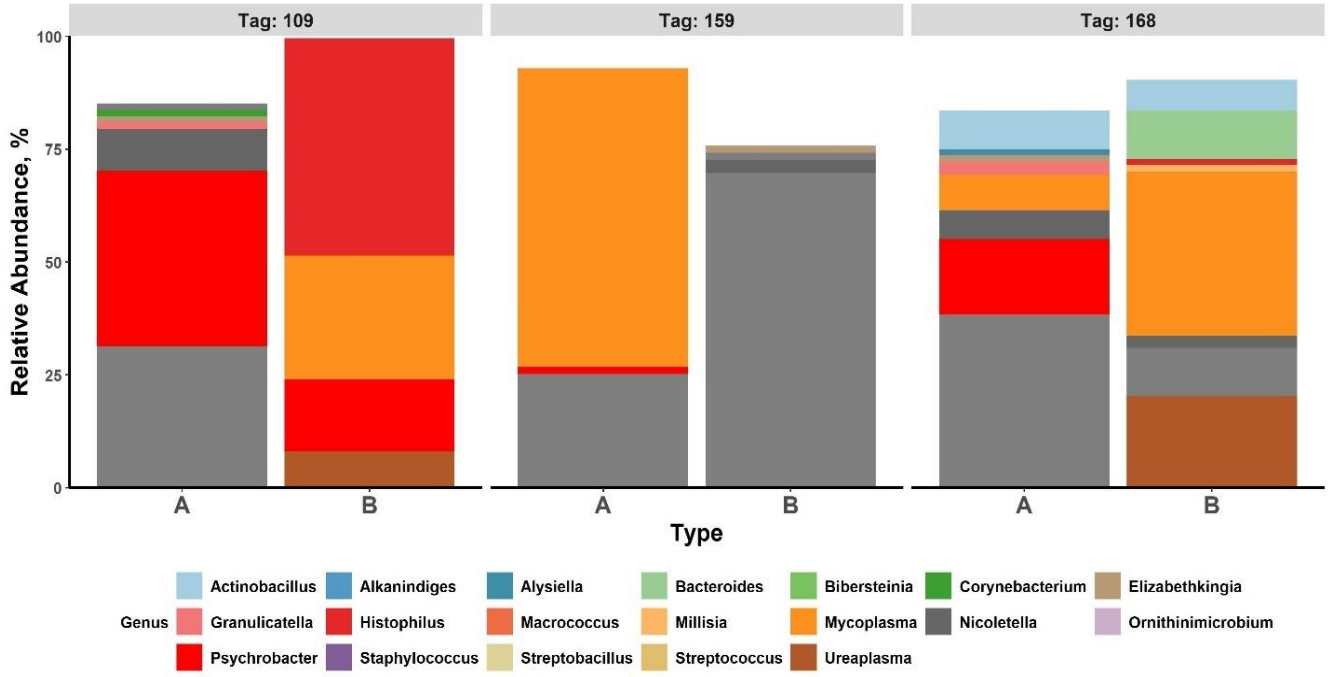

Comparison of nasopharyngeal bacterial microbiota structure between BRD CASE and CONT groups

Chao1 species richness did not differ between experimental groups or sample types within experimental group (P > 0.050; **Figure 14**). However, Shannon diversity was higher at arrival compared to enrollment within the CONT group (P = 0.039) and was higher at arrival in the CONT group compared to the CASE group (P = 0.009; **Figure 14**).

Figure 14. Chao1 species richness (left panel) and Shannon diversity index (right panel) of the microbial communities of the respiratory tract of steers classified as BRD cases and controls from samples extracted at induction (type A) and upon confirmation of BRD (type B).

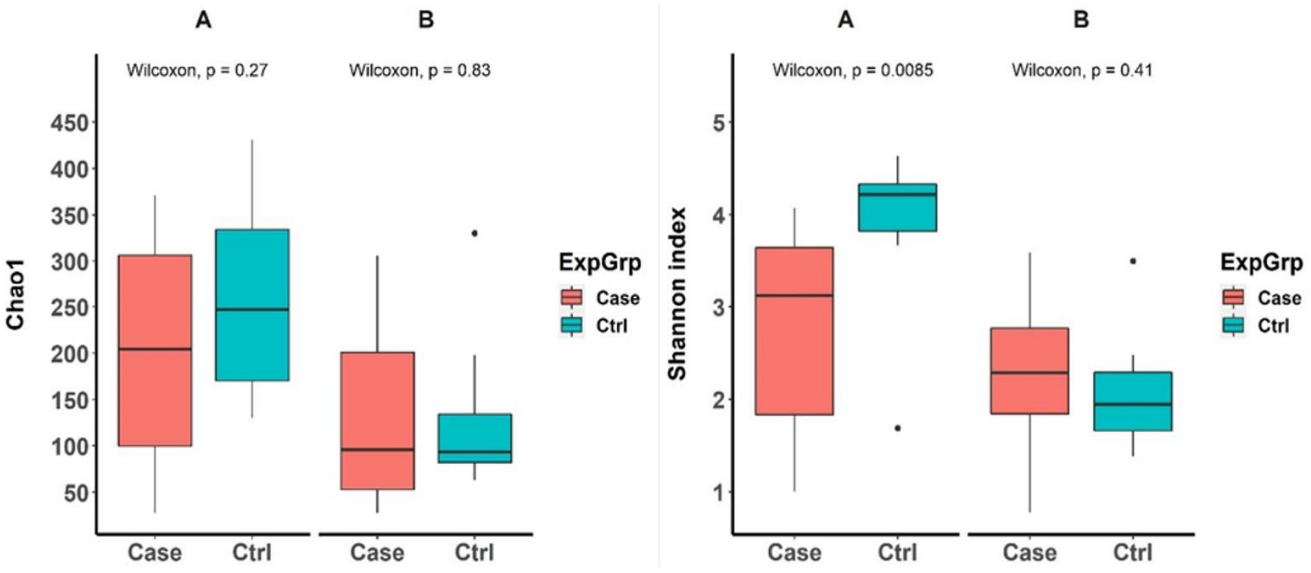

Based on PERMANOVA analyses, experimental group, ultrasound score, and Whisper score were not significant sources of variation in Chao1 index (P < 0.050; **Table 24**). Sample type was a significant source of variation (P < 0.001), although it only accounted for 9.84% of total observed variation.

Table 24. Effect of experimental group, sample type, lungs ultrasound score, and Whisper score on the variation in the microbial communities of the respiratory tract of feedlot steers – Chao1 index.

Factor	R^2	P-value	Beta-dispersion
Experimental group	0.02814	0.318	0.439
Sample type	0.09844	< 0.001	0.062
Ultrasound score	0.06512	0.827	0.027
Experimental group * Sample type	0.02225	0.632	-
Experimental group * Ultrasound score	0.03978	0.081	-
Sample type * Ultrasound score	0.08580	0.303	-
Experimental group * Sample type * Ultrasound score	0.03239	0.223	-

Similar results were found in Shannon index with only sample type being a significant source of variation (P < 0.001; **Table 25**). No pattern was observed between haptoglobin concentration and community composition (data not shown).

Table 25. Effect of experimental group, sample type, lungs ultrasound score, and Whisper score on the variation in the microbial communities of the respiratory tract of feedlot steers – Shannon index.

Factor	R^2	P-value	Beta-dispersion
Experimental group	0.02814	0.357	0.439
Sample type	0.09844	< 0.001	0.062
Whisper score	0.07586	0.604	0.031
Experimental group * Sample type	0.02225	0.632	-
Experimental group * Whisper score	0.06742	0.159	-
Sample type * Whisper score	0.05817	0.945	-
Experimental group * Sample type * Whisper score	0.05464	0.437	-

Figure 15. Non-metric multidimensional scale plots of the microbial communities of the respiratory tract of steers classified as BRD CASES and CONTs from samples extracted at induction (panel A) and upon confirmation of BRD (panel B), correlated to Whisper Score. No correlation is apparent.

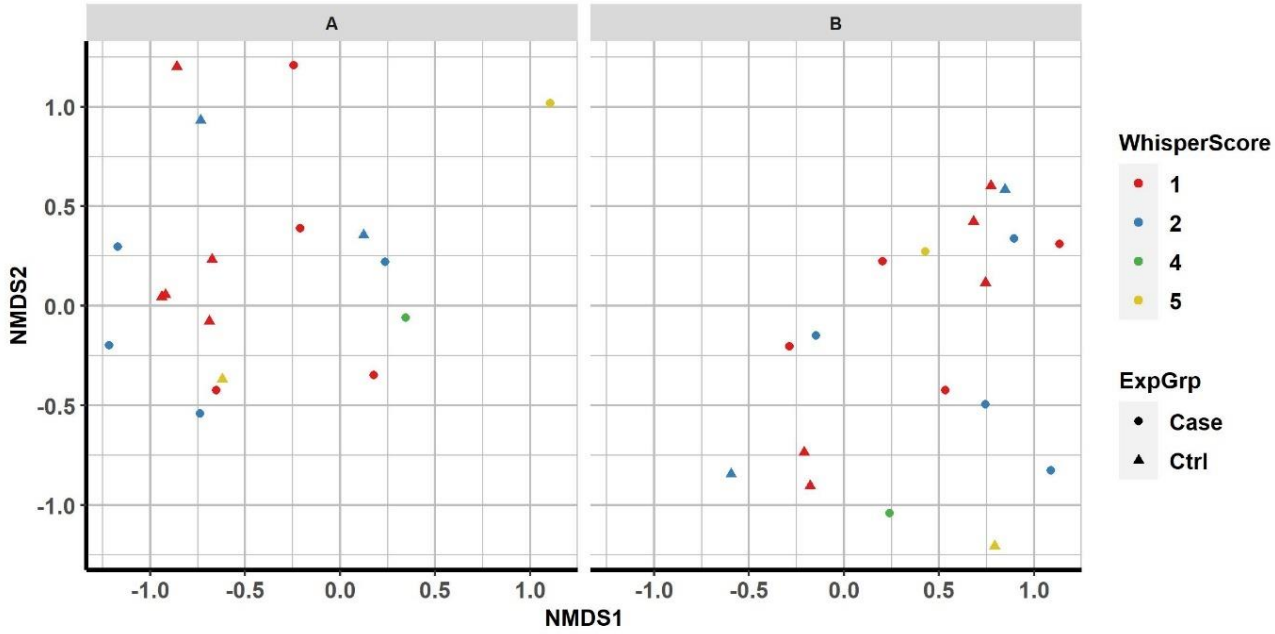

4.10 Computer aided auscultation

Each animal selected as final CASE or CONT were evaluated with computer aided auscultation (Whisper) at the time of diagnosis. Each animal had 3 readings recorded and classified by the computer. The final status was determined by creating a reading based on the most common reading (2/3) or when all readings disagreed, the central reading was recorded. Each feeder steer received the same score for each of the 3 readings in 4 out of 10 CASEs and 3 out of 10 CONT animals. These results highlight the low repeatability of the Whisper auscultation score. One challenge with evaluating data from the system is the inconsistency per animal resulting in potentially different aggregations of numbers if only one reading were recorded. Utilizing a single reading would have resulted in 4, 6, or 8 of the CONT cattle classified as normal if the first, second or third reading was utilized, respectively **(Table 26)**.

Table 26. Summary of Whisper scores for CASE / CONT study animals.

Feeder steer Tag	Status	Whisper 1	Whisper 2	Whisper 3	Whisper Aggregate	Whisper Aggregate Classification	Whisper (normal/ abnormal)
R1_110	CASE	2	2	2	2	mild acute	1
R1_130	CASE	5	4	3	4	severe acute	1
R1_89	CASE	3	1	2	2	mild acute	1
R2_101	CASE	2	3	2	2	mild acute	1
R2_181	CASE	1	1	1	1	normal	0
R2_2	CASE	1	1	1	1	normal	0
R2_25	CASE	4	5	5	5	chronic	1
R2_58	CASE	2	1	1	1	normal	0
R2_59	CASE	2	2	2	2	mild acute	1
R2_8	CASE	2	1	1	1	normal	0
R1_25	CONT	2	3	2	2	mild acute	1
R1_60	CONT	2	2	1	2	mild acute	1
R1_92	CONT	2	1	1	1	normal	0
R2_113	CONT	1	2	1	1	normal	0
R2_134	CONT	2	2	1	2	mild acute	1
R2_144	CONT	1	2	1	1	normal	0
R2_60	CONT	3	2	3	3	mod acute	1
R2_67	CONT	1	1	1	1	normal	0
R2_76	CONT	1	1	1	1	normal	0
R2_86	CONT	1	1	1	1	normal	0

The aggregate readings resulted in a scaled finding from 1 (normal) to 5 (Chronic) and number of readings by each level are presented in Table 27. Most CONT (n=9) animals were classified as normal or mild acute, however this was similar to the CASE cattle (n=8). Only 2 animals were classified as severe acute or chronic **(Table 27)**.

Table 27. Number of animals as classified by each aggregate reading through Whisper.

	1 Normal	2 Mild Acute	3 Mod Acute	4 Severe Acute	5 Chronic
CASE	4	4	0	1	1
CONT	6	3	1	0	0

Whisper scores were dichotomized to determine classification of each CASE/CONT as normal/abnormal (reading of = 1 or > 1). The resulting sensitivity and specificity calculations are listed in **Table 28.**

Table 28. Sensitivity and specificity based on Whisper classification as normal/abnormal.

		Whisper	
		ABNORM	**NORM**
TRUE	**CASE**	6	4
Status	**CONT**	4	6

Sensitivity:	*60%*
Specificity:	*60%*

Statistical comparison of the probability of Whisper diagnosis of abnormal at the time of diagnosis revealed no statistical (P = 0.36) differences in the probability of lesions at necropsy.

4.11 Remote early disease identification system

The REDI system utilizes data collected from real time location systems affixed to the cattle. The Eliko™ devices utilized for collecting remote locations suffered from significant technical challenges in the first replicate. The devises required significant maintenance resulting in multiple tag changes and battery replacements. For the whole replicate of study cattle, the proportion of sufficient data generation and monitoring declined through the feeding phase. For the first 24 days approximately 80% of the pen had sufficient data for monitoring, however during the date range 3rd – 5th April (28-30 DOF) a large proportion of the replicate lost sufficient data suddenly. Several modifications were made to the system between replicates resulting in significantly improved quantity of data in replicate 2 allowing collection of data through the feeding phase.

4.11.1 REDI Algorithm evaluations

The cattle were evaluated with several REDI algorithms for comparison as one of the objectives of this trial is to evaluate potential changes to the sensitivity and specificity of the system based on the situation.

The cattle were evaluated with several REDI algorithms for comparison as one trial objective is to evaluate potential changes to the sensitivity and specificity of the system based on the situation. REDI algorithms had been previously used in B.FLT.0242 in comparison with human observations at two Australian feedlots. In this (B.FLT.0242) original project the algorithms were based on data collected and evaluated in North American beef cattle production systems. The algorithms were further evaluated in a subsequent project (B.FLT.3005) where new algorithms were generated and refined based on Australian cattle in an Australian production system. The current project uses new algorithms based on the Australian versions but tweaked slightly to improve overall performance. These algorithms included:

Visual: based on observer
dccall: a sensitive REDI algorithm
ds3: a combination algorithm
rn2call: a combination algorithm
rn4call: a combination algorithm

The visual observations were the basis for disease calls; therefore, were perfectly aligned with CASE outcomes on this subset. Two algorithms called 8 of 10 CASE cattle and the other algorithms

identified 9 or 10 of the CASE cattle. In R1, many tags suffered from malfunctions and required replacements. One study animal was not identified as positive by 3 algorithms and another was not identified by one algorithm. These study animals were identified at d21 and d58, respectively. The REDI algorithms employ social data as one of the parameters and the impact of missing these data on many cattle in the pen on the final disease call is unknown. Specificity ranged from 60-80% with two CONT feeder steer (R2_144 and R2_67) called as false positives by multiple algorithms (Table 29).

Table 29. Disease calls for CASEs and CONT study animals by the REDI system.

Animal ID	Status	Visual	rn2call	rn4call	ds3	dccall
R1_110	CASE	1	0	1	1	1
R1_130	CASE	1	1	1	1	1
R1_89	CASE	1	0	0	0	1
R2_101	CASE	1	1	1	1	1
R2_181	CASE	1	1	1	1	1
R2_2	CASE	1	1	0	1	1
R2_25	CASE	1	1	1	1	1
R2_58	CASE	1	1	1	1	1
R2_59	CASE	1	1	1	1	1
R2_8	CASE	1	1	1	1	1
R1_25	CONT	0	0	0	0	0
R1_60	CONT	0	0	0	0	0
R1_92	CONT	0	0	0	0	0
R2_113	CONT	0	1	0	0	0
R2_134	CONT	0	0	0	0	1
R2_144	CONT	0	0	1	1	1
R2_60	CONT	0	0	0	0	0
R2_67	CONT	0	1	1	1	1
R2_76	CONT	0	0	0	0	1
R2_86	CONT	0	0	0	0	0

1 = detected by the REDI algorithm, 0 is not detected by the REDI algorithm.

The REDI algorithms each represented different diagnostic characteristics as presented in **Table 30**.

Table 30. Diagnostic evaluation of the 4 REDI algorithms.

		rn2call	
		ABNORM	**NORM**
TRUE Status	**CASE**	8	2
	CONT	2	8

Sensitivity:	*80%*
Specificity:	*80%*

		rn4call	
		ABNORM	**NORM**
TRUE Status	**CASE**	8	2
	CONT	2	8

Sensitivity:	*80%*
Specificity:	*80%*

		ds3	
		ABNORM	**NORM**
TRUE Status	**CASE**	9	1
	CONT	2	8

Sensitivity:	*90%*
Specificity:	*80%*

		dccall	
		ABNORM	**NORM**
TRUE Status	**CASE**	10	0
	CONT	4	6

Sensitivity:	*100%*
Specificity:	*60%*

4.11.2 Timing of REDI disease calls

Timing of disease calls is also important with most CASES having occurred around day 20 since arrival with one CASE early and two CASEs later **(Figure 16)**.

Figure 16. Timing of visual calls by number of calls per animal by day on feed post arrival.

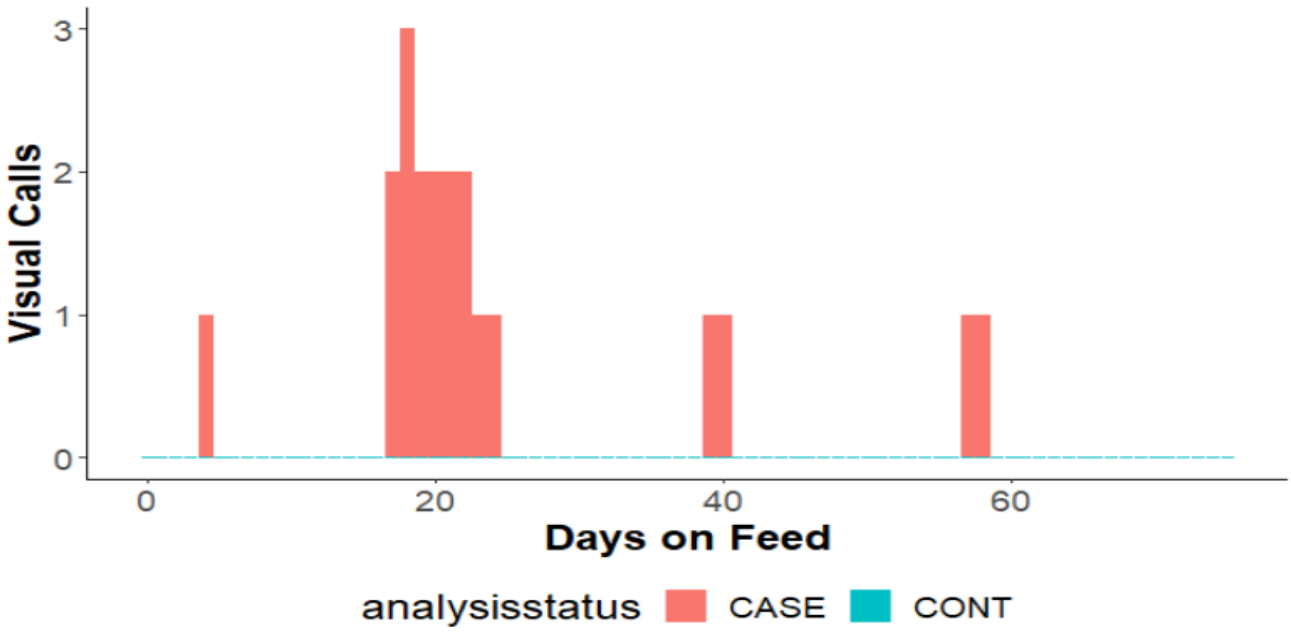

Using REDI algorithms resulted in similar patterns of disease calls among algorithms. The disease calls happened earlier and more frequently compared to visual calls; however, false positives were also presented. The two false positive animals were deemed as positive by REDI for multiple days **(Figure 17)**.

Figure 17. Distribution of REDI rn4 calls by day compared to true status (CASE/CONT). Each study animal had clinical status determined by REDI for each available day during the trial.

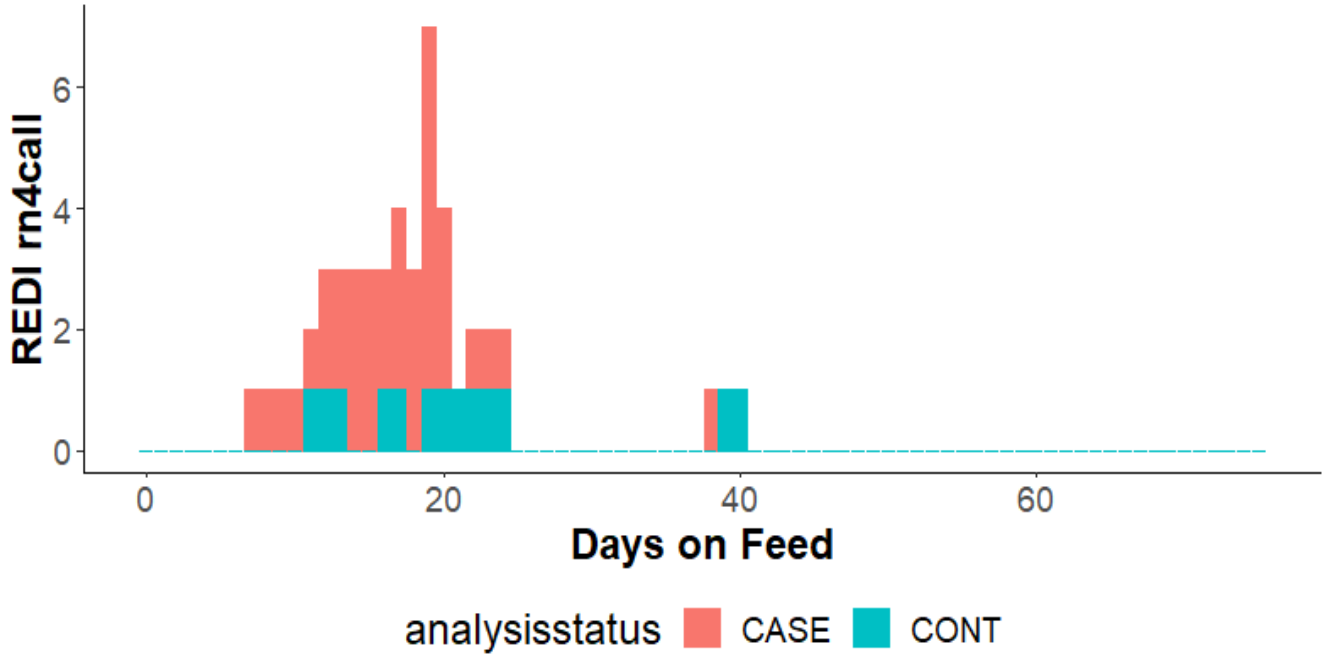

Further evaluation of timing of diagnosis by each REDI algorithm revealed that the algorithm diagnosed disease in CASE cattle prior to the human observer in every CASE where disease was identified by REDI **(Table 31)**. On average each REDI algorithm (rn2call, rn4call, ds3, and dccall) diagnosed disease 7.4, 8.9, 10.2, and 12.1 days prior to the diagnosis at necropsy. This timing effect does not account for the fact some CASE cattle were not diagnosed by REDI algorithms and some CONT cattle were false positives. Each of the false positives was consistently diagnosed as positive with R2_144 positive for at least 11 days with all four algorithms **(Table 31)**.

Table 31. Distribution of disease calls by timing based on each of the 4 evaluated REDI algorithms.

		rn2call			rn4call			ds3			dccall		
CASEs	**DOF @ Diag**	**DOF 1st call**	**days before visual**	**days pos.**	**DOF 1st call**	**days before visual**	**days pos.**	**DOF 1st call**	**days before visual**	**days pos.**	**DOF 1st call**	**days before visual**	**days pos.**
R1_110	58			0	19	39	5	19	39	7	19	39	7
R1_130	19	19	0	1	17	2	3	17	2	4	17	2	4
R1_89	21			0			0			0	17	4	2
R2_101	16	13	3	7	12	4	7	9	7	11	9	7	11
R2_181	19	15	4	4	14	5	6	13	6	8	13	6	8
R2_2	23	14	9	4			0	13	10	1	13	10	3
R2_25	16	15	1	5	11	5	7	11	5	9	11	5	9
R2_58	21	7	14	3	7	14	6	7	14	10	7	14	10
R2_59	18	15	3	5	17	1	1	10	8	6	10	8	6
R2_8	39	14	25	3	38	1	1	38	1	2	13	26	4
Average	***25.0***	***14.0***	***7.4***	***3.2***	***16.9***	***8.9***	***3.6***	***15.2***	***10.2***	***5.8***	***12.9***	***12.1***	***6.4***
CONTs													
R1_25	20			0			0			0			0
R1_60	59			0			0			0			0
R1_92	21			0			0			0			0
R2_113	17	7		1			0			0			0
R2_134	17			0			0			0	14		2
R2_144	38			0	39		1	15		7	15		9
R2_60	15			0			0			0			0
R2_67	22	12		11	11		11	11		12	11		14
R2_76	21			0			0			0	12		4
R2_86	21			0			0			0			0
Average	***25.1***			***1.2***			***1.2***			***1.9***			***2.9***

REDI comparison with individual additional CASEs

Replicate 1 BRD CASE

One animal (R1_194) was deemed as ill with BRD during the feeding phase after the REDI monitoring period ended in replicate 1. This feeder steer died from BRD at the end of the feeding phase. This feeder steer was not identified by REDI. However, the feeder steer had data ending on 4/17 (42 DOF) and thus was not monitored by REDI toward the end of the feeding period.

False positive at CASE diagnosis

Three potential CASEs (R1_113, R1_109, R1_159) were identified based on clinical signs and rectal temperature but failed to have significant lung lesions at necropsy; therefore, these animals were considered a false positive. Feeder steer R1_159 had a tag malfunction and did not have readings recorded. Feeder steer R1_113 and R1_109 had no positive calls for REDI.

False negative at CONT diagnosis

One individual animal (R1_168) was identified as a negative CONT because of a lack of clinical signs, met the temperature and evaluation criteria and was subsequently necropsied. This animal had lung lesions > 5% thus was considered a false negative. No REDI algorithm identified this animal as positive either, potentially indicating this animal had been ill prior to arrival at the feedlot with pre-existing pulmonary lesions

REDI Comparison with pulmonary lesions at harvest slaughter

Cattle were evaluated at slaughter and three cattle that received pulmonary scores did not receive REDI calls due to tag malfunctions (R1_53, R1_91, and R1_163). All other cattle receiving pulmonary lung scores were compared to the potential for REDI to call them positive through the period. Each algorithm was applied to those cattle through the feeding phase. The REDI algorithms represented a range in sensitivity (11%-56%) and specificity (43%-87%) (Table 32). Each algorithm could be applied in different situations depending on the current needs.

Table 32. Sensitivity and specificity of selected REDI algorithms based on detection of pulmonary lesions in non-clinical CASEs at harvest slaughter.

		rn4call	
		ABNORM	**NORM**
TRUE Status	**Lung les**	13	32
	No lung les	66	248

Sensitivity:	*29%*
Specificity:	*79%*

		rn2call	
		ABNORM	**NORM**
TRUE Status	**Lung les**	5	40
	No lung les	42	272

Sensitivity:	*11%*
Specificity:	*87%*

		dccall	
		ABNORM	**NORM**
TRUE Status	**Lung les**	22	23
	No lung les	148	166

Sensitivity:	*49%*
Specificity:	*53%*

		ds3	
		ABNORM	**NORM**
TRUE Status	**Lung les**	25	20
	No lung les	180	134

Sensitivity:	*56%*
Specificity:	*43%*

Note that due to data discrepancies and system malfunctions in R1, cattle in this replicate had fewer days available for monitoring. This may contribute to decreased overall accuracy although accuracy did not differ greatly among replicates.

Statistical analysis was performed on REDI algorithms comparing arrival and carcass characteristics based on algorithm differences **(Table 33)**. There was no difference in body weight, performance, or carcass traits between animals classified as normal or abnormal by the REDI system (P > 0.10).

Table 33. Statistical comparison of arrival and carcass characteristics based on REDI algorithm (rn4call) classifications as normal/abnormal at any point during the feeding phase for cattle that received pulmonary scores at harvest slaughter.

	REDI: rn4call				
	Normal	**SE**	**Abnormal**	**SE**	**P-value**
Head (n)	280		79		
Initial Weight (kg)	342.2	28.92	336.1	29.22	0.25
Initial Temperature (°C)	39.5	0.03	39.5	0.06	0.50
HSCW (kg)	262.6	5.61	258.8	5.88	0.17
P8 (mm)	10.09	0.864	10.50	0.932	0.38
EMA (cm^2)	64.8	1.29	63.8	1.61	0.45
MSA Index	56.4	0.08	56.5	0.16	0.17
ADG (kg/d)	1.99	0.051	1.90	0.063	0.11

4.12 Reticulo-ruminal temperature boluses

Reticulo-ruminal temperature boluses recorded core temperature throughout the trial period. These boluses were used to compare both CASE/CONT cattle as well as evaluate for lung lesions at harvest slaughter.

Data from the boluses was transmitted at approximately 5 minute intervals to a base station located within proximity of the trial pen and then uploaded to the Medria servers. Reports could be downloaded from the associated website (Farmlife™) such as raw data by individual for set date ranges, and branded reports related to pre-set alerts for hyperthermia. The threshold for hyperthermia set by the manufacturer is 41.2°C.

Descriptive data with regard to raw temperature captured for the CASE and CONT animals in both replicates are provided in the charts below in **Figures 18-41**. The manufacturer's hyperthermia alert threshold of 41.2°C is demonstrated by the red dash line. Recordings of significant temperature drops to below 38°C were associated with drinking episodes.

4.12.1 Replicate 1 CASE series: reticulo-rumen temperature temporal profiles

Figure 18. Study animal R1_89, diagnosed with BRD – reporting lung consolidation of 12.3% at necropsy.

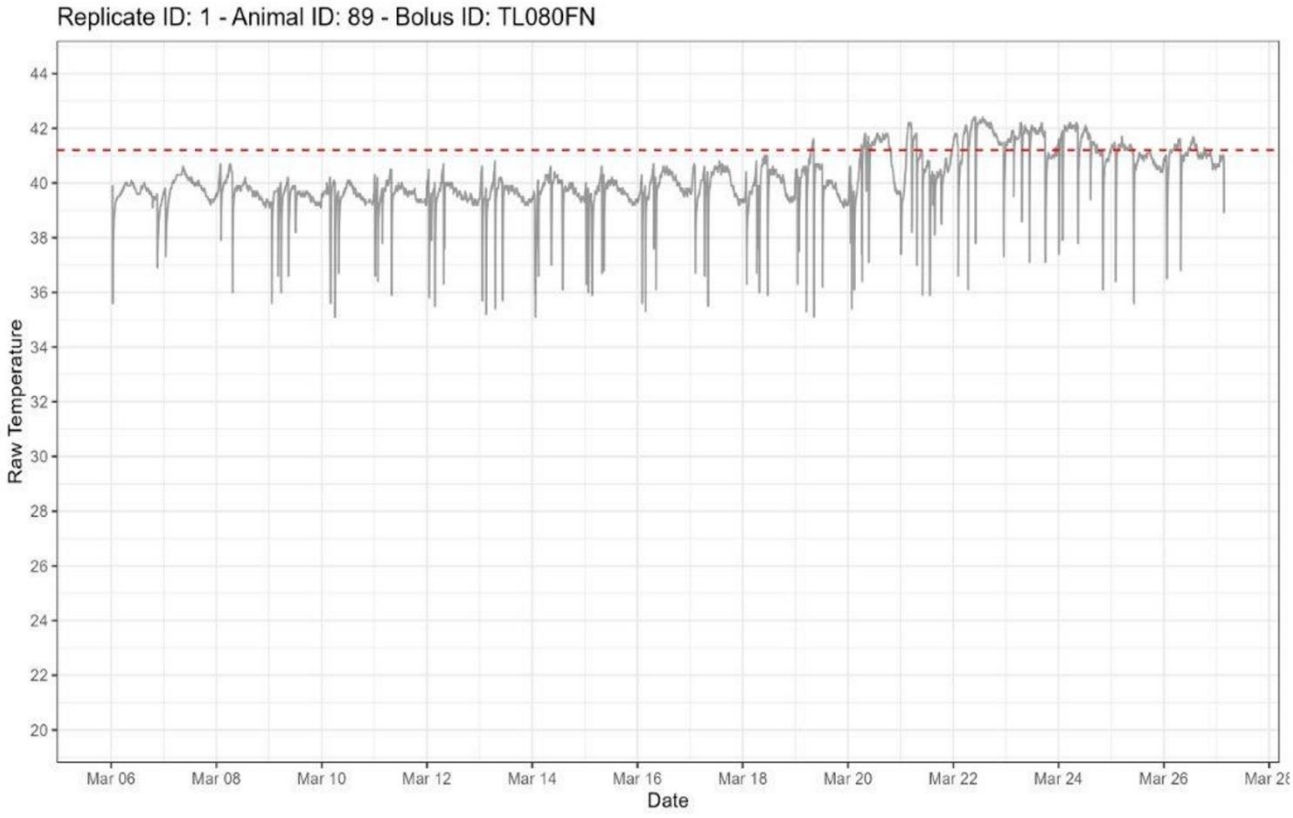

Figure 19. R1_110 - *Consolidation = 3.4%.*

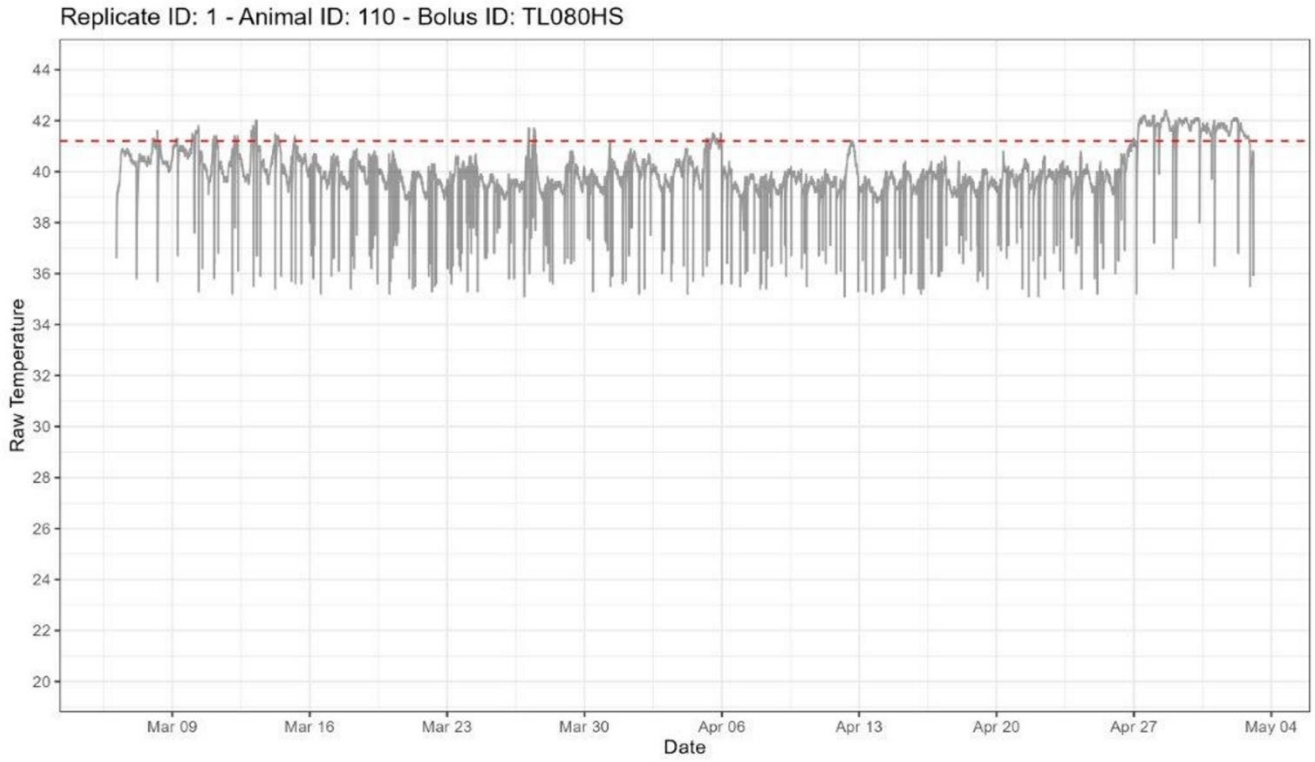

Figure 20. R1_130 - *Consolidation = 12.5%.*

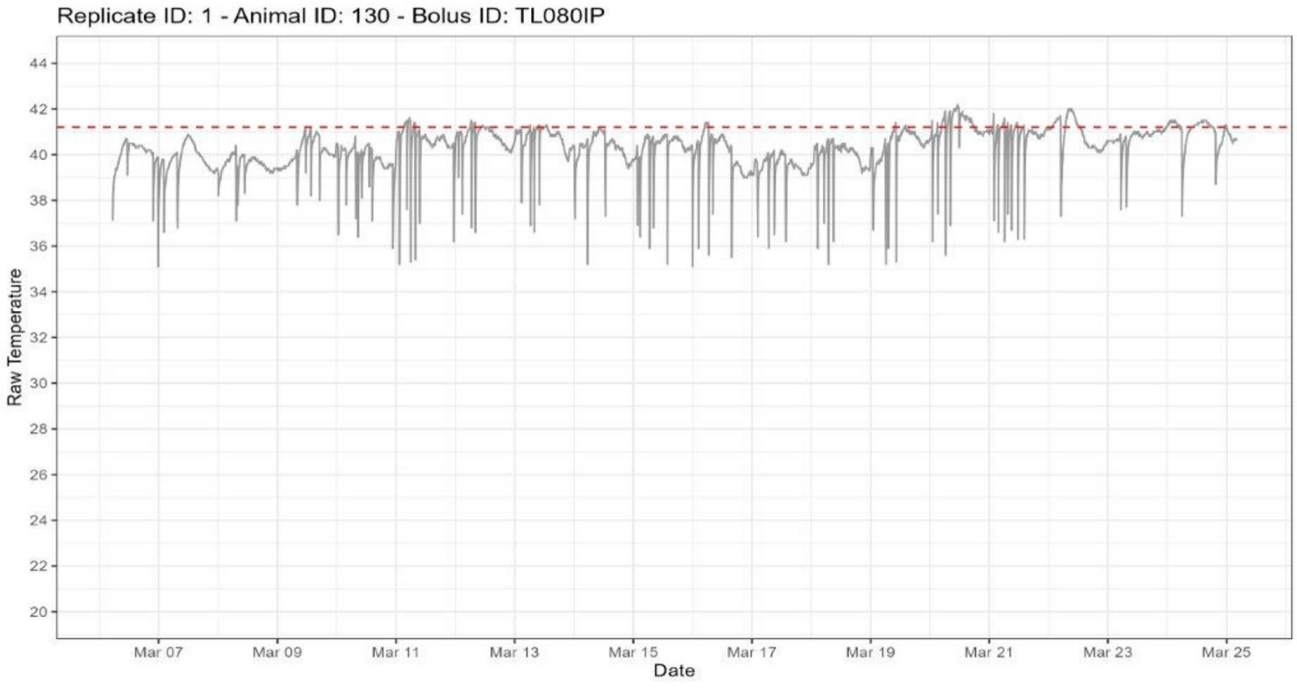

4.12.2 Replicate 1 FALSE NEGATIVE reticulo-rumen temperature temporal profile

Figure 21. R1_168 - *Consolidation = 2.5%.*

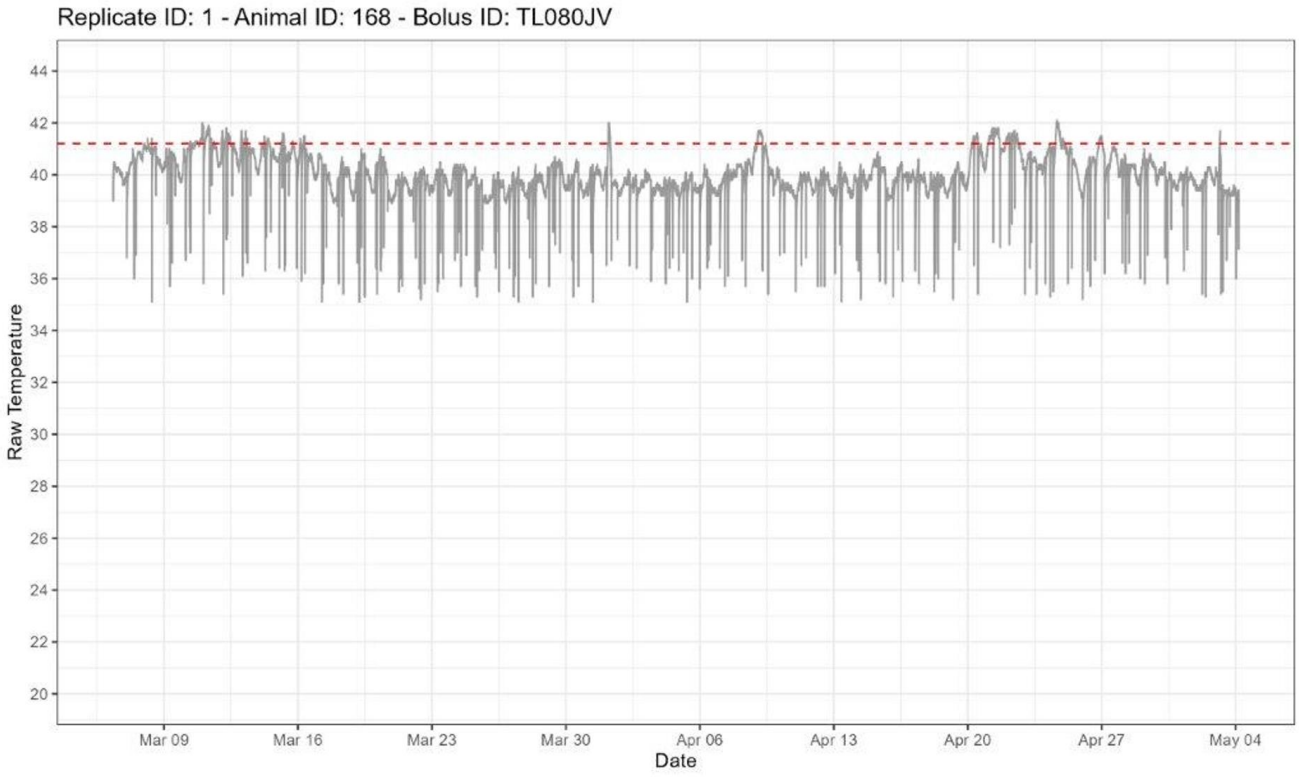

4.12.3 Replicate 1 CONT series reticulo-rumen temperature temporal profiles

Figure 22. R1_25.

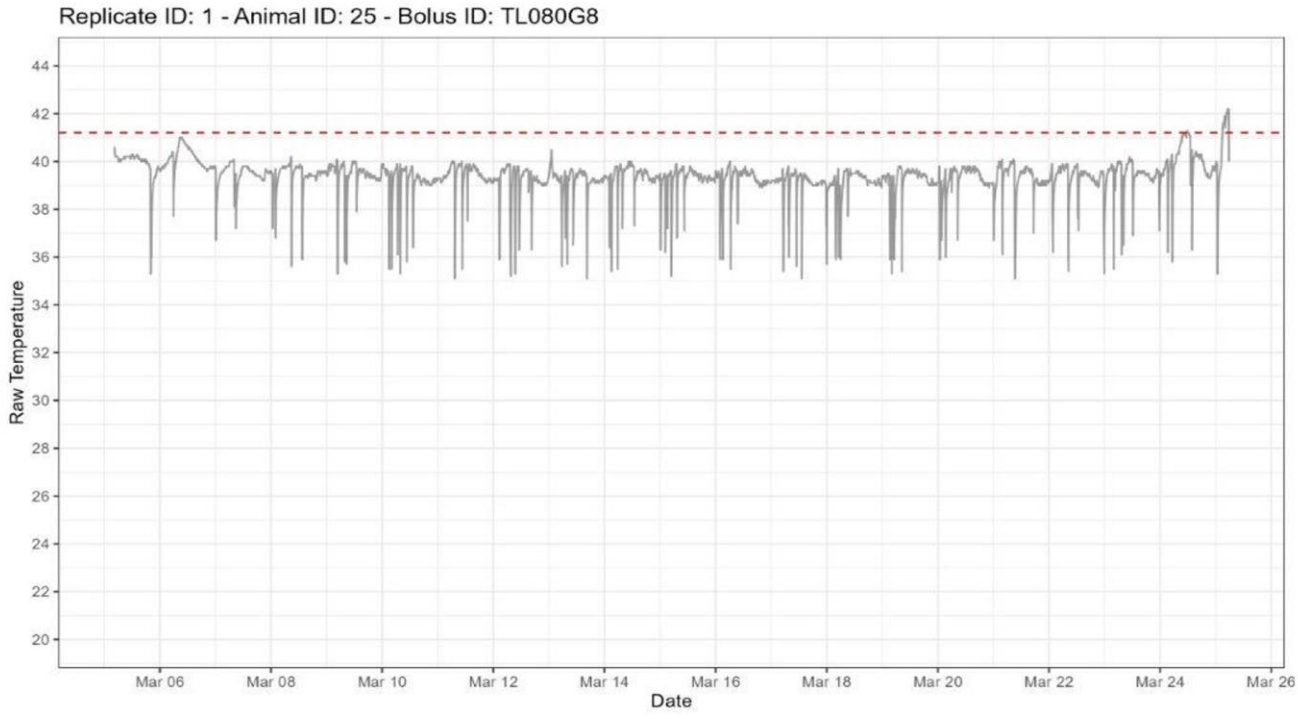

Figure 23. R1_60.

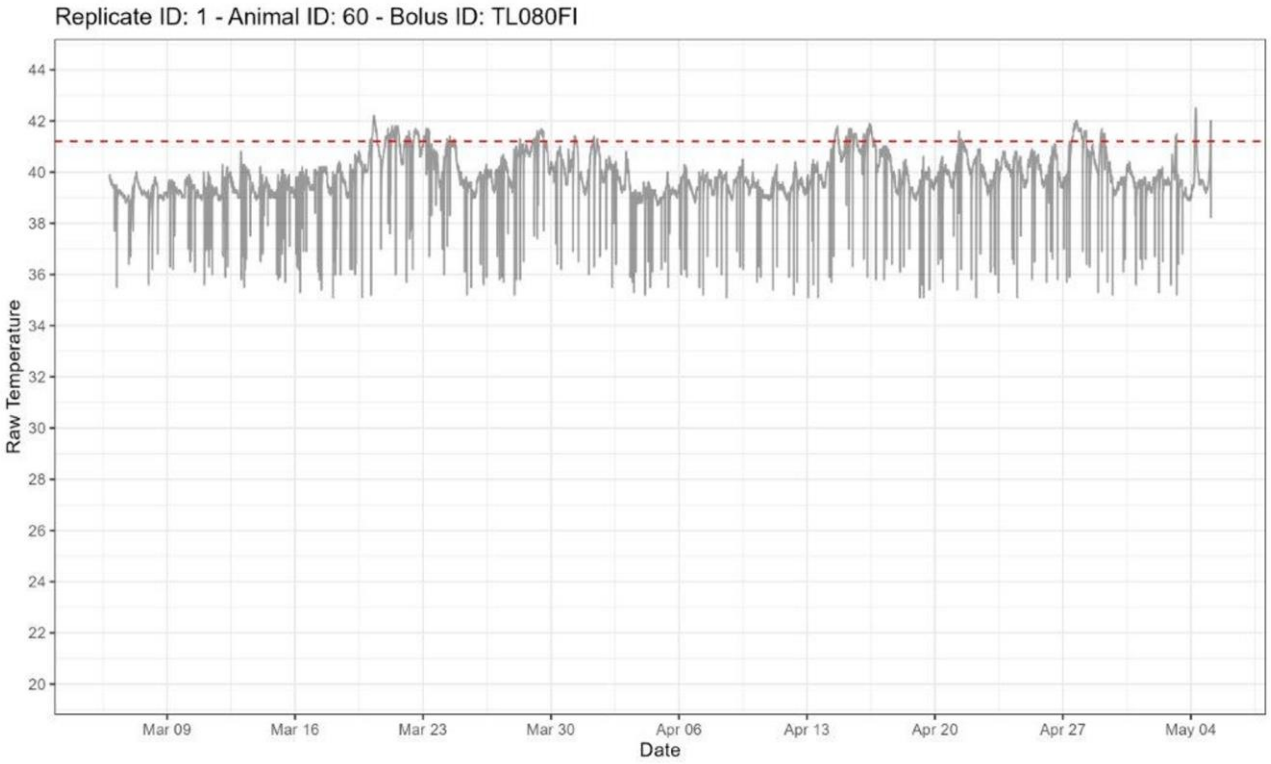

Figure 24. R1_92.

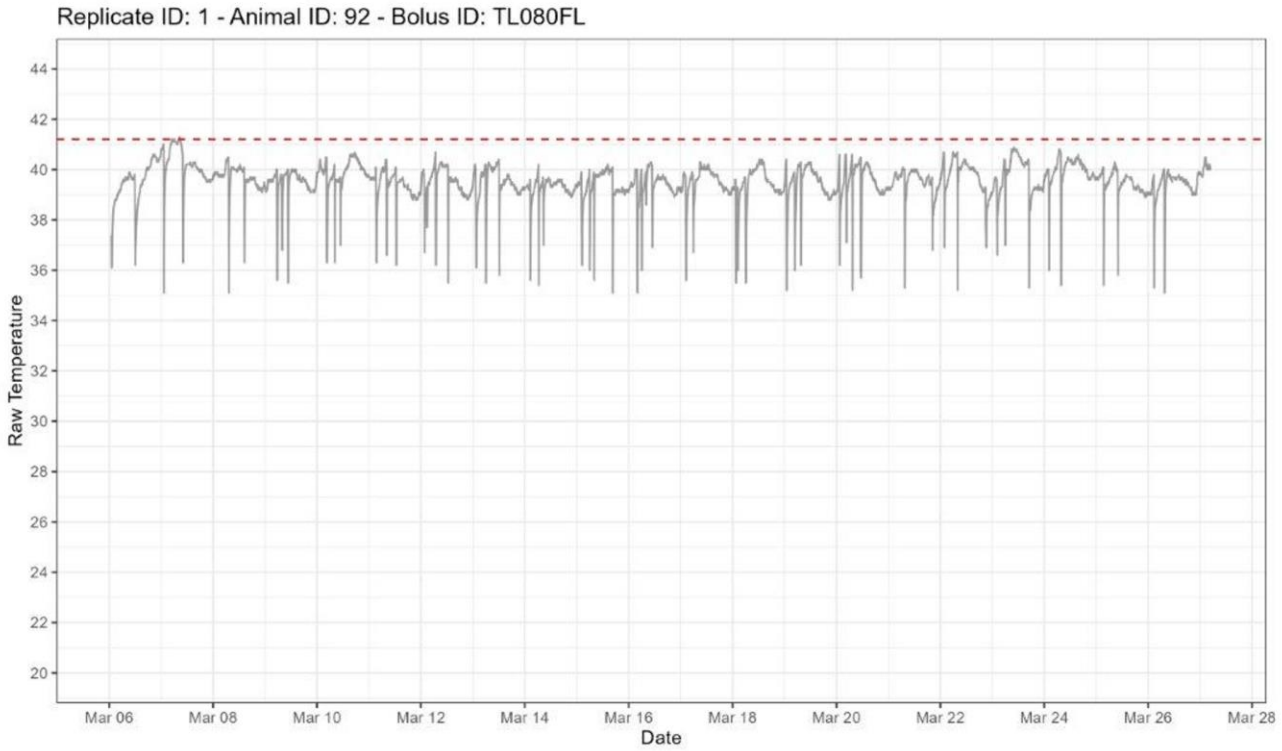

4.12.4 Replicate 1 FALSE POSITIVE series reticulo-rumen temperature temporal profiles

Figure 25. R1_109.

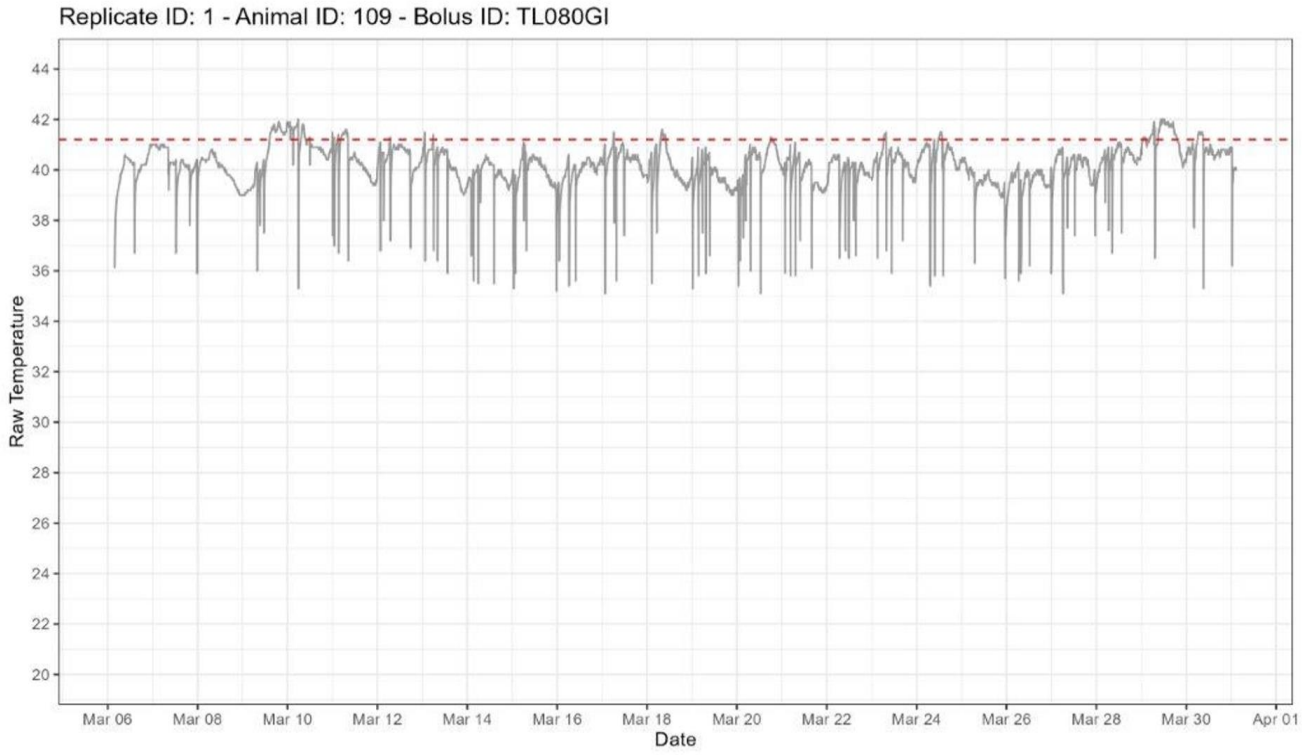

Figure 26. R1_113.

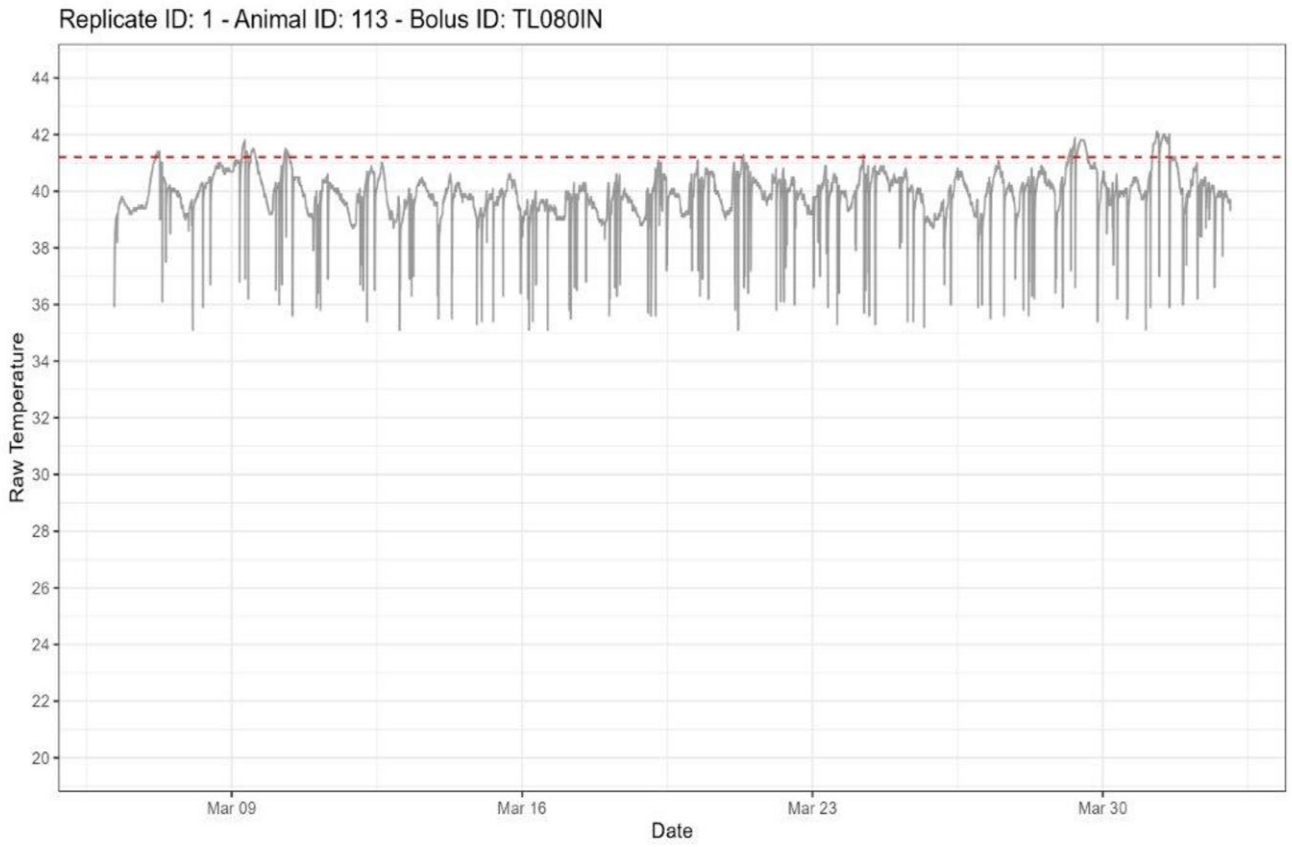

Figure 27. R1_159.

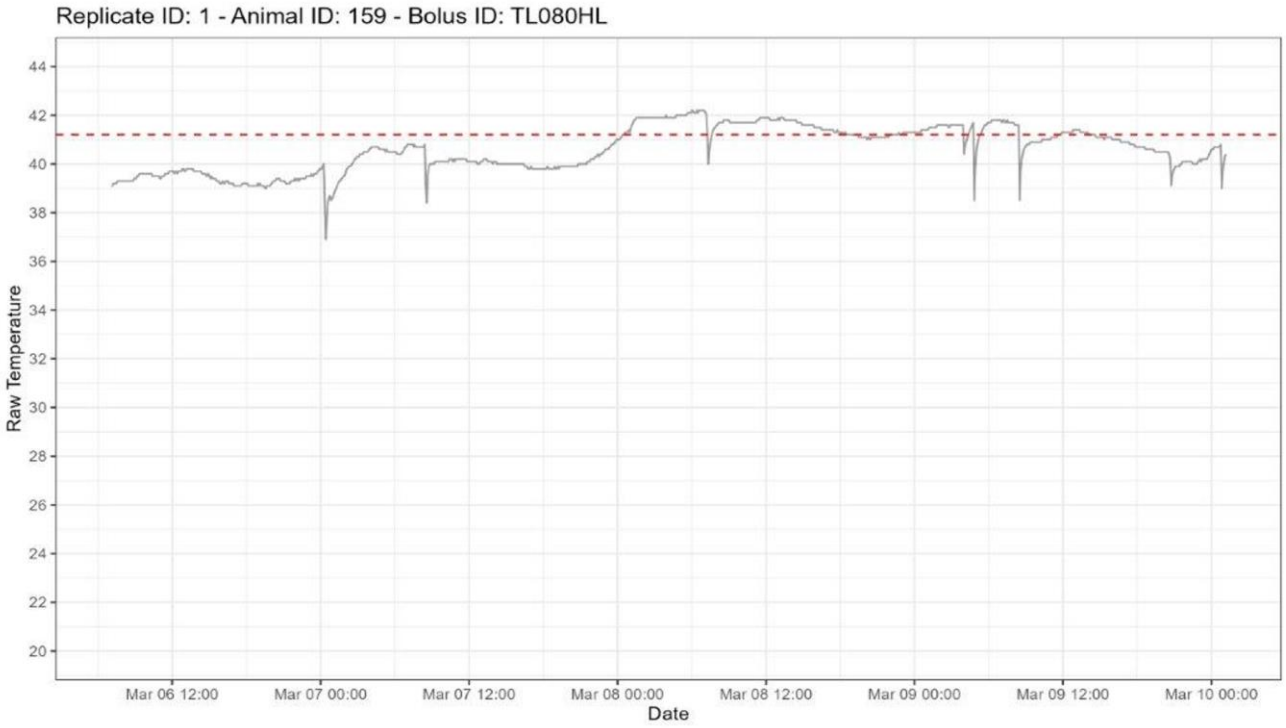

4.12.5 Replicate 2 CASE series reticulo-rumen temperature temporal profiles

Figure 28. R2_2 - *Consolidation = 64.11%.*

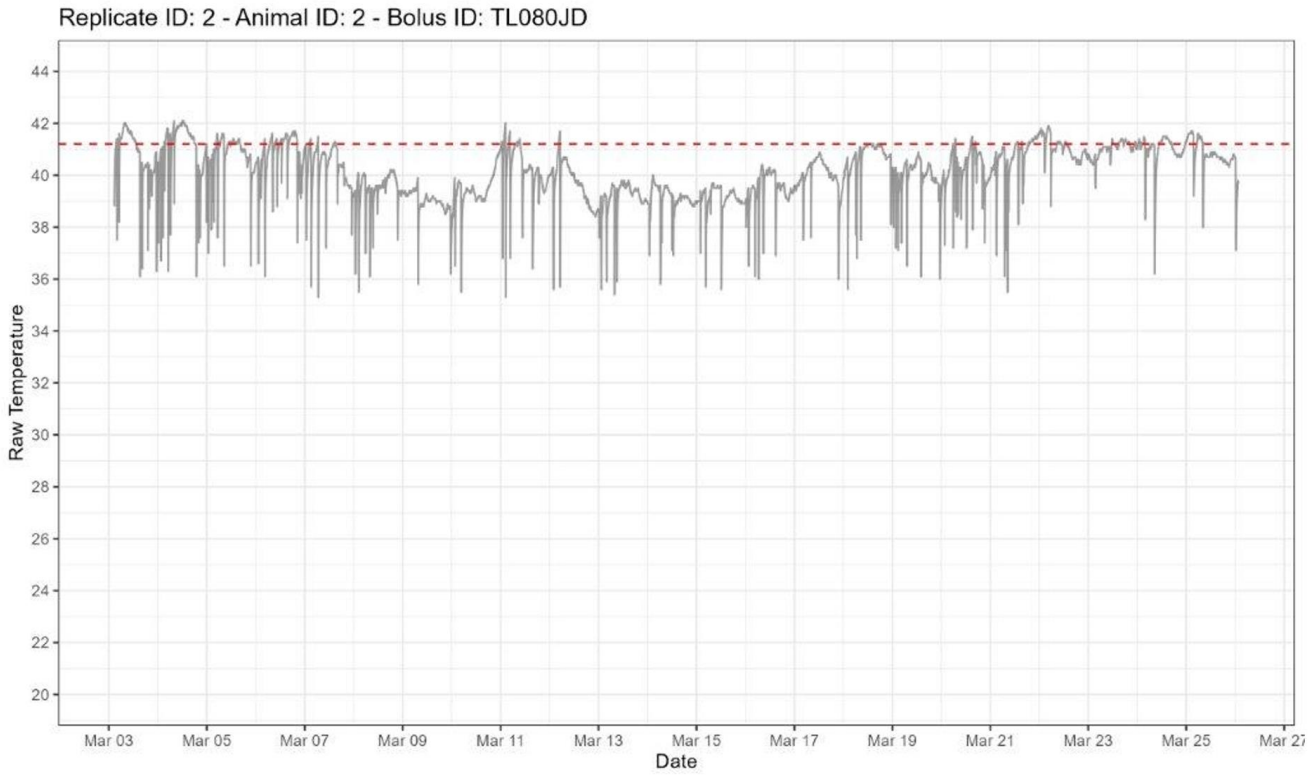

Figure 29. R2_8 - *Consolidation = 64.32%.*

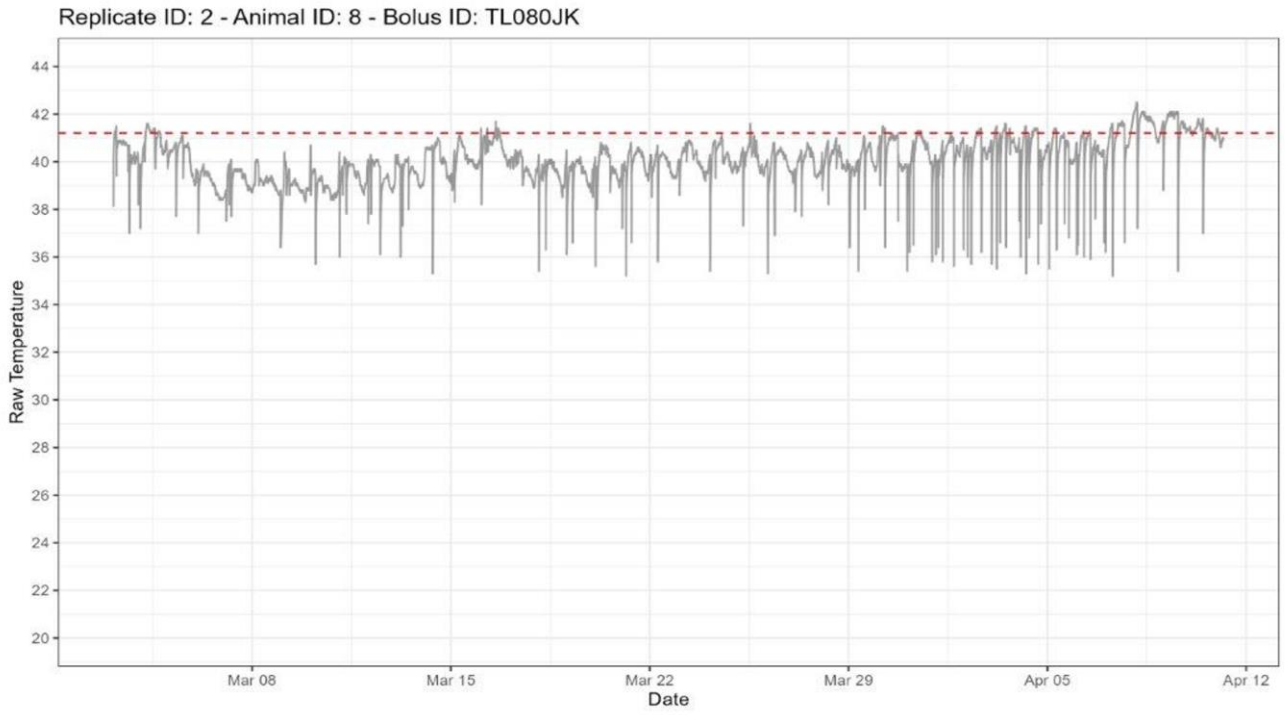

Figure 30. R2_25 - *Consolidation = 27.68%.*

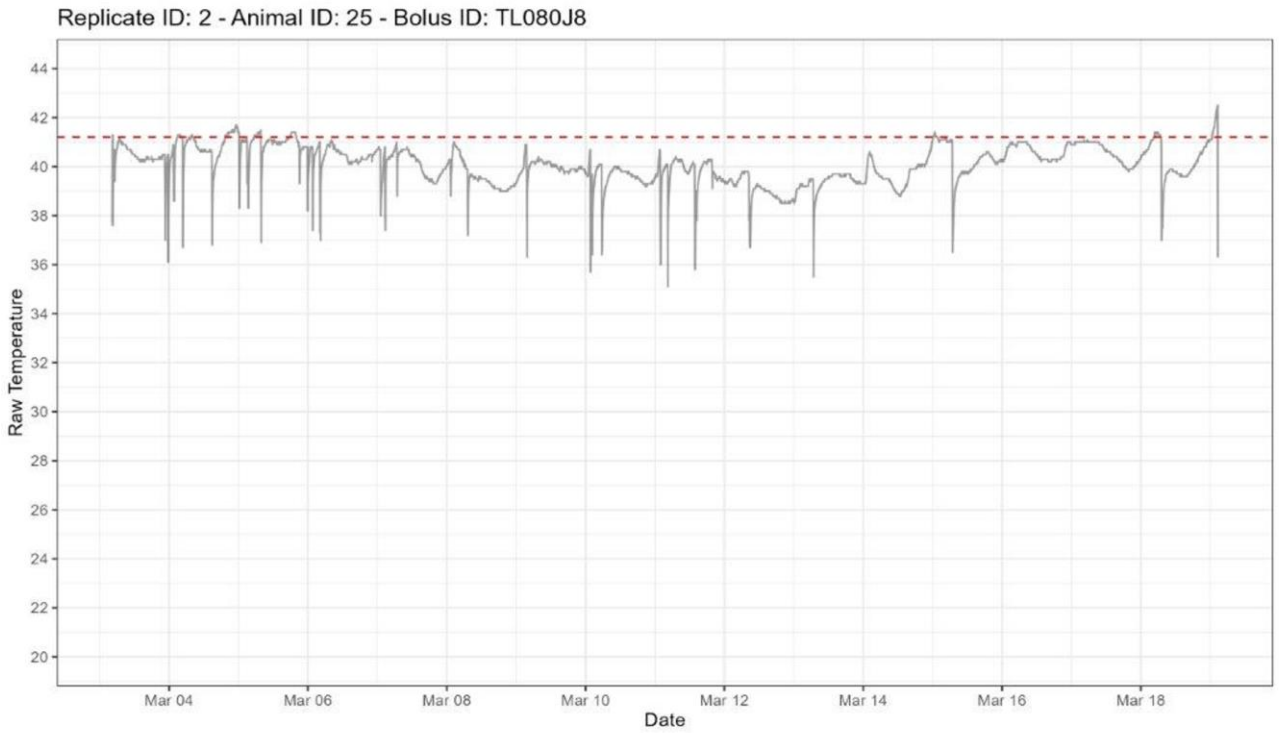

Figure 31. R2_58 - *Consolidation = 19.59%.*

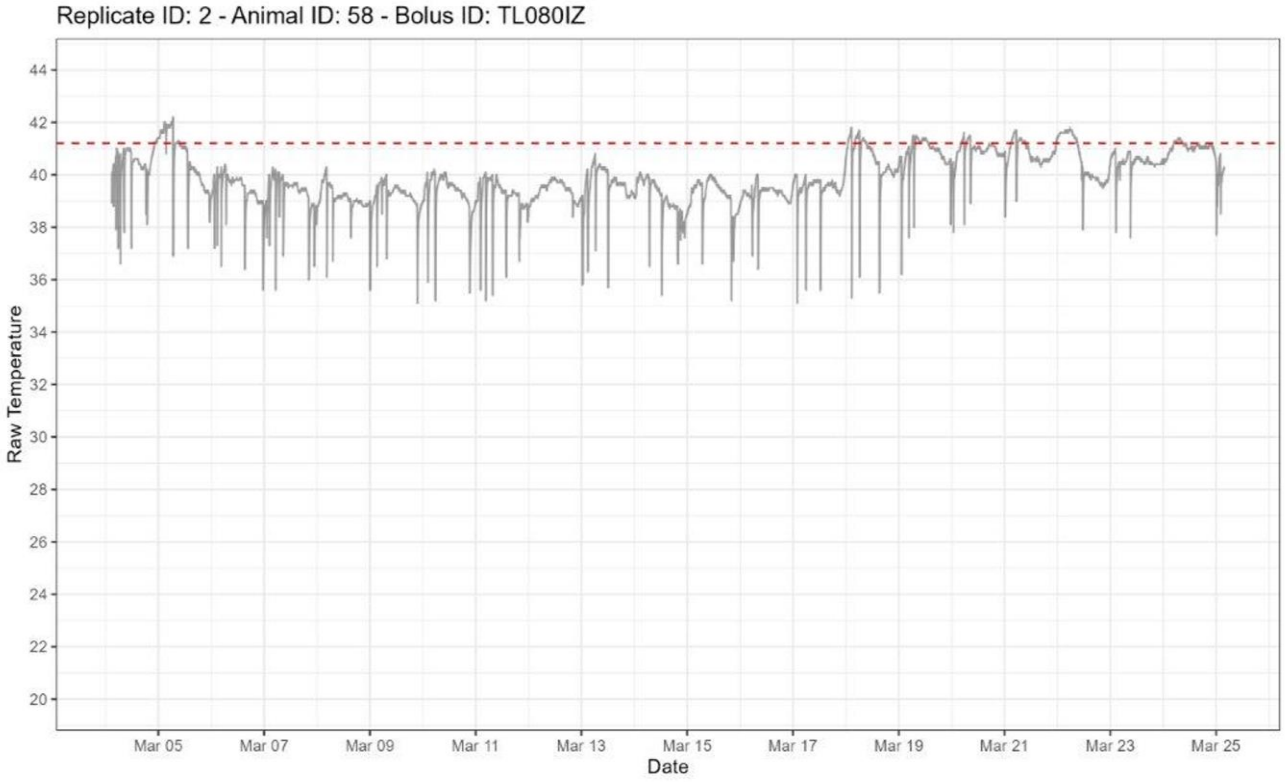

Figure 32. R2_59 - *Consolidation = 5.76%.*

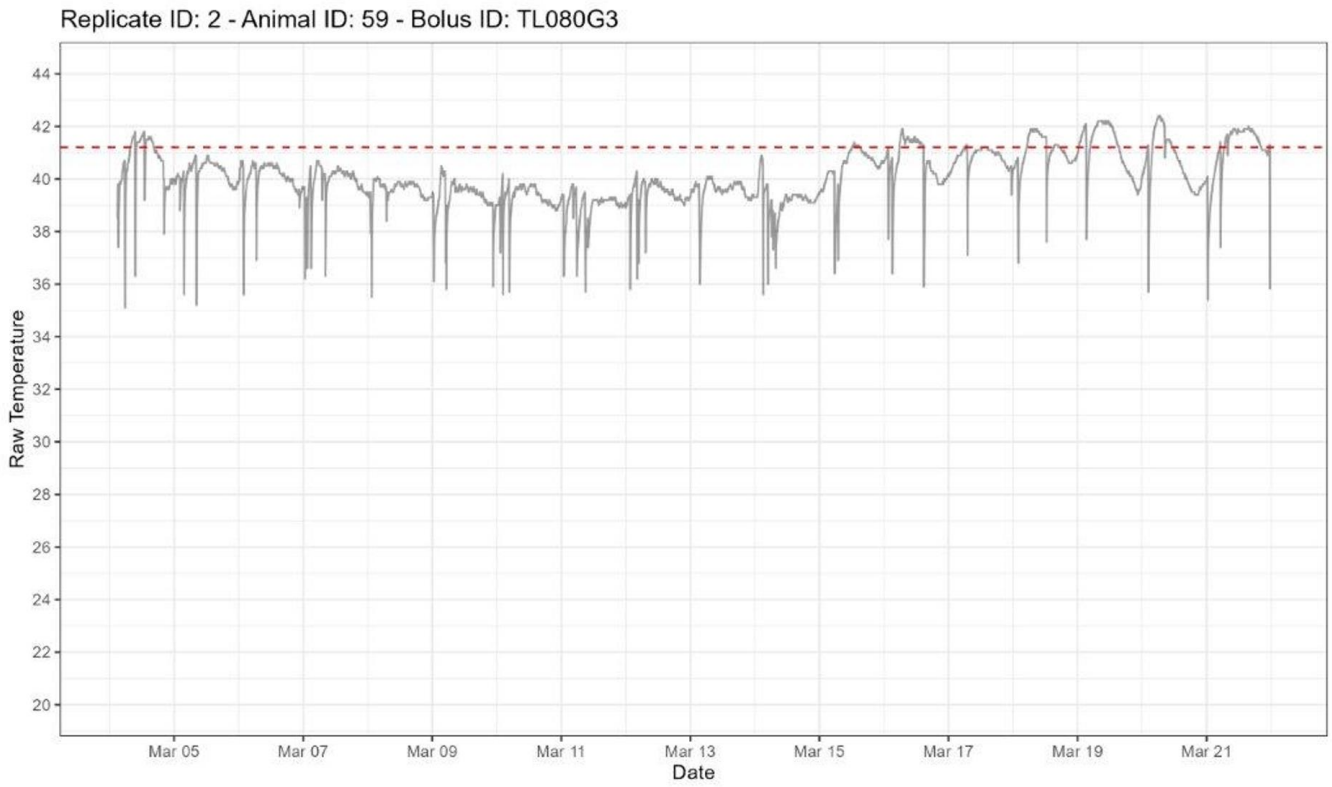

Figure 33. R2_101 - *Consolidation = 39.97%.*

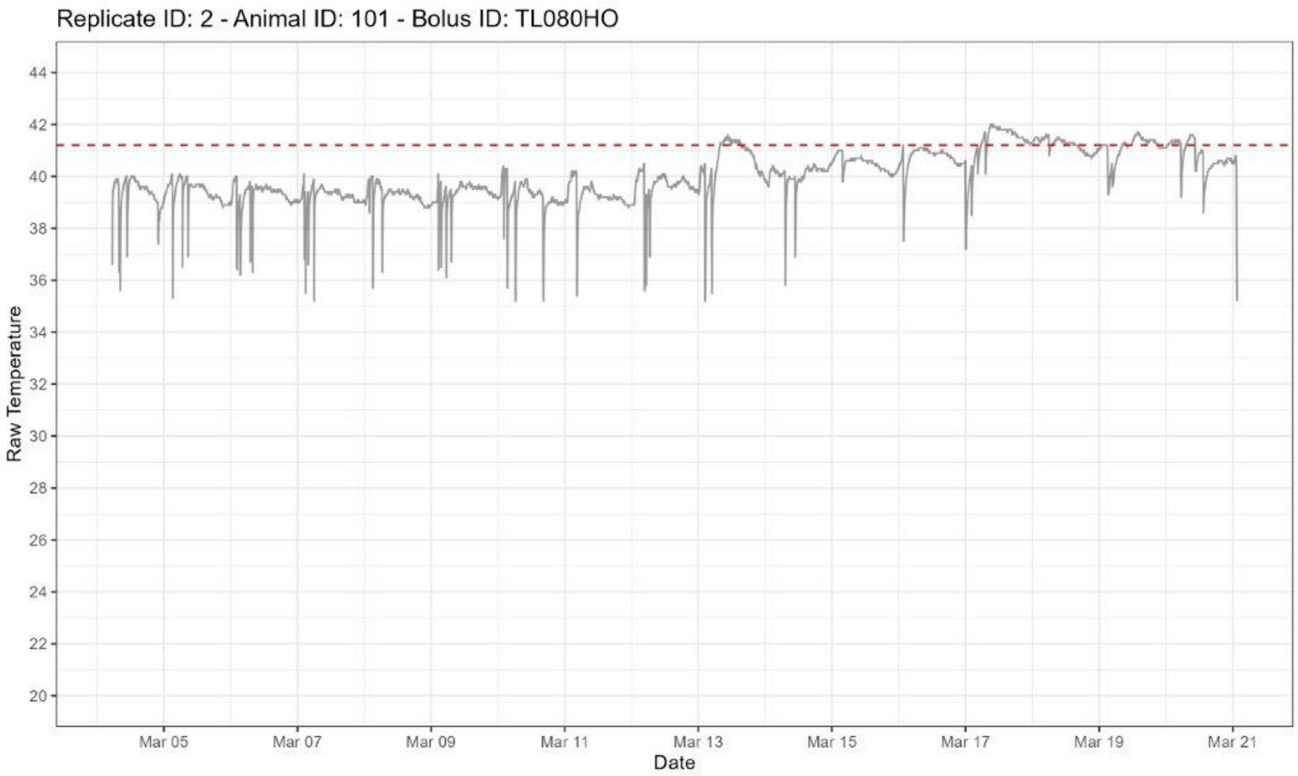

Figure 34. R2_181 - *Consolidation = 5.79%.*

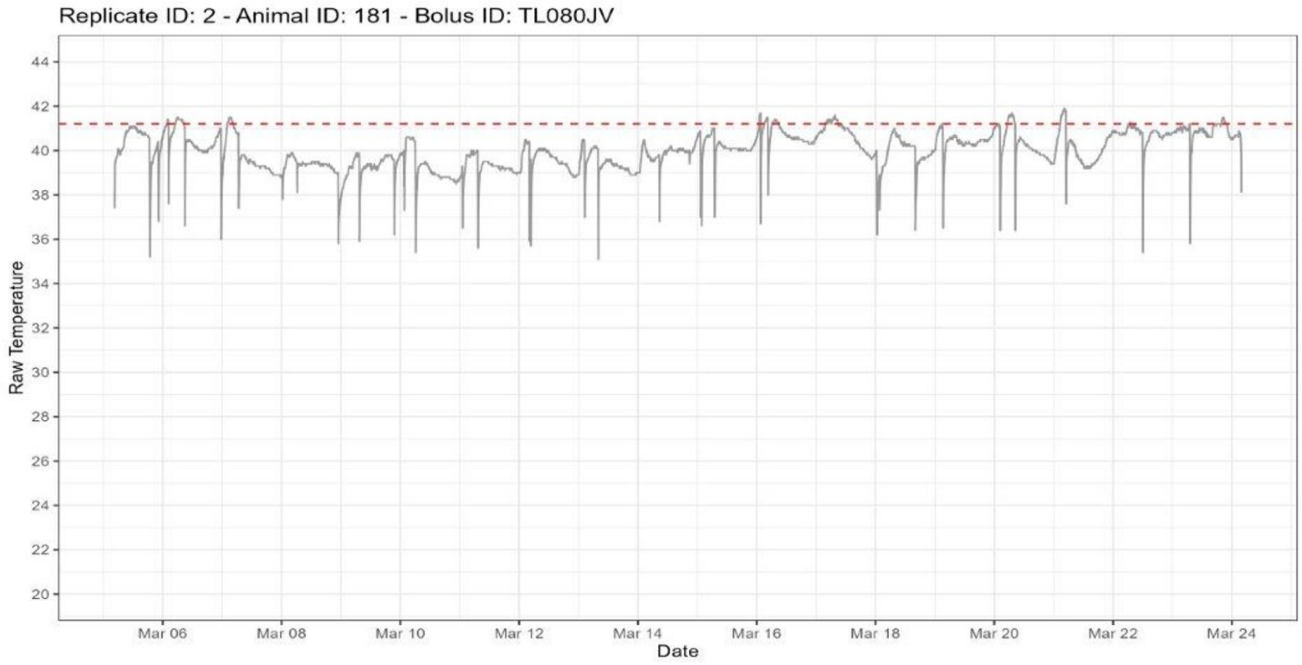

4.12.6 Replicate 2 CONT series reticulo-rumen temperature temporal profiles

Figure 35. R2_60.

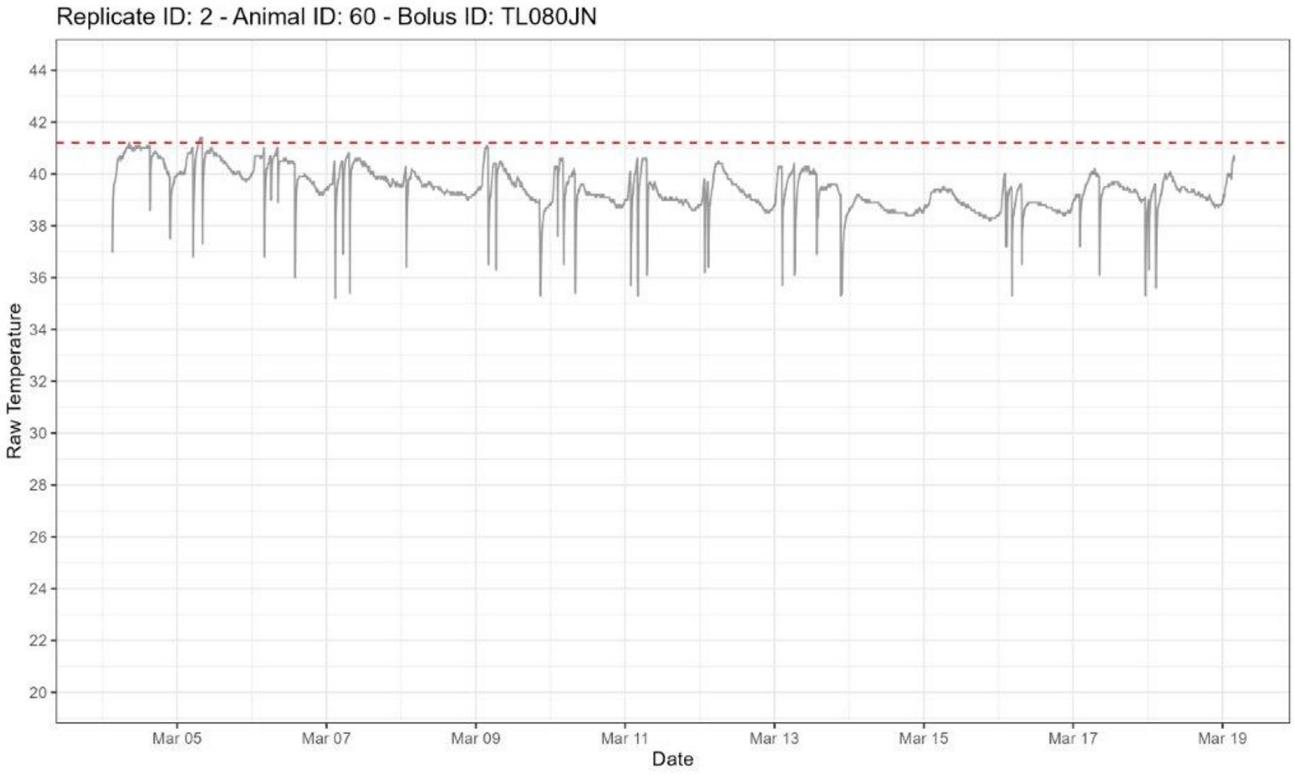

Figure 36. R2_67.

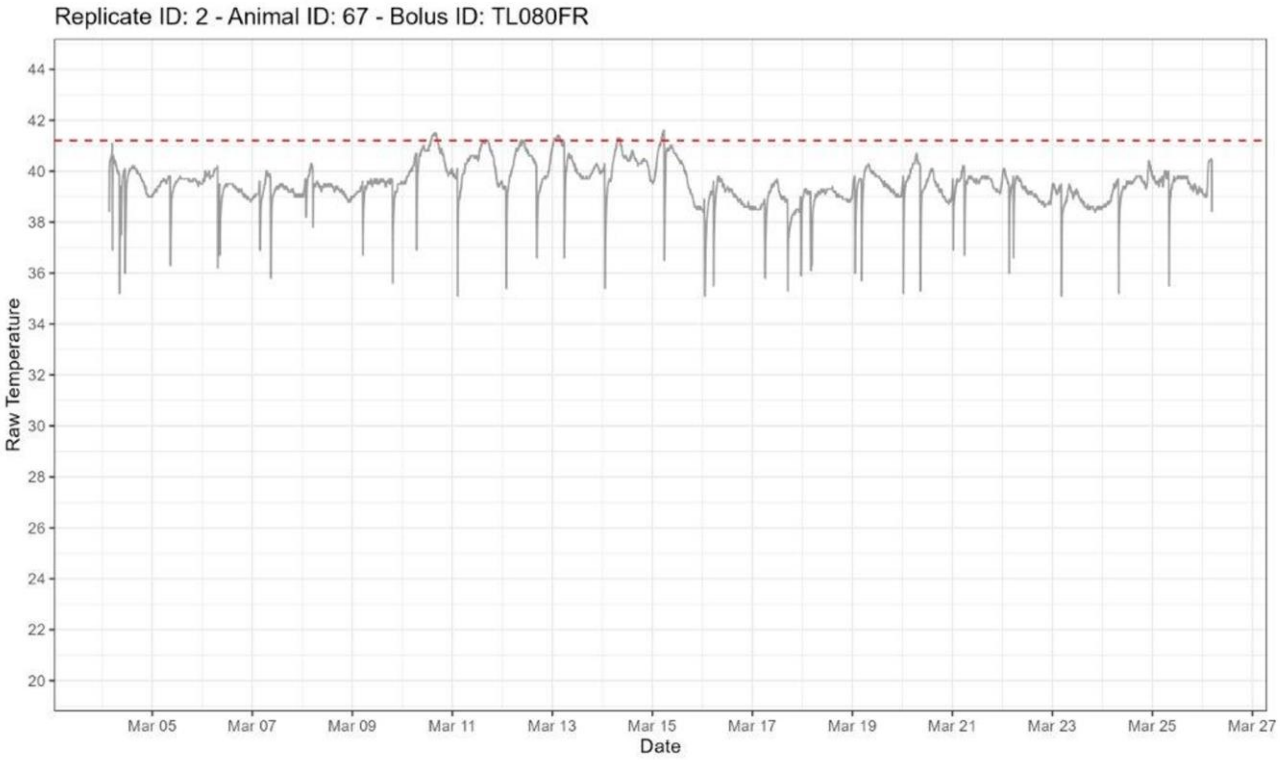

Figure 37. R2_76.

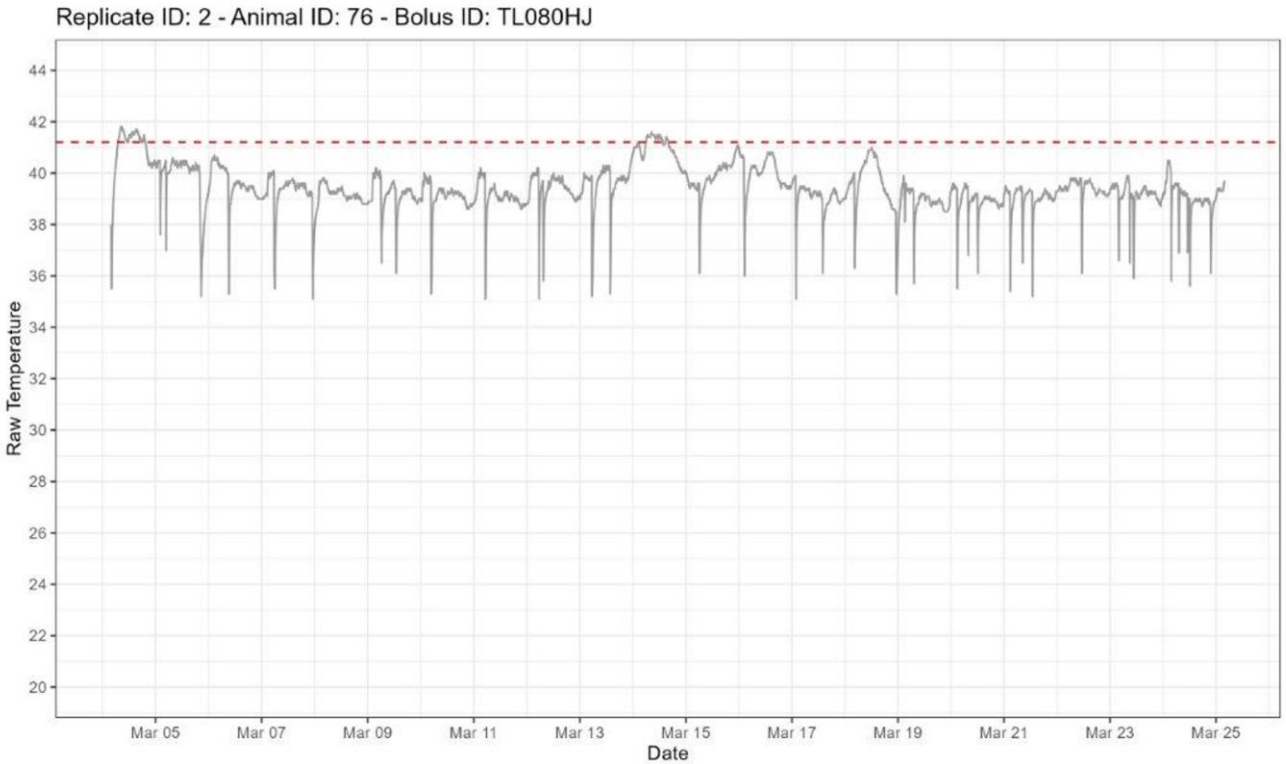

Figure 38. R2_86.

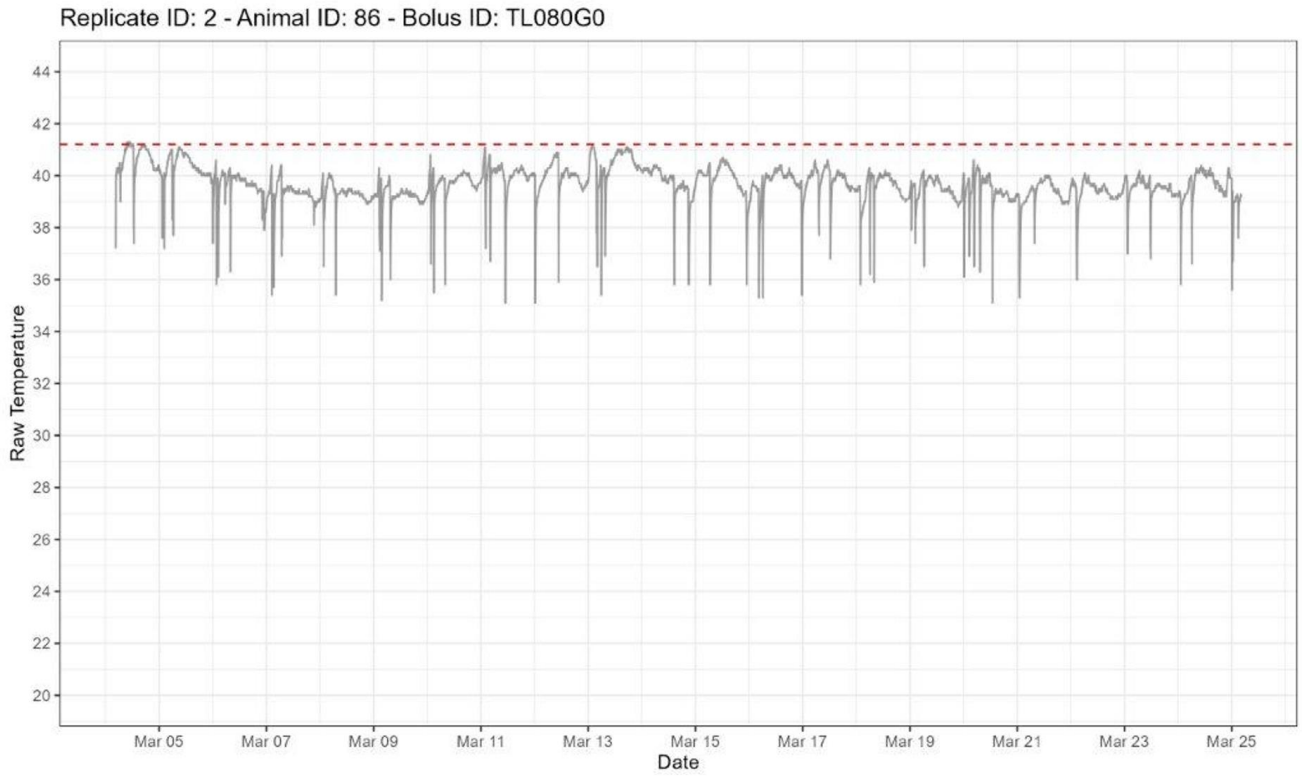

Figure 39. R2_113.

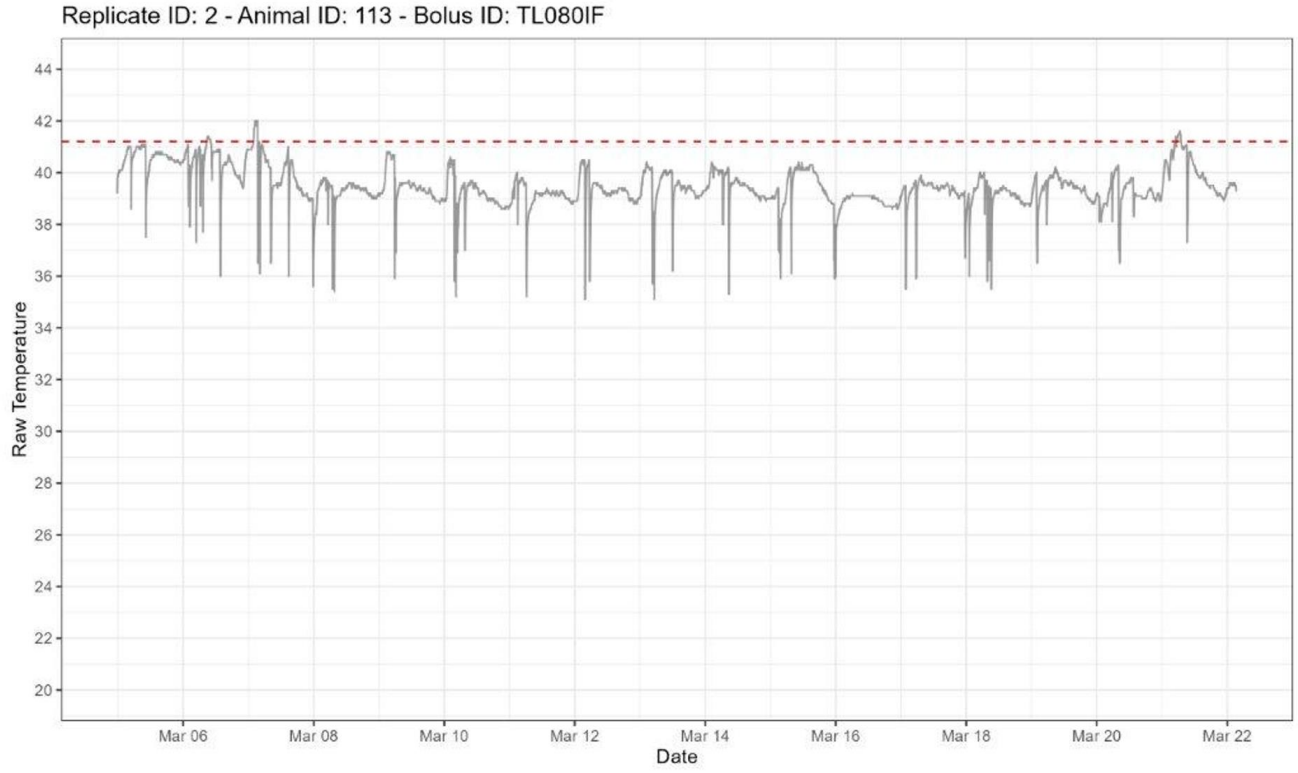

Figure 40. R2_134.

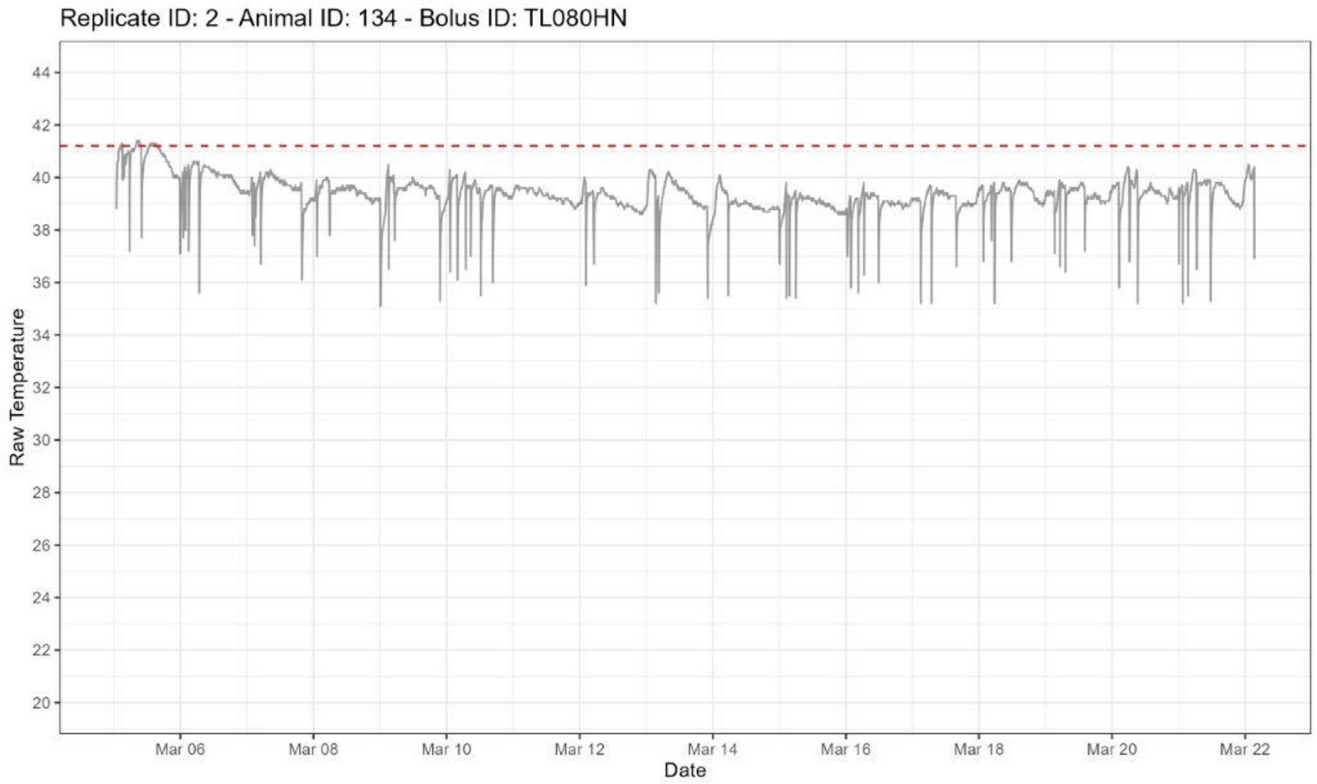

Figure 41. R2_144.

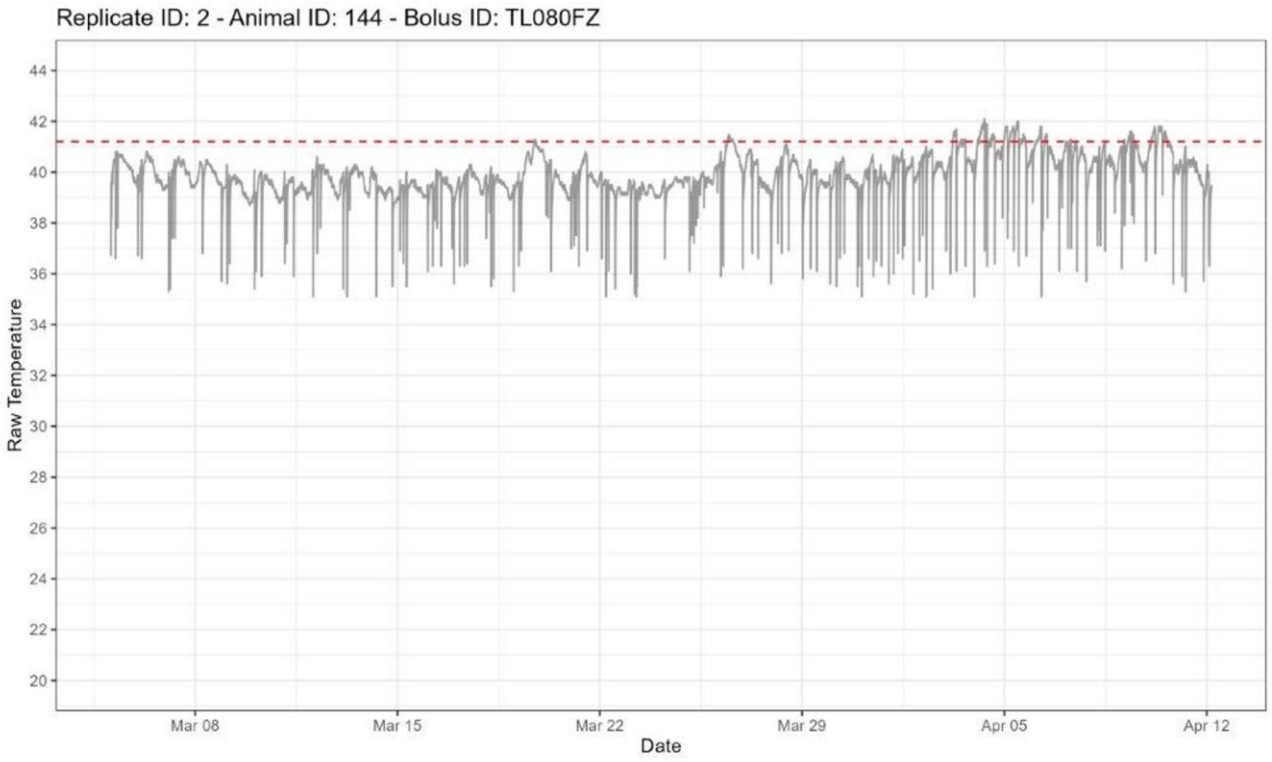

4.12.7 Diagnostic models based on reticulo-rumenal bolus temperature

Review of the plotted data indicated that formally enrolled CASE animals generally recorded temperatures above the manufacturer's hyperthermia threshold alert more frequently than CONT animals. A disparity existed between replicate 1 and 2 for data captured per individual bolus used, despite that fact that replicate 1 boluses were re-used for replicate 2. Extensive communication and engagement with the manufacturer couldn't resolve retrieving data that had similar data count numbers for similar time periods in each replicate. The differing temperature data count effect was equivalent within CASEs and CONTs of each replicate – i.e. data count disparity was not operating between the CASEs and CONTs of either replicate.

Consequently, an approach to build a model to explain the response variable of CASE or CONT classification, was to use *proportion* of temperature counts above the 41.2°C threshold as the explanatory variable. Given the query was one of dichotomous classification to identify CASE or CONT, a logistic regression was performed **(Figure 42)**.

Figure 42. Logistic regression model of proportion of temperature data counts above 41.2°C to classify CASE or CONT status.

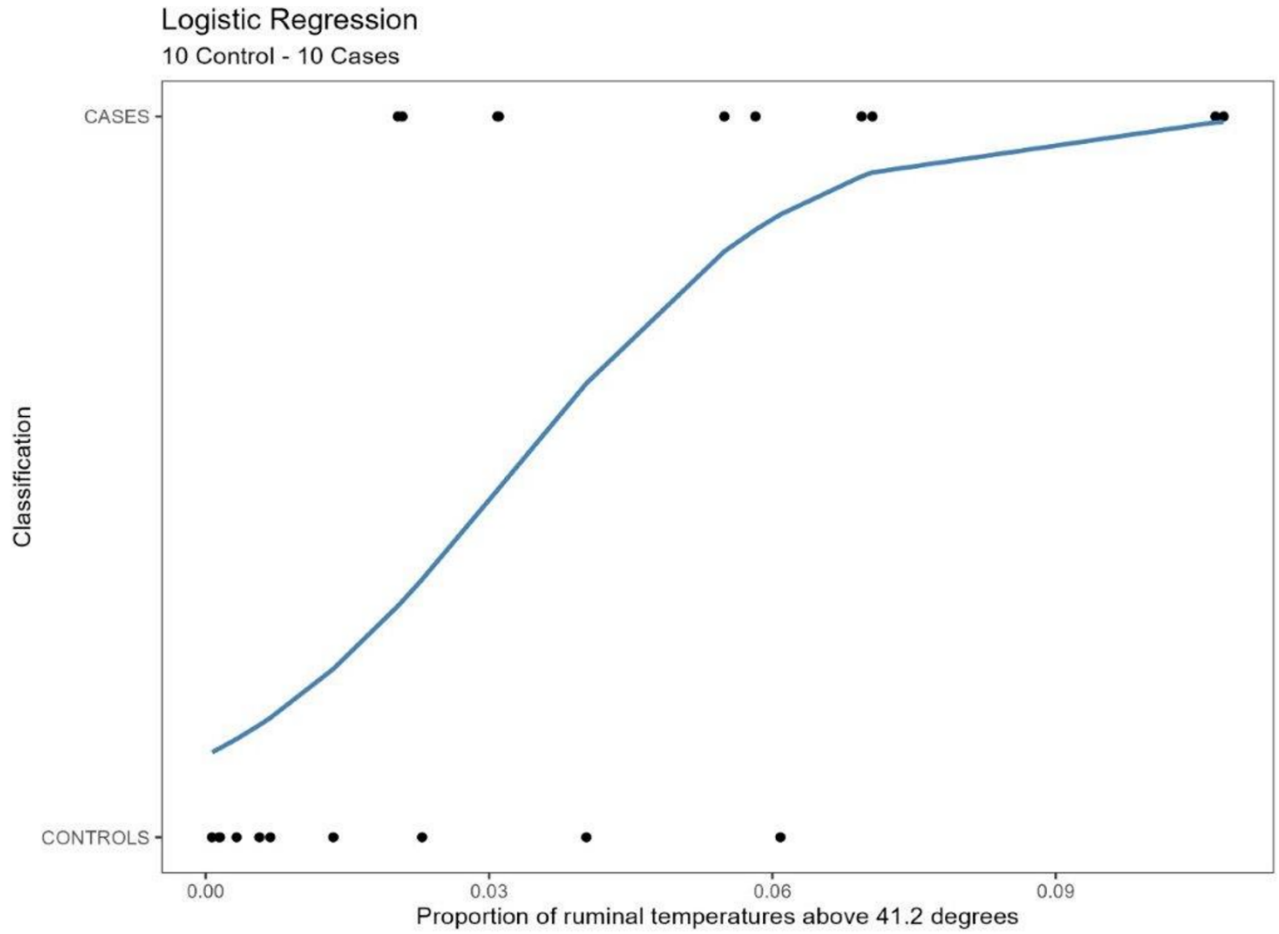

The model performed well to classify CASEs and CONTs using the explanatory variable as described.

In order to build prediction models to diagnose BRD CASEs by reticulo-rumen temperature, based on the experimental results, a classification tree approach was used, with the following elements included:

- Models based on prediction thresholds of 100, 180, 250 and 350 counts of data above the bolus hyperthermia threshold of 41.2°C, *since bolus placement.*
- Model training data was censored to within 72 hours of CASE and CONT formal enrolment, so as to examine the utility of the models as early detection modalities, replicating at least 36 hours detection in advance of the first CIS >= 2 observation as recorded in the study.

A summary of the output from the four classification tree models is provided below in **Table 34.**

Table 34. Heat map of thermobolus correct and misclassifications in replicate 1 and 2 with 72 hour censor.

Classification Tree Model with 72 Hour Censor

Thresholds: 1, 100, 180, 250, 350

					Outcome	Prediction Thresholds				
Replicate ID	Animal ID	Total Temp Count	Temp Count Above 41.2	Proportion Above 41.2	Analysis Status	1	100	180	250	350
1	25	5088	0	0.000	CONT	CONT	CONT	CONT	CONT	CONT
1	60	16366	1879	0.115	CONT	CASE	CASE	CASE	CASE	CASE
1	89	5428	1075	0.198	CASE	CASE	CASE	CASE	CASE	CASE
1	92	5399	24	0.004	CONT	CASE	CONT	CONT	CONT	CONT
1	110	15945	1850	0.116	CASE	CASE	CASE	CASE	CASE	CASE
1	130	4809	780	0.162	CASE	CASE	CASE	CASE	CASE	CASE
2	2	6007	1011	0.168	CASE	CASE	CASE	CASE	CASE	CASE
2	8	10611	927	0.087	CASE	CASE	CASE	CASE	CASE	CASE
2	25	3978	198	0.050	CASE	CASE	CASE	CASE	CONT	CONT
2	58	5426	532	0.098	CASE	CASE	CASE	CASE	CASE	CASE
2	59	4557	576	0.126	CASE	CASE	CASE	CASE	CASE	CASE
2	60	3694	18	0.005	CONT	CASE	CONT	CONT	CONT	CONT
2	67	5696	162	0.028	CONT	CASE	CASE	CONT	CONT	CONT
2	76	5374	270	0.050	CONT	CASE	CASE	CASE	CASE	CONT
2	86	5376	38	0.007	CONT	CASE	CONT	CONT	CONT	CONT
2	101	3959	322	0.081	CASE	CASE	CASE	CASE	CASE	CONT
2	113	4306	39	0.009	CONT	CASE	CONT	CONT	CONT	CONT
2	134	4291	79	0.018	CONT	CASE	CONT	CONT	CONT	CONT
2	144	10328	649	0.063	CONT	CASE	CASE	CASE	CASE	CASE
2	181	4832	297	0.061	CASE	CASE	CASE	CASE	CASE	CONT

A bar chart representation of temperature counts above the manufacturer's threshold for the 180 count model is demonstrated in **Figure 43**. For the individual CASE and CONT enrolments, the counts above the threshold and correct classification or misclassification are shown.

Figure 43. Classification tree prediction model at count threshold above 41.2°C = 180.

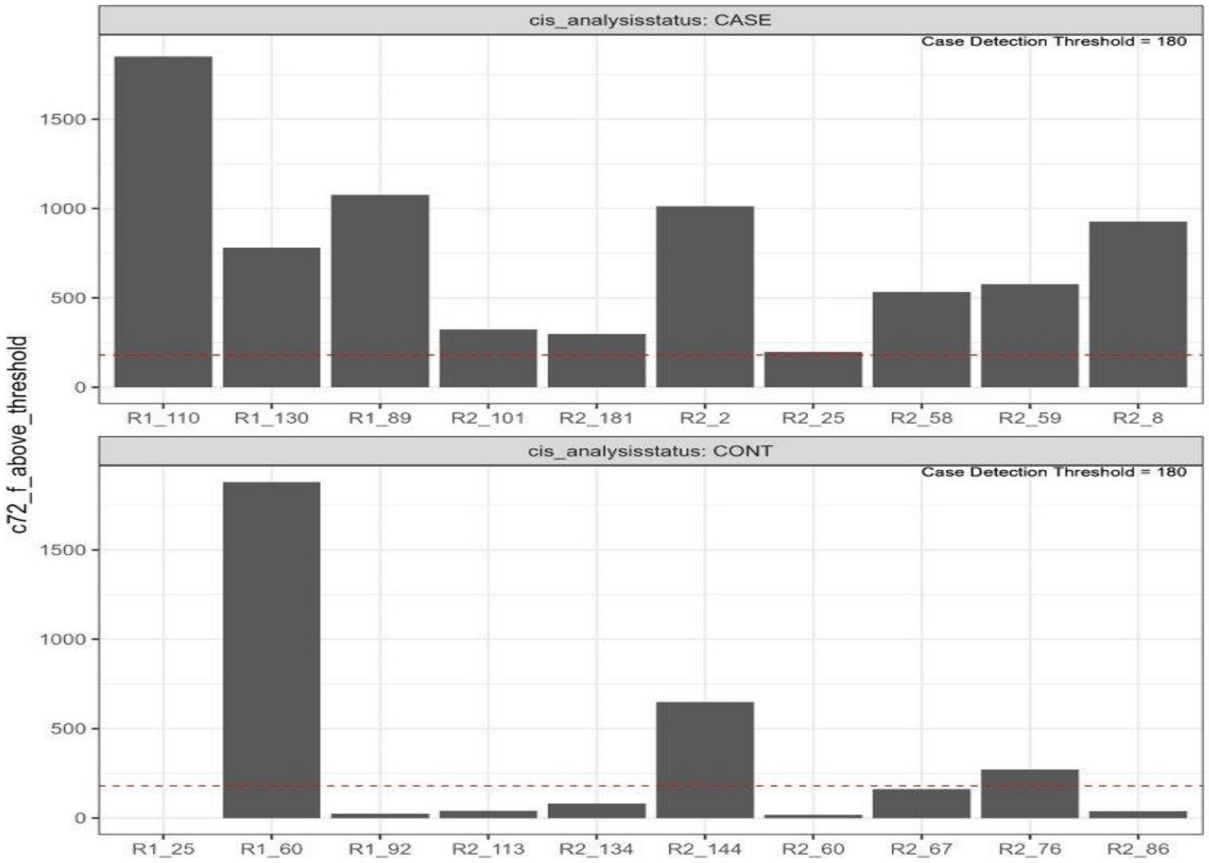

The reticulo-rumen bolus algorithms each represented different diagnostic characteristics as presented in **Table 35.**

Table 35. Diagnostic evaluation of the four bolus algorithms to classify animals with normal or abnormal rumen temperature.

		T-100	
		ABNORM	**NORM**
TRUE Status	**CASE**	10	0
	CONT	4	6

Sensitivity:	*100%*
Specificity:	*60%*

		T-180	
		ABNORM	**NORM**
TRUE Status	**CASE**	10	0
	CONT	3	7

Sensitivity:	*100%*
Specificity:	*70%*

		T-250	
		ABNORM	**NORM**
TRUE Status	**CASE**	9	1
	CONT	3	7

Sensitivity:	*90%*
Specificity:	*70%*

		T-350	
		ABNORM	**NORM**
TRUE Status	**CASE**	7	3
	CONT	2	8

Sensitivity:	*70%*
Specificity:	*80%*

4.12.8 Study animals with lung lesions at slaughter and reticulo-rumen temperature data

For study animals pulmonary scored at slaughter and having logged thermobolus data for the whole study period, the following analysis were conducted.

Figure 44. Logistic regression - pulmonary lesion score (normal/mild = < 5% consolidation and/or pleural score = 1 versus abnormal (case) => 5% consolidation and/or pleural score > 1) and average daily gain until harvest slaughter.

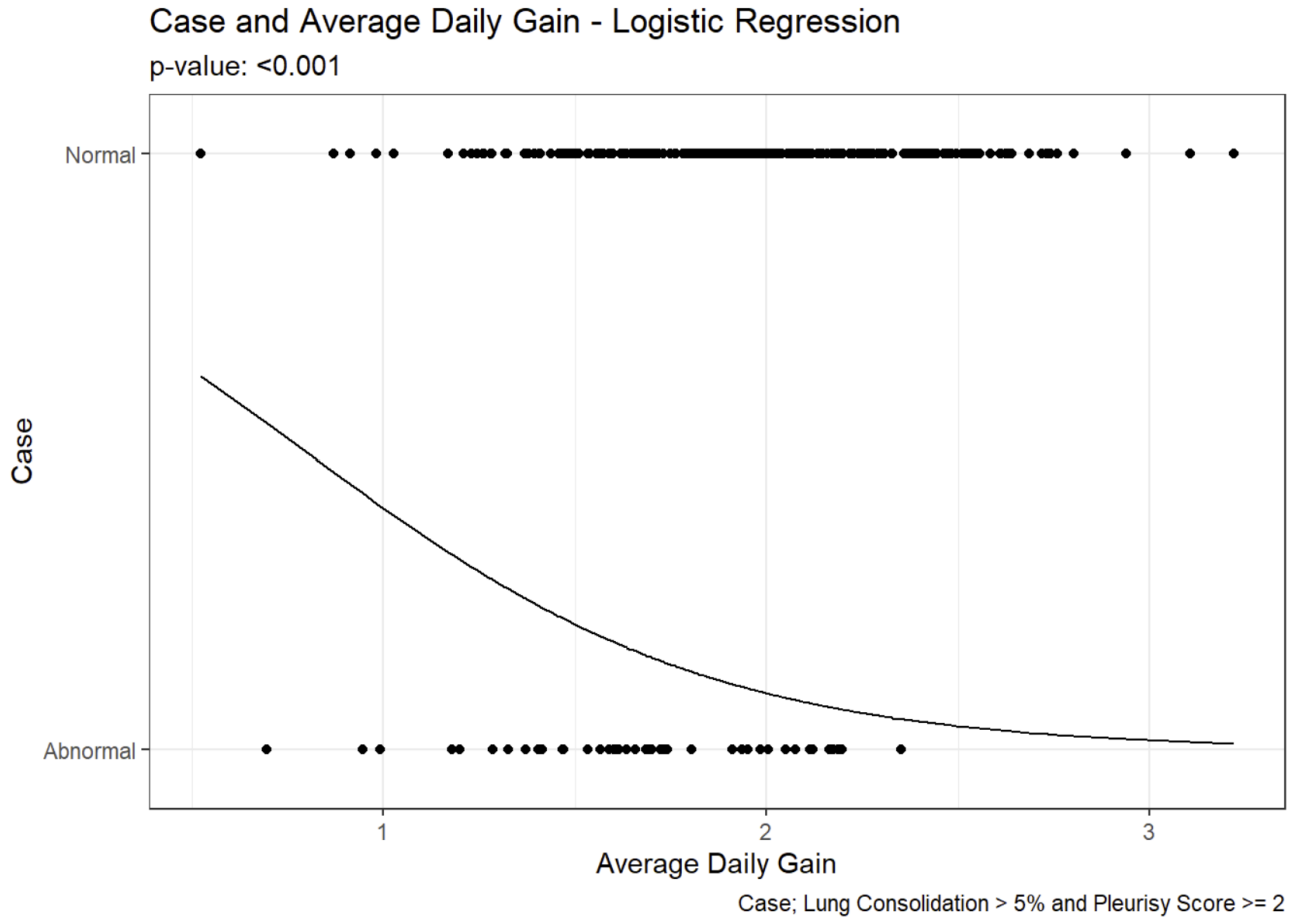

In **Figure 44**, there is a significant negative association (at the 95% confidence level) demonstrated between pulmonary lesions at slaughter (abnormal – case) and average daily gain. This holds agreement with findings in **Table 9.**

Figure 45. Boxplot of pulmonary score (normal/mild = < 5% consolidation and/or pleural score = 1, abnormal (case) => 5% consolidation and/or pleural score > 1) and thermobolus temperature count above manufacturers threshold = 41.2°C.

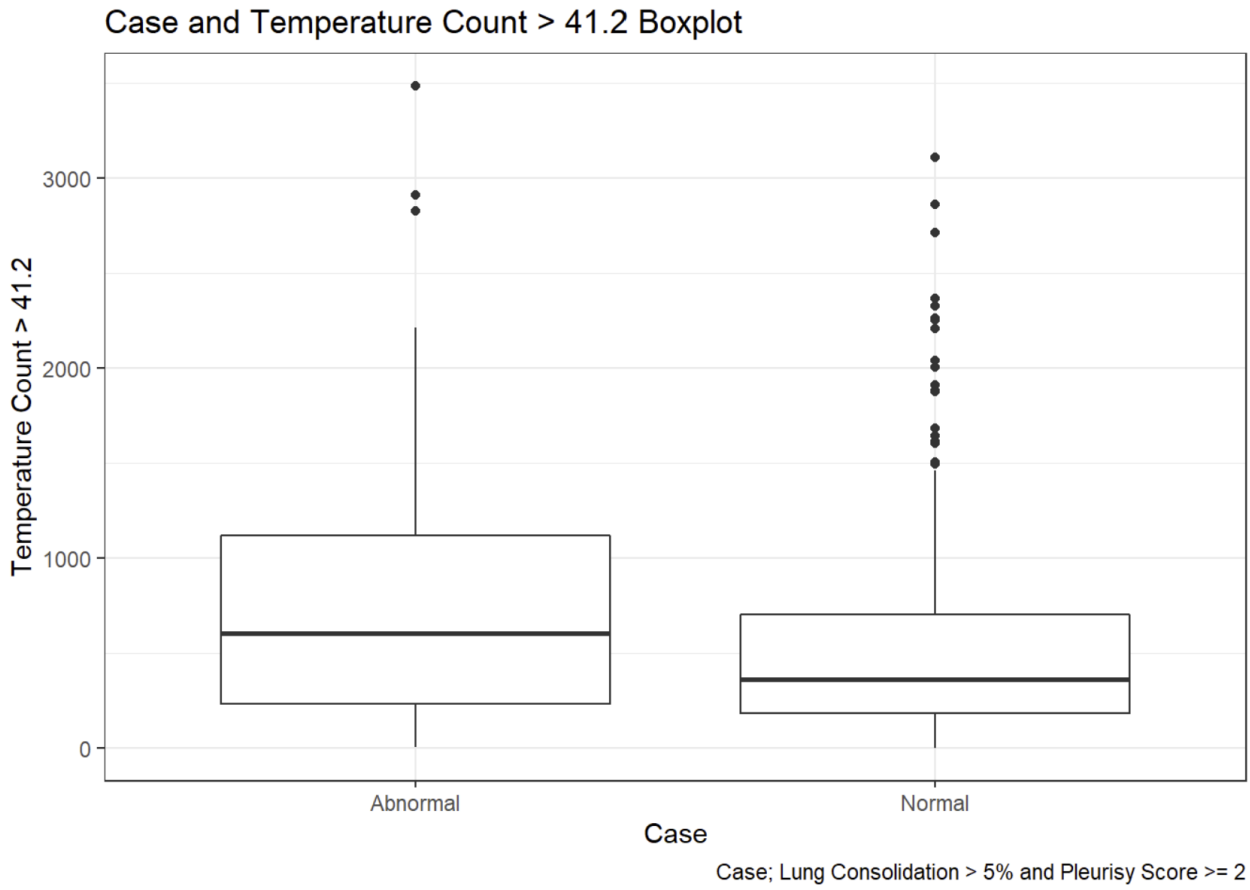

Boxplots in **Figure 45** demonstrate a positive association between a high number of temperature counts above threshold 41.2°C and abnormal (case) status of pulmonary pathology at slaughter.

Figure 46. Logistic regression - pulmonary score (normal/mild = < 5% consolidation and/or pleural score = 1, abnormal (case) => 5% consolidation and/or pleural score > 1) and thermobolus counts > 41.2°C.

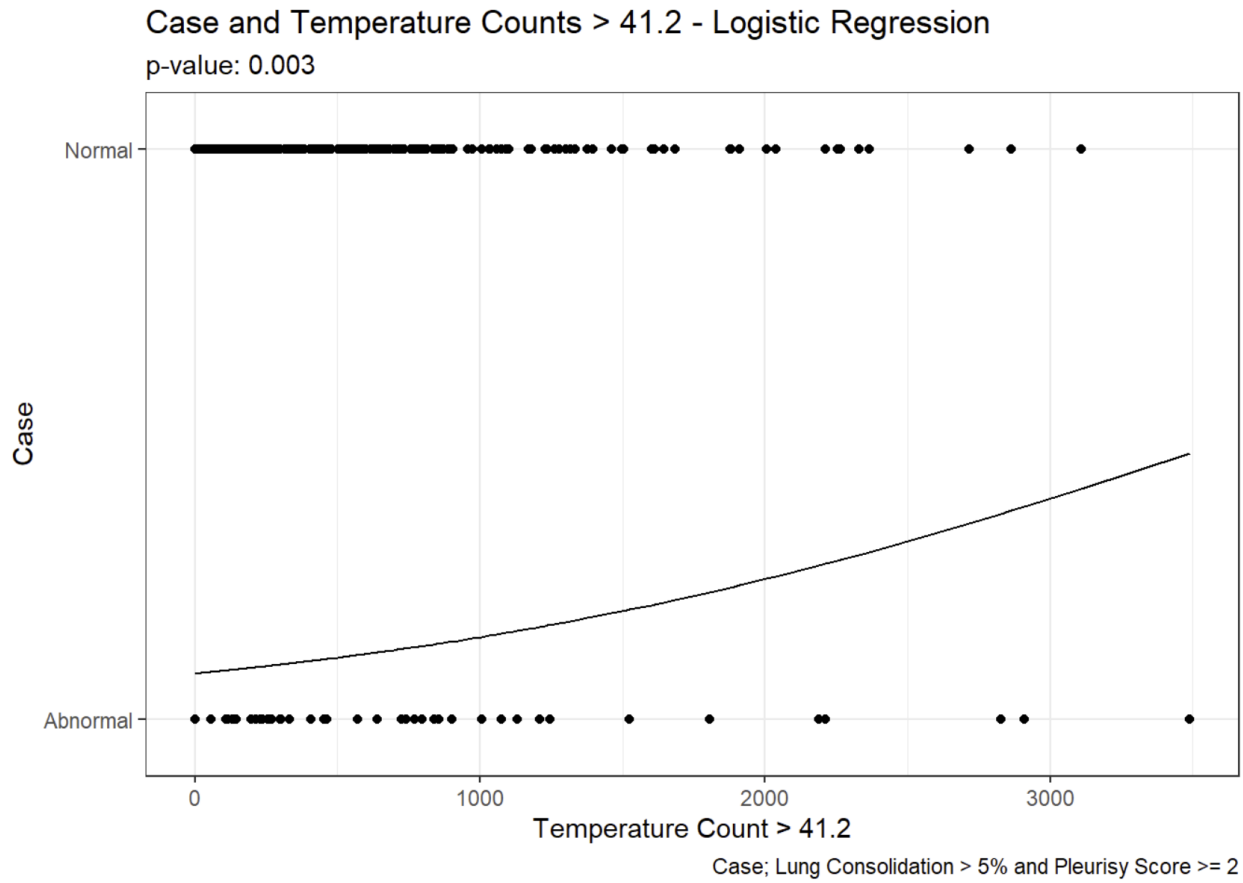

A significant association (at the 95% confidence level) is demonstrated between increasing temperature counts above 41.2°C and abnormal pulmonary lesion status (case).

In **Table 36** heat map below, the four thermobolus classification models have been applied to the study animals that were pulmonary lesion scored at slaughter, without 72 hour sensor (since none of these animals were enrolled as CASE or CONT in the feedlot phase). True CASE or CONT status is shown in the Outcome column and the relevant model prediction shown in the Prediction Thresholds column. Red shading indicates a missclassification whereas green shading indicates correct.

In **Table 37**, 2x2 table calculations of diagnostic sensitivity and specificity of the four thermobolus classification models (without 72 hour sensor) applied to the study animals that were pulmonary lesion scored at slaughter demonstrate true trade-off between sensitivity and specificity when utilising these models.

Table 36. Heat map of thermobolus correct and misclassification examples in replicate 1 and 2, *without* 72-hour sensor, and based on abnormal (CASE) definition => 5% lung consolidation and/or pleural score > 1 at harvest slaughter.

Classification Tree Model

Thresholds: 1, 100, 180, 250, 350

					Outcome			Prediction Thresholds				
Replicate ID	Animal ID	Total Temp Count	Temp Count Above 41.2	Proportion Above 41.2	Case	Lung Consolidation %	Pleurisy Score >= 2	1	100	180	250	350
1	15	21049	157	0.007	CONT	0.000	0	CASE	CASE	CONT	CONT	CONT
1	23	21063	368	0.017	CONT	0.000	0	CASE	CASE	CASE	CASE	CASE
1	28	21030	1876	0.089	CONT	0.000	0	CASE	CASE	CASE	CASE	CASE
1	42	21005	181	0.009	CONT	0.000	0	CASE	CASE	CASE	CONT	CONT
1	43	21068	327	0.016	CONT	0.000	0	CASE	CASE	CASE	CASE	CONT
1	48	21156	2716	0.128	CONT	0.000	0	CASE	CASE	CASE	CASE	CASE
1	56	21031	2827	0.134	CASE	0.610	1	CASE	CASE	CASE	CASE	CASE
1	84	27317	1877	0.069	CONT	1.575	0	CASE	CASE	CASE	CASE	CASE
1	126	26957	382	0.014	CONT	0.000	0	CASE	CASE	CASE	CASE	CASE
1	145	20676	279	0.013	CONT	0.000	0	CASE	CASE	CASE	CASE	CONT
1	154	20764	2188	0.105	CASE	9.300	1	CASE	CASE	CASE	CASE	CASE
1	156	20781	420	0.020	CONT	0.000	0	CASE	CASE	CASE	CASE	CASE
1	173	20865	1246	0.060	CASE	6.045	0	CASE	CASE	CASE	CASE	CASE
1	175	20824	3488	0.167	CASE	3.670	1	CASE	CASE	CASE	CASE	CASE
1	188	19777	1806	0.091	CASE	5.325	0	CASE	CASE	CASE	CASE	CASE
1	191	19926	237	0.012	CASE	9.225	1	CASE	CASE	CASE	CONT	CONT
1	199	20022	1460	0.073	CONT	0.000	0	CASE	CASE	CASE	CASE	CASE
2	15	18417	315	0.017	CONT	0.000	0	CASE	CASE	CASE	CASE	CONT
2	22	18391	73	0.004	CONT	0.000	0	CASE	CONT	CONT	CONT	CONT
2	28	22114	1210	0.055	CASE	0.980	1	CASE	CASE	CASE	CASE	CASE
2	29	18382	740	0.040	CASE	0.000	1	CASE	CASE	CASE	CASE	CASE
2	39	18321	146	0.008	CASE	0.000	1	CASE	CASE	CONT	CONT	CONT
2	41	18353	478	0.026	CONT	0.000	0	CASE	CASE	CASE	CASE	CASE
2	46	18773	406	0.022	CASE	4.880	1	CASE	CASE	CASE	CASE	CASE
2	47	17960	130	0.007	CONT	0.000	0	CASE	CASE	CONT	CONT	CONT
2	55	18173	231	0.013	CASE	0.000	1	CASE	CASE	CASE	CONT	CONT
2	61	18172	872	0.048	CONT	0.000	0	CASE	CASE	CASE	CASE	CASE
2	81	18120	229	0.013	CASE	0.000	1	CASE	CASE	CASE	CONT	CONT
2	90	18286	2253	0.123	CONT	0.000	0	CASE	CASE	CASE	CASE	CASE
2	93	18232	197	0.011	CASE	0.000	1	CASE	CASE	CASE	CONT	CONT
2	95	18212	453	0.025	CASE	0.000	1	CASE	CASE	CASE	CASE	CASE
2	103	18144	108	0.006	CASE	0.000	1	CASE	CASE	CONT	CONT	CONT
2	114	18640	502	0.027	CONT	0.000	0	CASE	CASE	CASE	CASE	CASE
2	122	17907	40	0.002	CONT	0.000	0	CASE	CONT	CONT	CONT	CONT
2	151	17915	145	0.008	CASE	0.000	1	CASE	CASE	CONT	CONT	CONT
2	152	17941	55	0.003	CONT	0.000	0	CASE	CONT	CONT	CONT	CONT
2	162	17944	480	0.027	CONT	0.000	0	CASE	CASE	CASE	CASE	CASE
2	165	17929	214	0.012	CASE	0.000	1	CASE	CASE	CASE	CONT	CONT
2	170	17879	464	0.026	CASE	0.000	1	CASE	CASE	CASE	CASE	CASE
2	172	17983	725	0.040	CASE	0.000	1	CASE	CASE	CASE	CASE	CASE
2	173	17954	269	0.015	CASE	0.000	1	CASE	CASE	CASE	CASE	CONT

Table 37. Diagnostic evaluation of the 4 thermobolus algorithms for the sub-clinical dataset from Table 34.

		T-100	
		ABNORM	**NORM**
	CASE	40	5
	CONT	271	46

Sensitivity:	*91%*
Specificity:	*15%*

		T-180	
		ABNORM	**NORM**
TRUE Status	**CASE**	35	10
	CONT	240	77

Sensitivity:	*80%*
Specificity:	*24%*

		T-250	
		ABNORM	**NORM**
	CASE	30	15
	CONT	203	114

Sensitivity:	*68%*
Specificity:	*36%*

		T-350	
		ABNORM	**NORM**
TRUE Status	**CASE**	25	20
	CONT	167	150

Sensitivity:	*57%*
Specificity:	*47%*

Figures 47-52 report the temporal profile of thermobolus recordings of various study animals from **Table 36** for the entire feeding period to harvest slaughter. Thermobolus data has been cleaned where indicated, which involved primarily removing large temperature declines associated with drinking events. Classification according to pulmonary lesion scoring case definition is also indicated

Figure 47. Animal R1_154 (cleaned).

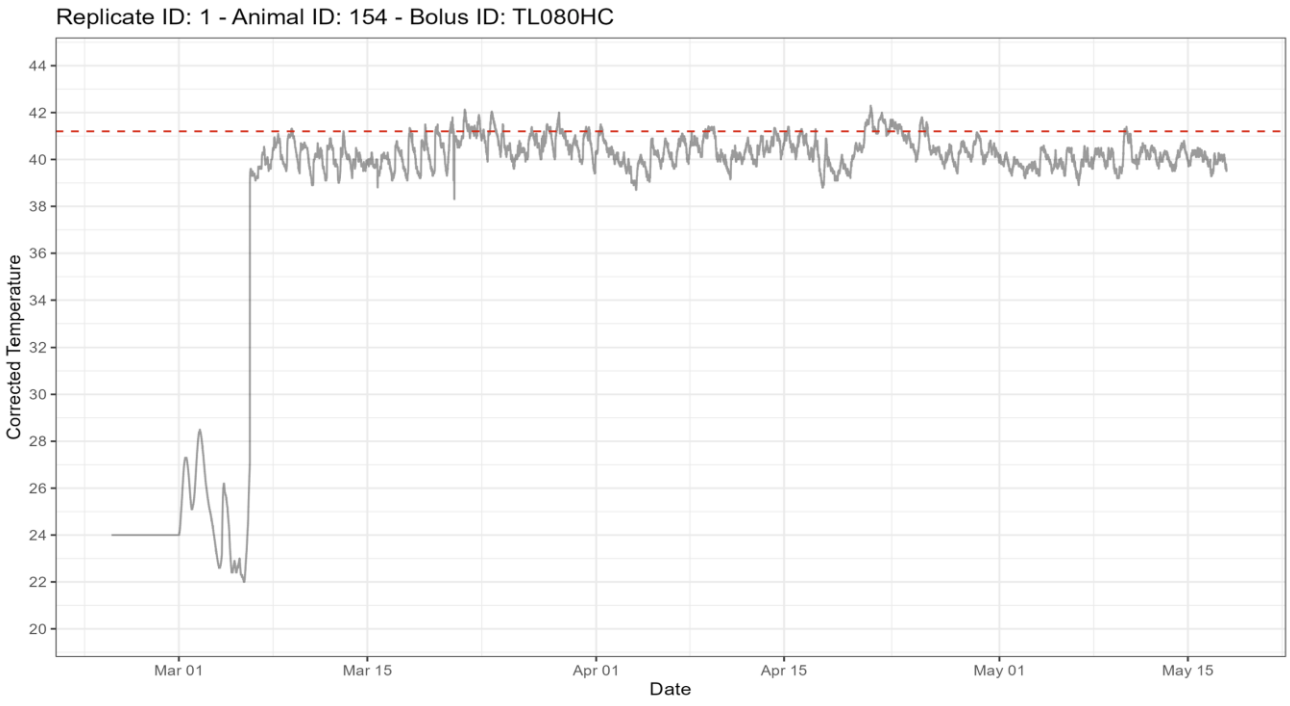

- Correctly classified a case by all algorithms

Figure 48. Animal R1_188 (cleaned).

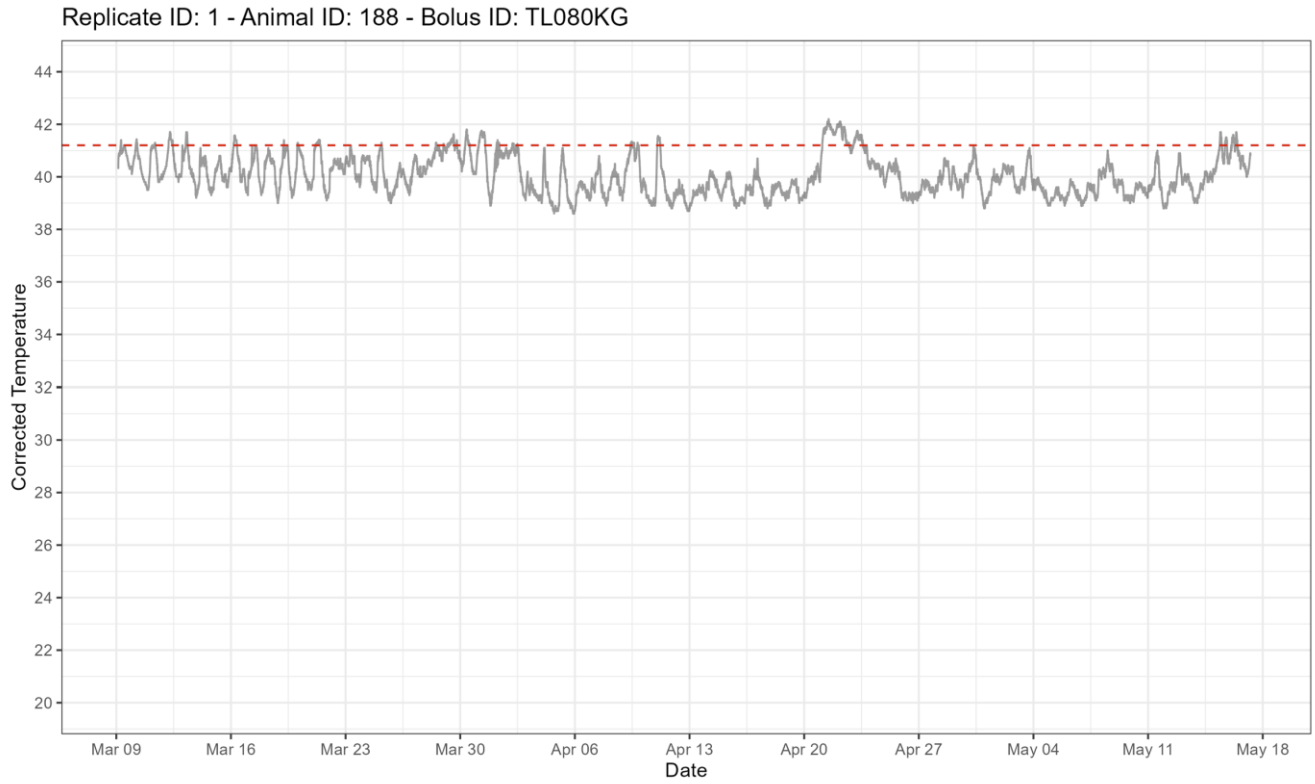

- Correctly classified a case by all algorithms

Figure 49. Animal R1_148 (cleaned).

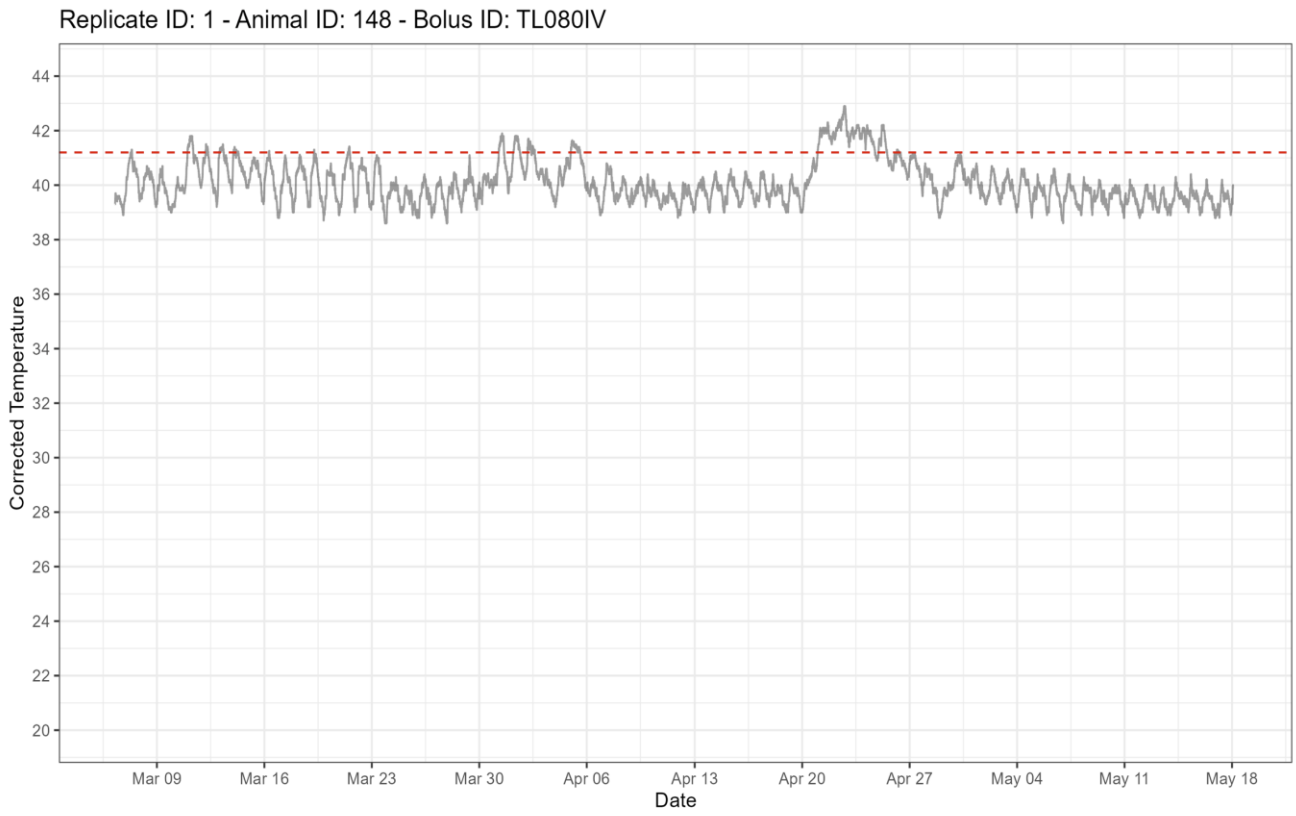

- The study animal R1_148 was scored at harvest slaughter with *6.5%* lung consolidation and nil pleural score. There were no clinical illness scores assigned to this animal at any time during the study, however all prediction threshold algorithms of the classification tree model correctly classified this animal as a case. Note the sustained period between 20th April and 27th April of reticulo-rumen temperature above manufacturer's threshold 41.2°C.

Figure 50. Animal R1_191 (cleaned) thermobolus temporal profile for the feeding period to harvest slaughter.

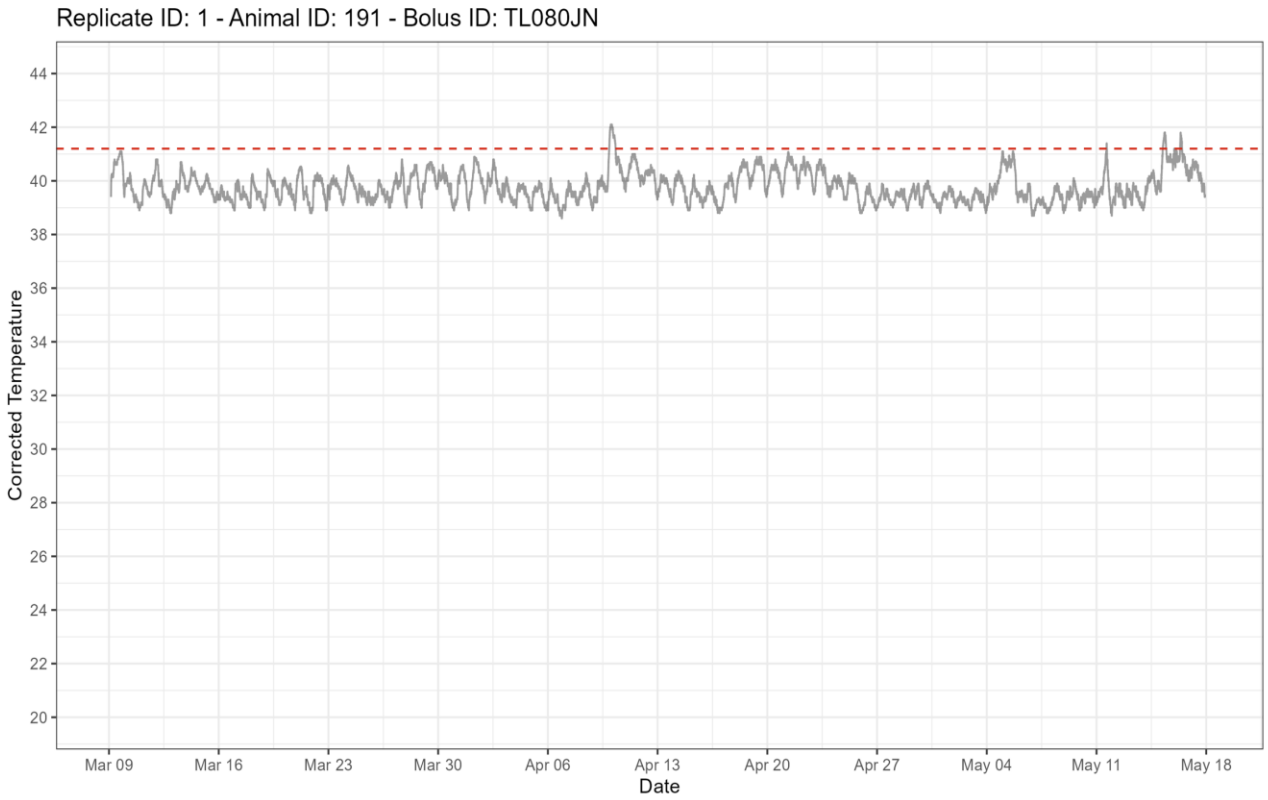

- Incorrectly classified a control by T-250 and T-350 algorithms, but correctly classified by the T-100 and T-180 models. Total lung consolidation = *9.225%* at slaughter.

Figure 51. Animal R2_22 (raw).

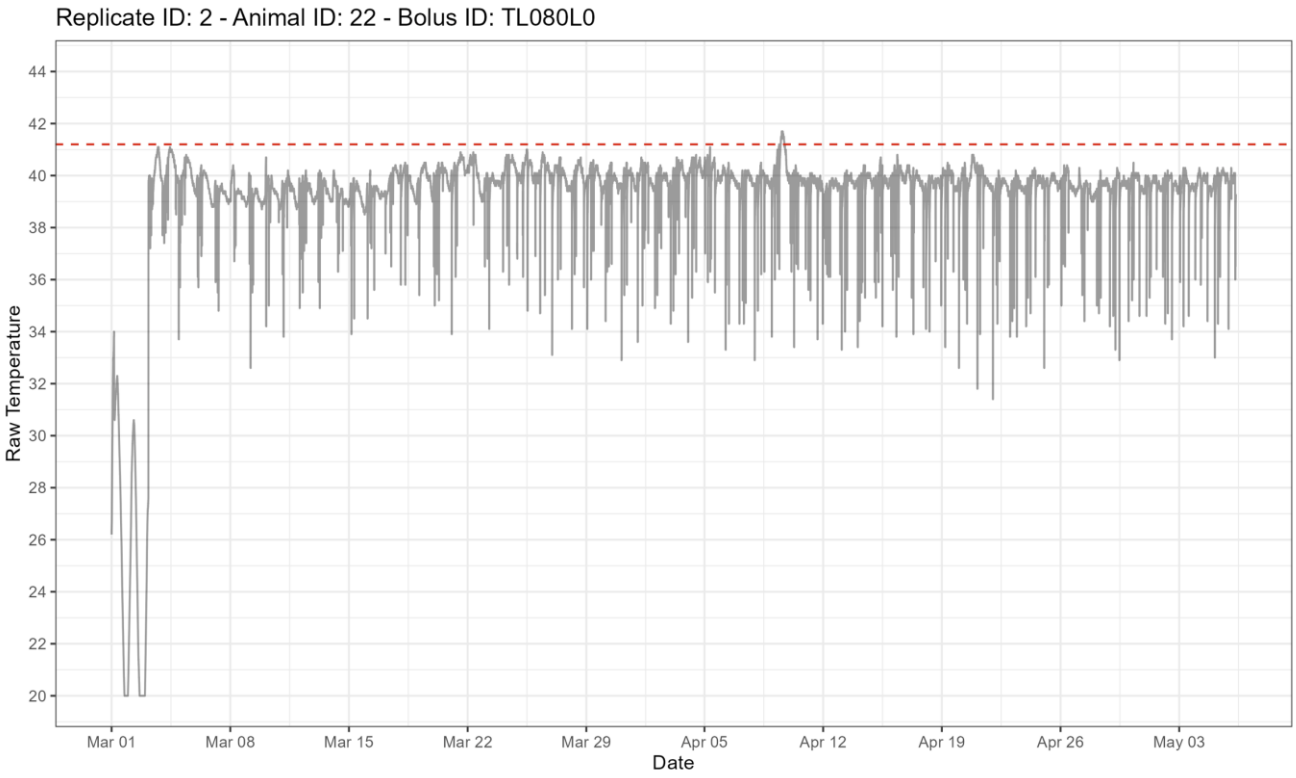

- Study animal R2_22 recorded pleural score = 1 at harvest slaughter, and zero lung consolidation. A clinical illness score = 2 was recorded on 20th March 2021. This animal was correctly classified a control by all algorithms.

Figure 52. Animal R2_159 (raw).

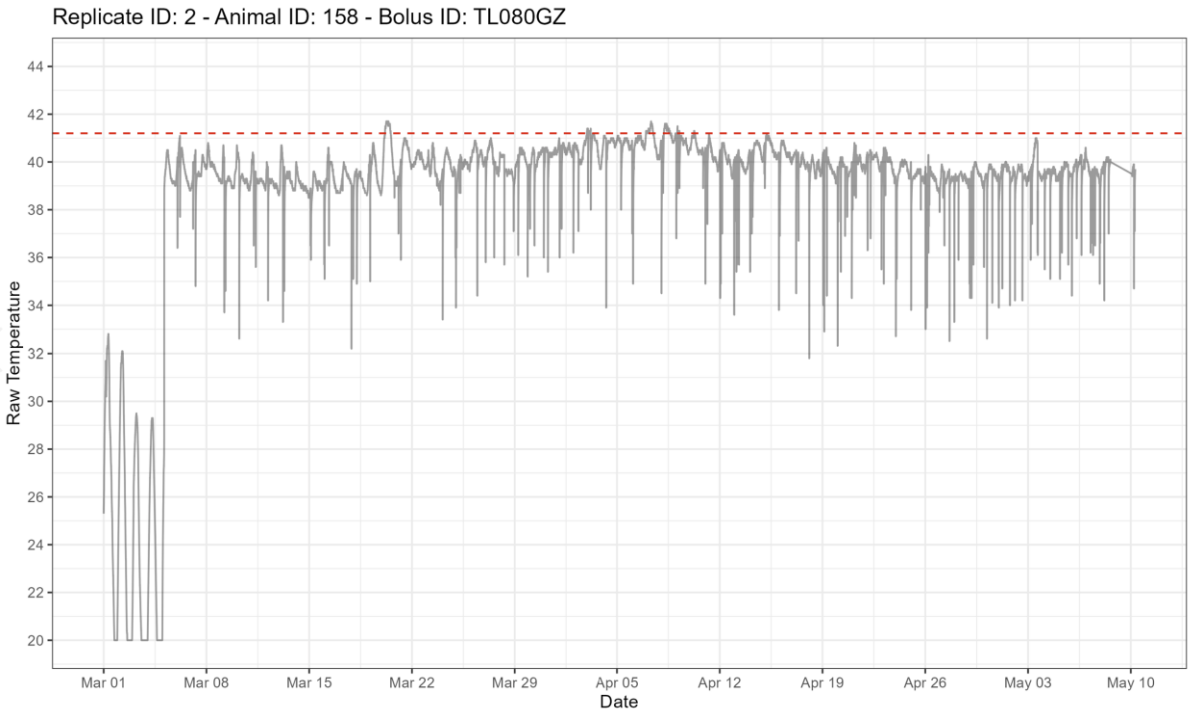

- This animal received clinical illness scores => 2 through the study period, and was correctly classified a control by all algorithms.

4.12.9 Study animals observed with heat load signs and reticulo-rumen temperature data

In the second replicate of the study, a number of animals were observed with visible heat load signs, in a range of severity analogous to industry standard of Pant Score = 1 to Pant Score = 3 as described in B.FLOT 307,308,309 (2001). Heat load signs were evident on various observation days through March and early April, and always at the afternoon clinical illness scoring events. No heat load signs were evident in any study animals at any of the morning clinical illness scoring events. Using the classification tree model algorithms as above for enrolled CASE/CONT animals, per the study protocol, prediction results for these animals are reported in **Table 38**.

Table 38. Heat map of replicate 2 study animals with observed heat load at afternoon clinical illness scoring and correct or misclassifications as CASE/CONT according to the study protocol.

Classification Tree Model

Thresholds: 1, 100, 180, 250, 350

				Outcome		Prediction Thresholds				
Replicate ID	Animal ID	Total Temp Count	Temp Count Above 41.2	Heat Load Status	Proportion Above 41.2	1	100	180	250	350
2	11	18569	292	OBSERVED	0.016	CASE	CASE	CASE	CASE	CONT
2	40	18243	217	OBSERVED	0.012	CASE	CASE	CASE	CONT	CONT
2	61	18172	872	OBSERVED	0.048	CASE	CASE	CASE	CASE	CASE
2	63	18366	216	OBSERVED	0.012	CASE	CASE	CASE	CONT	CONT
2	70	18181	643	OBSERVED	0.035	CASE	CASE	CASE	CASE	CASE
2	73	18075	223	OBSERVED	0.012	CASE	CASE	CASE	CONT	CONT
2	85	18386	594	OBSERVED	0.032	CASE	CASE	CASE	CASE	CASE
2	87	18240	377	OBSERVED	0.021	CASE	CASE	CASE	CASE	CASE
2	96	18171	337	OBSERVED	0.019	CASE	CASE	CASE	CASE	CONT
2	102	18061	350	OBSERVED	0.019	CASE	CASE	CASE	CASE	CASE
2	106	18026	75	OBSERVED	0.004	CASE	CONT	CONT	CONT	CONT
2	112	17969	421	OBSERVED	0.023	CASE	CASE	CASE	CASE	CASE
2	132	18544	356	OBSERVED	0.019	CASE	CASE	CASE	CASE	CASE
2	186	17949	335	OBSERVED	0.019	CASE	CASE	CASE	CASE	CONT
2	190	17928	285	OBSERVED	0.016	CASE	CASE	CASE	CASE	CONT

All of the animals in **Table 38** are study controls (CONT) in that they did not meet CASE preliminary or enrolment criteria and were not identified and treated for BRD per the feedlot site health management protocol. Two of the animals did receive clinical illness score => 2: R2_22 on 21st March and R2_73 on three occasions – 24th / 25th / 31st March. Only 6 of the listed animals received any pulmonary scoring at harvest slaughter: pleural score = 1 for R2_22, R2_40 R2_70 R2_73 and R2_85,

and lung consolidation of 0.63% for R2_190. The best performing algorithm for classifying these heat load observed study animals as CONT was the 350-count threshold (model T350) at 53% specificity.

Figures 53 and 54 report the temporal profiles of thermobolus data for the entire feeding period to harvest slaughter for study animals R2_61 and R2_70 who were heat load observed during the project **(Table 38).**

Figure 53. Animal R2_61 (raw).

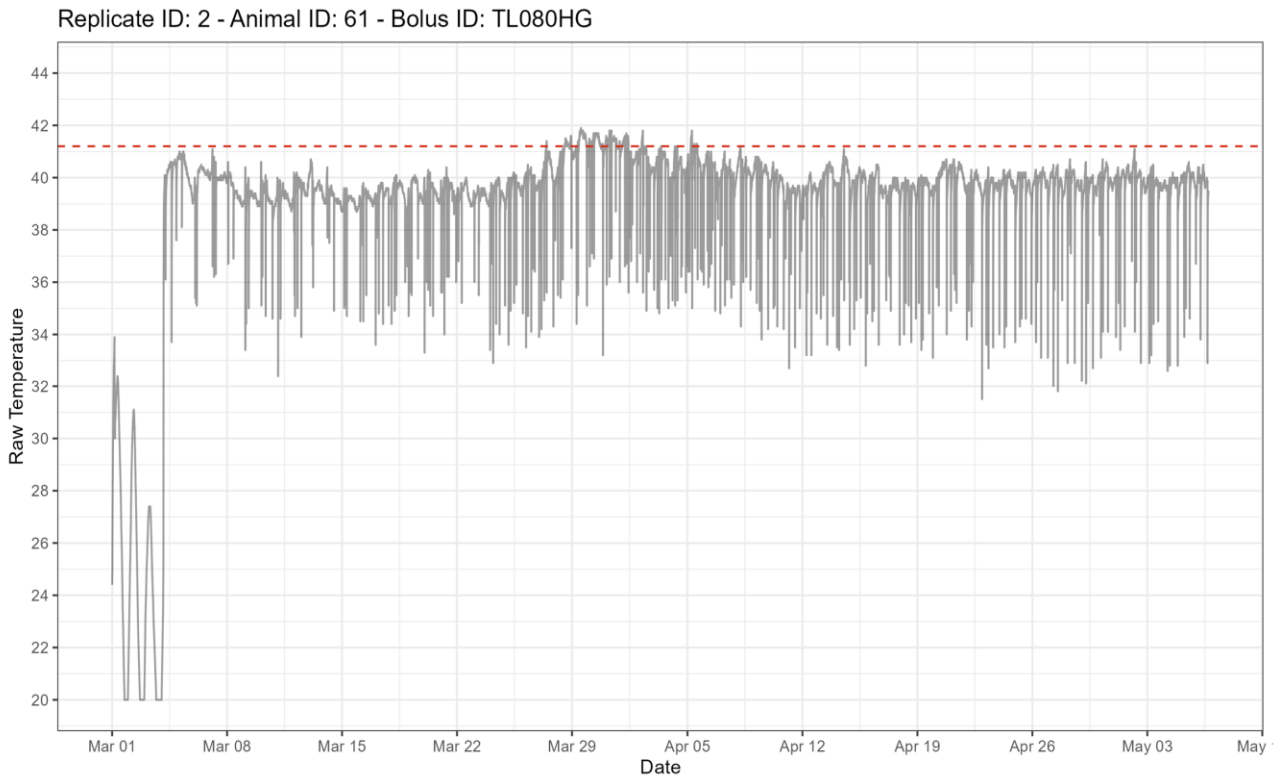

Figure 54. Animal R2_70 (raw).

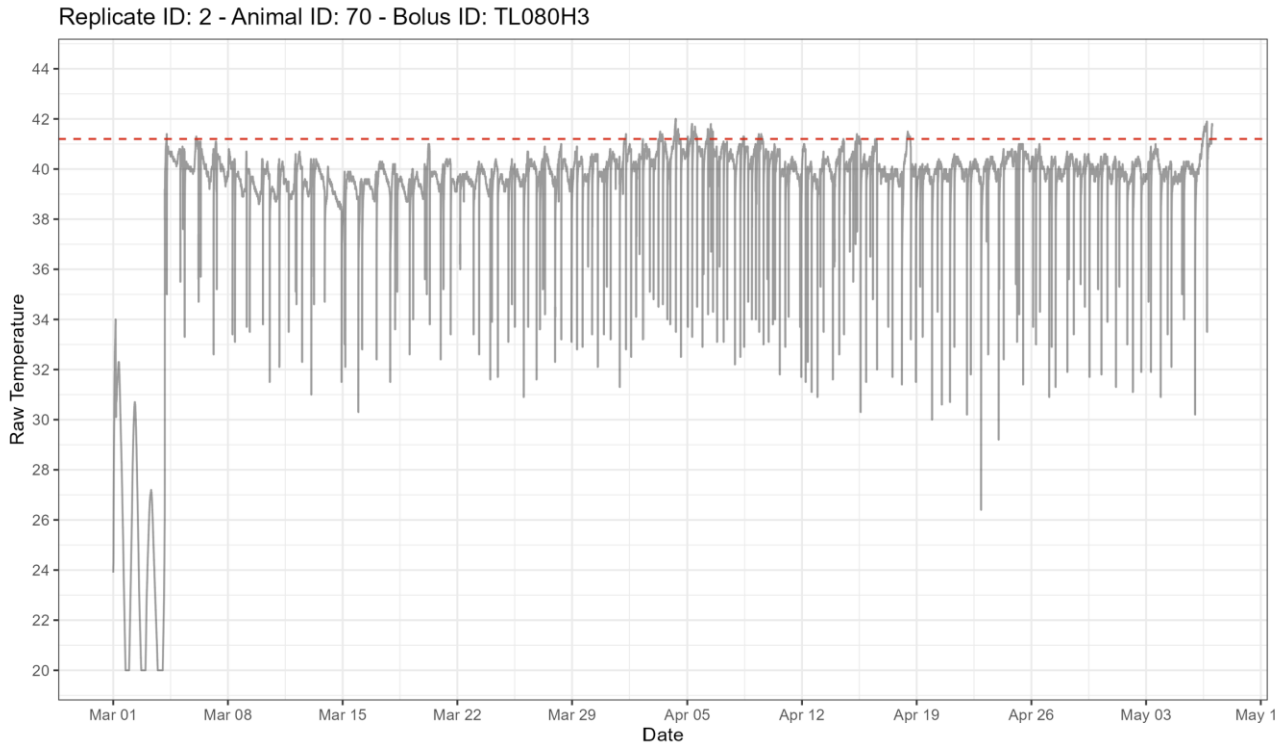

5 Summary of diagnostic modalities

The results obtained from this project are the first to evaluate diagnostic modalities compared to the gold standard of pulmonary lesions at the time of clinical illness. Additionally, several tests were evaluated relative to the final lung score of the cattle at harvest slaughter. These overall results are summarized in **Tables 39 and 40**.

Table 39. Diagnostic characteristics of each tested modality evaluating the CASE (n=10) and CONT (n=10) cattle in the study against lung lesions of euthanised and necropsied feedlot cattle as the "gold standard", or reference test. Sensitivity and Specificity reported.

	TP	FP	TN	FN	SE	SP
Visual assessment and rectal T	10	3	10	1	91%	77%
Thoracic Ultrasound	9	0	10	1	90%	100%
CPU Aided Auscultation.	6	4	6	4	60%	60%
BOLUS: T-100	10	4	6	0	100%	60%
BOLUS: T-180	10	3	7	0	100%	70%
BOLUS: T-250	9	3	7	1	90%	70%
BOLUS: T-350	7	2	8	3	70%	80%
REDI_rn4call	8	2	8	2	80%	80%
REDI_rn2call	8	2	8	2	80%	80%
REDI_dccall	10	4	6	0	100%	60%
REDI_ds3	9	2	8	1	90%	80%
HAPTOGLOBIN	9	2	7	0	100%	78%
METABOLOMICS – visual signs: Classif Tree	7	2	8	2	80%	78%
METABOLOMICS – visual / clinical: Rand Forest	7	0	10	2	100%	78%
METABOLOMICS – lung lesions: Neural Net	7	1	9	2	90%	78%

Visual assessment was used at one of the criteria for determining CASE/CONT status of euthanised animals; therefore, this variable exhibits perfect agreement with final animal status.

Table 40. Diagnostic accuracy of each modality compared to final pulmonary status as determined by pleural lesions and pulmonary consolidation at harvest slaughter.

	TP	FP	TN	FN	SE	SP	Acc	Bal Acc	App Prev	True Prev
Visual assessment	3	26	291	42	7%	92%	81%	50%	8.0%	12.4%
Thoracic Ultrasound	2	9	157	24	9%	100%	88%	55%	1.1%	12.7%
REDI_rn4call	13	66	248	32	29%	79%	73%	54%	22.0%	12.5%
REDI_rn2call	5	42	272	40	11%	87%	77%	49%	13.1%	12.5%
REDI_dccall	22	148	166	23	49%	53%	52%	51%	47.4%	12.5%
REDI_ds3	25	180	134	20	56%	43%	44%	50%	57.1%	12.5%
BOLUS: T-100	40	265	45	2	95%	15%	24%	55%	86.7%	11.9%
BOLUS: T-180	35	234	76	7	83%	25%	32%	54%	76.4%	11.9%
BOLUS: T-250	30	198	112	12	71%	36%	40%	54%	64.8%	11.9%
BOLUS: T-350	25	162	148	17	60%	48%	49%	54%	53.1%	11.9%

Total number of tests are not equal for all modalities, some limitations in reliable data recorded resulted in variations in dataset size.

Definitions for the diagnostic metrics presented in **Table 40**;

- **Accuracy** is the proximity of measurement results to the true value. It is the amount of agreement between the results from the diagnostic test under study, and those from a reference (gold standard) test.
  - Formula = (true positives + true negatives)/total number of tests

- **Balanced accuracy** is useful to consider, especially in classification model diagnostic tests (i.e. class = disease or no disease), when datasets are relatively unbalanced – such as when only a small number of study subjects have the disease.
  - Formula = (Sensitivity + Specificity)/2

As described previous in **Table 17**;

- **Apparent (detection) prevalence** is the proportion of the population that tests positive for the target disease
  - Formula = (true positives + false positives) / total number of tests

- **True prevalence** is the proportion of the population that is *actually* infected
  - Formula = (true positives + false negatives) / total number of tests

6 Conclusions/recommendations

Results from the trial showed several meaningful differences among diagnostic modalities.
A summary list of conclusions and recommendations for the study to date follow below:

- An accurate standard for BRD diagnosis in living animals facilitates future research and negates the requirement to euthanase specifically for confirmatory diagnosis.
- Sensitivity and specificity are widely used metrics, however other measurements should be considered when designing an overall diagnostic strategy for research or commercial purposes such as accuracy, prevalence, repeatability, amongst others. A highly specific test may not be very useful when the disease condition has high (true) prevalence, but in clinical settings where there is low prevalence, a highly specific test will protect against the inefficiency of many false positive detections and the work practices and operations this generates. Many false positive case animals presented for clinical treatment in feedlot production systems also does not align with good antimicrobial stewardship.
- Receiver operating characteristic curves (ROC) are plots of sensitivity vs false positive rate, for a range of diagnostic test results. The ROC curve graphically represents the compromise between sensitivity and specificity in test, and the area under this ROC produce results on a numerical scale, rather than binary (positive vs negative results). The ROC curve can be used to determine the cut-off point at which the sensitivity and specificity are optimal.
  If the area under the curve (AUC) is high, then the more accurate the test is, and it is the single parameter that summarises all possible combinations of Sensitivity and Specificity that can be achieved by changing the tests cut-off value. When comparing two tests, the more accurate test is the one with a larger ROC curve with a higher AUC. The best cut-off point for a test is the point on the ROC curve which is closest to the top left corner of the graph. A further desktop analysis, utilising the data generated from this study, to build ROC plots for each of the diagnostics examined could also assist to inform an overall strategy to deploy combinations of the modalities.
- Remote continuous monitoring can be utilised as a screening diagnostic test, with confirmation determination carried out by ultrasound, and possibly a combination of haptoglobin, and/or metabolomics. At this stage, combining these modalities in a diagnostic strategy would define the best working practical gold standard of BRD diagnosis in living animals for research purposes, and for further validation of the continuous monitors. For commercial purposes, considering real-time requirements, combining the continuous monitoring screening test with ultrasound as confirmation, defines the best working practical gold standard of BRD diagnosis in living animals, noting that in this study the disease was allowed to progress enough to cause lung tissue damage that was detectable. This diagnostic strategy does form the foundation of an extension of this project to further validate the identified most workable modalities to sufficient study power, precluding the need to euthanase animals as the gold standard.
- Combining diagnostics into an optimal diagnostic strategy has merit as outlined above, and further to this, combining remote continuous monitors into the best combination of Sensitivity and Specificity – *between* the two modalities utilised – may optimise diagnostic *screening* such that the most relevant animals are presented for confirmation diagnostics. Based on the non-clinical dataset of study animals with pulmonary scoring data obtained at slaughter, the Specificity advantage of REDI could be combined with the Sensitivity advantage of reticulo-rumen thermobolus for ultimate screening purposes .
- This study confirms that the standard feedlot visual observation method, with rectal temperature not utilised, has low operating accuracy when compared to (necropsied) CASEs that demonstrated lung pathology.

- Adding rectal temperature (40.0°C threshold) to visual observation and clinical illness scoring did improve diagnosis, in terms of rejecting preliminary CASEs for enrolment that ultimately were never enrolled as CASEs at later dates in the study, and, did not demonstrate respiratory pathology at slaughter. However, there were instances of false positive and false negative CASE and CONT animals on the basis of rectal temperature, with 40.0°C as the threshold for final determination.
- In the course of this study, no animal in the study pen was a non-detection misdiagnosis by visual observation as the method, to the extent of discovering animals very advanced with BRD and/or spontaneous deaths due to BRD without any preceding detection. It is important to note however, that these cattle were observed twice daily and for longer periods per session than the industry norm (up to 30 minutes in total daily). Even with this augmented version of the typical feedlot process, many of the cattle with pulmonary lesions at harvest were not identified as clinically ill.
- Ultrasound performs well as a BRD diagnostic method but requires training to conduct the surveys and interpret images, minimum machine capability, an appropriate restraint facility that allows access to both sides of the chest and the forward chest area, and a minimum of 5 minutes available to conduct the more basic level survey. It should also be noted that presumptive CASEs presented for examination had demonstrated a minimum of three clinical illness scores of 2 or greater over a 24-hour period. These CASEs therefore represent moderate to severe morbidity where the disease (and lung lesions) are allowed to progress longer than in typical feedlot clinical settings. Nonetheless, this diagnostic modality showed the best accuracy.
- For commercial application of ultrasound, where a truncated survey would be required to save time, prioritising anteroventral (forward and low) positions on the right hemithorax (right chest side) would yield the best probability of detecting pulmonary lesions if they are present. This orientation of lesions was evident when performing pulmonary scoring at slaughter in this project.
- Remote, continuous monitoring through wearable technologies demonstrated promising accuracy with the added advantage of early detection in the case of REDI, especially in comparison to the industry standard of visual observation. Reticulorumen thermobolus modalities have the potential for early detection however more advanced algorithms would need to be developed, targeting above threshold temperature counts in a more condensed time period near the presentation of clinical illness.
- Remote continuous monitoring offers the most promise commercially because of the ability to capture clinical and subclinical cases across the whole cohort under surveillance, as opposed to select animals presented as individuals to a restraint facility. As such, remote continuous monitors can facilitate early, targeted, treatment intervention across both clinical presentations and maximise treatment, productivity and welfare outcomes.
- In the case of BRD in Australian beef feedlots, the usual epidemiology involves incidence concentrating between approximately 10 and 60 days after arrival. The continuous monitoring modality REDI made all its detection of BRD CASEs in this period, which aligns with the prior high probability estimates of the disease in a typical beef feedlot clinical setting. This is a significant advantage for the REDI modality in that it differentiates behaviour variables associated with disease status in this defined period.
- Remote continuous monitoring modalities carry the capacity to operate with varying mixes of diagnostic Sensitivity and Specificity, which can be applied to varying levels of BRD risk as presented in the feedlot clinical setting. A working example could be utilising more sensitive algorithms for high BRD risk cohorts that are candidates for targeted metaphylaxis and/or more intensive daily pen riding.
- Haptoglobin is an acute phase protein that performed well as a diagnostic for BRD in this study, however specific cut-offs for levels of haptoglobin present in plasma have not been

established for BRD, and this modality remains very non-specific to a spectrum of disease conditions. BRD is necessarily a very inflammatory process, so elevated levels in enrolled CASEs can be expected, however there remains low differentiation from other inflammatory disease processes.

- Plasma metabolomics in this study utilised a set of algorithms generated from an independent dataset and project (B.FLT.0164). There was good overall performance classifying CASE and CONT status in this group of study animals, with the random forest for visual / clinical signs model likely being a good candidate for confirmatory diagnostic test as part of a wider diagnostic strategy.
- Nasopharyngeal microbiota offers potential in the living animal to describe changes in the structure of microbiota that might align with increased resilience or susceptibility to BRD. In this study, the most prominent identified phyla across all CASE and CONT samples were Proteobacteria (40.50%), Tenericutes (33.27%), Firmicutes (8.78%), Bacteroidetes (6.22%), and Actinobacteria (6.21%). However, the order of both phyla and genera by abundance differed between experimental CASEs and CONTs, and between induction and CASE / CONT enrolment sample types. The most prominent identified genera across all CASE and CONT samples were *Mycoplasma* (32.15 %), *Psychrobacter* (12.68%), *Actinobacillus* (4.54%), *Histophilus* (4.14%), and *Nicotella* (3.04%). However, the order of genera by abundance differed between experimental groups and sample types (Genus abundance) Genera also varied between individual animals across experimental groups and sample types (individual animal abundance). It was notable that CASE animals possessed comparatively higher abundance of *Mycoplasma* at induction and CASE enrolment.
- Computer aided electronic auscultation performed with low accuracy, as well as low repeatability (precision) in this study, across all animals in both replicates. A significant limitation of this modality is the requirement to limit all ambient noise to conduct the recording, which involves at minimum, removing all animals from the restraint apparatus adjacent to the presented patient. This results in considerable interruption to animal flow through the facility. To ensure mitigation of ambient noise further and obtain a diagnostic recording, vehicles travelling on the feedlot must be diverted from proximity to the restraint facility. Even under these conditions, computer aided electronic auscultation performed with the lowest accuracy and repeatability of all the studied modalities and offers very limited commercial application.
- Staging of disease and assessment of level of severity was not well elucidated in this study. Either the diagnostics employed were performing as a classifier only (i.e. determining disease present or not only), or, severity functions were not fully utilised (ultrasound) or didn't perform well (computer aided auscultation). Intuitively, longer ultrasound surveys could construct cross-sectional area "maps" of both sides of the chest where pathology exists and estimate a total lung volume of consolidation and/or pleuritis described. Timsit (2019) did report an association with depth of lesions detected by ultrasound and clinical outcome of BRD treatment. However, it should be noted that in this study, the clinical presentation (and clinical illness scores) of confirmed CASEs in the feedlot phase, and their calculated area of lung consolidation at necropsy didn't appear to demonstrate a direct relationship between the severity of clinical signs and the recorded extent of consolidation. It is likely that individual differences in immune response and the prevailing pathogens involved in separate infections play significant roles.
- Presence of pulmonary lesions as defined in this study (> 1 pleurisy score and/or => 5% pulmonary consolidation) at slaughter was significantly associated with reduced average daily gain. This highlights a potential value proposition for remote monitoring diagnostic modalities to identify feeder cattle that are subclinical cases so that they can be treated during the feeding phase to realise more optimal health, welfare, and productivity.

- Remote continuous monitoring, in this study delivered by the REDI system and reticulo-rumen thermobolus, can be utilised as a screening diagnostic test, with confirmation determination carried out by ultrasound when presumptive CASEs are presented to the hospital restraint facility. At this stage in the study, combining these modalities would define the best working model of a gold standard of BRD diagnosis in living animals.
- Changes in the structure of nasopharyngeal microbiota might be related to the development of BRD. While not strictly a diagnostic test, certain structures of commensal bacteria in the nasopharynx at induction (arrival) into the feedlot might be associated with higher or lesser BRD susceptibility.
- The standard feedlot visual observation method with any clinical illness scores recorded has low operating accuracy as evaluated by presence or absence of pulmonary and pleural lesions at slaughter matched against the observation history. This highlights the need for alternative BRD detection methods.
- One animal in this study demonstrated detectable lesions on ultrasound during the feeding period that were not detectable at slaughter, seemingly resolving on account of BRD treatment. This indicatesthat the pulmonary scoring method of validation may not be perfectly specific, and in studies relying on this method, this particular animal would have been classified as a false positive.
- In the thermobolus data, utilising the simple classification models built within this report, there was an error effect on account of observed heat load in some of the study animals. Visual assessment, utilising pant scores, allowed differentiation between BRD and heat load. Robotic following of bolus data, and the simple algorithms used here, would lead to erroneous BRD cases identified in the summer months. There is a need to further the classification algorithms to account for this, possibly by defining the period above the 41.2°C threshold further, and/or add weighting to the time of day for the increased temperature recordings or review the temperature threshold itself.
- Further desktop analysis possible includes an opportunity to conduct cross-validation analysis, such as agreement between the REDI system and reticulo-rumen boluses of diagnosing false positive/negative animals. The two continuous monitoring modalities can also be examined for agreement between detection and estimation of variables such as drinking behaviour. Extended analysis will involve, where appropriate, receiver operating characteristic curves (ROC) and development of diagnostic algorithms which combine extra modalities than is contained within this report. Metabolomics showed good diagnostic accuracy using algorithms developed in independent studies. Further research is recommended to identify these biomarkers and explore opportunities to develop crush side tests.

7 Key messages

- Visual observation in this study demonstrated good sensitivity in CASE cattle (consider that no trial cattle were “missed” and presented as very late detections or non-detection deaths). However, the process was carried out atypical to the industry norm in that at least two observation sessions, in extended elapsed time (minimum 10 minutes per session), in combination with standard feedlot surveillance, was carried out each day of the study. It would appear impractical to apply this modality in this manner in normal industry operations. In addition, approximately 12% of the animals that went to slaughter had lung tissue damage indicative of past BRD episodes but these were not detected during visual observations.
- Wearable technology for continuous monitoring can deliver good operating diagnostic accuracy. However, fixation and in-situ application methods need to be robust since wearable technology is only useful if it’s actually being worn. Externally worn devices need also to withstand all climatic conditions and continue transmitting. The continuous monitoring systems used in this study, REDI and reticulo-rumen boluses, require on-site infrastructure such as base station, wall point antenna / transmitter etc which must also be included in the consideration (cost, maintenance, all weather durability etc) to deploy as a diagnostic.
- In this study, computer aided electronic auscultation had a low diagnostic accuracy. This modality also had a low utility in a standard feedlot operating site if all requirements of mitigating/cancelling ambient noise were met, since not only did the cattle handling facility allow only the examined animal, but all nearby feedlot traffic had to be stopped or diverted.
- Ultrasonography to detect respiratory pathology in clinical CASEs performed well as a diagnostic when animals were transferred to a suitable handling and restraint facility. The restraint apparatus must provide access to all required locations on both sides of the chest for best diagnostic potential and accuracy however while still maintaining safe and effective restraint for feedlot operations. Most standard feedlot facilities are not designed for and are not suitable for this purpose. Realistically, given these limitations, hospital facilities would be the most feasible to consider installing ultrasound as a diagnostic of any potential (screening/confirmatory diagnosis) since volume and cattle flow requirements precludes ultrasound from induction and/or drafting operations.
- All limitations notwithstanding, the ultimate living animal gold standard for BRD diagnosis, real-time in the feedlot clinical setting, based on accuracy reported in this study, is a screening combination of REDI and thermobolus continuous monitors, confirmed by ultrasound by an experienced operator. Device advancement, cost competitiveness and data transfer and processing will likely all improve appreciably in the near future and if combined with attractive cost-benefit on the diagnostic accuracy outcomes, reasonable incentive would exist to adapt feedlot infrastructure to operate these modalities.
- The continuous monitoring modalities operate an advantage of being able to apply machine learning or similar methods to improving diagnostic accuracy against future observations that have robust CASE definitions. As above, future studies utilising ultrasound as a diagnosis confirmation will assist this process and preclude the need to utilise necropsy as the gold standard.
- Metabolomics showed good accuracy and robustness to detect BRD animals because the algorithms were independently developed in another project. This can also be used as confirmatory test. Further research could focus on identifying the chemical structure of the biomarkers and exploring opportunities to develop crush-side tests with these biomarkers.
- Further replicates added to this study could be done with less expense and complexity if a truncated list of modalities was utilised based on all – ultimate – results once available.

- Prevalence, accuracy and precision, among other diagnostic measures, are also important considerations along with Sensitivity and Specificity. For a complex disease such as BRD, including these when designing a diagnostic strategy, as opposed to considering limited measures, and tests in isolation, would provide the best opportunity to achieve maximal accuracy.

8 Appendix

8.1 CASE series images: clinical presentation pen and hospital lane, select ultrasound, necropsy

Figure 55. R2_2: CASE – study pen clinical presentation at 3rd clinical illness score =>2.

Figure 56. R2_2: CASE ultrasound image 1 – arrow demonstrates fibrinosuppurative pleural effusion between chest wall and consolidated lung edge in right anterior chest field.

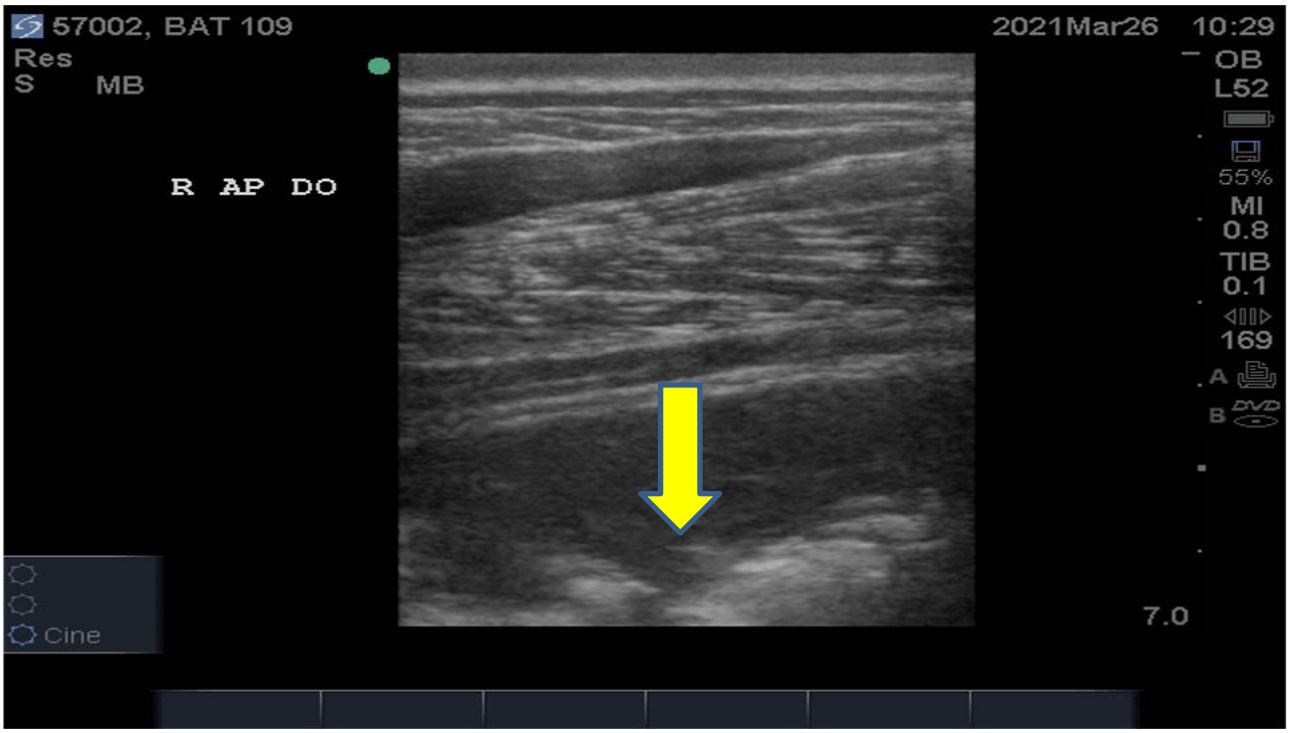

Figure 57: CASE ultrasound image 2 – arrow demonstrates comet tail artefact from imaging one of multiple miliary caseous abscess foci in consolidated lung of right mid-chest field.

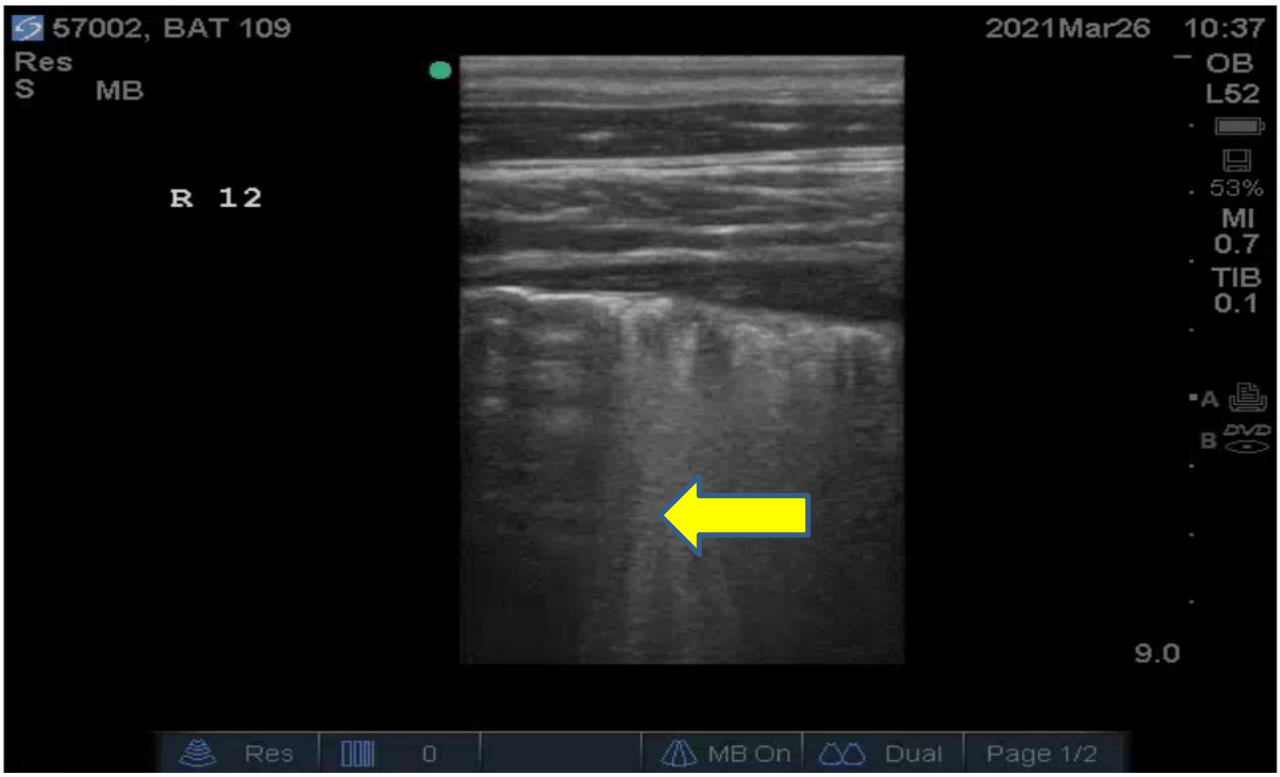

Figure 58. R2_2: CASE ultrasound image 3 – arrow demonstrates large fibrin deposit in suppurative pleural effusion in left anterior chest field.

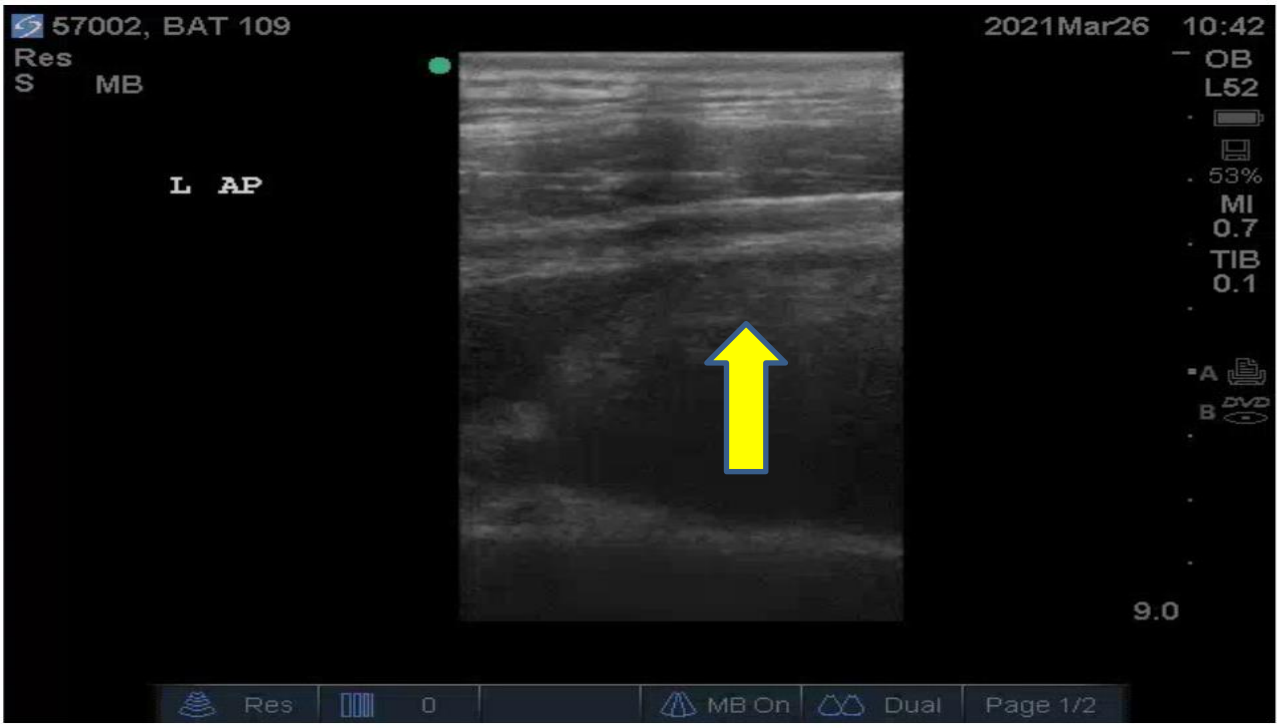

Figure 59. R2_2: CASE ultrasound image 4 – arrow demonstrates lobar consolidation of lung lobe in left mid chest field adjacent to pleural effusion.

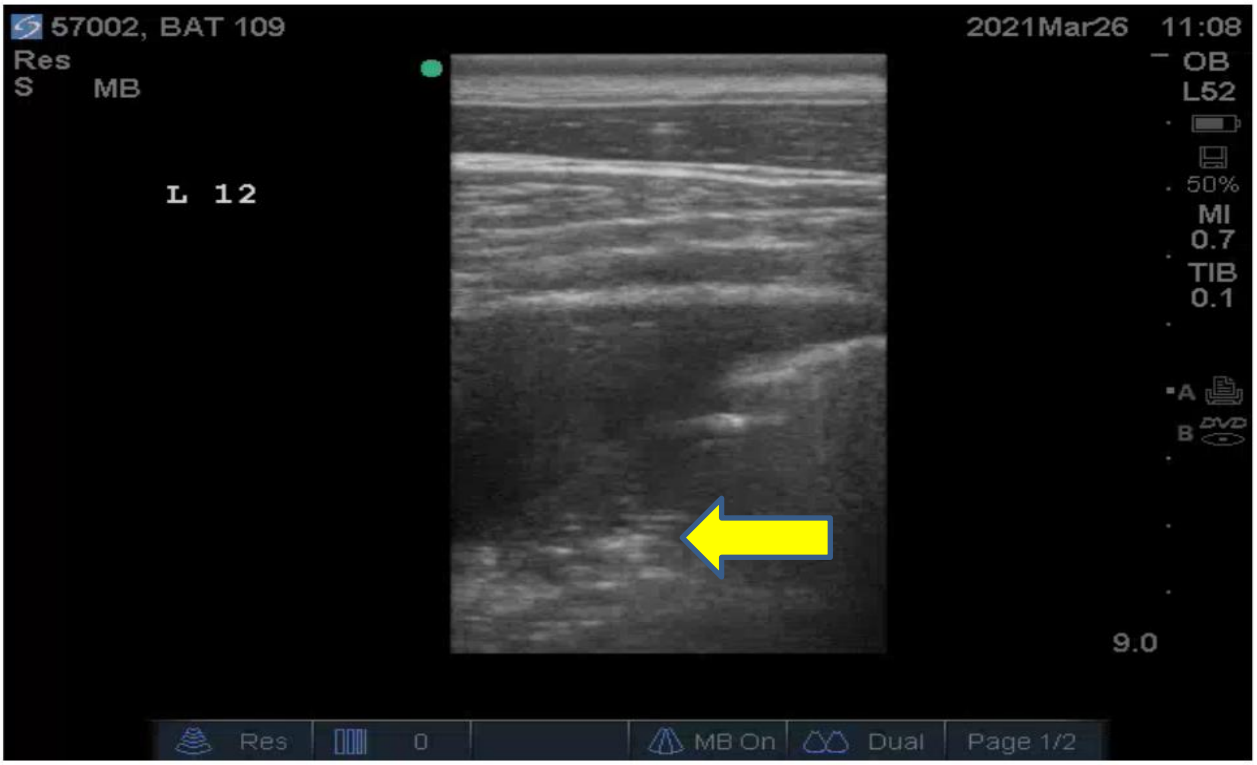

Figure 60. R2_2: CASE ultrasound image 5 – arrow demonstrates lobar lung consolidation in left posterior lung field.

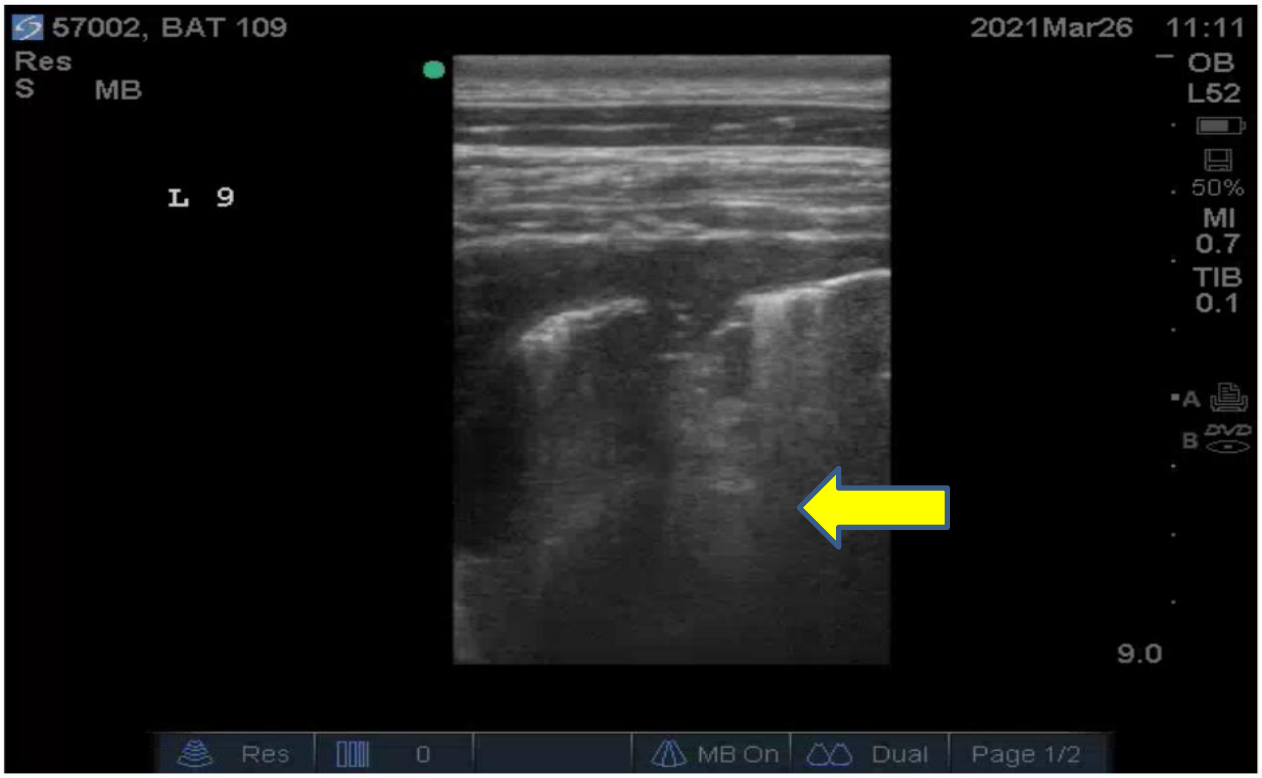

Figure 61: R2_2: CASE necropsy photo – left lung field.

If you are a lot feeder, veterinarian, animal scientist or agricultural/veterinary student, please contact MLA to access version of final report with lung images.

Figure 62. R2_2: CASE necropsy photo – right lung field.

Figure 63. R2_8: CASE – study pen clinical presentation at 3rd clinical illness score =>2, photo 1.

Figure 64. R2_8: CASE - study pen clinical presentation at 3rd clinical illness score =>2, photo 2.

Figure 65. R2_8: CASE ultrasound image 1 – arrow demonstrates lobar lung consolidation adjacent pleural effusion in left mid chest field.

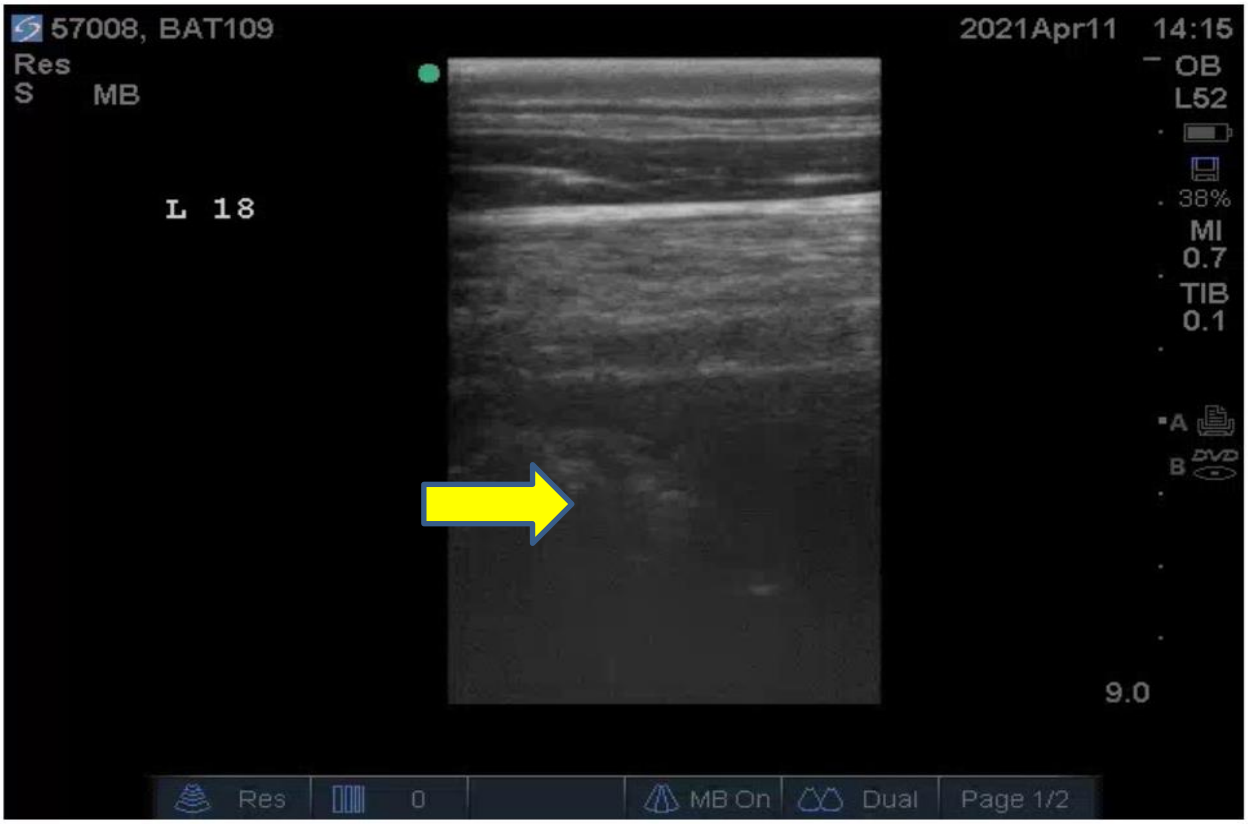

Figure 66. R2_8: CASE ultrasound image 2 – arrow demonstrates lobular lesions and associated comet tail artefacts in left mid chest field.

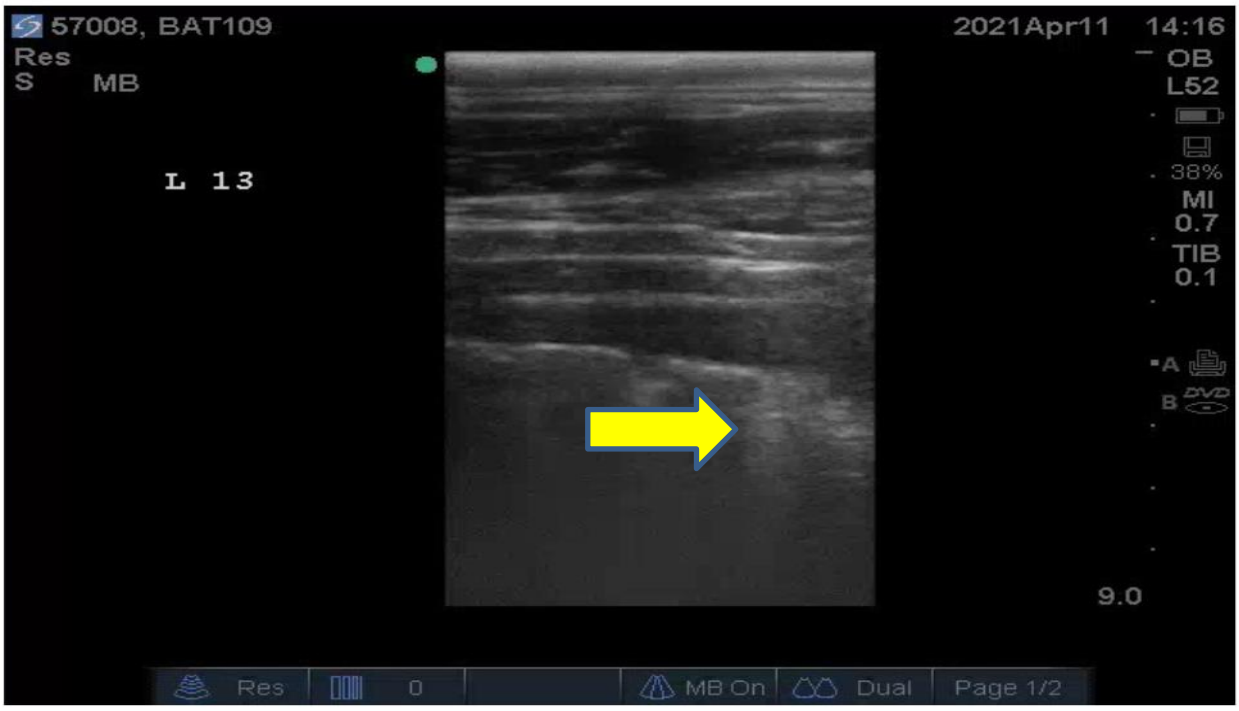

Figure 67. R2_8: CASE ultrasound image 3 – arrow demonstrates pleural effusion adjacent lobar lung consolidation in right anterior chest field.

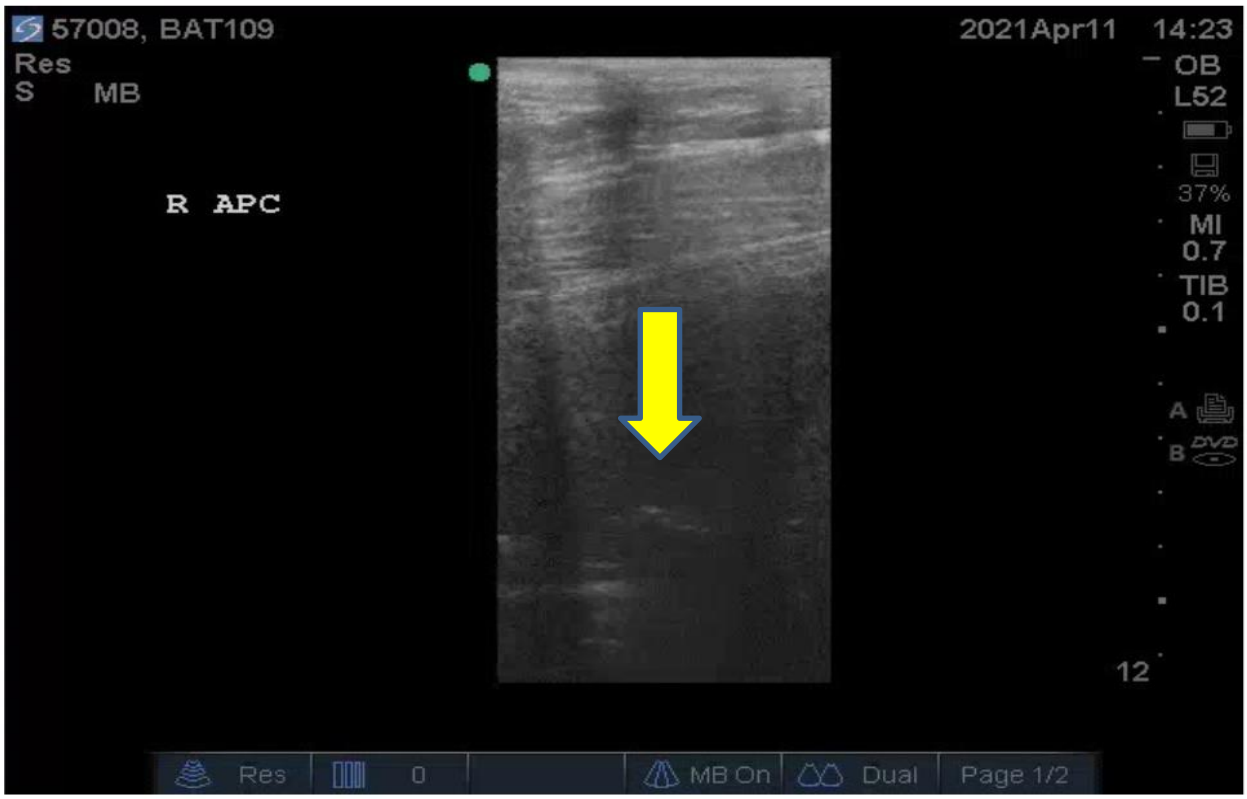

Figure 68. R2_8: CASE ultrasound image 4 – arrow demonstrates lobar lung consolidation in right posterior chest field.

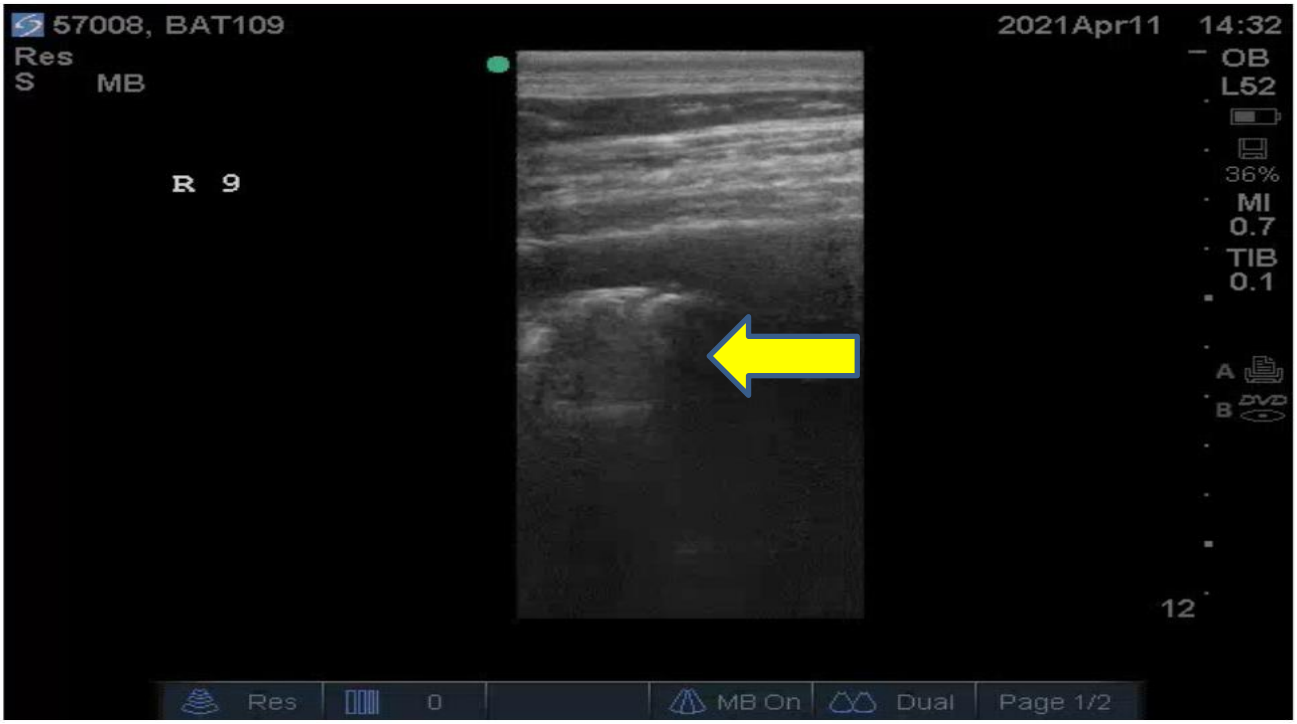

Figure 69: R2_8: CASE necropsy photo – left lung field.

Figure 70: R2_8: CASE necropsy photo – right lung field.

Figure 71. R2_25: CASE - study pen clinical presentation at 3rd clinical illness score =>2.

Figure 72. R2_25: CASE ultrasound image 1 – arrow demonstrates lobar lung consolidation in left anterior chest field.

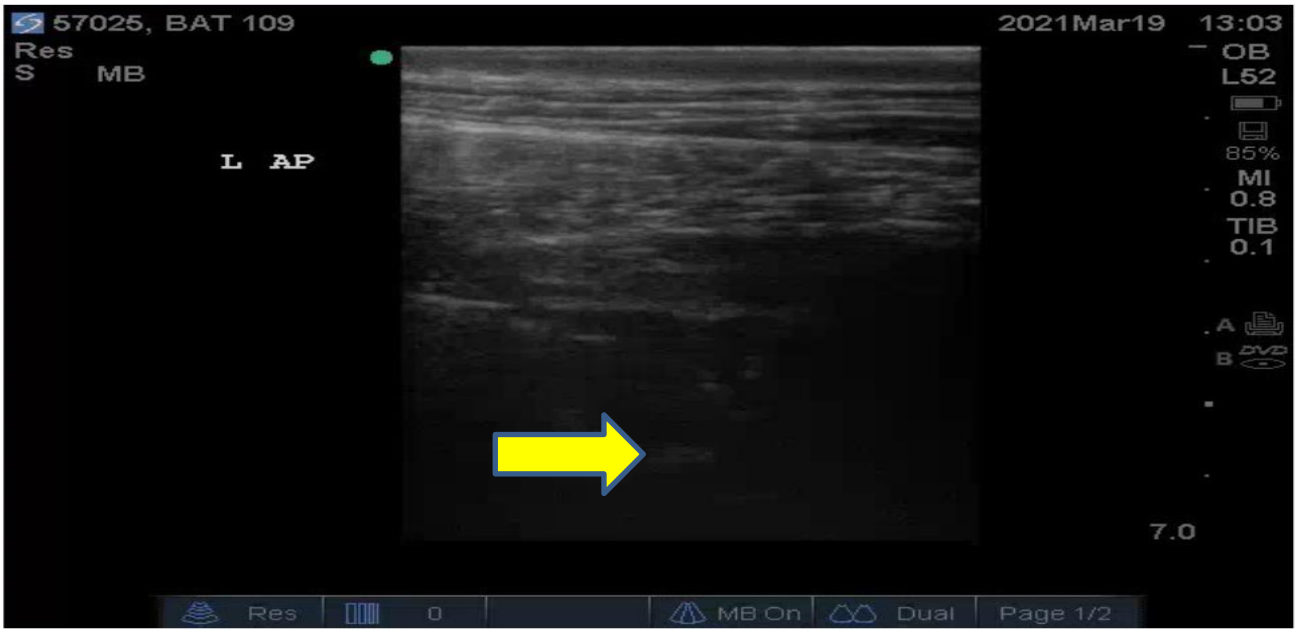

Figure 73. R2_25: CASE ultrasound image 2 – arrow demonstrates fibrin density in pleural effusion, adjacent to lung lobe in right middle chest field.

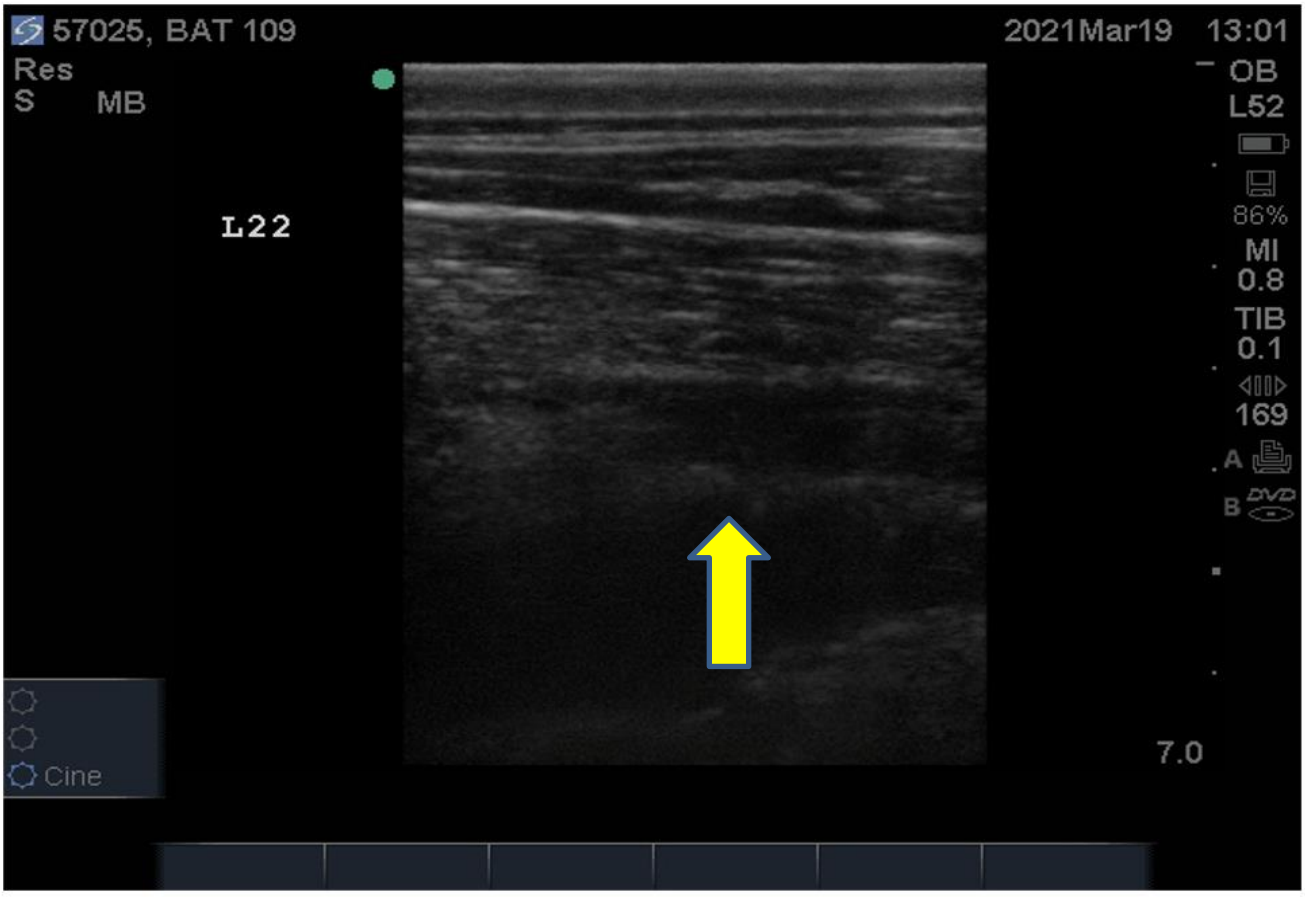

Figure 74. R2_25: CASE ultrasound image 3 – arrow demonstrates lobar lung consolidation adjacent to suppurative pleural effusion in right middle chest field.

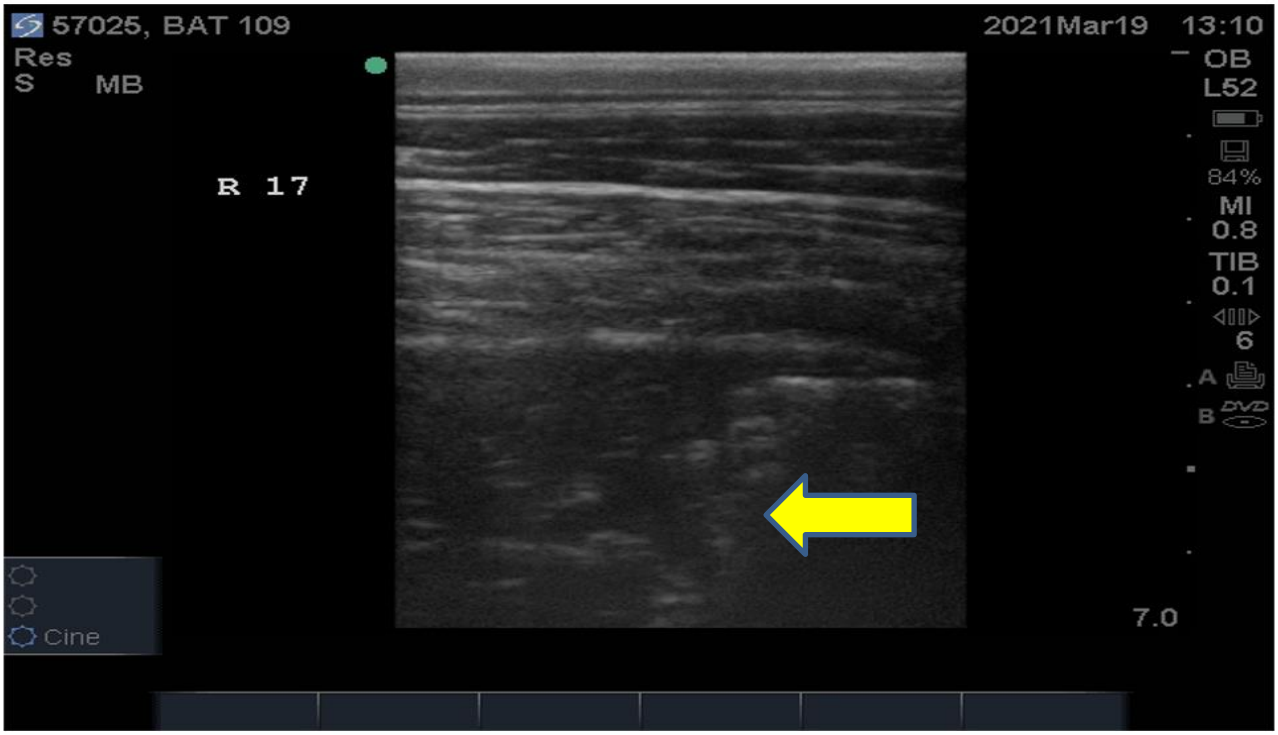

Figure 75: R2_25: CASE necropsy photo – left lung field.

Figure 76: R2_25: CASE necropsy photo – left lung field photo 2, demonstrating suppurative pericardial effusion.

Figure 77: R2_25: CASE necropsy photo – right lung field.

Figure 78. R2_58: CASE - study pen clinical presentation at 3rd clinical illness score =>2.

Figure 79. R2_58: CASE ultrasound image 1 – arrow demonstrates large lobar lung consolidation of bronchopneumonia in right anterior chest field.

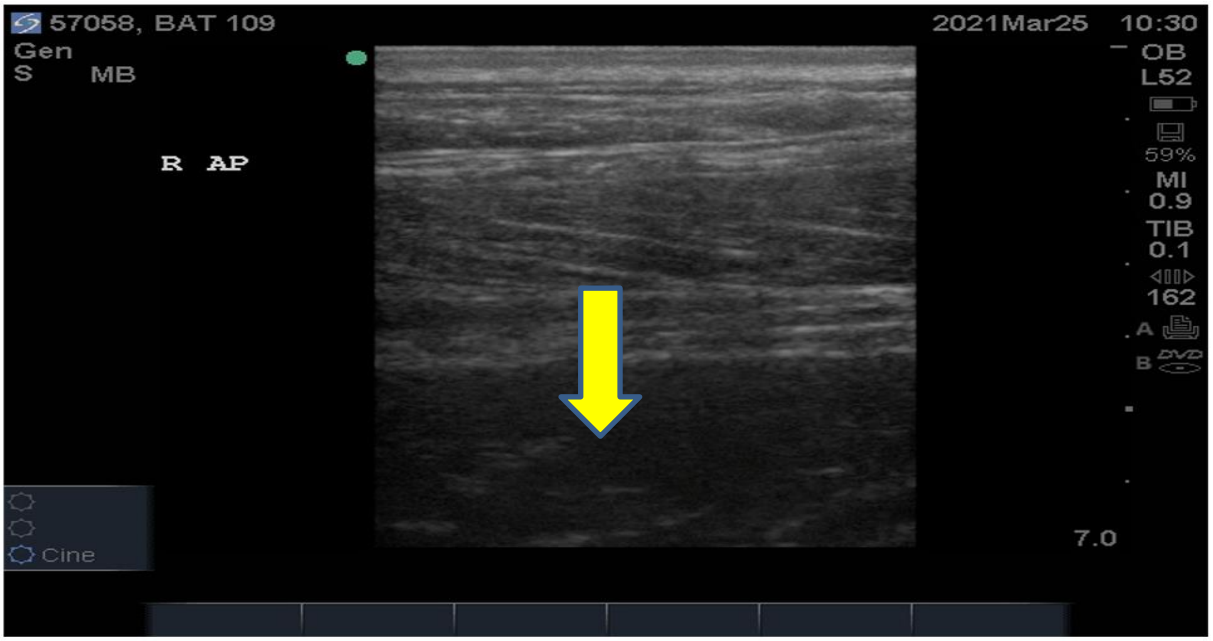

Figure 80. R2_58: CASE ultrasound image 2 – arrow demonstrates lobar lung consolidation in right middle chest field.

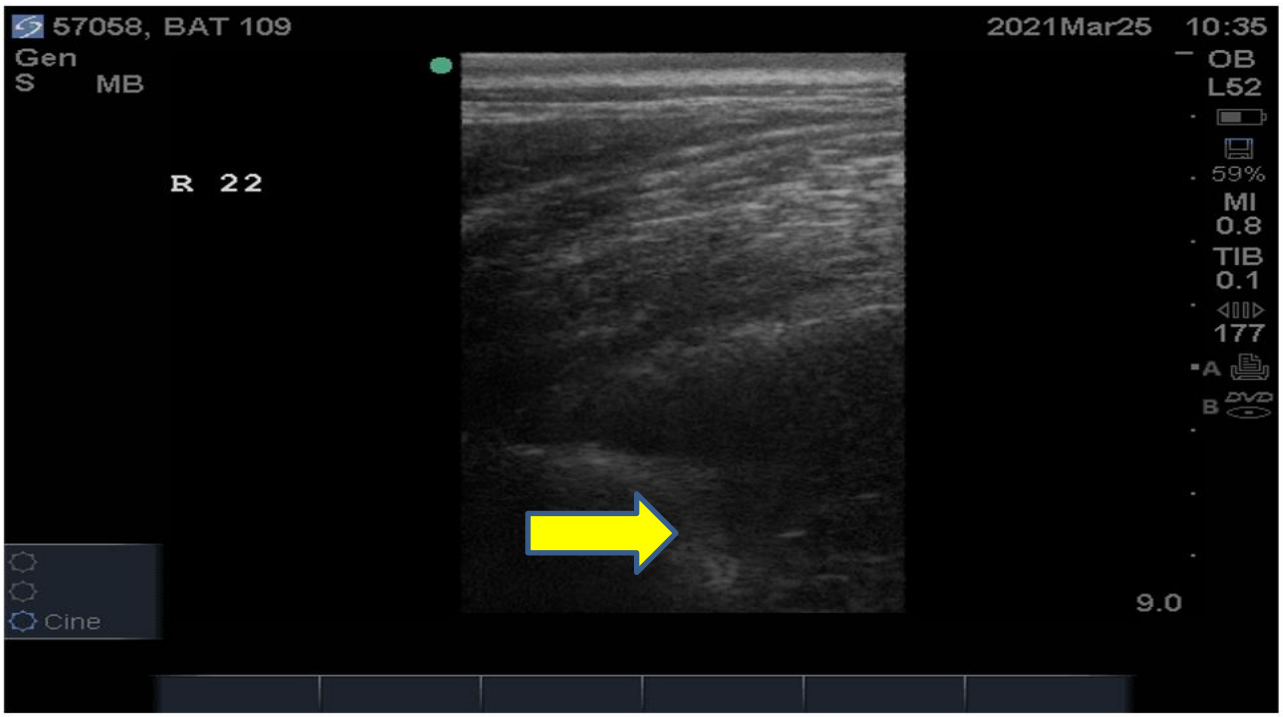

Figure 81. R2_58: CASE ultrasound image 3 – arrow demonstrates nil findings in left anterior chest field.

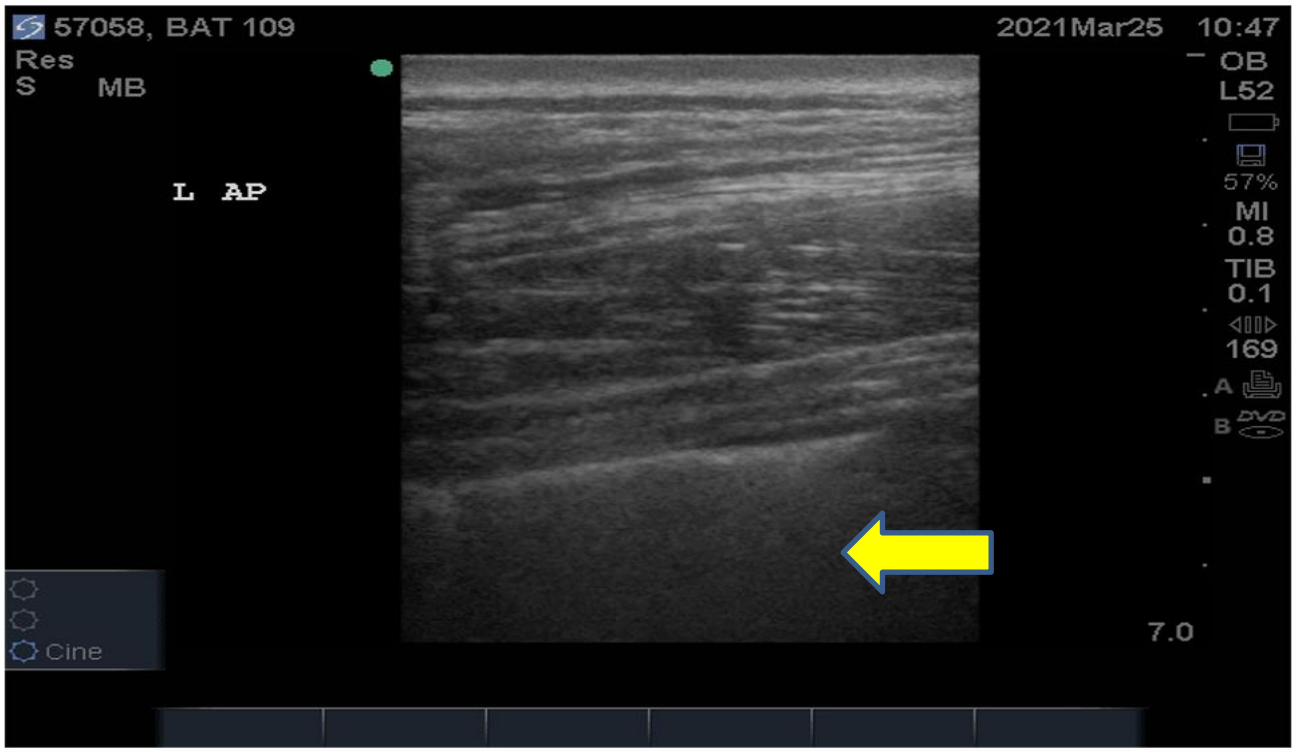

Figure 82. R2_58: CASE ultrasound image 4 – arrow demonstrates lobar lung consolidation in left middle chest field.

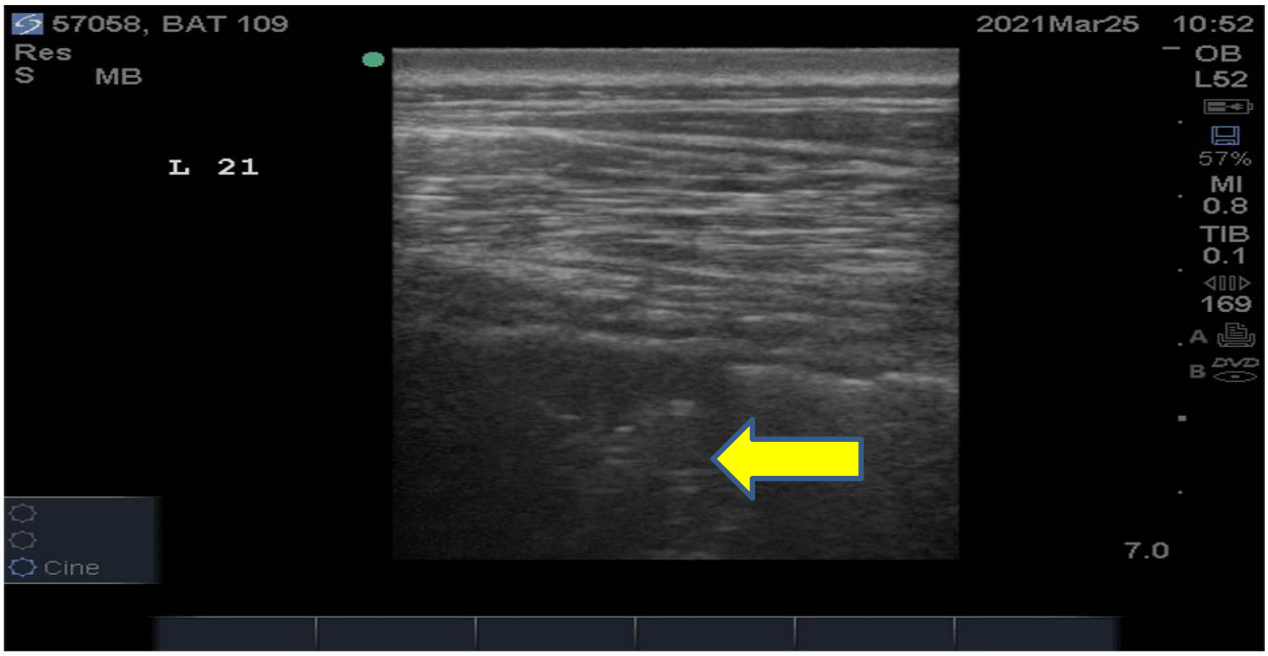

Figure 83: R2_58: CASE necropsy photo – left lung field, demonstrating normal gross appearance in anterior and posterior chest fields, with consolidation in middle lung field. Note agreement with ultrasound imaging above.

Figure 84: R2_58: CASE necropsy photo – right lung field.

Figure 85. R2_59: CASE - study pen clinical presentation at 3rd clinical illness score =>2.

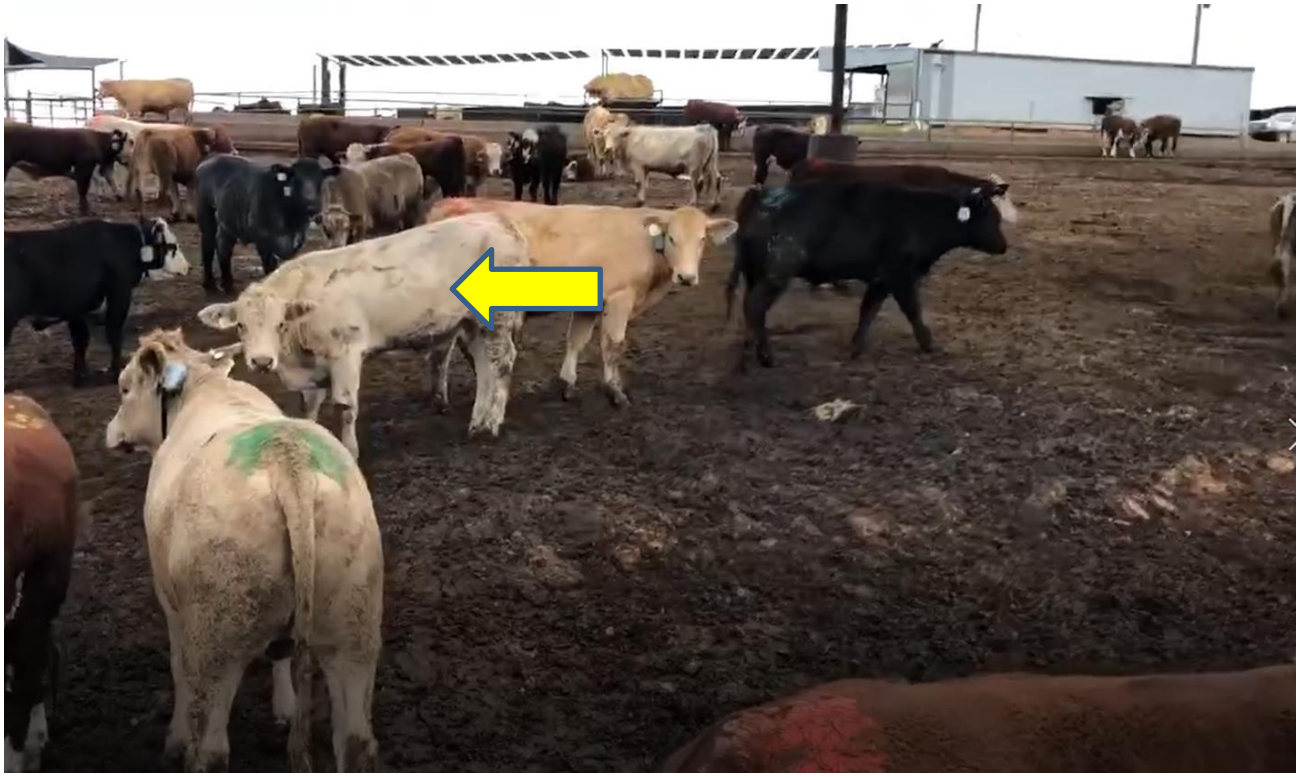

Figure 86. R2_59: CASE ultrasound image 1 – arrow demonstrates lobar lung consolidation of bronchopneumonia in right anterior chest field.

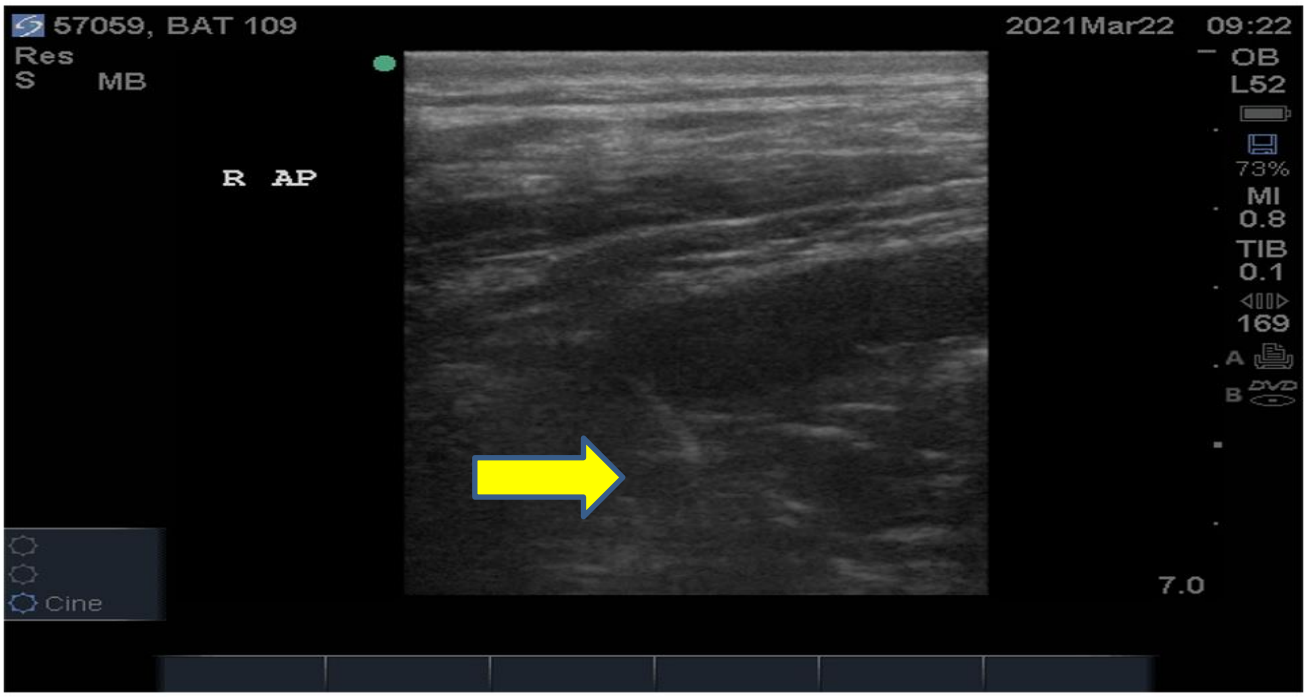

Figure 87. R2_59: CASE ultrasound image 2 – arrow demonstrates junction of normal lung and lobar lung consolidation of bronchopneumonia in right middle chest field.

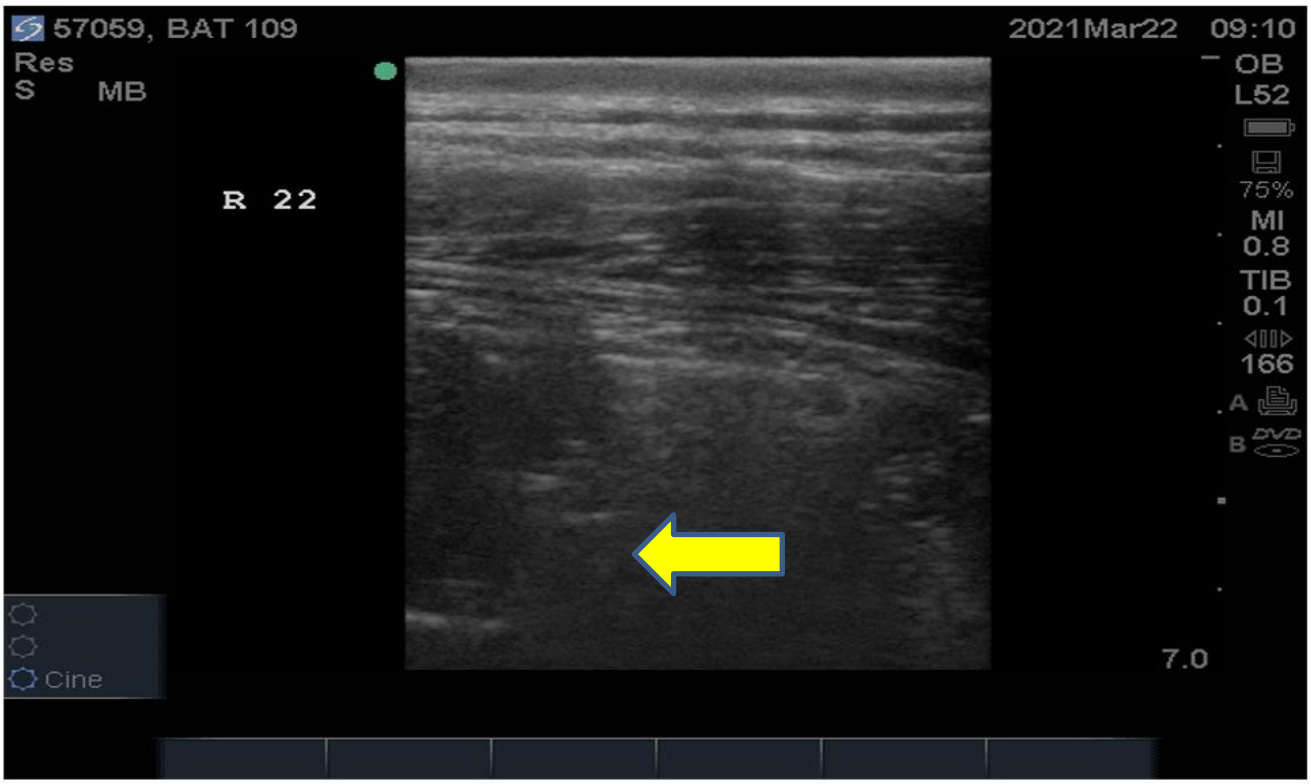

Figure 88: R2_59: CASE necropsy photo – left lung field.

Figure 89: R2_59: CASE necropsy photo – right lung field.

Figure 90. R2_101: CASE - study pen clinical presentation at 3rd clinical illness score =>2.

Figure 91. R2_101: CASE – hospital lane clinical presentation at 3rd clinical illness score =>2, photo 2.

Figure 92. R2_101: CASE ultrasound image 1 – arrow demonstrates lobar lung consolidation of bronchopneumonia adjacent pleural effusion in the right anterior chest field.

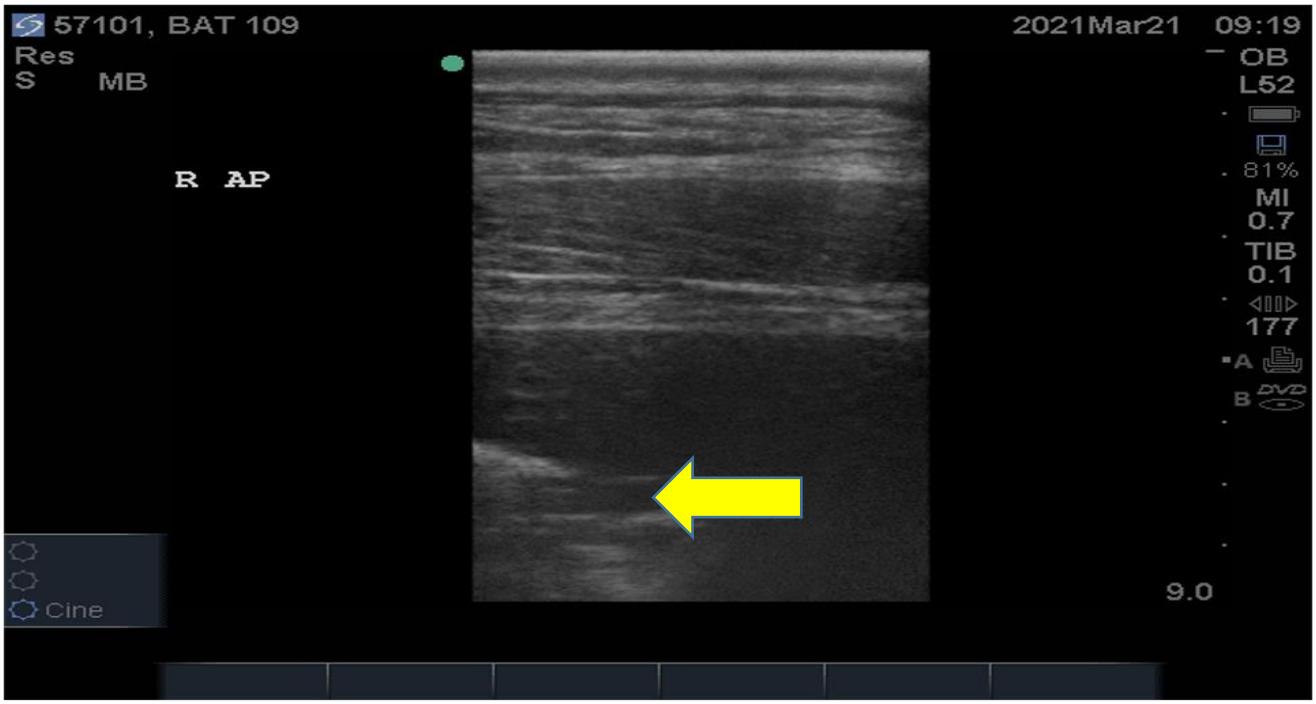

Figure 93. R2_101: CASE ultrasound image 2 – arrow demonstrates lobar lung consolidation of bronchopneumonia in the right anterior chest field.

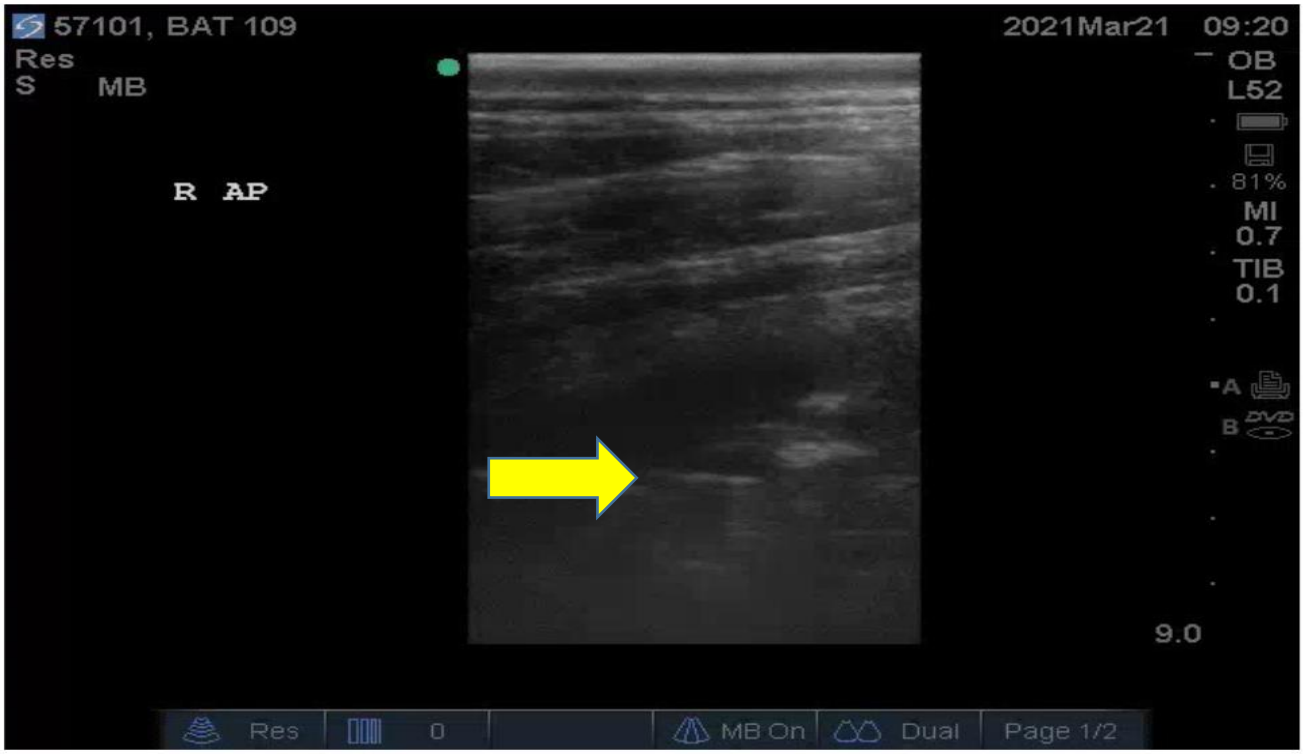

Figure 94. R2_101: CASE ultrasound image 3 – arrow demonstrates large lobar lung consolidation of bronchopneumonia, adjacent fibrin densities in pleural effusion in the right middle chest field.

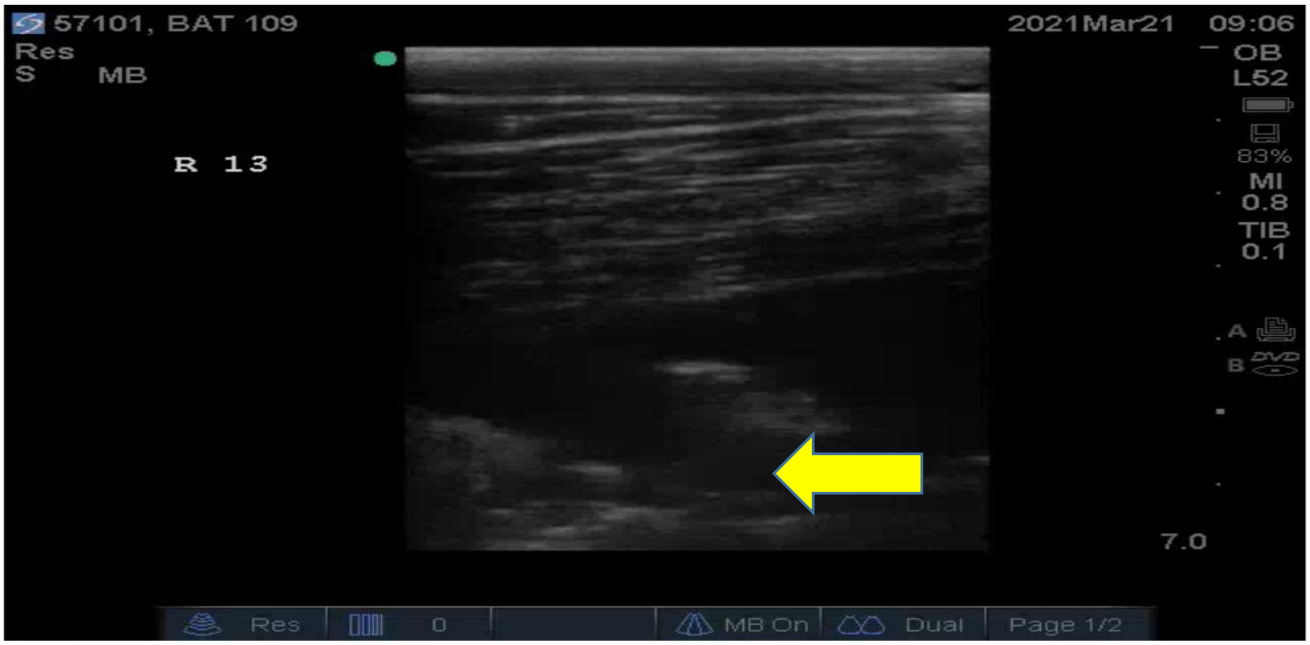

Figure 95: R2_101: CASE necropsy photo – left lung field.

Figure 96: R2_101: CASE necropsy photo – right lung field.

Figure 97. R2_181: CASE – study pen clinical presentation at 3rd clinical illness score =>2.

Figure 98. R2_181: CASE ultrasound image 1 – arrow demonstrates lobar lung consolidation, adjacent to normal lung, in left anterior chest field.

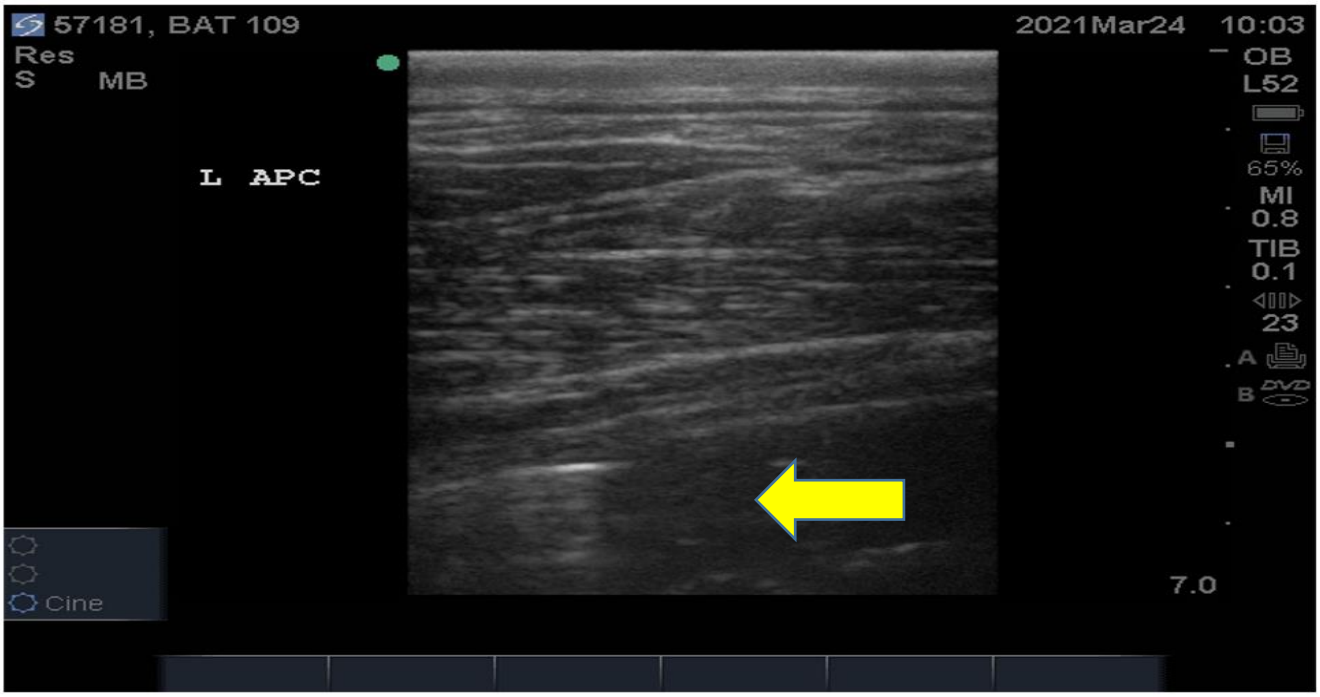

Figure 99. R2_181: CASE ultrasound image 2 – arrow demonstrates fibrinosuppurative density in pleural effusion in left anterior chest field.

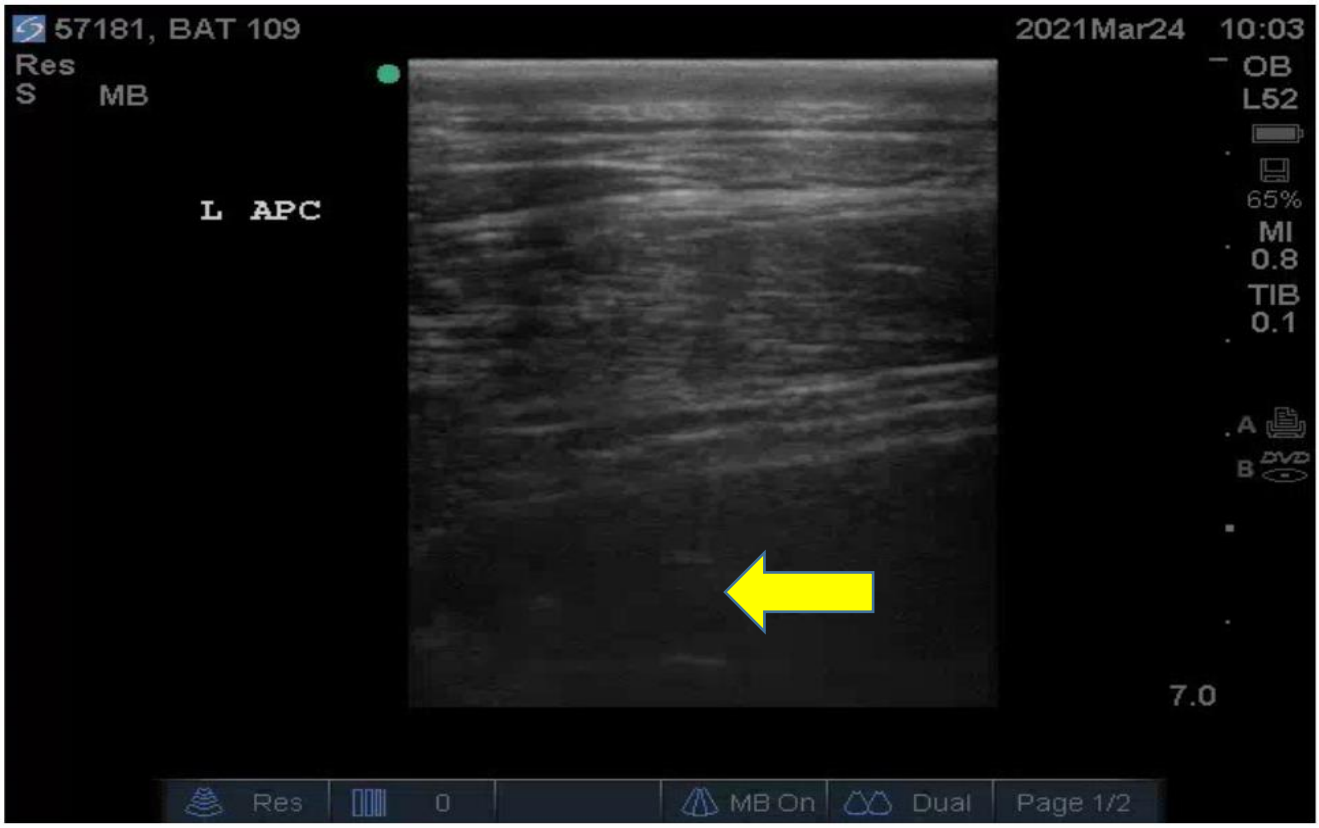

Figure 100: R2_181: CASE necropsy photo – left lung field.

Figure 101: R2_181: CASE necropsy photo – right lung field.

Figure 102: R2_181: CASE necropsy photo – both sides of chest field viewed from dorsal (top) aspect.

Figure 103. R1_130: CASE – study pen clinical presentation at 3rd clinical illness score =>2.

Figure 104. R1_130: CASE ultrasound image 1 – arrow demonstrates large lobar consolidation in left middle chest field.

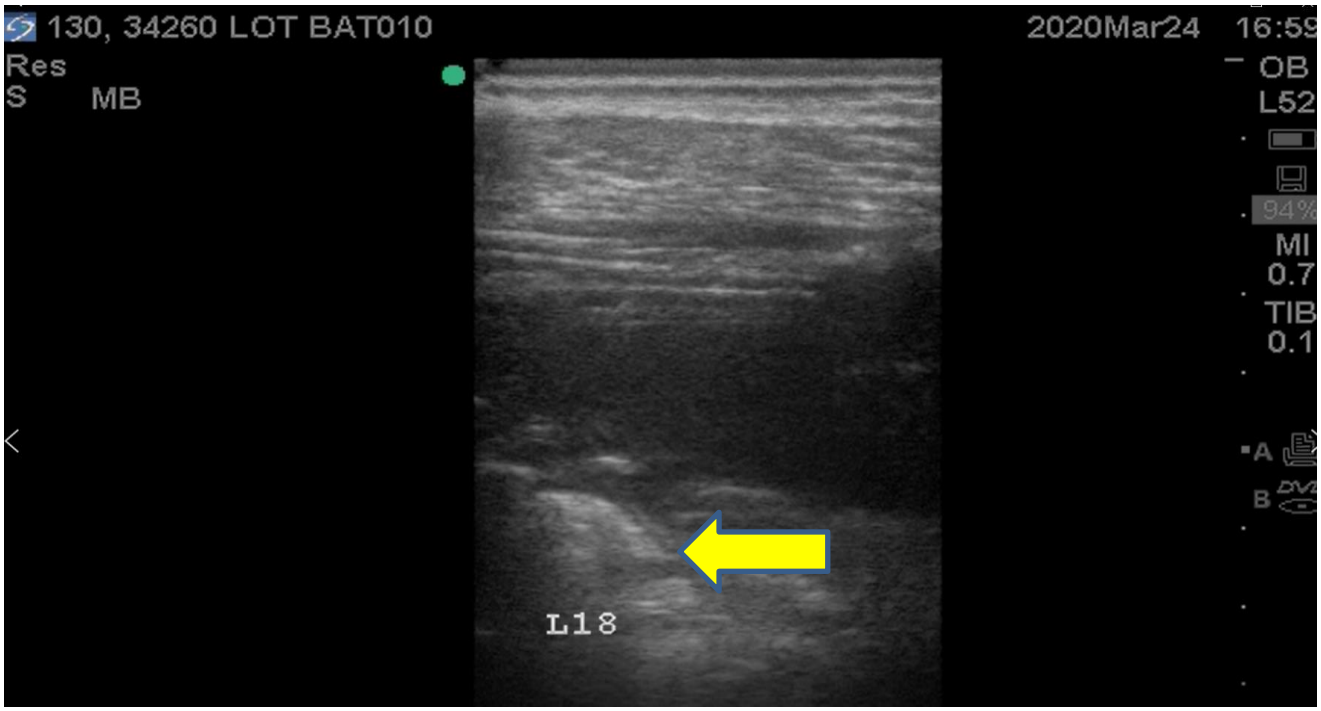

Figure 105. R1_130: CASE ultrasound image 2 – arrow demonstrates lobular lesion comet tail artefacts and pleural effusion adjacent in left upper middle chest field.

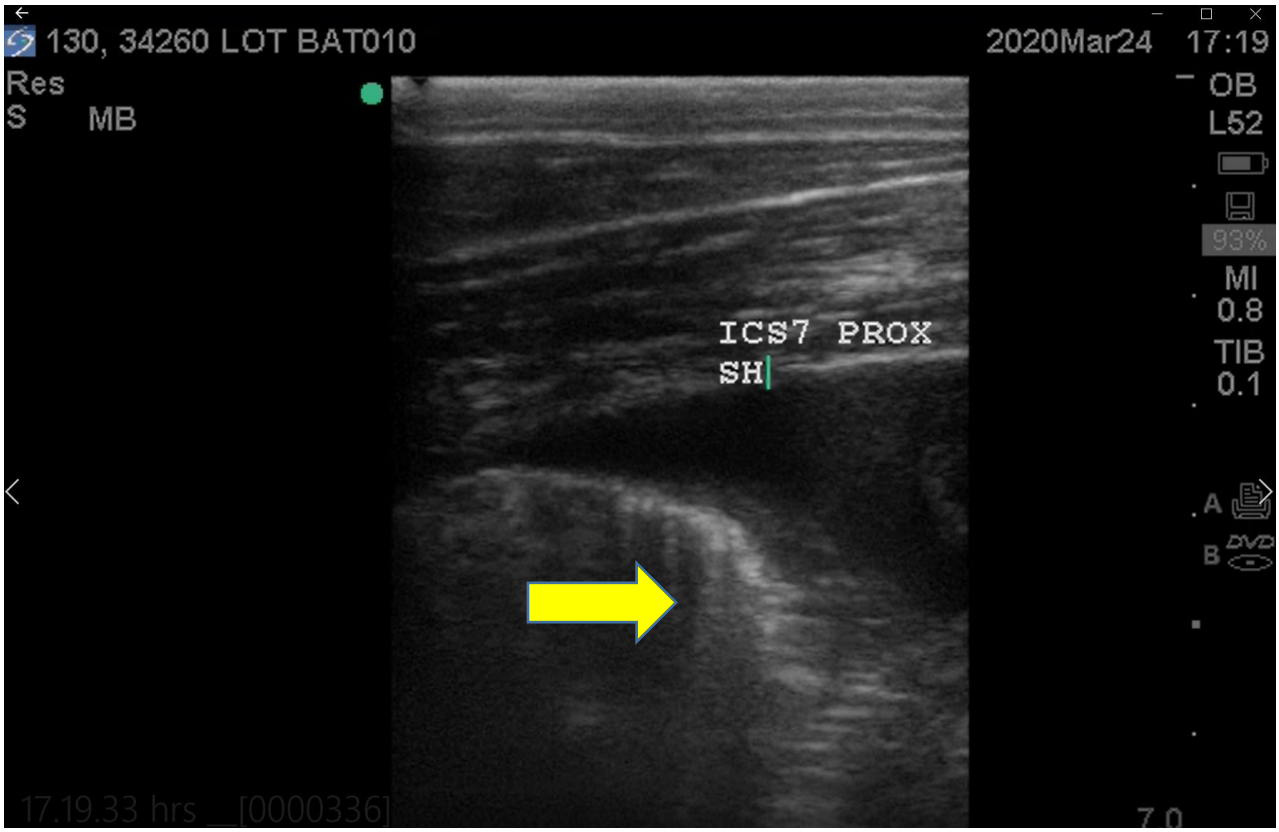

Figure 106. R1_130: CASE ultrasound image 3 – arrow demonstrates large lobar consolidation and adjacent pleural effusion in left upper middle chest field.

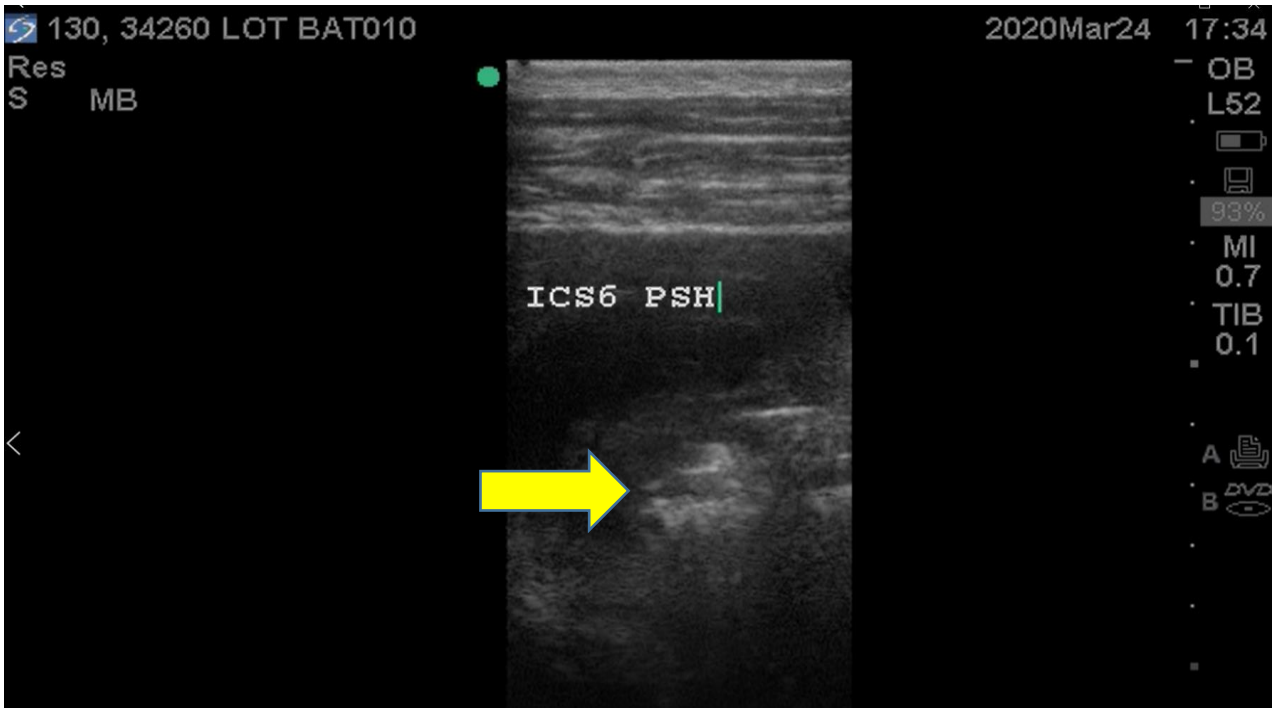

Figure 107. R1_130: CASE ultrasound image 4 – arrow demonstrates large lobar consolidation and adjacent pleural effusion in left middle chest field.

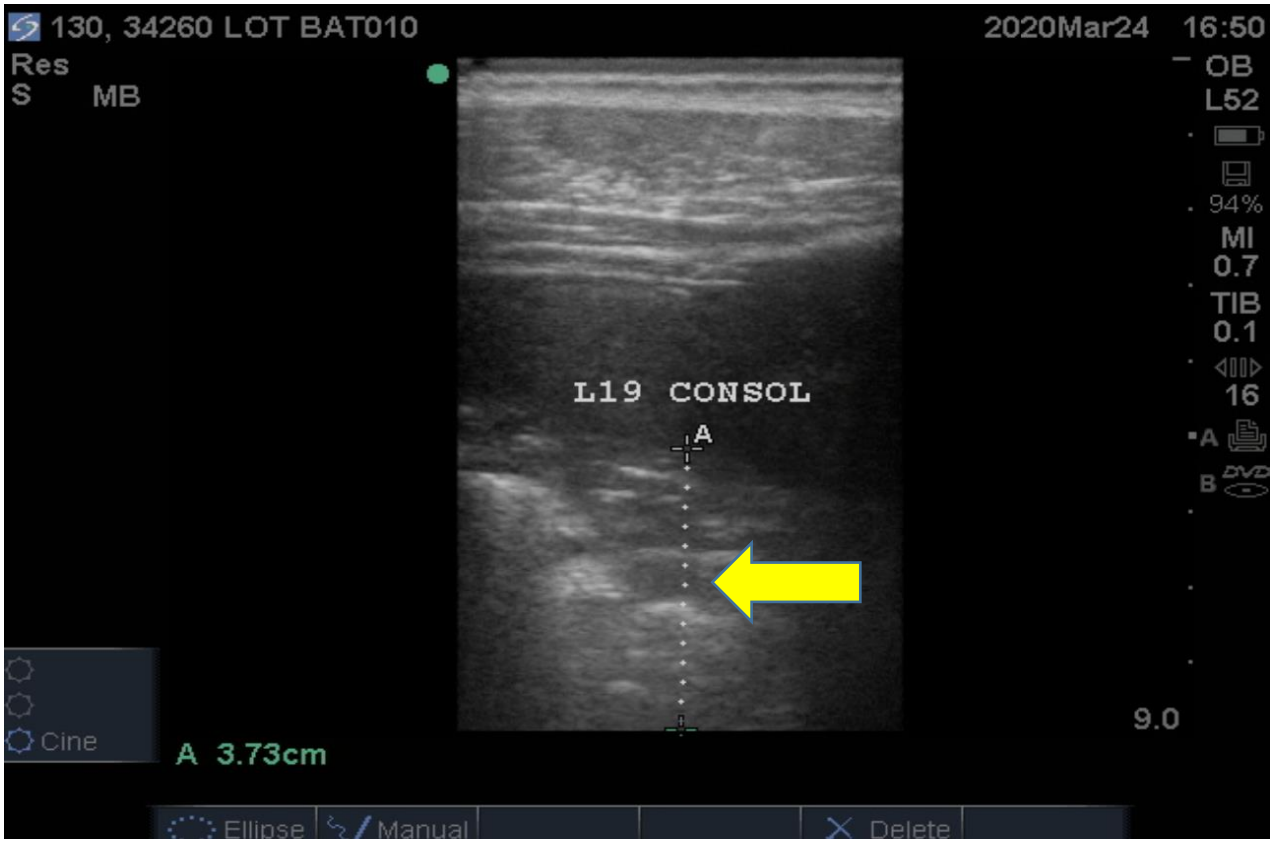

Figure 108: R1_130: CASE necropsy photo – left lung field.

Figure 109: R1_130: CASE necropsy photo – right lung field.

Figure 110. R1_89: CASE ultrasound image 1 – arrow demonstrates edge of lobar consolidation and adjacent lobular lesions with associated comet tail artefacts in right middle chest field.

This first CASE in the series informed the ultrasonography researcher on finalising a technique for gaining maximum access to the axillary area of the bovine patient in order to image the more cranial (anterior) lung field.

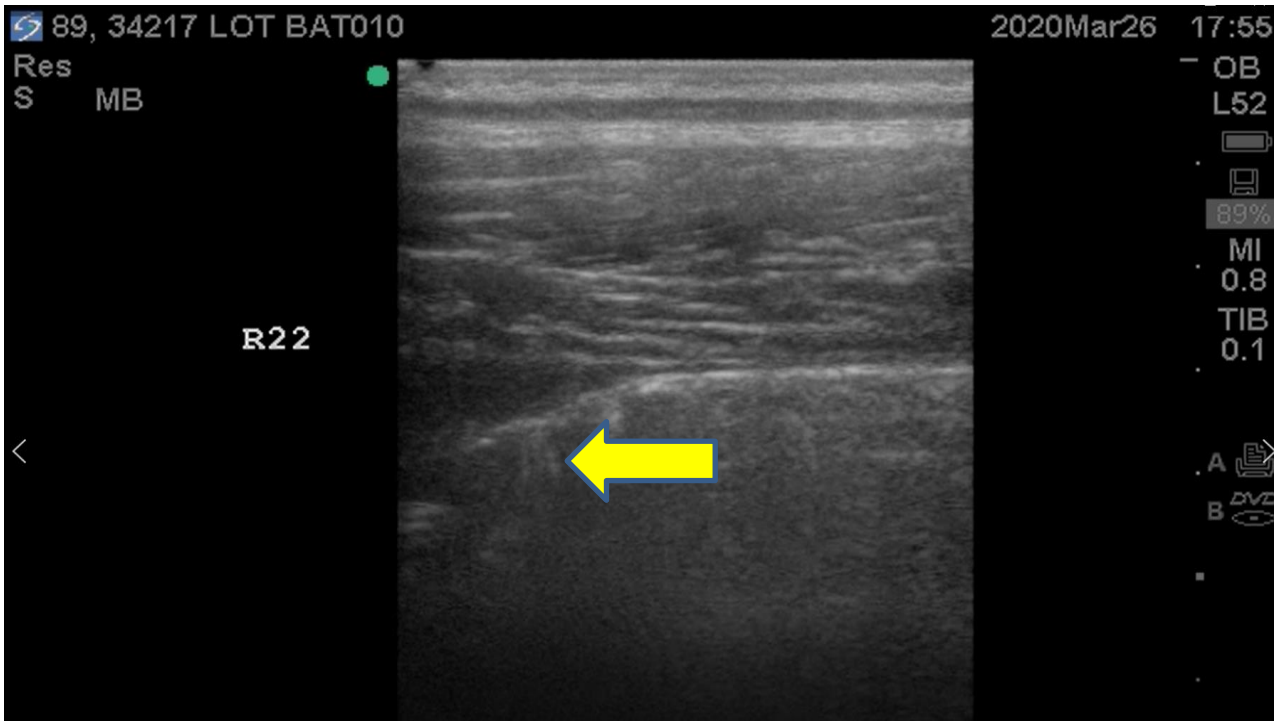

Figure 111. R1_89: CASE necropsy photo – dorsal view, ear tags adjacent right lung field.

Figure 112. R1_89: CASE necropsy photo 2 – right lung field, post-mortem knife indicating anterior lung lobe consolidation.

Figure 113. R1_110: CASE necropsy photo 1 – dorsal lung field with no gross pathology evident.

Figure 114. R1_110: CASE necropsy photo 2 – left lung field with no gross pathology evident.

Figure 115. R1_110: CASE necropsy photo 3 – right accessory lung lobe consolidation.

Figure 116. R1_110: CASE necropsy photo 4 – right dorsal lung lobe consolidation.

Total consolidation area taken from pathology present in figures 112 and 113 = 3.4%

Figure 117. R1_110: CASE necropsy photo 5 – necrotic laryngitis lesions demonstrated. These lesions contributed to clinical illness scoring per the study protocol.

8.2 Non-CASE/CONT study animals' examinations

Figure 118. R2_158: study pen clinical presentation on 13th April 2021.

This animal received clinical illness score >= 2 on five occasions, however didn't meet the study criteria for preliminary CASE candidature because of insufficient rectal temperature at 3rd call (13/4/21). These scores occurred on the following dates; 31/3/21, 3/4/21, 12/4/21 (am and pm), and 13/4/21.

Harvest slaughter occurred on 24/5/21; lesions present on all lung lobes except accessory, and most consolidation in the left and right apical lobes. Total consolidation = 28%.

Figure 119. R2_158 ultrasound image 1 – arrow demonstrates junction of lobar consolidation and normal lung architecture in the left middle chest field.

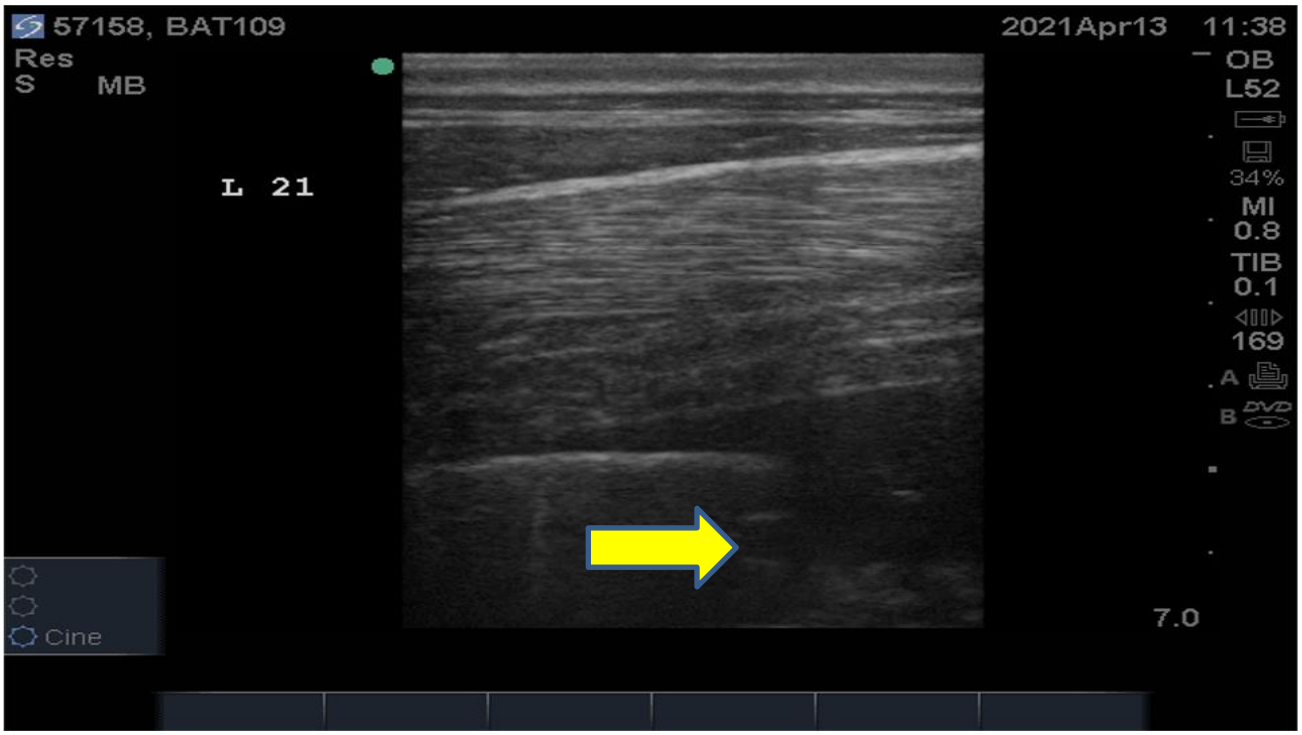

Figure 120. R2_158 ultrasound image 2 – arrow demonstrates lobar consolidation in the left middle chest field, further caudal (backwards) compared to **Figure 119**.

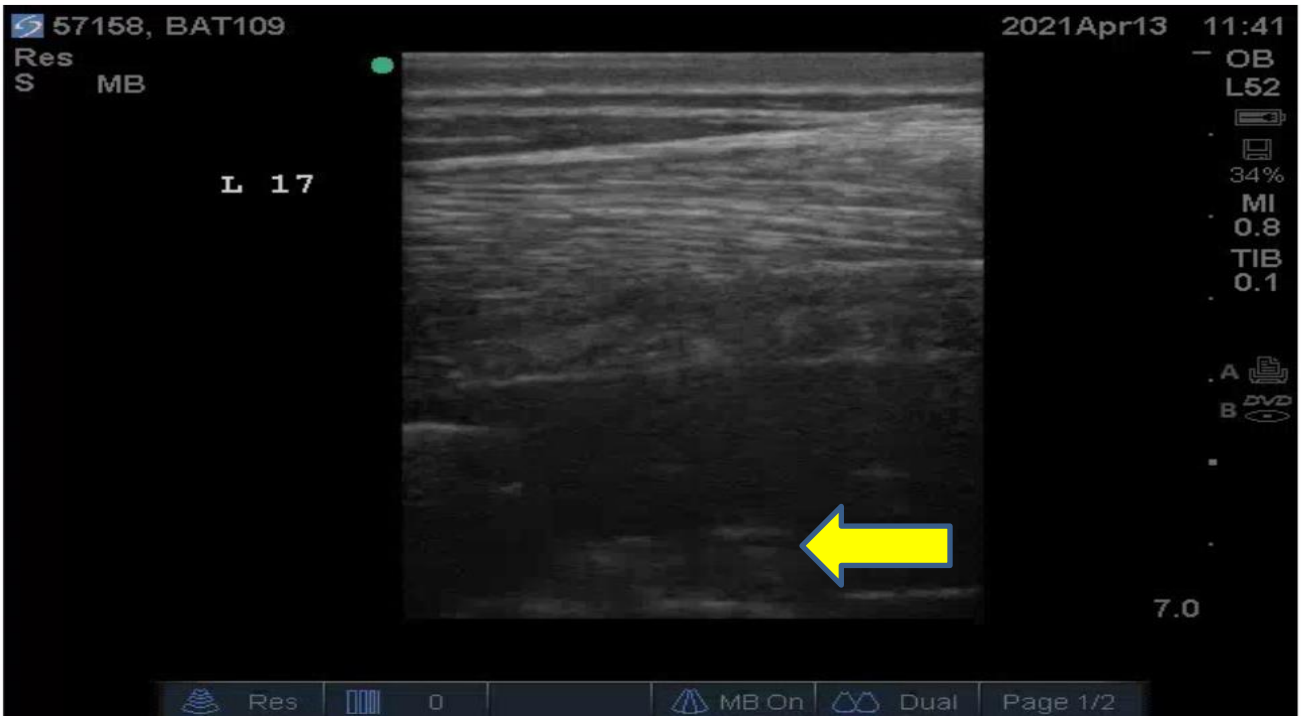

Figure 121. R2_158 ultrasound image 3 – arrow demonstrates significant fibrin deposition in pleural effusion in the left anterior chest field.

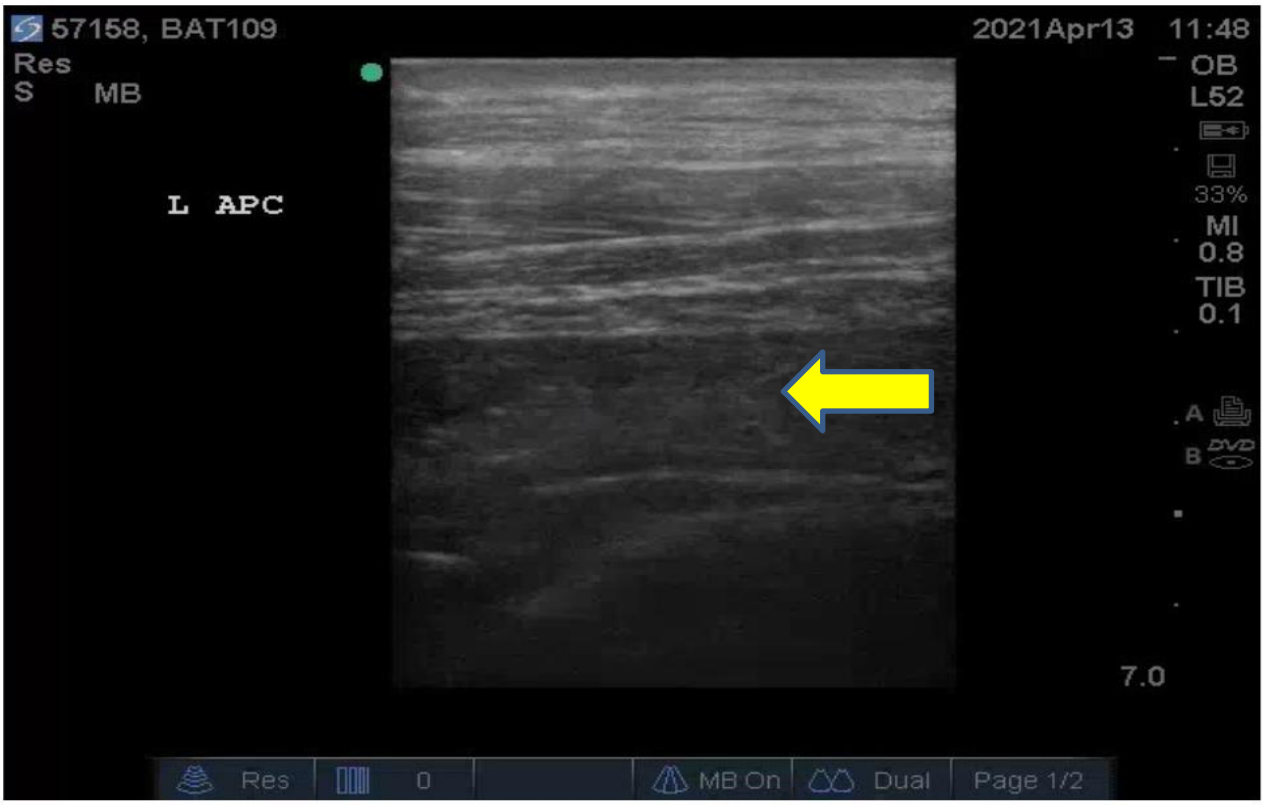

Figure 122. R2_158 ultrasound image 4 – arrow demonstrates lobar consolidation and pleural effusion in the right anterior chest field.

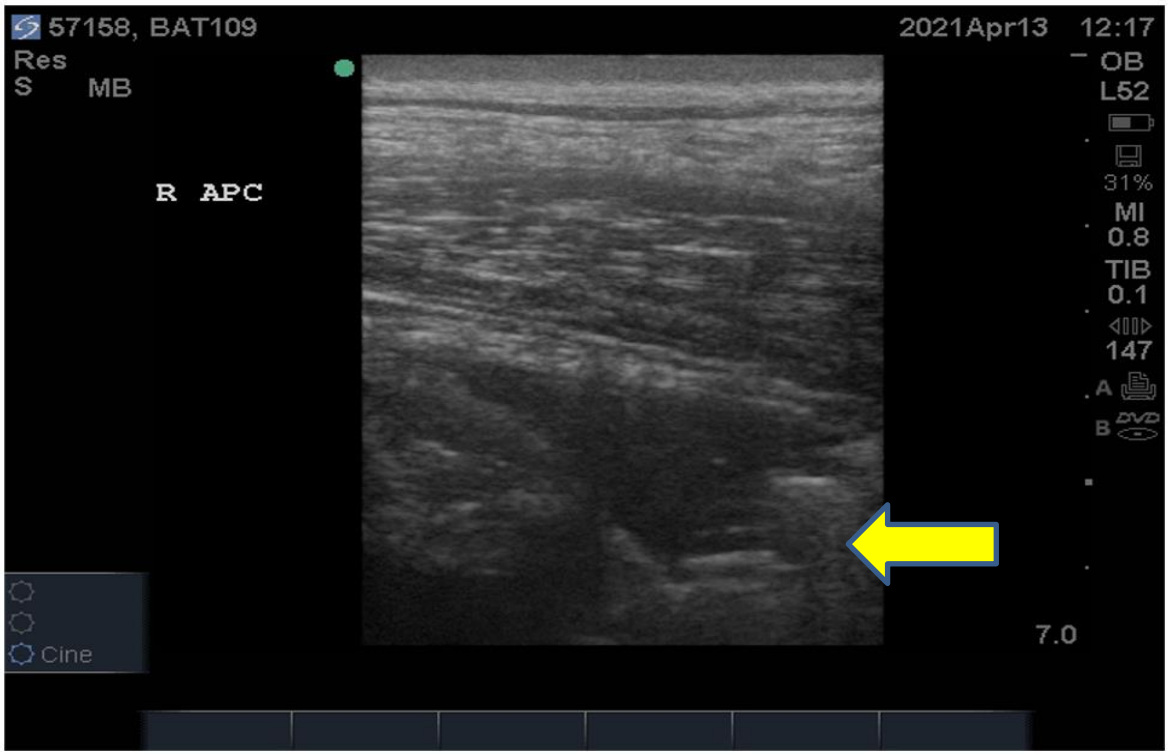

Figure 123. R1_136 ultrasound image 1 – arrow demonstrates lobar consolidation in right anterior chest field (11th May, 2021).

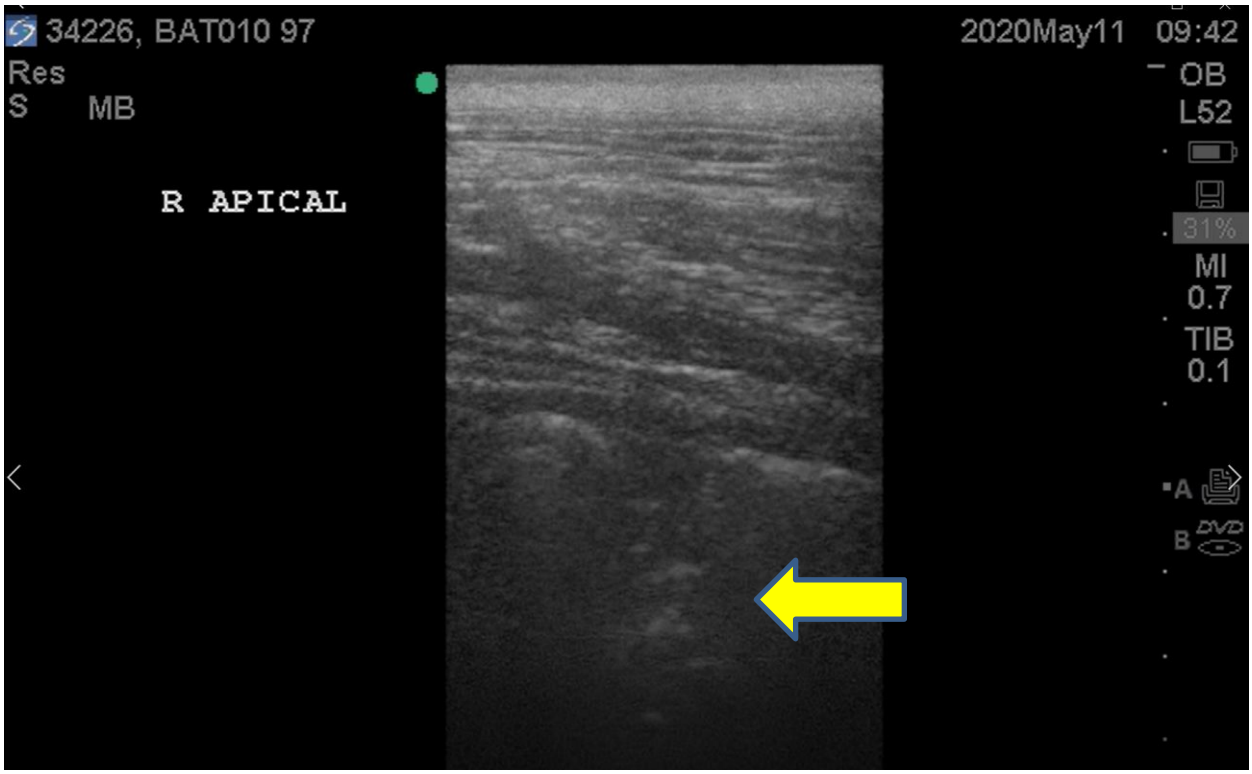

This animal received one clinical illness score = 2 on 9th March 2020 and thus became ineligible for "CONT" candidate.

Presented for Eliko tag change on 17th April 2020, which presented an opportunity for ultrasound survey to be conducted bilateral (both sides of chest); no lesions detected.

On 11th May, the animal pulled under normal feedlot protocol for BRD treatment per the conditions of the animal ethics approval whereby the study design could be overridden. Accordingly, this animal was not a candidate for "CASE" enrolment. Ultrasound imaging from this examination is above in Figure 120. Pathology was evident in the right apical lung lobes (right anterior chest field). The animal was treated with tulathromycin (Draxxin®) and monitored in the hospital recovery pen. At the feedlot protocol re-treatment interval assessment, sufficient recovery for return to home (study) pen was determined.

This animal was subsequently presented for an ultrasound screening survey on exit from the feedlot (per the original study protocol) on 11th June (+ 30 days from Draxxin® treatment) – no lesions in the right chest field were detected.

This animal was then presented for slaughter on 19th June (+38 days from Draxxin treatment) – no lung lesions were detected on visual inspection of the respiratory offal.

The history of this study animal appears to support a successful resolution of BRD pathology in the right apical lung lobes such that lesions could not be detected 38 days after initial presentation.

The other significant interpretation of these findings is that validating a diagnostic modality on slaughter findings alone, against treatment records in this particular case, would have (mis)classified the feedlot treatment as a “false positive” given that there were no lesions at slaughter.

Figure 124. R1_136 temporal profile of reticulo-rumen temperature for the study period.

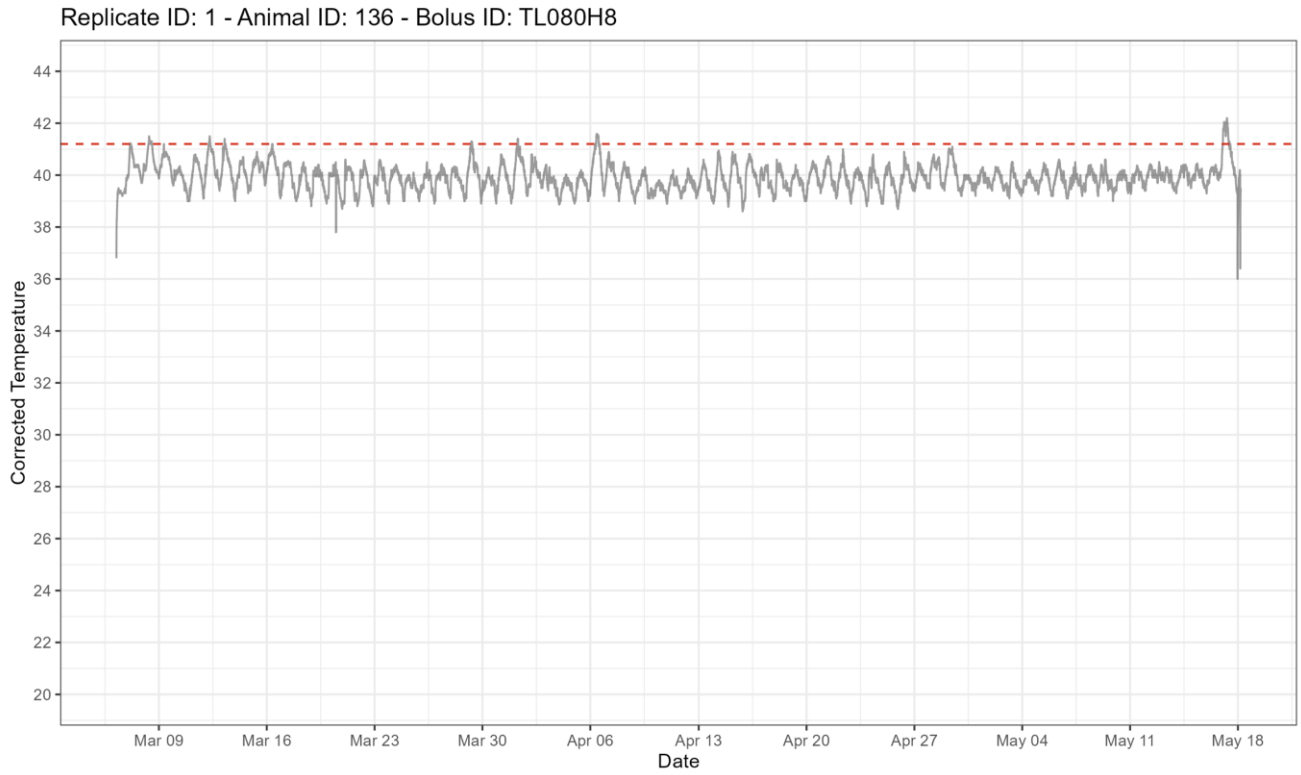

Table 41. WinPepi output for estimates of group size required for sufficient study power at expected sensitivity and specificity of 90% and 50% for the test diagnostics.

Expected sensitivity	No. animals with BRD enrolled (these are animals that truly have BRD ie based on the gold standard)	95% CI[1]
90%	30	0.7347 to 0.9789
90%	50	0.7819 to 0.9667
90%	70	0.8048 to 0.9588
90%	90	0.8186 to 0.9532
90%	110	0.8281 to 0.9490
90%	130	0.8351 to 0.9457
90%	150	0.8404 to 0.9429
50%	30	0.313 to 0.687
50%	50	0.355 to 0.645
50%	70	0.378 to 0.622
50%	90	0.393 to 0.607
50%	110	0.403 to 0.597
50%	130	0.411 to 0.589
50%	150	0.417 to 0.583

[1] Fisher's exact 95% confidence intervals calculated using WinPepi version 11.65 (Describe version 3.18; http://www.brixtonhealth.com/pepi4windows.html)

Expected specificity	No. animals without BRD enrolled (these are animals that truly don't have BRD ie based on the gold standard)	95% CI[1]
90%	30	0.7347 to 0.9789
90%	50	0.7819 to 0.9667
90%	70	0.8048 to 0.9588
90%	90	0.8186 to 0.9532
90%	110	0.8281 to 0.9490
90%	130	0.8351 to 0.9457
90%	150	0.8404 to 0.9429
50%	30	0.313 to 0.687
50%	50	0.355 to 0.645
50%	70	0.378 to 0.622
50%	90	0.393 to 0.607
50%	110	0.403 to 0.597
50%	130	0.411 to 0.589
50%	150	0.417 to 0.583

[1] Fisher's exact 95% confidence intervals calculated using WinPepi version 11.65 (Describe version 3.18; http://www.brixtonhealth.com/pepi4windows.html)

9 Bibliography

Abdallah, A., Hewson, J., Francoz, D., Selim, H., Buczinski, S., (2016). Systematic Review of the Diagnostic Accuracy of Haptoglobin, Serum Amyloid A, and Fibrinogen versus Clinical Reference Standards for the Diagnosis of Bovine Respiratory Disease. Journal of Veterinary Internal Medicine 30(4): 1356-1368 https://doi.org/10.1111/jvim.13975

Amrine, D. E., White, B.J., Larson, R., Anderson, D. E., Mosier, D.A. & Cernicchiaro, N. (2013). Precision and accuracy of clinical illness scores, compared with pulmonary consolidation scores, in Holstein feeder steer with experimentally induced Mycoplasma bovis pneumonia. Am J Vet Res 74(2):310-315. doi: 10.2460/ajvr.74.2.310

Bolyen, E., Rideout, J.R., Dillon, M.R., Bokulich, N.A., Abnet, C.C., Al-Ghalith, G.A., Alexander et al (2019). Reproducible, interactive, scalable and extensible microbiome data science using QIIME 2. Nature Biotechnology 37: 852–857. https://doi.org/10.1038/s41587-019-0209-9

Buczinski, S., et al. (2018). Inter-rater agreement and reliability of thoracic ultrasonographic findings in feedlot feeder steer, with or without naturally occurring bronchopneumonia. Journal of veterinary internal medicine 32(5): 1787-1792.

Buczinski, S., et al. (2016). Incremental Value (Bayesian Framework) of Thoracic Ultrasonography over Thoracic Auscultation for Diagnosis of Bronchopneumonia in Preweaned Dairy Feeder steer. Journal of veterinary internal medicine 30(4): 1396-1401.

Buczinski, S., et al. (2014). Comparison of Thoracic Auscultation, Clinical Score, and Ultrasonography as Indicators of Bovine Respiratory Disease in Preweaned Dairy Feeder steer. Journal of veterinary internal medicine 28(1): 234-242.

Callahan, B.J., McMurdie, P.J., Rosen, M.J., Han, A.W., Johnson, A.J.A., & Holmes, S.P. (2016). DADA2: High-resolution sample inference from Illumina amplicon data. Nat. Meth. 13: 581-583.

Cramer, M. C. & T. L. Ollivett. (2019). Growth of preweaned, group-housed dairy feeder steer diagnosed with respiratory disease using clinical respiratory scoring and thoracic ultrasound—A cohort study. Journal of Dairy Science 102(5): 4322-4331.

Cramer, C., et al. (2020). Automated feeding behaviors associated with subclinical respiratory disease in preweaned dairy feeder steer. Animals (Basel) 10(6): 1-9.

Dixon, P. (2003). VEGAN, a package of R functions for community ecology, Journal of Vegetation Science 14 (6): 927-930.

Galyean, M. L., L. J. Perino, & G. C. Duff. (1999). Interaction of cattle health/immunity and nutrition. J Anim Sci 77(5): 1120-1134.

Hanthorn, C. J., et al. (2014). Serum concentrations of haptoglobin and haptoglobin-matrix metalloproteinase 9 (Hp-MMP 9) complexes of bovine calves in a bacterial respiratory challenge model. BMC veterinary research 10(1): 285.

Hanthorn. C.J, Dewell. G.A, Dewell. R.D, Cooper. V.L., Wang. Chong, Plummer. P.J., & Lakritz. J. (2014). Serum concentrations of haptoglobin and haptoglobin-matrix metalloproteinase 9

(Hp-MMP 9) complexes of bovine calves in a bacterial respiratory challenge model. BMC Veterinary Research 10: 285.

Kassambara, A. (2017). ggpubr: 'ggplot2' Based Publication Ready Plots. R package version 0.1.6. https://CRAN.R-project.org/package=ggpubr.

Lechtenberg, K. F., C. S. Daniels, G. C. Royer, D. T. Bechtol, S. T. Chester, J. Blair, & R. K. Tessman. (2011). Field efficacy study of gamithromycin for the CONT of bovine respiratory disease in cattle at high risk of developing the disease. Intern J Appl Res Vet Med 9(2):184-192.

Mang, A. V., S. Buczinski, C. W. Booker, & E. Timsit. (2015). Evaluation of a Computer-aided Lung Auscultation System for Diagnosis of Bovine Respiratory Disease in Feedlot Cattle. Journal of Veterinary Internal Medicine 29(4):1112-1116. doi: 10.1111/jvim.12657

McMurdie, P.J., & Holmes, S. (2013). phyloseq: an R package for reproducible interactive analysis and graphics of microbiome census data. PloS one 8, e61217.

Moisá, S.J., Aly, S.S., Lehenbauer, T.W., Love, W.J., Rossitto, P.V., Van Eenennaam, A.L., Trombetta, S.C., Bortoluzzi, E.M., & Hulbert. (2019). Association of plasma haptoglobin concentration and other biomarkers with bovine respiratory disease status in pre-weaned dairy calves. Journal of Veterinary Diagnostic Investigation, 31(1):40-46.

NAHMS. (2011a). Part III: Trends in Health and Management Practices on U.S. Feedlots, 1994-2011. In: C. USDA:APHIS:VS, National Animal Health Monitoring System (ed.), Fort Collins, CO.

NAHMS. (2011b). Part IV: Health and Health Management on U.S. Feedlots with a Capacity of 1,000 or More Head. In: C. USDA:APHIS:VS, National Animal Health Monitoring System (ed.), Fort Collins, CO.

Nickell, J., & White, B. (2010). Metaphylactic Antimicrobial Therapy for Bovine Respiratory Disease in Stocker and Feedlot Cattle. Veterinary Clinics of North America-Food Animal Practice 26(2):285-+. doi: 10.1016/j.cvfa.2010.04.006

Ollivett, T. L. & Buczinski, S. (2016). On-Farm Use of Ultrasonography for Bovine Respiratory Disease. The Veterinary clinics of North America. Food animal practice 32(1): 19-35.

Ollivett, T. L., et al. (2015). Thoracic Ultrasonography and Bronchoalveolar Lavage Fluid Analysis in Holstein Feeder steer with Subclinical Lung Lesions. Journal of veterinary internal medicine 29(6): 1728-1734.

Pardon, B., et al. (2019). Accuracy and inter-rater reliability of lung auscultation by bovine practitioners when compared with ultrasonographic findings. Veterinary Record 185(4): 109-109.

Quast, C., Pruesse, E., Yilmaz, P., Gerken, J., Schweer, T., Yarza, P., Peplies, J., & Glöckner, F.O. (2013). The SILVA ribosomal RNA gene database project: improved data processing and web-based tools. Nucleic Acids Research 41, D590-D596.

R Development Core Team. (2010). R: A language and environment for statistical computing. http://R-project.org.

Rezac, D. J., D. U. Thomson, S. J. Bartle, J. B. Osterstock, F. L. Prouty, & C. D. Reinhardt. (2014). Prevalence, severity, and relationships of lung lesions, liver abnormalities, and rumen health scores measured at slaughter in beef cattle. J Anim Sci 92(6):2595-2602. doi: 10.2527/jas.2013-7222

Sackett D, H. P. & Abbott K et al. (2006). Assessing the economic cost of endemic disease on the profitability of Australian beef cattle and sheep producers. Meat & Livestock Australia, Sydney.

Sparke, E.J., Young, B.A., Gaughan, J.B., Holt, M., Goodwin, P.J. (2001). Heat Load in Feedlot Cattle. BFLOT 307,308,309. Meat and Livestock Australia, Sydney.

Theurer, M.E., Anderson, D.E., White, B.J., Miesner, M.D., Mosier, D.A., Coetzee, J.F., Lakritz, J. & Amrine, D.E. (2013a). Effect of Mannheimia haemolytica pneumonia on behavior and physiologic responses of feeder steer during high ambient environmental temperatures. J. Anim. Sci. 91(8):3917-3929. doi: 10.2527/jas.2012-5823

Theurer, M.E., White, B.J., Anderson, D.E., Miesner, M.D., Mosier, D.A., Coetzee, J.F. & Amrine, D.E. (2013b). Effect of transportation during periods of high ambient temperature on physiologic and behavioral indices of beef heifers. Am. J. Vet. Res. 74(3):481-490. doi: 10.2460/ajvr.74.3.481

Theurer, M.E., White, B.J., Larson, R.L. & Schroeder, T.C. (2015). A stochastic model to determine the economic value of changing diagnostic test characteristics for identification of cattle for treatment of bovine respiratory disease. J Anim Sci 93(3):1398-1410. doi: 10.2527/jas.2014-8487

Timsit, E., Dendukuri, N., Schiller, I. & Buczinski, S. (2016). Diagnostic accuracy of clinical illness for bovine respiratory disease (BRD) diagnosis in beef cattle placed in feedlots: A systematic literature review and hierarchical Bayesian latent-class meta-analysis. Prev. Vet. Med. 135:67-73. doi: 10.1016/j.prevetmed.2016.11.006

Timsit, E., et al. (2019). Association of lung lesions measured by thoracic ultrasonography at first diagnosis of bronchopneumonia with relapse rate and growth performance in feedlot cattle. Journal of veterinary internal medicine 33(3): 44-50. doi:10.2527/af.2016-0022

Timsit, E., Holman, D., Hallewell, J., Alexander, T., (2016). The nasopharyngeal microbiota in feedlot cattle and its role in respiratory health. Animal Frontiers 6(2): 44-50. doi: 10.2527/af

White, B., Goehl, D., Theurer, M. & Abell, K. (2017). Determining health, performance, and economic value of using a Remote Early Disease Identification system compared to conventional method for diagnosis of Bovine Respiratory Disease. J Anim Health and Behav Sci 1(106).

White, B., Goehl, D.R. & Amrine, D. (2015a). Comparison of a remote early disease identification (REDI) system to visual observations to identify cattle with bovine respiratory diseases. J of Appl Res Vet Med 13(1): 2015

White, B.J., Amrine, D.E. & Goehl, D.R. (2015b). Determination of value of bovine respiratory disease CONT using a remote early disease identification system compared with conventional methods of metaphylaxis and visual observations. J Anim Sci 93(8):4115-4122. doi: 10.2527/jas.2015-9079

White, B.J., Goehl, D.R. & Amrine, D.E. (2014). Comparison of a remote early disease identification (REDI) system to metaphylaxis and conventional management for CONT of bovine respiratory disease in high risk beef feeder steer. Proceedings of the Forty-Seventh Annual Conference of the American Association of Bovine Practitioners, Albuquerque, New Mexico, USA, 18-20 September 2014:115.

White, B.J. & Renter, D.G. (2009). Bayesian estimation of the performance of using clinical observations and harvest lung lesions for diagnosing bovine respiratory disease in post-weaned beef feeder steer. J Vet Diagn Invest 21(4):446-453. doi: 10.1177/104063870902100405

Wolfger, B., Timsit, E., White, B. & Orsel, K. (2015). A Systematic Review of Bovine Respiratory Disease Diagnosis Focused on Diagnostic Confirmation, Early Detection, and Prediction of Unfavorable Outcomes in Feedlot Cattle. The Veterinary Clinics of North America. Food Animal Practice 31(3):351-65.

10 Acknowledgements

Thanks to the following research team members

Professor Brad White

Professor Luciano Gonzalez

Dr Emilie Flatot

Dr Christopher McMullen

Dr Kay Anantanawat

Dr Barbara Rodriguez

Dr Edouard Timsit

Dr Calvin Booker

Dr David Frith

Dr Hugh Ryan

Dr Robert Hayward

Mr Andrew Hale